Novel Aluminium Polyoxocation-based Materials and Their Potential Applications

Saranphong Yimklan

The University of Liverpool

February, 2016

Thesis submitted in accordance with the requirements of the University of Liverpool for the degree of Doctor in Philosophy

The work described in this thesis was carried out at the Department of Chemistry, Crown Street, Liverpool between March 2012 and February 2016 under the supervision of Professor Matthew Jonathan Rosseinsky (70%) and Dr John Bleddyn Claridge (30%). All work in my own, except where otherwise stated, and has not been submitted by the author for any other degree at this, or any other university,

Saranphong Yimklan.
February 2016

Novel Aluminium Polyoxocation-based Materials and Their Potential Applications

Submitted for the degree of Doctor of Philosophy by

Saranphong Yimklan, the University of Liverpool, Liverpool, February 2016

Abstract

This thesis presents the discovery, synthesis, and characterisation of novel polyoxocations of aluminium. The first polyoxocation is **Al_{30}-acetate**, $[Al_2(\mu_4\text{-}O)_8(Al_{28}(\mu_2\text{-}OH)_{50}\ (\mu_2\text{-}OH)_6(\eta\text{-}H_2O)_{22}(\eta_2\text{-}CH_3COO)_2]^{16+}$. It was crystallised by supramolecular assemblies with naphthalene-2,6-trisulphonate anion, formulated $[Al_2(\mu_4\text{-}O)_8Al_{26}(\mu_2\text{-}OH)_{56}(\eta\text{-}H_2O)_{22}Al_2(\eta_2\text{-}CH_3COO)_2](2,6\text{-}NDS)_7(CH_3COO)_2{\cdot}2H_2O$, characterised by single crystal X-ray diffraction. The structure comprises of both coordinated and uncoordinated acetate anions which were generated *in situ* by hydrolysis of acetonitrile. Protonation states of oxygen atoms were calculated by Bond Valence Sum (BVS) method. Analysis of hydrogen bonding and π-π interactions offered the understanding of supramolecular assemblies of the structure. Details of the discovery, synthesis and characterisation of Al_{30}-cetate are described in Chapter 3.

The second novel structure is a gigantic polyoxocation, $[2SO_4{\subset}Al_{162}(\mu_4\text{-}O_{44})(\mu_2\text{-}O)_2(\mu_3\text{-}OH)_{32}\ (\mu_2\text{-}OH)_{276}(\eta\text{-}H_2O)_{100}(\eta\text{-}SO_4)_{16}]^{50+}$ or ***megaKeggin*-Al_{162}**. It is the largest polyoxocation based on research literatures reported so far. It is also the first structure which combine two different isomers of *Keggin*-Al_{13} polyoxocation *i.e.* δ- and γ-isomer. Local structure of the materials was studied by MAS ^{27}Al NMR. Its supramolecular assemblies generate three rotational polymorphs (**MK-A**, **MK-B** and **MK-C**). All of the polymorphs are open frameworks with large pores in their crystal structures. Among these three polymorphs, **MK-A** has been successfully synthesised and investigated the potential applications as a sorbent for alkali metal cations and also anions *i.e.* sulphate, arsenate, as well as, organic dye *i.e.* $(Chromis\text{-}A)^{2-}$. X-ray crystal structures are key evidences which indicate the presences of the alkali metal cations in the materials after sorption. Details of the discovery and characterisation of the *megaKeggin*-Al_{162} based materials are described in Chapter 4. The studies of sorption properties of MK-A are described in Chapter 5.

Acknowledgements

It is a pleasure to thank my supervisor, Professor Matthew Jonathan Rosseinsky, for his helps over the past three years. His enthusiasms have been invaluable in helping me overcome the numerous problems encountered during the course of this work.

I am also very grateful to the people who have contributed to the project and the megaKeggin paper during the period; Dr Marco Zanella, Dr Alexandros Katsoulidis, Dr Sanjit Nayak, Dr Susanna Jansat and Dr Troy Manning deserve a special mention for their great suggestions and research coordination. Dr George Whitehead, Dr John E Warren, and Dr Gary Miller provided valuable assistances in crystallographic works.

Thanks are due to Dr Frédéric Blanc, Mona Kab Omir and Kenneth Kazuya Inglis for their great helps and valuable discussions on Solid State NMR experiments.

Thanks are also due to the Department of Chemistry at the University of Liverpool including Centre for Materials Discovery (CMD) and Chemical Analysis Units for research facilities and supports, especially, George Miller for ICP-OES analysis. I thank I19 Beamline at Diamond Light Source (DLS) in Harwell, Oxfordshire, for Synchrotron X-ray diffraction facilities and experiences.

I would like to thank the 14th BCA/CCG Intensive Teaching School in X-ray Structure Analysis at Durham University for great opportunity to learn about crystallography and also the school of topological methods in crystal chemistry and materials science at EPFL for great lecture series about topology and reticular chemistry and a good trip in Lausanne, Switzerland.

I would like to thank the Development and Promotion of Science and Technology Talented Project (DPST), Thailand, for fully financial supports since 2004.

I am very grateful to my family for helping me throughout my education, and to numerous friends, Mona, Maria, Darren, Tom, Leopoldo, who have made Liverpool such a pleasant place to work in. Thank you to Ken for good memories and being my luck complement. Finally, thanks to Tom, Mai, p'Nook and Micky for a warm family in Liverpool.

ปญฺญายตฺถํ วิปสฺสติ

Table of Contents

Abbreviations

1,3,6(7)-NTS	1,3,6(7)-Naphthalene Trisulphonate (Mix Isomers)
1,3,6-NTS	1,3,6-Naphthalene Trisulphonate
1,3,7-NTS	1,3,7-Naphthalene Trisulphonate
1,5-NDS	1,5-Napthalene Disulphonate
2,6-NDS	2,6-Napthalene Disulphonate
BVS	Bond Valence Sum
DMF	*N*,*N*-Dimethylformalmide
EDX	Energy Dispersive X-Ray spectrometer
EtOH	Ethanol
FT-IR	Furrier Transform Infrared Spectroscopy
ICP-OES	Inductively Coupled Plasma Optical Emission Spectrometry
IDA	Iminodiacetic Acid
M	Molarity
MAS	Magic Angle Spinning
MeCN	Acetonitrile, Ethanenitrile
MeOH	Methanol
mL	Milli Litre
NMR	Nuclear Magnetic Resonance
NTA	Nitrilotriacetic Acid
ppm	parts per million
PXRD	Powder X-Ray Diffraction
SEM	Scanning Electron Microscope
SBU	Secondary Building Unit

Chapter 1
Introduction

1.1 Polyoxometalates and Polyoxocations

Polyoxometalates (POMs) are discrete anionic metal oxides, which have well-organised chemistries and exhibit potential applications in many fields *e.g.* catalysis, pigments, recording materials, gas sensors, selective electrodes, protein precipitation agents, *etc*.[1–5] Aqueous chemistry of high oxidation state group 5 and 6 elements *i.e.* V(IV/V), Nb(V), W(VI), and Mo(VI) promotes the formations of polyoxoanion as simply illustrated by the following equations:[6–9]

$$8H^{+}\,(aq) + 7[WO]_4^{2-}\,(aq) \rightarrow [W_7O_{14}]^{6-}\,(aq) + 4H_2O\,(l) \qquad (1.1)$$

$$23H^{+}\,(aq) + [HPO_4]^{2-}\,(aq) + 12[MO_4]^{2-}\,(aq) \rightarrow [PMo_{12}O_{40}]^{3-}\,(aq) + 12H_2O\,(l). \qquad (1.2)$$

Normally, polyoxometalates compose of metal oxide building blocks with a general formula $[MO_x]_n$, where M = Mo, W, V, and Nb and x = 4-7.[10] POMs can be broadly classified into (i) isopolyanions ($[H_xM_yO_z]^{n-}$) and (ii) heteropolyanions ($[X_xM_yO_z]^{m-}$), where X = heteroatom *e.g.* a *p*-block element or a first-row transition metal). Despite their diverse compositions, POMs can be found as isostructures of distinct clusters, for example, *Lindqvist*-$[M_6O_{19}]^{n-}$, *Anderson*-$[XM_6O_{24}]^{n-}$, *Keggin*-$[XM_{12}O_{40}]^{n-}$, *Wells–Dawson*-$[X_2M_{18}O_{62}]$, *Preyssler*-$[X_5M_{30}O_{110}]^{n-}$, *etc*. (where M =W, V, Nb, Mo and X is a tetrahedral template), as shown in Figure 1.1. Among these structures, *Keggin*-type structure is the most well-known structure exhibiting five theoretical geometries.[11,12] Not only in POMs chemistry, the *Keggin* structure also exists isostructurally in polyoxocations of Al(III), Ga(III), Ge(IV) as well as Fe(III).[13–22] Considering about size of anionic polynuclear metal oxide clusters, a molybdenum POMs Mo_{268} size, reported by Achim Müller *et al.*, reaches a scale of protein![23] In contrast, the largest cationic cluster of aluminium amongst a handful distinct structures reported to date is $[Al_{32}O_8(OH)_{60}(H_2O)_{28}(SO_4)_2]^{16+}$, Al_{32}.[24] Thus, the discoveries of large aluminium polyoxocations are interesting. Aqueous chemistry of aluminium is described below.

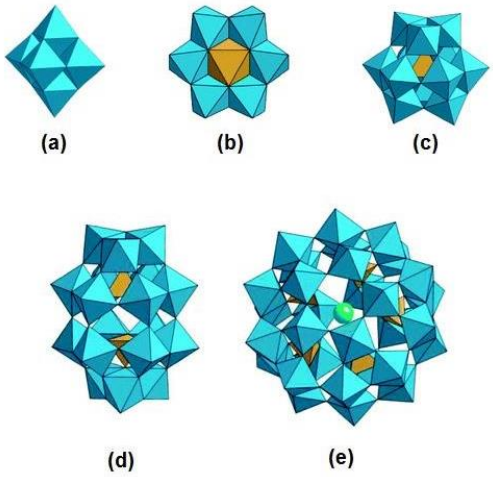

Figure 1.1 Polyhedral representation of (a) Lindqvist, (b) Anderson, (c) ***Keggin***, (d) Wells–Dawson and (e) Preyssler polyoxoanions. (Reprinted with permission from Ref. 3).

1.2 Hydrolysis of aluminium

Metal cations in aqueous solution generally hydrolyse to form a series of mononuclear and polynuclear hydroxyl complexes. The general equation is

$$xM^{n+}\,(aq) + yH_2O\,(l) \quad \rightleftharpoons \quad M_x(OH)_y^{n-y}\,(aq) + yH^+\,(aq) \qquad (1.3)$$

Iron(III), for example forms $[Fe(OH)]^{2+}$, $[Fe(OH)_2]^{+}$, $Fe(OH)_3$, $[Fe(OH)_4]^{-}$, $[Fe_2(OH)_2]^{4+}$ and probably other polynuclear species.[25] Aluminium, the third most abundant element in earth crust, has similar hydrolysis chemistry. Al(III), with an ionic radius of 0.535 Å, has hydration number of six and is unhydrolysed below pH 3.0.[26,27]. The hexaaquaaluminium cation, $[Al(OH_2)_6]^{3+}$, is the most simple species formed in aqueous solution of acidic aluminium salts. Successive addition of base leads to the formation of mononuclear species *e.g.* $[Al(OH_2)_5(OH)]^{2+}$, $[Al(OH_2)_4(OH)_2]^{+}$, and $[Al(OH)_4]^{-}$.[25] Like many other cations, Aluminium cation can be partially hydrolysed to r_{OH}, $[OH^-]/[Al^{3+}]$, of 2.50 to form polyaluminiumoxocations which can be stable indefinitely in solution but are metastable with respect to precipitate of the stable phase $Al(OH)_3$ (gibbsite), beyond r_{OH} of 2.50.[28,29] Speciation of partially hydrolysed aluminium fall into two broad structural classes *i.e.* (i) *"Cage-like"* or *"Baker-Figgis-Keggin"* structure and (ii) "*Core-link*" or "Mögel" structure. Structural diversity of polyaluminiumoxocation depends on the synthetic conditions *e.g.* (i) degree of hydrolysis, $r_{OH,}$ (ii) rate of base injection, (iii) concentration, (iv) time.[30] Direct addition of hydroxide base tends to form "*Cage-like*" structures (*see* Figure 1.2) because the

formation requires a tetrahedral $[Al(OH)_4]^-$ anion which is an origin of $\{AlO_4\}$ core as a tetrahedral template of the structures.[30] The application of hydroxide-free precursor, for example, reduction of H^+ using Zn powder leads the formation of "*Core-link*" structures (Figure 1.2).[31,32]

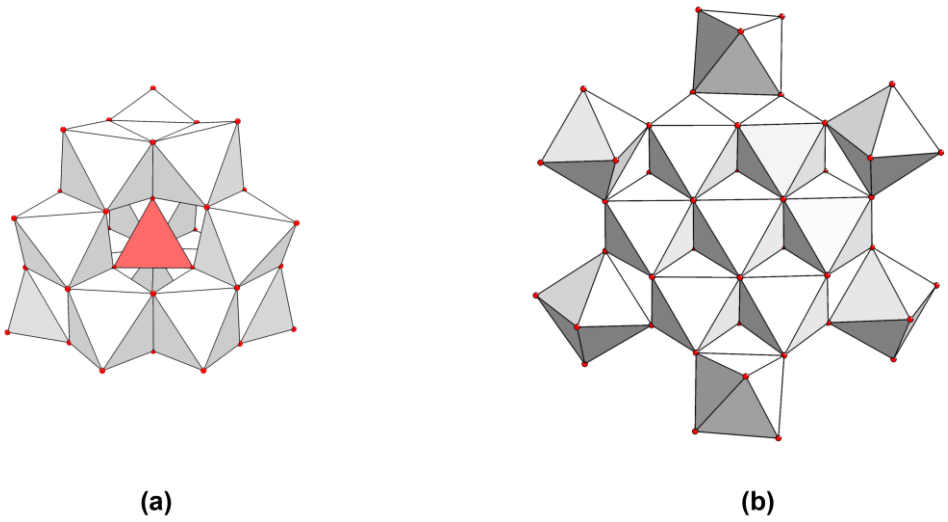

Figure 1.2 (A) Polyhedral representation of "*Cage-like" ε-Keggin*-$[MO_4M_{12}(OH)_{24}(H_2O)_{12}]^{n+}$, where M = Al(III) or Ga(III), comprising twelve octahedral metal centres that share vertices with a central tetrahedral MO_4 metal centre. (B) Polyhedral representation of "*Core-link*" M_{13} structure.

To describe the structural properties of aluminium, formula notations are employed that η indicates terminal oxygens, while μ_i refers to ligating oxygens that bridge *i* aluminium atoms.[33] The coordination number of Al(III) is also denoted as 'AlO_j' where *j* refers to the number of oxygens bonded to an aluminium.

1.2.1 Polyoxocations of aluminium

1.2.1.1 Aluminium monomers, dimers, trimers and octamers

Aluminium monomers, $[Al(H_2O)_6]^{3+}$, are dominant species in highly acidic aqueous solutions of aluminium salts as reflected in ^{27}Al-NMR spectra (δ= 0.00 ppm).[26] At low pH, Al(III) is six-coordinated to oxygens as $[Al(H_2O)_6]^{3+}$ and changed successively to $[Al(OH)(H_2O)_5]^{2+}$, $[Al(OH)_2(H_2O)_4]^+$, and $[Al(OH)_4]^-$ at near-neutral pH and higher.[26] Aluminium monomers can polymerise to larger cluster at concentration above 1×10^{-5} M.[34] They are important as primary octahedral $\{AlO_6\}$ building blocks for larger polyoxocations.

Al(III) dimerises with bridging dihydroxy groups (μ_2-OH), which has been crystallised in form of selenate (SeO_4^{2-}) salt, formulated $[Al_2(\mu_2\text{-}OH)_2(H_2O)_8](SeO_4)_2\cdot(H_2O)_{10}$, originally isolated by *Johansson* in 1962.[35] It can be stabilised by aminocarboxylates like iminodiacetate (IDA), nitrilotriacetate (NTA), hydroxyethyliminodiacetate (HEIDI), *e.g.* $[Al_2(\mu_2\text{-}OH)_2(H_2O)_2(IDA)_2]$, $[Al_2(\mu_2\text{-}OH)_2(NTA)_2]^{2-}$, and $[Al(HEIDI)\ (H_2O)]_2$.[36]

A flat-aluminium trimer is proposed as an important building block of the *Keggin*-Al_{13} and larger polyoxocations.[36,13] An aluminium trimer has been crystallised by *Feng et al*. in 1990 using citrate.[37]

An aluminium tetramer exists in form of bromide salt, $[Al_4(OH)_6(H_2O)_{12}][Al(H_2O)_6]_2Br_{12}$, reported by *S. Du et al.* in 2011.[38] The tetramer, $[Al_4(OH)_6(H_2O)_{12}]^{6+}$ (**Al_4**), comprises four identical distorted $\{AlO_6\}$ octahedra connecting with each other by corner sharing to form a regular tetrahedron with ideal T_d symmetry. Beside the aluminium trimer, an octamer, $[Al_8(\mu_3\text{-}OH)_2(\mu_2\text{-}OH)_{12}(\eta\text{-}H_2O)_{18}]^{10+}$ (**Al_8**), also has a flat structure (*see* Figure 1.3) isolated as sulphate salt, $[Al_8(OH)_{14}(H_2O)_{18}](SO_4)_5\cdot 16H_2O$.[39] Its crystallisation process takes more than a year![39]

1.2.1.2 Aluminium tridecamers

Partial hydrolysis of Al(III) leads to the formation of tridecamers (**Al_{13}**) with a highly positive charge. There are two classes of aluminium tridecamers *i.e. Mögel*- and *Keggin*-type structures.

1.2.1.2.1. Mögel isomer

Due to its very high charge, Mögel isomer, formulated $[M_{13}(\mu_3\text{-}OH)_6(\mu_2\text{-}OH)_{12}(\eta\text{-}H_2O)_{24}]^{15+}$ (**Mögel-M_{13}**), where M = Al(III) or Ga(III), is stable only in solid state structures in forms of salts of monovalent anions *i.e.* nitrate and chloride.[31,40–42] It can transform to *Keggin*-Al_{13} structure during aging or dilution process.[43,44] Similar to Al_8, the *Mögel*-Al_{13} also comprises of edge-sharing $\{AlO_6\}$ units like brucite structure.[45] It can be simply synthesised in *non-aqueous* or *alkali-free aqueous solution* to prevent the formation of *Keggin*-Al_{13} isomer, which requires a tetrahedral $Al(OH)_4^-$ unit from base as a structural template.[31,46] Even though it is unstable in solution phase, it can be stabilised by anions *i.e.* nitrate (NO_3^-), chloride (Cl^-), as well as aminocarboxylate *i.e.* $HEIDI^{3-}$ and $HPDTA^{5-}$.[31,40–42] Recently, it was isolated as a

column-like metal–organic framework with a 2-aminobenzene dicarboxylate linker coordinated to aluminium.[47] There are five solid state structures which contain a *Mögel*-Al_{13}-based cluster, reported in Chemical Database Service (CDS) (*see* Table 1.1).

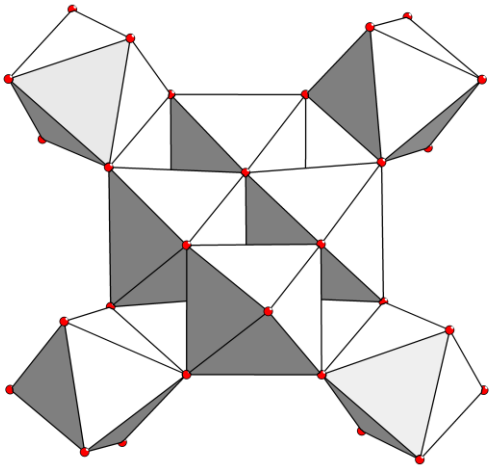

Figure 1.3 Graphical representation shows the structure of Al_8.

1.2.1.2.2. Baker-Faggis-Keggin isomers

In 1933, *James Fargher Keggin*, a doctoral student of Nobel laureate Lawrence Bragg at the University of Manchester, published his paper which described the polyoxometalate-structure of phosphotungstic acid, $H_3[PO_4W_{12}O_{18}(OH)_{36}]\cdot nH_2O$ using X-ray single crystal diffraction.[11] The cluster comprises of a regular tetrahedral centre of phosphate surrounded by twelve octahedrally coordinated $\{WO_6\}$ sharing edges. The structure has been described as a new fundamental type of inorganic complex and five geometrical isomers have been proposed by *Louis C. W. Baker* and *Jane S. Figgis* in 1970.[12] The $[Al(\mu_4\text{-}O)_4Al_{12}(\mu_2\text{-}OH)_{24}(H_2O)_{12}]^{7+}$ (***Keggin*-Al_{13}**), is a dominant polycationic species in aqueous solution of partialy hydrolysed Al(III), synthesised by titration of an aluminium solution with base to $2.10 < r_{OH} < 2.50$.[36] It is derived from five *Baker–Faggis–Keggin or Keggin* isomers (*see* Figure 1.4), which are familiar with well-known polyoxometalates *e.g.* tungstates and molybdates. The structure of *Keggin*-Al_{13} comprises of one Al(III) tetrahedrally coordinated to oxide ions $\{AlO_4\}$ at the centre. The $\{AlO_4\}$ core is then encapsulated in cage of twelve octahedrally coordinated

Al(III) ions, which contains four $[Al_3(\mu_2\text{-}OH)_6(H_2O)_3]^{3+}$ trimers sharing their edges as shown in Figure 1.4.

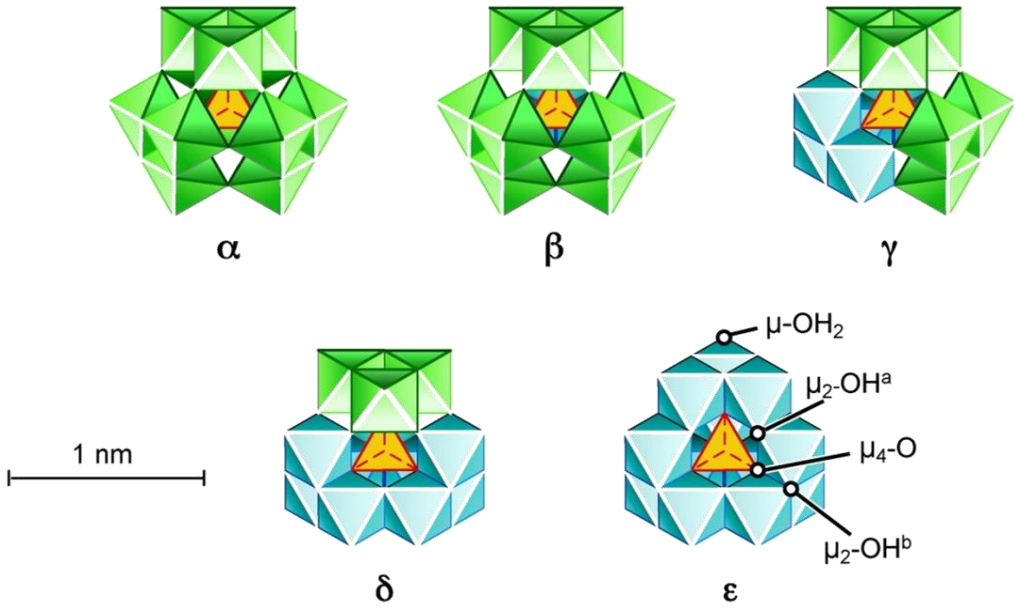

Figure 1.4 Five *Baker–Faggis–Keggin* isomers. (Reprinted with permission from Ref. 48)

The ε isomer is the most stable species among the five isomers. The *Keggin* isomers stability follows this order: ε-Al_{13} > δ-Al_{13} > α-Al_{13} > γ-Al_{13} > β-Al_{13} as it is observed experimentally and in nature. The δ-, γ- and ε-Al_{13} been isolated and structurally characterised and the α-Al_{13} is found in a natural mineral zunyite. The γ-Al_{13} has been synthesised from a complicated amino-acid-assisted method, and β-Al_{13} has not been reported so far (*see* **Error! Reference source not found.**).[13,20,49–51] The *Keggin*-Al_{13} cluster has been isolated as salts of divalent anions *e.g.* SO_4^{2-}, SeO_4^{2-}, as well as naphthalene-2,6-disulphonate (2,6-NDS^{2-}) anion and a polyoxovanadate tungstate, $[(V_2W_4O_{19})]^{4-}$, which has *even* number of charge, –2 , –4, and –14, respectively.[24,52] Due to its *odd* charge, +7, *Keggin*–Al_{13} prefers to be capped by a monovalent cation like Na^+ to obtain an even-number charge, +8, Na-δ-$[Al(\mu_2\text{-}O)_4Al_{12}(\mu_2\text{-}OH)_{24}(\eta\text{-}H_2O)_{12}]^{8+}$.[53] Polyoxocations reported in CDS database are listed in Table 1.1.

Table 1.1 Summary of polyoxocations of aluminium reported in literatures and CDS[†]

Polyoxocation/anions	**Counter ions**	**Ref.**
Mögel-Al_{13} based		
$[Al_{13}(\mu_3\text{-}OH)_6(\mu_2\text{-}OH)_{18}(H_2O)_{24}]^{15+}$	Cl^-	40
$[Al_{13}(\mu_3\text{-}OH)_6(\mu_2\text{-}OH)_{18}(H_2O)_{24}]^{15+}$	NO_3^-	31
$[Al_{13}(\mu_3\text{-}OH)_6(\mu_2\text{-}OH)_{12}(HEIDI)_6(H_2O)_6]^{3+}$	NO_3^-	54
$[Al_{15}(\mu_3\text{-}O)_4(\mu_3\text{-}OH)_6(\mu\text{-}OH)_{14}(HPDTA)_4]^{3-}$	$pipzH_2^{2+}$	55
$[Al_{13}(OH)_{27}(H_2O)_6(BDC\text{-}NH_2)_3Cl_6(C_3H_7OH)_6]$	–	47
Keggin-Al_{13} based		
Na-ε-$[Al(\mu_2\text{-}O)_4\,Al_{12}(\mu_2\text{-}OH)_{24}(H_2O)_{12}]^{8+}$	SO_4^{2-}	56
ε-$[Ga(\mu_4\text{-}O)_4Al_{12}(\mu_2\text{-}OH)_{24}(H_2O)_{12}]^{7+}$	SO_4^{2-}	19
ε-$[Al(\mu_4\text{-}O)_4Al_{12}(\mu_2\text{-}OH)_{24}(\mu\text{-}OH)(H_2O)_{12}(SO_4)]^{4+}$	SO_4^{2-}	24
ε-$[Al(\mu_4\text{-}O)_4Al_{12}(\mu_2\text{-}OH)_{24}(H_2O)_{12}]^{7+}$	K^+, NO_3^-, tris(cucurbit[6]uril)	57
ε-$[Al(\mu_4\text{-}O)_4Al_{12}(\mu_2\text{-}OH)_{24}(H_2O)_{12}]^{7+}$	NO_3^{2-}, tris(cucurbit[6]uril)	57
ε-$[Al(\mu_4\text{-}O)_4Al_{12}(\mu_2\text{-}OH)_{24}(H_2O)_{12}]^{7+}$	$[Na(18\text{-crown-}6)(H_2O)_2L_2(H^+)_w]^{x-}$	58
δ-$[Al(\mu_4\text{-}O)_4Al_{12}(\mu_2\text{-}OH)_{24}(H_2O)_{12}]^{7+}$	$[XW_{12}O_{40}](OH)^{7-}$ (X = H_2 and Co)	59
γ-$[Al(\mu_4\text{-}O)_4Al_{12}(\mu_2\text{-}OH)_{23}(H_2O)_{13}]^{6+}$	SO_4^{2-}	50
$[Al(\mu_4\text{-}O)_4Al_{12}(\mu_2\text{-}OH)_{24}(H_2O)_{12}]^{7+}$	$[V_2W_4O_{19}]^{4-}$	60
Na-δ-$[Al(\mu_4\text{-}O)_4Al_{13}(\mu_2\text{-}OH)_{24}(H_2O)_{12}]^{8+}$	2,6-NDS^{2-}	53
$[(Al_2(\mu_4\text{-}O)_8(Al_{24}(\mu_2\text{-}OH)_{50}(H_2O)_{20})]^{12+}$	2,6-NDS^{2-}	53
$[(Al_2(\mu_4\text{-}O)_8(Al_{28}(\mu_2\text{-}OH)_{56}(H_2O)_{26})]^{18+}$	Cl^-, 2,6-NDS^{2-}	53
$[(Al_2(\mu_4\text{-}O)_8(Al_{28}(\mu_2\text{-}OH)_{56}(H_2O)_{26})]^{18+}$	SO_4^{2-}	52,56
$[W_2Al_{28}O_{18}(OH)_{48}(H_2O)_{24}]^{7+}$	$[H_2W_{12}O_{40}]^{7-}$	60
$[(Al_2(\mu_4\text{-}O)_8(Al_{28}(\mu_2\text{-}OH)_{56}(H_2O)_{26})]^{18+}$	Na^+, NO_3^-, tris(cucurbit[6]uril)	57
$[Al_{32}O_8(OH)_{60}(H_2O)_{28}(SO_4)_2]^{16+}$	Cl^-, SO_4^{2-}	24
$[(Al(IDA)(H_2O)_2(Al_{30}O_8(OH)_{60}(H_2O)_{22})]^{16+}$	Cl^-, SO_4^{2-}, 2,6-NDS^{2-}	61
$[(Zn(NTA)(H_2O)_2(Al(NTA)(OH)_2)_2(Al_{30}(OH)_{60}(O)_8(H_2O)_{20}]^{10+}$	2,6-NDS^{2-}	61
$[(TBP)_2Al_2(\mu_4\text{-}O)_8(Al_{28}(\mu_2\text{-}OH)_{56}(H_2O)_{22})]^{14+}$	2,6-NDS^{2-}	62
$[(Cu(H_2O)_2(Al_2O_8Al_{28}(OH)_{60}(H_2O)_{22}]^{18+}$	2,6-NDS^{2-}	63
Dawson Al_{20} based structure		
$[Al_{20}O_8(OH)_{36}(H_2O)_{12}]^{8+}$	2,5-NDS^{2-}	19
$[Ga_2Al_{18}O_8(OH)_{36}(H_2O)_{12}]^{8+}$	2,5-NDS^{2-}	19

[†] Chemical Database Service (CDS); The databases comprise Cambridge Structural Database, ICSD, CrystMet and the NIST Crystal Data Files.

1.2.1.3 Al_{26} and Al_{30} class

Dimerisation of *Keggin*-Al_{13} can lead to the formation of larger polyoxocations which are classified into two distinct classes *i.e.* (i) an Al_{26} class, and (ii) an Al_{30} class.[24,52,53,56,61,63] The Al_{26}, $[(Al_2(\mu_4\text{-}O)_8(Al_{24}(\mu_2\text{-}OH)_{50}(H_2O)_{20})]^{12+}$, comprises of two δ-*Keggin*-Al_{13} linked together *via* two bridging μ_2-OH corners as illustrated in Figure 1.5 a. It has been isolated as a salt of 2,6-NDS^{2-} and reported in 2012.[53] There is only one structure in this class. The Al_{30}, $[(Al_2(\mu_4\text{-}O)_8(Al_{28}(\mu_2\text{-}OH)_{56}(H_2O)_{26})]^{18+}$, is another distinct class of *Keggin*-Al_{13} dimer. It was firstly reported by two independent groups in 2000.[52,56] The polyoxocation comprise of two *Keggin*-Al_{13} linked *via* a tetramer which is a group of four $\{AlO_6\}$ units as illustrated in Figure 1.5 b. There are many derivatives of this Al_{30} structure. The derivatives of the Al_{30} structure are shown in Figure 1.6.

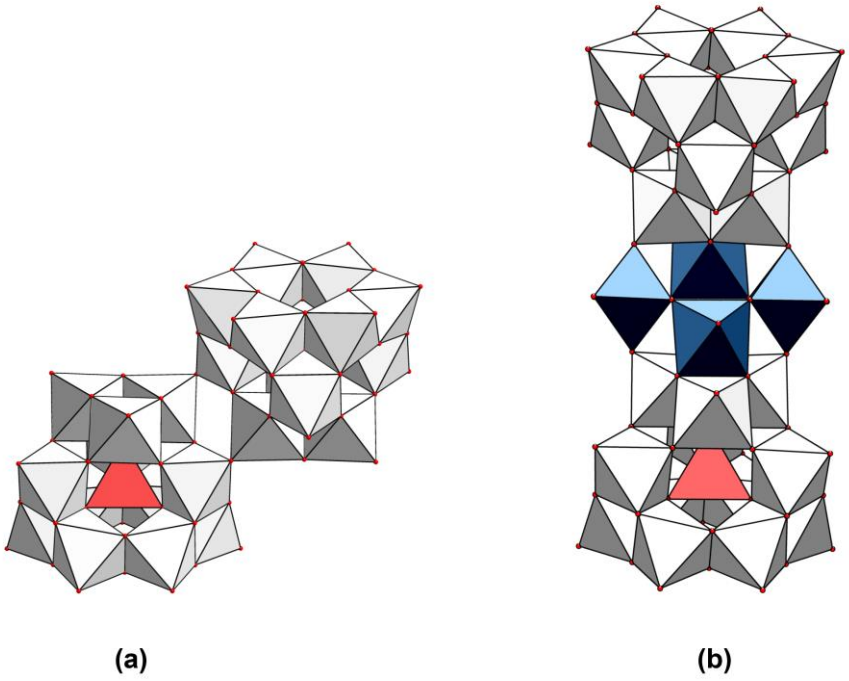

Figure 1.5 Polyhedral representations of (a) $[(Al_2(\mu_4\text{-}O)_8(Al_{24}(\mu_2\text{-}OH)_{50}(H_2O)_{20})]^{12+}$ (Al_{26}) and (b) $[(Al_2(\mu_4\text{-}O)_8(Al_{28}(\mu_2\text{-}OH)_{56}(H_2O)_{26})]^{18+}$ (Al_{30}). Tetrahedral $\{AlO_4\}$ cores and an $\{AlO_6\}$ tetramer are represented by red and blue polyhedra, respectively.

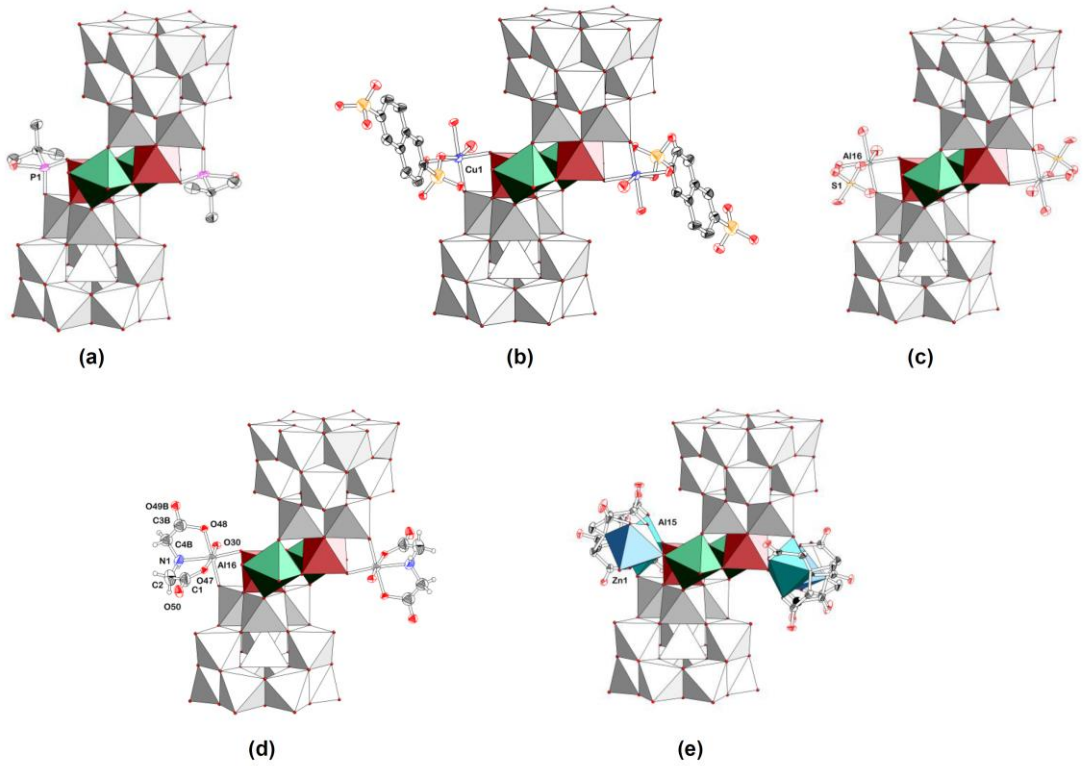

Figure 1.6 Polyhedral representations showing the derivatives of Al_{30} polyoxocations *i.e.* (a) $[(TBP)_2Al_{30}O_8(OH)_{56}(H_2O)_{22})]^{14+}$ (Al_{30}TBP), (b) $[(Cu(H_2O)_3(2,6\text{-NDS})_2Al_{30}O_8(OH)_{60}(H_2O)_{22}]^{18+}$ (Cu_2 Al_{30}NDS), (c) $[Al_{32}O_8(OH)_{60}(H_2O)_{28}(SO_4)_2]^{16+}$ ($Al_{32}SO_4$), (d) $[(Al(IDA)H_2O)_2(Al_{30}O_8(OH)_{60}(H_2O)_{22})]^{16+}$ (Al_{32}IDA), (e) $[(Zn(NTA)H_2O)_2(Al(NTA)(OH)_2)_2(Al_{30}O_8(OH)_{60}(H_2O)_{20}]$ (Zn_2Al_{32}NTA). (TBP = *tert*-butylphosphonate, IDA = iminodiacetate, 2,6-NDS = naphthalene-2,6-disulphonate, NTA = nitrilotriacetate)

1.2.1.4 Dawson Al_{20} structure

In 2015, a novel heterometallic cluster $[Ga_2Al_{18}O_8(OH)_{36}(H_2O)_{12}]^{8+}$ (**Ga_2Al_{18}**) has been isolated using 2,7-NDS^{2-} and structurally characterised using single-crystal X-ray diffraction.[19] The polyoxocation has Wells–Dawson structure topology as illustrated in Figure 1.7. The Well-Dawson structure is well-known in polyoxometalate chemistry. The general formula of the Wells–Dawson structure is $[(X^{n+})_2M_{18}O_{62}]^{(16-2n)-}$ where X^{n+} represents a central atom, *e.g.* P(V), As(V), S(VI); surrounded by a cage of M addenda atoms, *e.g.* W(VI), Mo(VI) or a mixture of elements, each of them composing $\{MO_6\}$octahedral units.[64,65] The presence of $[Al_{20}O_8(OH)_{36}(H_2O)_{12}]^{8+}$ (**Al_{20}**) was computationally studied and reported in the same paper.[19]

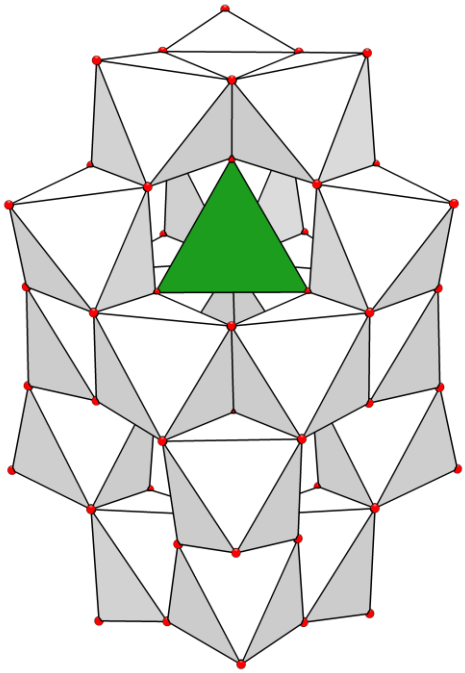

Figure 1.7 Polyhedral representation of a Well-Dawson $[Ga_2Al_{18}O_8(OH)_{36}(H_2O)_{12}]^{8+}$ (Ga_2Al_{18}) polyoxocation. The $\{GaO_4\}$ core are represented by green tetrahedrons.

1.3 Protonation state of oxygen in polyoxocations

In polyoxocation chemistry, Bond Valence Sum (BVS) calculation is applied as a key method to assign the protonation state of oxygens in polyoxocations. Oxygen atoms in each polyoxocations can be assigned to oxide (O^{2-}), hydroxide (OH^-) and water (H_2O). Valency (V) of oxygen depends on its protonation state. Valency of oxygen in O^{2-} is about 2.0, in OH^- is between 0.5 - 1.5, and in H_2O is below 0.5.[66] It can be calculated as the summation of bond valence (v_i). The bond valence can be evaluated by following equation:

$$v_i = \exp((R_o - R_i)/b), \tag{1.4}$$

where R_i is the length of a bond between the two given atoms reflecting the strength of the bond, b is a bond valence parameter (for any Al(III)—O(II) bond, b = 0.37, R_o = 1.622 Å).[67–69] In early 2016, *Pavel Karen et al.* are working on the "Comprehensive Definition of Oxidation State" in order to define the term officially after their IUPAC technical report has been published two years ago.[70,71] They proposed that the *oxidation*

state is the atom's charge after ionic approximation of its bonds.[70] The BVS calculation is one of the most famous approaches to estimate the oxidation state of chemical elements in compounds.

In this thesis, we applied the BVS method to calculate protonation state of oxygen atoms in all polyoxocations of aluminium and to classify chemical identities of each atom into oxide (O^{2-}), hydroxide (OH^{-}), or water (H_2O).

1.4 Intermolecular Interactions

Non-covalent intra- and intermolecular interactions are important in supramolecular assemblies of polyoxocations crystal structures. Coulombic or ionic interaction is a simple attractive force between polycationic species and its counter anion. Hydrogen bond is one of the most important intermolecular interactions in crystal structure of aluminium polyoxocations because they have a number of coordinating OH^{-} and H_2O. Recently, *Keggin*-type structures could be isolated by naphthalene sulphonate, 2,6-NDS^{2-}, anion.[53] The naphthalene ring has ability to form "π-π interaction" or "π-π stacking" between each other. Important intramolecular interactions in crystal structures of the compounds reported in this thesis are hydrogen bonds and π-π interactions. Details of each type of interactions are described below.

1.4.1 Hydrogen bond

Hydrogen bond is an important inter- and intramolecular interaction in aluminium polyoxocation chemistry. It is an attractive interaction between hydrogen atom which bonds to an electronegative atom, and other electronegative atom(s) in the same or different molecules. *Linus Pauling* mentioned in his famous book, The Nature of the Chemical Bond, that *T.S. Moore* and *T.F. Winmill* were the who developed the concept of hydrogen bond.[73] In 1912, they published an account of the fact that trimethylammonium hydroxide is a weaker base than tetramethylammonium hydroxide by using the concept of hydrogen bond.[74]

1.4.1.1 Definition of hydrogen bond

In 2011, IUPAC has published a definition of hydrogen bond with some essential criteria in "Definition of the hydrogen bond (IUPAC Recommendations 2011)".[75,76] The hydrogen bond is officially defined as the following:

"*The hydrogen bond is an attractive interaction between a hydrogen atom from a molecule or a molecular fragment X—H in which X is more electronegative than H, and an atom or a group of atoms in the same or a different molecule, in which there is evidence of bond formation.*"

A hydrogen bond is usually represented as **X—H···Y—Z**, where the three dots denote the hydrogen bond, **X—H** represents the hydrogen bond donor and **Y** represents the hydrogen bond acceptor. The Y may be an atom or an anion, or a fragment or a molecule **Y—Z**. The X and Y may be the same element. In any ways, the hydrogen acceptor is an electron rich region *e.g.* a lone pair of Y or π-bonded pair of Y—Z.[75] The IUPAC recommendation also states that the *"evidence for hydrogen bond formation may be experimental or theoretical, or ideally, a combination of both"*.[75] There are six criteria (E1-E6) for hydrogen bond formation as listed below.

1.4.1.2 List of criteria for hydrogen bond

For a hydrogen bond X—H···Y—Z: [75,76]

(E1) The forces involved in the formation of a hydrogen bond include those of an electrostatic origin, those arising from charge transfer between the donor and acceptor leading to partial covalent bond formation between H and Y, and those originating from dispersion.

(E2) The atoms X and H are covalently bonded to one another and the X—H bond is polarized, the H···Y bond strength increasing with the increase in electronegativity of X.

(E3) The X—H···Y angle is usually linear (180°) and the closer the angle is to 180°, the stronger is the hydrogen bond and the shorter is the H···Y distance.

(E4) The length of the X—H bond usually increases on hydrogen bond formation leading to a red shift in the infrared X—H stretching frequency and an increase in the infrared absorption cross-section for the X—H stretching vibration. The greater the lengthening of the X—H bond in X—H···Y, the stronger is the H···Y bond. Simultaneously, new vibrational modes associated with the formation of the H···Y bond are generated.

(E5) The X—H···Y—Z hydrogen bond leads to characteristic NMR signatures that typically include pronounced proton deshielding for H in X—H, through hydrogen bond spin–spin couplings between X and Y, and nuclear Overhauser enhancements.

(E6) The Gibbs energy of formation for the hydrogen bond should be greater than the thermal energy of the system for the hydrogen bond to be detected experimentally.

1.4.1.3 Evidence and classification of hydrogen bond

As mentioned above, an assignment of hydrogen bond using the official definition needs evidence for the bond formation. This evidence may be from crystallographic, spectroscopic, as well as, computational studies.[76] Bond distances and bond angles can be obtained from crystallography. IR and NMR spectroscopy can offer direct evidence of the hydrogen bond formation. Microwave spectroscopy also provides a structural information of isolated hydrogen-bonded complexes.[77] *G. A. Jeffrey* classified hydrogen bonds into three type *i.e.* weak, moderate and strong hydrogen bonds. The criteria for his classification are listed in Table 1.2.

Table 1.2 Physicochemical properties of weak, moderate and strong H-bonds.[78]

Hydrogen bond	**Strong**	**Moderate**	**Weak**
A–H···B	mostly covalent (only 2-centred)	mostly electrostatic (2- and more centred)	Electrostatic (2- and more centred)
Bond lengths	A—H ≈ H···B	A—H < H···B	A—H << H···B
H···B (nm)	~ 0.12 – 0.15	~ 0.15 – 0.22	0.22 – 0.32
A···B (nm)	0.22 – 0.25	0.25 – 0.32	0.32 – 0.40
Bond angles A—H···B (°)	175 – 180	130 – 180	90 – 150
Bond energy [kcal mol^{-1} (kJ mol^{-1})]	14 – 40 (59 – 167)	4 – 15 (17 – 63)	< 4 (<17)
Relative IR ν vs vibration shift (cm^{-1})	25 % (< 1600 cm^{-1})	10 – 25 % (< 2000 - 3000 cm^{-1})	< 10 % (~ 3000 cm^{-1})
^{1}H NMR chemical shift downfield (ppm)	14 – 22	< 14	-
Example	Gas-phase dimers with strong acid or strong bases Acid salts Proton sponges Pseudohydrates HF complexes	Acids Alcohols Phenols Hydrates All biological molecules	Gas phase dimers with weak acids or weak bases Minor components of 3-centre bonds C—H···O/N bonds O/N—H···π bonds

1.4.2 π-π interaction

The terms "π-π interaction" and "π-stacking" are used to describe situations in which two or more aromatic rings are associated in some fashion for half centuries.[79,80] The origin of this interaction is the attractive force between a partially positive σ-framework of the aromatic ring and an electron cloud in π-system.[80] It can be found in three main orientations *i.e.* (i) parallel face-centred or sandwich, (ii) perpendicular T-shaped, and (iii) parallel displaced or off-set parallel as shown in Figure 1.8 (a). Quadrupole moments of the aromatic rings are different in benzene and hexafluorobenzene due to their different electron distributions as illustrated in Figure 1.8 (b). Electrostatic views of each orientation of π-π interactions are shown in Figure 1.9. In case of two electron-rich aromatic rings, the parallel stacking is disfavoured due to the repulsion between the π-electron clouds (*see* Figure 1.9 (a)). Off-set parallel and T-shape stacking is more favoured because of the attractive interaction between partially positive σ-framework and π-electron cloud (*see* Figure 1.9 (b) and (c)). In contrast, the parallel π-stacking interaction between an electron-rich and another electron-deficient ring is favoured (*see* Figure 1.9 (d)).

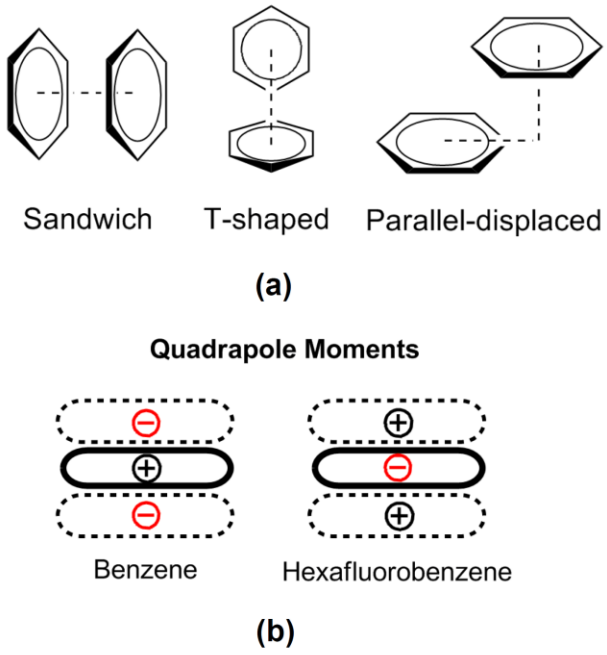

Figure 1.8 (a) Possible aromatic stacking arrangements: parallel face-centred or sandwich (left), perpendicular T-shaped (centre), and parallel displaced (right). (b) Quadrupole moments of benzene and hexafluorobenzene. The polarity is inverted due to differences in electronegativity for hydrogen and fluorine relative to carbon.

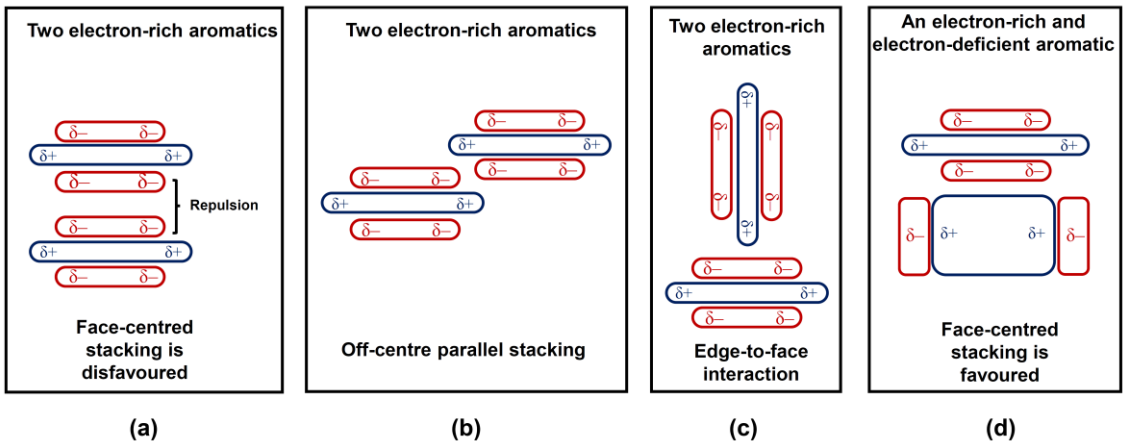

Figure 1.9 Schemes for describing the electrostatic view of aromatic interactions (a) face-centred stacking, (b) off-set parallel stacking, (c) Edge-to-face or T-shape interaction, and (d) face-centred stacking of electron rich and electron deficient aromatic rings.

1.5 Project overview

The aims of this project are focused on the synthesis and characterisation of novel polyoxocations of aluminium and new open frameworks from the assemblies of the polyoxocations for use as sorbent of molecules and ions, and catalyst. Single crystal and powder X-ray diffraction techniques are the main tools employed to characterise the obtained structures. Analyses and calculations of charges and also intermolecular interactions *i.e.* hydrogen bond and π-stacking interactions offer understandings of structure-properties of the materials. The results presented in this thesis demonstrate the discoveries of new kind of Al_{30}-based polyoxocation and a novel gigantic polyoxocation mega*Keggin*-Al_{162} which forms three polymorphically ionic structures with finite synthetic procedures.

Bibliography

(1) Ammam, M. *J. Mater. Chem. A* **2013**, *1* (21), 6291–6312.

(2) Song, Y.-F.; Tsunashima, R. *Chem. Soc. Rev.* **2012**, *41* (22), 7384–7402.

(3) López, X.; Carbó, J. J.; Bo, C.; Poblet. *Chem. Soc. Rev.* **2012**, *41* (22), 7537–7571.

(4) Katsoulis, D. E. *Chem. Rev.* **1998**, *98* (1), 359–388.

(5) Mizuno, N.; Yamaguchi, K. *Chem. Rec.* **2006**, *6* (1), 12–22.

(6) Pope, M. T.; Müller, A. *Angew. Chemie Int. Ed. English* **1991**, *30* (1), 34–48.

(7) Nyman, M. *Dalt. Trans.* **2011**, *40* (32), 8049–8058.

(8) Ma, P.; Wang, G.; Chen, G.; Wang, J.; Niu, J. *J. Mol. Struct.* **2011**, *997* (1), 126–130.

(9) Bontchev, R. P.; Nyman, M. *Angew. Chemie Int. Ed.* **2006**, *45* (40), 6670–6672.

(10) Long, D.-L.; Tsunashima, R.; Cronin, L. *Angew. Chemie Int. Ed.* **2010**, *49* (10), 1736–1758.

(11) *Keggin*, J. F. *Nature* **1933**, *131* (3321), 908–909.

(12) Baker, L. C. W.; Figgis, J. S. *J. Am. Chem. Soc.* **1970**, *92* (12), 3794–3797.

(13) Casey, W. H. *Chem. Rev.* **2006**, *106* (1), 1–16.

(14) Lee, A. P.; Furrer, G.; Casey, W. H. *J. Colloid Interface Sci.* **2002**, *250* (1), 269–270.

(15) Loring, J.; Yu, P.; Phillips, B. L.; Casey, W. H. *Geochim. Cosmochim. Acta* **2004**, *68* (13), 2791–2798.

(16) Lee, A. P.; Phillips, B. L.; Casey, W. H. *Geochim. Cosmochim. Acta* **2002**, *66* (4), 577–587.

(17) Reusser, D.; Schliesser, J.; Woodfield, B. F.; Navrotsky, A. *J. Chem. Thermodyn.* **2015**, *89*, 296–305.

(18) Casey, W. H.; Phillips, B. L. *Geochim. Cosmochim. Acta* **2001**, *65* (5), 705–714.

(19) Fairley, M.; Corum, K. W.; Johns, A.; Unruh, D. K.; Basile, M.; de Groot, J.; Mason, S. E.; Forbes, T. Z. *Chem. Commun. (Camb).* **2015**, *51* (62), 12467–12469.

(20) Reusser, D.; Casey, W. H.; Navrotsky, A. *Angew. Chem. Int. Ed. Engl.* **2015**, *54* (32), 9253–9256.

(21) Rustad, J. R.; Loring, J. S.; Casey, W. H. *Geochim. Cosmochim. Acta* **2004**, *68* (14), 3011–3017.

(22) Sadeghi, O.; Zakharov, L. N.; Nyman, M. *Science* **2015**, *347* (6228), 1359–1362.

(23) Müller, A.; Beckmann, E.; Bögge, H.; Schmidtmann, M.; Dress, A. *Angew. Chemie Int. Ed.* **2002**, *41* (7), 1162–1167.

(24) Sun, Z.; Wang, H.; Tong, H.; Sun, S. *Inorg. Chem.* **2011**, *50* (2), 559–564.

(25) Barnum, D. W. *Inorg. Chem.* **1983**, *22* (16), 2297–2305.

(26) Charles Frederick Baes, R. E. M. *The Hydrolysis of Cations*; A Wiley-Interscience Publication, 1924.

(27) Shannon, R. D. *Acta Crystallogr. Sect. A* **1976**, *32* (5), 751–767.

(28) Bottero, J. .; Axelos, M.; Tchoubar, D.; Cases, J. .; Fripiat, J. .; Fiessinger, F. *J. Colloid Interface Sci.* **1987**, *117* (1), 47–57.

(29) Li, H.; Addai-Mensah, J.; Thomas, J. C.; Gerson, A. R. *J. Cryst. Growth* **2005**, *279* (3-4), 508–520.

(30) Bi, S. *Coord. Chem. Rev.* **2004**, *248* (5-6), 441–455.

(31) Gatlin, J. T.; Mensinger, Z. L.; Zakharov, L. N.; Macinnes, D.; Johnson, D. W. *Inorg. Chem.* **2008**, *47* (4), 1267–1269.

(32) Ma, Z. L.; Wentz, K. M.; Hammann, B. A.; Chang, I.-Y.; Kamunde-Devonish, M. K.; Cheong, P. H.-Y.; Johnson, D. W.; Terskikh, V. V.; Hayes, S. E. *Chem. Mater.* **2014**, *26* (17), 4978–4983.

(33) Hartshorn, R. M.; Hellwich, K.-H.; Yerin, A.; Damhus, T.; Hutton, A. T. *Pure Appl. Chem.* **2015**, *87* (9-10), 1039–1049.

(34) Casey, W. H.; Phillips, B. L.; Furrer, G. *Rev. Mineral. Geochemistry* **2001**, *44* (1), 167–190.

(35) Johansson, G. *Acta Chem. Scand.* **1960**, *14* (3), 771–773.

(36) Casey, W. H.; Phillips, B. L.; Furrer, G. *Rev. Mineral. Geochemistry* **2001**, *44* (1), 167–190.

(37) Feng, T. L.; Gurian, P. L.; Healy, M. D.; Barron, A. R. *Inorg. Chem.* **1990**, *29* (3), 408–411.

(38) Sun, Z.; Wang, H.; Feng, H.; Zhang, Y.; Du, S. *Inorg. Chem.* **2011**, *50* (19), 9238–9242.

(39) Casey, W. H.; Olmstead, M. M.; Phillips, B. L. *Inorg. Chem.* **2005**, *44* (14), 4888–4890.

(40) Seichter, W.; Mögel, H.-J.; Brand, P.; Salah, D. *Eur. J. Inorg. Chem.* **1998**, *1998* (6), 795–797.

(41) Gerasko, O. A.; Mainicheva, E. A.; Naumov, D. Y.; Kuratieva, N. V; Sokolov, M. N.; Fedin, V. P. *Inorg. Chem.* **2005**, *44* (12), 4133–4135.

(42) Rather, E.; Gatlin, J. T.; Nixon, P. G.; Tsukamoto, T.; Kravtsov, V.; Johnson, D. W. *J. Am. Chem. Soc.* **2005**, *127* (10), 3242–3243.

(43) Bi, Z.; Feng, C.; Wang, D.; Ge, X.; Tang, H. *Colloids Surfaces A Physicochem. Eng. Asp.* **2013**, *416*, 73–79.

(44) Bi, Z.; Feng, C.; Wang, D.; Ge, X.; Tang, H. *Colloids Surfaces A Physicochem. Eng. Asp.* **2012**, *407*, 91–98.

(45) J. Stuart Anderson. *Nature* **1937**, *140*, 850.

(46) Kamunde-Devonish, M. K.; Fast, D. B.; Mensinger, Z. L.; Gatlin, J. T.; Zakharov, L. N.; Dolgos, M. R.; Johnson, D. W. *Inorg. Chem.* **2015**, *54* (8), 3913–3920.

(47) Reinsch, H.; Marszałek, B.; Wack, J.; Senker, J.; Gil, B.; Stock, N. *Chem. Commun. (Camb).* **2012**, *48* (76), 9486–9488.

(48) Casey, W. H.; Rustad, J. R. *Annu. Rev. Earth Planet. Sci.* **2007**, *35* (1), 21–46.

(49) Yang, W.; Qian, Z.; Lu, B.; Zhang, J.; Bi, S. *Geochim. Cosmochim. Acta* **2010**, *74* (4), 1220–1229.

(50) Smart, S. E.; Vaughn, J.; Pappas, I.; Pan, L. *Chem. Commun. (Camb).* **2013**, *49* (97), 11352–11354.

(51) Kloprogge, J. T.; Frost, R. L. *Spectrochim. Acta Part A Mol. Biomol. Spectrosc.* **1999**, *55* (7-8), 1505–1513.

(52) Allouche, L.; Gérardin, C.; Loiseau, T.; Férey, G.; Taulelle, F. *Angew. Chem. Int. Ed. Engl.* **2000**, *39* (3), 511–514.

(53) Abeysinghe, S.; Unruh, D. K.; Forbes, T. Z. *Cryst. Growth Des.* **2012**, *12* (4), 2044–2051.

(54) Icente, M.A., Lambert, J.-F. *Phys. Chem. Chem. Phys.* **1999**, *1* (7), 1633–1639.

(55) Schmitt, W.; Baissa, E.; Mandel, A.; Anson, C. E.; Powell, A. K. *Angew. Chem. Int. Ed. Engl.* **2001**, *40* (19), 3577–3581.

(56) Rowsell, J.; Nazar, L. F. *J. Am. Chem. Soc.* **2000**, *122* (15), 3777–3778.

(57) Mainicheva, E. A.; Gerasko, O. A.; Sheludyakova, L. A.; Naumov, D. Y.; Naumova, M. I.; Fedin, V. P. *Russ. Chem. Bull.* **2006**, *55* (2), 267–275.

(58) Drljaca, A.; Hardie, M. J.; Raston, C. L. *J. Chem. Soc. Dalt. Trans.* **1999**, No. 20, 3639–3642.

(59) Son, J.-H.; Kwon, Y.-U. *Inorg. Chem.* **2004**, *43* (6), 1929–1932.

(60) Son, J. H.; Kwon, Y.-U.; Han, O. H. *Inorg. Chem.* **2003**, *42* (13), 4153–4159.

(61) Abeysinghe, S.; Unruh, D. K.; Forbes, T. Z. *Inorg. Chem.* **2013**, *52* (10), 5991–5999.

(62) Corum, K. W.; Fairley, M.; Unruh, D. K.; Payne, M. K.; Forbes, T. Z.; Mason, S. E. *Inorg. Chem.* **2015**, *54* (17), 8367–8374.

(63) Abeysinghe, S.; Corum, K. W.; Neff, D. L.; Mason, S. E.; Forbes, T. Z. *Langmuir* **2013**, *29* (46), 14124–14134.

(64) Briand, L. E.; Baronetti, G. T.; Thomas, H. J. *Appl. Catal. A Gen.* **2003**, *256* (1), 37–50.

(65) Dawson, B. *Acta Crystallogr.* **1953**, *6* (2), 113–126.

(66) Donnay, G. and A. *Am. Mineral.* **1970**, *55*, 1003–1015.

(67) Brown, I. D.; Altermatt, D. *Acta Crystallogr. Sect. B Struct. Sci.* **1985**, *41* (4), 244–247.

(68) Brown, I. D. *J. Appl. Crystallogr.* **1996**, *29* (4), 479–480.

(69) Brown, I. D. *Chem. Rev.* **2009**, *109* (12), 6858–6919.

(70) Karen, P.; McArdle, P.; Takats, J. *Pure Appl. Chem.* **2014**, *86* (6), 1017–1081.

(71) Karen, P.; McArdle, P.; Takats, J. IUPAC - International Union of Pure and Applied Chemistry: Comprehensive Definition of Oxidation State.

(72) Desiraju, G. R.; Ho, P. S.; Kloo, L.; Legon, A. C.; Marquardt, R.; Metrangolo, P.; Politzer, P.; Resnati, G.; Rissanen, K. *Pure Appl. Chem.* **2013**, *85* (8), 1711–1713.

(73) Pauling, L. *The Nature of the Chemical Bond and the Structure of Molecules and Crystals: An Introduction to Modern Structural Chemistry*, 3rd ed.; Cornell University Press: New York, 1960.

(74) Moore, T. S.; Winmill, T. F. *J. Chem. Soc. Trans.* **1912**, *101*, 1635.

(75) Arunan, E.; Desiraju, G. R.; Klein, R. A.; Sadlej, J.; Scheiner, S.; Alkorta, I.; Clary, D. C.; Crabtree, R. H.; Dannenberg, J. J.; Hobza, P.; Kjaergaard, H. G.; Legon, A. C.; Mennucci, B.; Nesbitt, D. J. *Pure Appl. Chem.* **2011**, *83* (8), 1637–1641.

(76) Arunan, E.; Desiraju, G. R.; Klein, R. A.; Sadlej, J.; Scheiner, S.; Alkorta, I.; Clary, D. C.; Crabtree, R. H.; Dannenberg, J. J.; Hobza, P.; Kjaergaard, H. G.; Legon, A. C.; Mennucci, B.; Nesbitt, D. J. *Pure Appl. Chem.* **2011**, *83* (8), 1619–1636.

(77) Legon, A. C. *Chem. Soc. Rev.* **1990**, *19* (3), 19197–19237.

(78) George A. Jeffrey. *An Introduction to Hydrogen Bonding*; Oxford, 1997.

(79) Martinez, C. R.; Iverson, B. L. *Chem. Sci.* **2012**, *3* (7), 2191–2201.

(80) Hunter, C. A.; Sanders, J. K. M. *J. Am. Chem. Soc.* **1990**, *112* (14), 5525–5534.

Chapter 2

Synthetic and Experimental Techniques

2.1 Introduction

Although the details of specific experimental techniques for syntheses, crystal growths, and characterisations will be illustrated and discussed in each of following chapters, it is appropriate to describe in term of theory and general details before. The aim is to provide an overview of methodology, key theory and relevant literatures about the syntheses, crystal growths and characterisations applied in this thesis. As we will discuss later the complexity of the synthetic procedures adopted arise from the dryness-sensitive nature of the materials. Emphasis shall be placed on the information available from, and the limitations of, the analytical techniques described and their application to polyoxocations.

2.2 Hydrothermal synthesis

Hydrothermal synthesis is one of the most important synthetic techniques in inorganic materials chemistry. The hydrothermal reaction is usually defined as heterogeneous reactions in aqueous media above 100°C and 1 bar.[1] An obvious example of this process is found in nature, specially, the formation of minerals under the earth crust. Geologists and mineralogists have developed the hydrothermal method to their studies of mineral formation, crystal growth and hydrometallurgy for decades. Materials chemists also apply this technique for the syntheses of various materials *e.g.* zeolitic materials. The hydrothermal condition has advantages in the synthesis of (i) compounds which contain various oxidation states, especially, transition metals (ii) low temperature phases and (iii) metastable compounds.[2–4] These advantages may be due to properties of water under hydrothermal conditions.

2.2.1 Properties of water under hydrothermal condition

To understand the properties of water in autoclave under hydrothermal condition, it is necessary to study its behaviour under various conditions of pressure, volume, and temperature. Pressure in the autoclave is originally from vapour pressure

of water which depends on temperature and degree of filling as illustrated in Figure 2.1. The line A–C is the vapour pressure curve along with liquid and vapour coexist. C is the critical point of water (220 bar, 374°C). At the critical point, the density of liquid and vapour water are identical, 0.322 g cm^{-3}. An autoclave at room temperature is filled to 80% of its capacity and then heated, the pressure inside will rise as represented by the line B–D in Figure 2.1. At B point, the density will be 0.80 g cm^{-3} under these conditions.

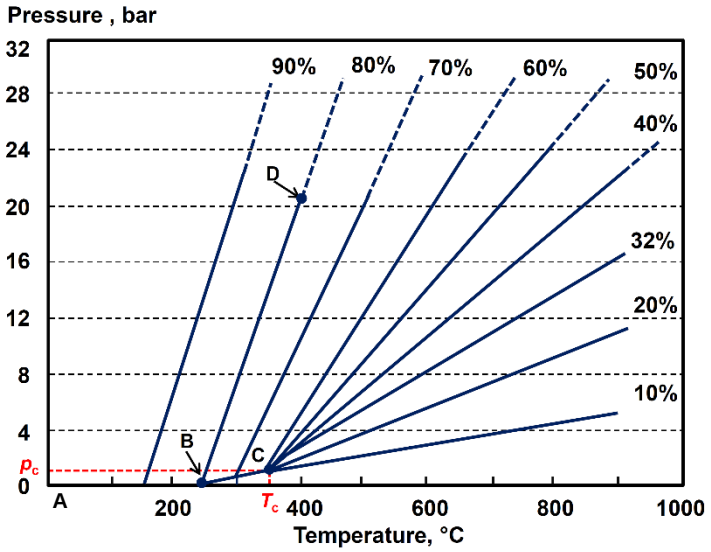

Figure 2.1 Pressure–temperature dependence of water for different degree of filling of the hydrothermal reaction vessel. B, C and D are triple point, critical point and boiling point, respectively, and T_c and p_c stand for critical temperature and critical pressure, respectively.[5]

The density (or volume) of water depends on temperature. The density of liquid water decreases and the density of water vapour increases as the temperature rises (Figure 2.2).[6] The *pvT* data up to 1000°C and 10 kbar are known accurately within 1% error.[1] In this range, the ion product of water (K_w) increases sharply with pressure and temperature as shown in Table 2.1. At 1000°C and 10 kbar, pK_w (–log K_w) is 7.85 ± 0.3. At 150 - 200 kbar and 1000°C, water has density of 1.7 - 1.9 g cm^{-3} and is completely dissociated into H_3O^+ and OH^-. Water at this condition has behaviour like a molten salt and is isoelectric with NH_4F and NaOH.[1] The critical filling volume for any hydrothermal autoclave is 32%. Any autoclave with the degree of filling more than 32%, the liquid level in the autoclave rises until the autoclave is entirely filled with liquid water at 250°C as shown in the top row of diagrams in Figure 2.3. In any

autoclave filled 32% with water the liquid water remains unchanged as the temperature risen. When the autoclave is filled less than 32% with water, the level of liquid water will drop as the temperature has risen because the liquid water is lost due to boiling. If the autoclave is filled initially more than 32% with water, the level of liquid water will increase due to is expansion as shown in Figure 2.3.

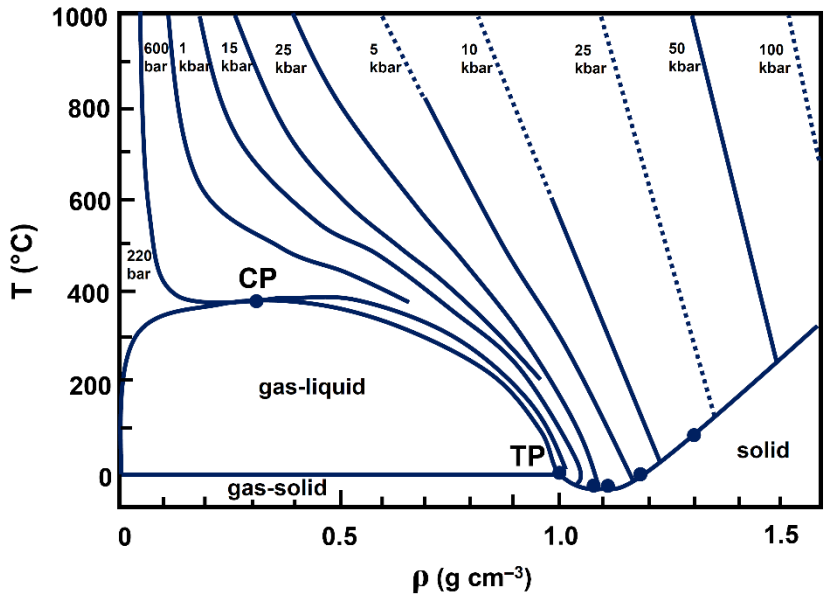

Figure 2.2 Density–temperature dependence of water; The critical temperature (T_c) and critical density (ρ_c) of water are 373.946°C (647.096 K) and 0.322 g cm^{-3}(322 kg m^{-3}), respectively.[7,8]

Table 2.1 Negative logarithm (base 10) of ionisation constant of water, pK_w, at different temperature and pressure.

Temperature (°C)	**Pressure (MPa)**[†]	**pK_w**
0	0.10	14.95
25	0.10	13.99
50	0.10	13.26
75	0.10	12.70
100	0.10	12.25
150	0.47	11.64
200	1.5	11.31
250	4.0	11.20
300	8.7	11.34
350	17	11.92

[†] 0.1 MPa for T < 100°C. Saturation pressure for T ≥ 100°C.

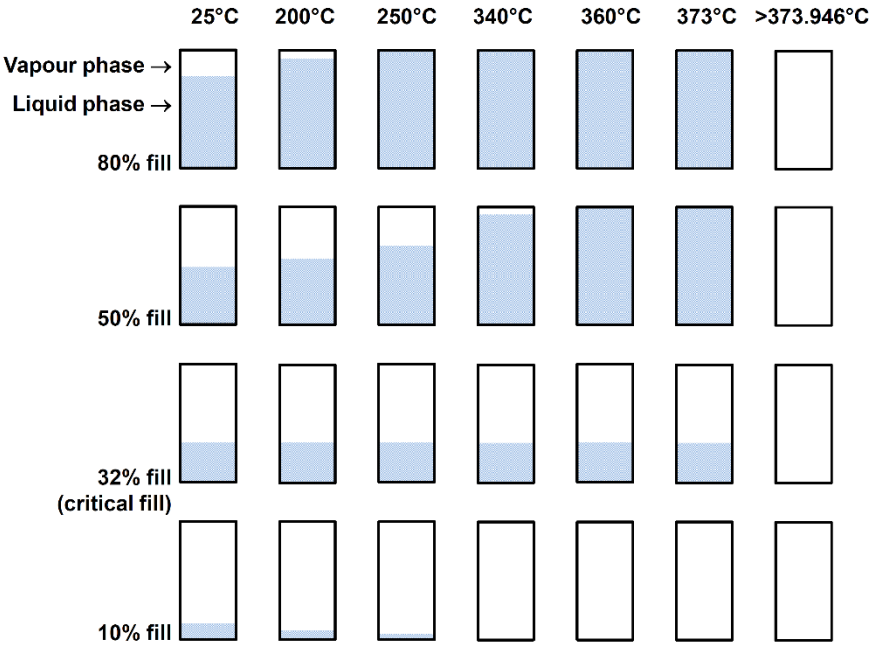

Figure 2.3 Filling diagram of vapour–liquid water as a function of filling degree and temperature; 32% is critical filling.(Adapted with permission from Ref. 6)

Viscosity of water decreases with temperature. At 120°C and 100 bar, the viscosity of water is about 26% of the viscosity at normal condition.[9] This enhances the mobility of ions and molecules in the solution comparing to the reaction media under normal conditions.

2.2.2 Autoclave

The reaction vessel or autoclave for hydrothermal synthesis has been designed specifically for its applications with high temperature, high pressure and chemically corrosive conditions. Materials selection for the reaction vessel is important. The corrosive properties and side reaction(s) under the desired condition must be considered carefully. The autoclave generally comprises of a Teflon liner and a set of steel case as shown by the diagram in Figure 2.4. Teflon or polytetrafluoroethylene (PTFE) is inert for various chemicals and solvents under hydrothermal condition. As it melts at 375°C, the Teflon liner is only suitable for the reaction below 300°C.

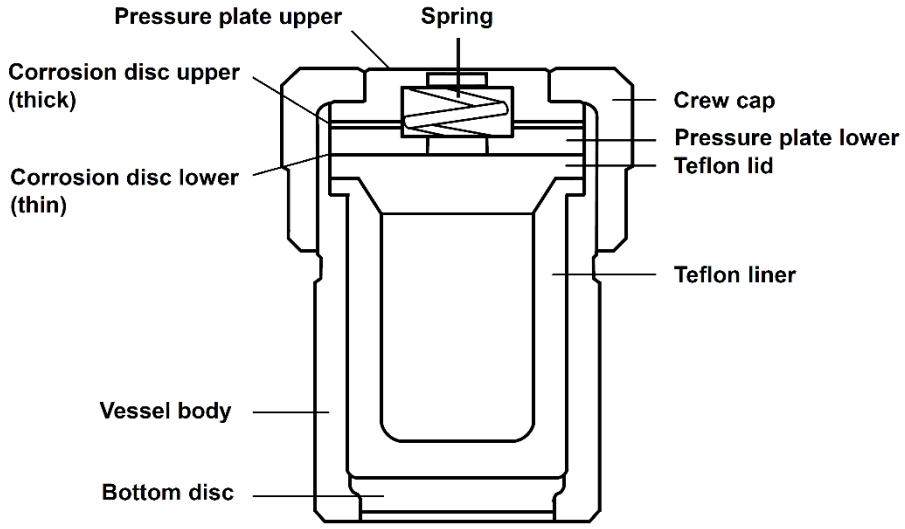

Figure 2.4 Diagram showing the composition of autoclave for hydrothermal synthesis.

Borosilicate and quartz glass are quite stable under acidic and neutral condition with exception of hydrogen fluoride. In NaOH-containing solutions, the formation of a protective surface layer of insoluble acmite, $NaFeSi_2O_6$, can occur.[1] Glass and quartz glass can be applied with a limited pressure and temperature range. The maximum pressure and temperature depends on the diameter of the vessel, strength of the glass wall, and mechanical properties of the glass. The useful range for borosilicate glasses at higher temperature is 250 – 300°C.

2.2.3 Alternative solvents

Other solvents *i.e.* NH_3, EtOH, *i*-PrOH, ionic liquids *etc.* can be applied as reaction media in the synthesis. The reaction using non-aqueous solvent(s) in an autoclave above the boiling point of the solvent(s) is known as solvothermal synthesis.

In this thesis, most of the syntheses have been done under hydrothermal condition at 120°C in 40-mL glass vials. The glass vials are suitable up to 140°C. In chapter 3, an acetonitrile-water mixture was applied as a reaction media. Glass vials were heated by Carbolite electric oven coupled with Eurotherm temperature controller.

2.3 X-ray crystallography

2.3.1 Basic crystal symmetry

Since the discovery of quasicrystals or aperiodic crystals has been reported by *Dan Shechtman* in 1984, the definition of crystal or crystalline solid has changed.[10,11] Referring to the International Union of Crystallography (IUCr) terminology, a crystal is defined as "*a material which has essentially a sharp diffraction pattern*".[12] For periodic crystals, it is always possible to select a small parallelepipedon. Translations of this parallelepipedon in all three dimensions will generate the entire crystal structure. This parallelepipedon is called the "*unit cell*" and is defined by six "*unit cell parameters*" *i.e.* three noncoplanar vectors (*a*, *b*, *c*) and (ii) three angles between the vectors (α, β, γ). The directions of the vectors are also chosen as the axes *x*, *y*, and *z* of the crystal coordinate system (*see* Figure 2.5 a). The dimensions of the unit cell are described by three edge lengths (*a*, *b*, *c*) and three angles between them (α, β, γ). Any point in a unit cell is described by fractional coordinates. The direction of such a plane is described by a set of three integers *h*, *k*, and *l*, written in parentheses as (*hkl*) called "*Miller indices*". It means that the plane intersects the axes *x*, *y*, and *z* at the distances from the origin, equal to rational fractions of the corresponding unit cell parameters *a*/*h*, *b*/*k*, and *c*/*l*, respectively (*see* Figure 2.5 b).

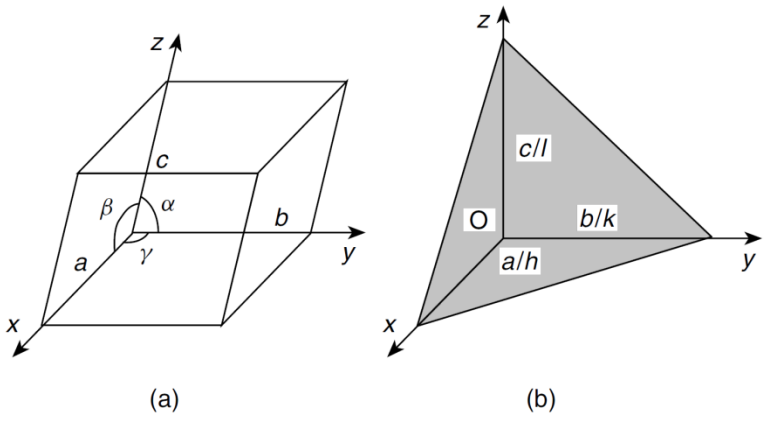

Figure 2.5 (a) Primitive unit cell showing its six defining parameters. (b) lattice, or Miller plane (*hkl*), O is the origin of the unit cell. (Reprinted with permission from Ref. 13)

There are seven different types of lattice symmetry or "*crystal systems*". Each type of crystal system corresponds to a distinct shape of the unit cell (*see* Table 2.2). If we consider all centring conditions with each crystal system, there are 14 different types

of lattices called "*Bravais lattices*" as shown in Figure 2.6. There are 230 possible combinations of symmetry elements with lattice translations, called "*crystallographic space groups*". The space groups describe the symmetries of all crystal structures that can exist, and some of those have not been observed so far. A space group symbol includes a capital letter describing the lattice type, followed by the essential symmetry elements present.

Table 2.2 Relations between Unit Cell Parameters and Lattice Symmetry.

Crystal system	**Bravais lattices**	**Unit cell constraints**	**Laue symmetry**
1. Triclinic	*P*	$a \neq b \neq c$, $\alpha \neq \beta \neq \gamma$	$\bar{1}$
2. Monoclinic	*P*, *C*	$a \neq b \neq c$, $\alpha = \gamma = 90°$, $\beta > 90°$	2/*m*
3. Orthorhombic	*P*, *C*, *I*, *F*	$a \neq b \neq c$, $\alpha = \beta = \gamma = 90°$	*mmm*
4. Tetragonal	*P*, *I*	$a = b \neq c$, $\alpha = \beta = \gamma = 90°$	4/*m* or 4/*mmm*
5. Trigonal	*P*, *R*†	$a = b \neq c$, $\alpha = \beta = 90°$, $\gamma = 120°$	$\bar{3}$ or $\bar{3}m$
Rhombohedral†	*R*	$a = b = c$, $\alpha = \beta = \gamma < 120°$	Ditto
6. Hexagonal	*P*	$a = b \neq c$, $\alpha = \beta = 90°$, $\gamma = 120°$	6/*m* or 6/*mmm*
7. Cubic	*P*, *I*, *F*	$a = b = c$, $\alpha = \beta = \gamma = 90°$	$m\bar{3}$ or $m\bar{3}m$

†Alternative setting for centred trigonal lattices

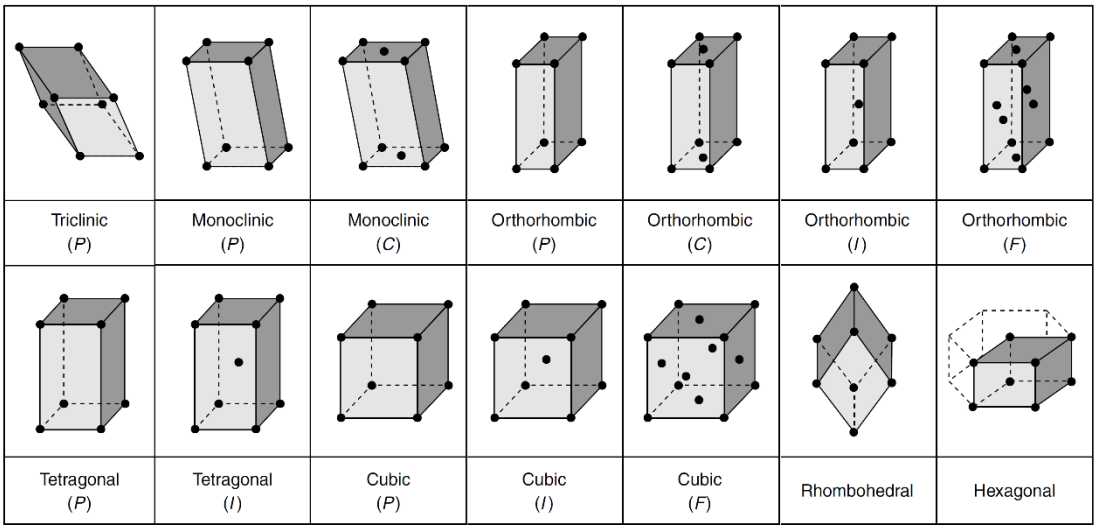

Figure 2.6 The 14 Bravais lattices. (Reprinted with permission from Ref. 13)

2.3.2 X-ray diffraction

2.3.2.1 Bragg's law

Although a relationship between the physical appearance of crystals and their atomic arrangements has been proposed over centuries, the determination of crystal structures in atomic resolution was intensively studied after the discovery of X-ray by *Wilhelm Conrad Röntgen* in the last decade of nineteen century.[14] During intense debates about particle-wave behaviour of light, *Max Theodor Felix von Laue* discovered that X-ray can be diffracted by single crystals and he suggested physicists to apply this single crystal which had the same order of magnitude of interatomic spacing as diffraction grating for X-ray.[14] *William Lawrence Bragg* then discovered that crystalline solid produce patterns of reflected X-ray and published the observation in 1913.[15] *Bragg* proposed that the X-ray reflected from stacks of the parallel planes of atoms in 3D structure of the crystal, the angle of incidence being equal to the angle of reflection, θ. A diffraction beam occurs only at certain θ values, when the waves reflected from all parallel planes are all in phase, that is, path differences between waves reflected from adjacent planes equal an integer number of wavelengths λ (see Figure 2.7), as defined by Bragg's law:

$$n\lambda = 2d_{hkl} \sin \theta \tag{2.2}$$

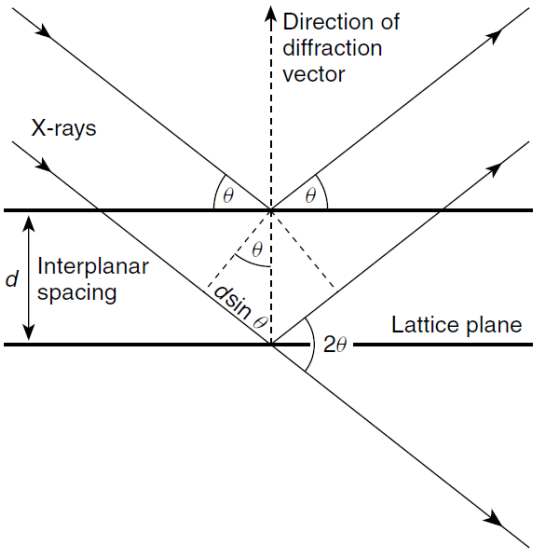

Figure 2.7 Bragg's law illustrated. (Reprinted with permission from Ref. 13)

Thus each diffracted beam is regarded as a reflection from a plane with Miller indices (*hkl*) and is named by the same indices. Since d_{hkl} depends on the unit cell parameters, as $d_{hkl} = X/Y$, where

$$X = [1 - \cos^2\alpha - \cos^2\beta - \cos^2\gamma + 2\cos\alpha\cos\beta\cos\gamma]^{1/2} \quad (2.3)$$

$$Y = [(h/a)^2 \sin^2\alpha + (k/b)^2 \sin^2\beta + (l/c) \sin^2\gamma - 2(kl/bc)(\cos\alpha - \cos\beta\cos\gamma) - 2(lh/ca)(\cos\beta - \cos\alpha\cos\gamma) - 2(hk/ab)(\cos\gamma - \cos\beta\cos\alpha)]^{1/2} \quad (2.4)$$

it is possible to determine the unit cell if λ and the directions of several diffracted beams are known.

2.3.2.2 Intensities of diffracted beams

The intensity of the diffracted beam depends on the types and positions of atoms in the cell. The intensity, I_{hkl}, depends on many factors. For X-ray diffraction,

$$I_{hkl} = \frac{e^4\Omega}{m^2c^4V} I_0 \lambda LPTE|F_{hkl}|^2 \quad (2.5)$$

where I_0 is the intensity of the incident beam, Ω is the volume of the crystal, V the volume of the unit cell, e and m are the charge and mass of the scattering particle, in this case. L is the Lorentz factor, accounting for the time needed for the reflection to pass through the Ewald sphere. P is the polarisation factor. Both L and P are dependent on θ and the precise geometry of the particular X-ray instrument. The transmission factor T depends on the absorption of X-rays in the crystal. The factor E accounts for two different effects (i) the diffracted beam being diffracted again in the crystal and (ii) the decrease of the incident beam intensity I_0 during its progress through the crystal, because some energy is taken away by the diffracted beam.

I_{hkl} depends on the distribution of electron density in the unit cell. It can be represented by the structure factor F_{hkl} of a reflection,

$$F_{hkl} = \int_V \rho(x,y,z)\exp[2\pi i(hk+ky+lz)]\mathrm{d}V \quad (2.6)$$

where ρ is the electron density at a point with the fractional coordinates x, y, z. Equation 2.6 can be simplified if we present ρ not as a continuous function but as a superposition of atoms,

$$F_{hkl} = \sum_j f_j \exp\left[2\pi i(hk_j + ky_j + lz_j)\right] \quad (2.7)$$

where f_j is the atomic scattering factor (form factor) for the j-th atom and x_j, y_j, z_j are the fractional coordinates of this atom. The f_j is not a constant. It is a function of sin θ/λ (*see* Figure 2.8). The maximum value equal to the total number of electrons in the atom and it decreases to approach zero at high sin θ/λ. This dependence is because of the fact that the size of electron is comparable to the wavelength.

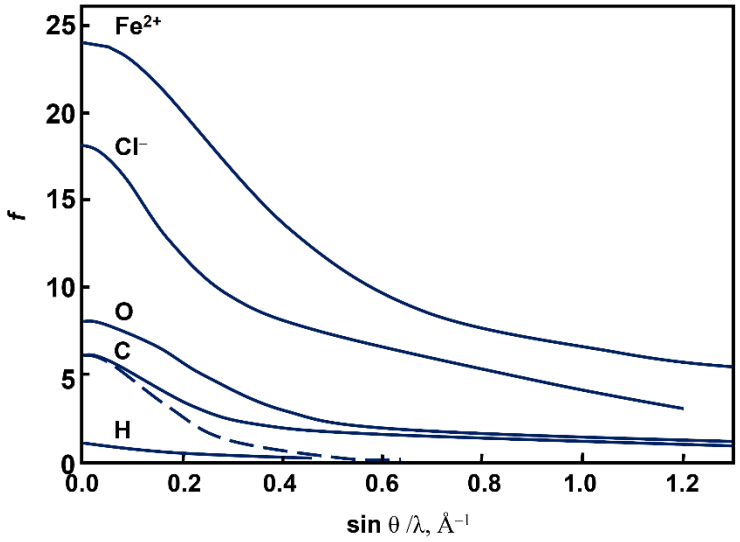

Figure 2.8 Variation of X-ray form factors, *f*, with sin *θ*/*λ*. Solid lines: stationary atoms, dashed line: C atom with U = 0.1 Å^2 (Adapted with permission from Ref. 13)

2.3.2.3 Generation of X-rays

X-ray can be generated by (i) synchrotron, or (ii) ionising atoms by fast-moving electrons. Synchrotron generates a continuous spectrum because the energy of a free electron is not quantised, whereas, the ionised atom gives narrow characteristic lines. The latter occur when the energy of the colliding electrons higher than a threshold potential of the target metal atom and knocks an electron of the atom. The vacancy is then filled rapidly by an electron from a higher shell. The electron releases its potential energy in form of X-ray. Photon wavelength of the X-ray is constant depending on type of the target metal. The wavelength which generally applied in crystallography are Cu-K_α and Mo-K_α, with λ of 1.54178 and 0.71073 Å, respectively. These wavelengths are comparable to the distances between atoms in crystals.

The most powerful sources of X-ray radiation are synchrotrons. A synchrotron is a type of circular particle accelerator. It works by accelerating charged particles *i.e.* electrons or positrons through sequences of magnets until they reach almost the speed of light. These fast-moving electrons produce very bright radiation, called synchrotron light. Synchrotrons can be classified into two types *i.e.* (i) high energy physics machines and (ii) sources of synchrotron light. They were first developed to study high energy particle collisions. These particle colliders are still used today *e.g.* the Large Hadron Collider (LHC) at CERN. Synchrotrons for light sources have been established around the world. They can produce synchrotron light that supports a range of experiments with numbers of applications. Diamond Light Source (DLS) is the largest synchrotron in the United Kingdom. It could support around 40 beamlines at maximum (*see* Figure 2.9). Beamline for small molecule X-ray diffraction is I19. Details of the beamline is listed in Table 2.3.

Table 2.3 Details of I19 beamline.[16]

Beamline name	**I19 small-molecule single-crystal diffraction beamline at Diamond**
Source type	In-vacuum U21 undulator
Mirrors	A pair of bimorph mirrors (one vertically focusing, one horizontally focusing)
Monochromator	Double-crystal monochromator with Si 111 cryo-cooled crystals
Energy range (keV)	5 to 28
Wavelength range (Å)	0.44 to 2.48
Flux (photons s^{-1})	2.571×10^{12} for approximate Gaussian ~170 µm (h) by 85 µm (v) FWHM defocused beam at 150 mA at $\lambda = 1$ Å measured at the first sample position using a calibrated diode
Divergence	82 µrad (h) × 31 µrad (v) for unfocused beam at the first sample position at $\lambda =$ 0.6889 Å

(a)

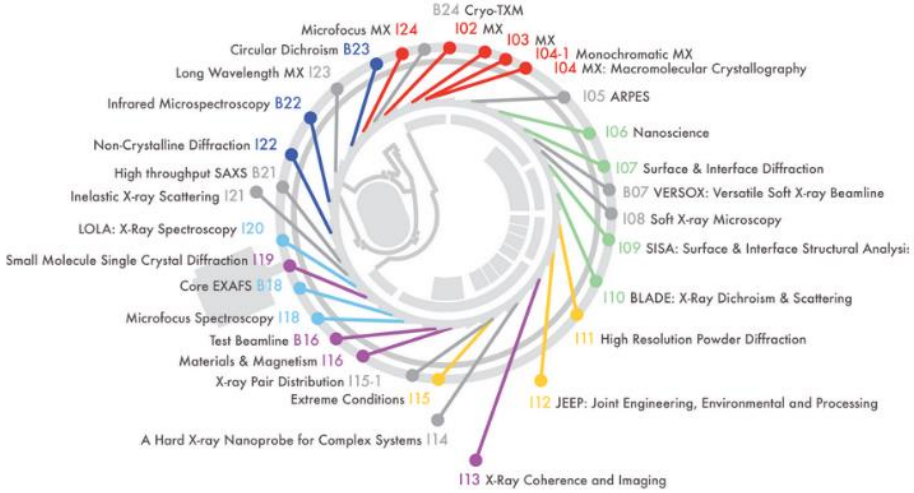

(b)

Figure 2.9 (a) Diamond Light Source Synchrotron, Harwell, Oxfordshire (b) diagram showing beamlines in the synchrotron. (Reprinted with permission from Ref. 16)

2.3.2.4 X-Ray detectors

The crystal and detector can be controlled by a four-circle diffractometer (*see* Figure 2.10). It is a computer-controlled machine with four independently rotating axes. A goniometric head with the crystal attached is mounted on the shaft of the φ circle, and moves along the χ circle. This block is rotated on the vertical axis ω, while θ (or 2θ) axis moves the arm of the detector. All axes and the beam from the X-ray source intersect in the same point. The crystal remains centred in this point during any rotation.

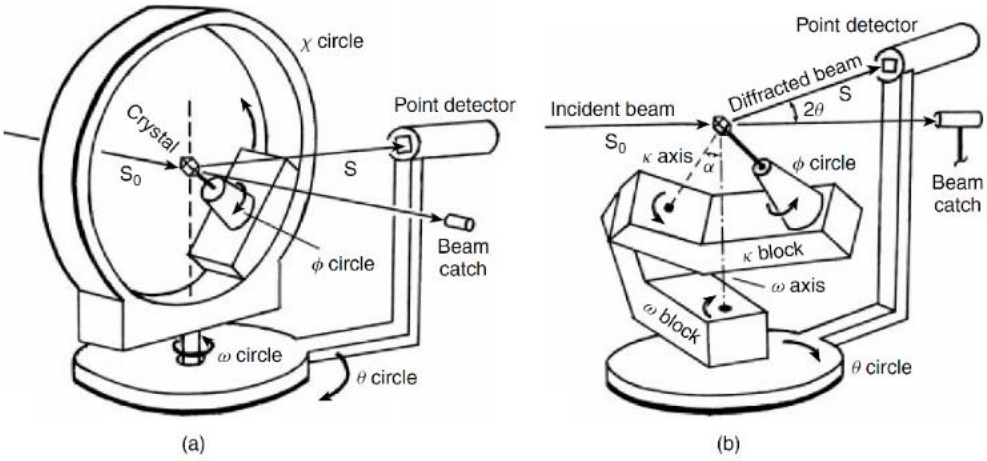

Figure 2.10 Scheme of a four-circle diffractometer: (a) conventional geometry, (b) κ (kappa) geometry. (Reprinted with permission from Ref. 13)

Alternatively, the four-circle diffractometer can have a κ (kappa) geometry, in which the χ circle is replaced by two arcs, one of which ('ω block') rotates around the vertical ω axis and the other ('κ block') around the κ shaft, mounted on the ω block (*see* Figure 2.10). The κ and ω axes always form the 'magic angle' (α = 54°).

In this thesis, the Rigaku diffractometer with CrystalClear software, Mo-K_α, and the Rigaku diffractometer, Diamond Light Source synchrotron, I19 beamline, CCD detector were applied. Specific details of diffraction experiments are described in each chapter.

2.3.2.5 Data Correction and reduction

The results of data collection are a list of reflections including its hkl index and measured intensity (I). Each intensity has an associated standard uncertainty ($\sigma(I)$) which is a measure of precision or reliability if the instrument. However, the measure intensity is affected by several factors, for which corrections are needed. The process is

colled "data correction". A correction may be needed for changes in the incident X-ray beam intensity or in the scattering power of the crystal during the experiments, which weakening the measured intensity of the diffracted X-ray beam. Absorption effects are also significant and a correction must be applied. There are many different types of absorption correction. For example, SADABS is designed for correcting the data obtained from Bruker CCD detector. It provides useful diagnostics and can correct for errors *e.g.* variation in the volume of the crystal radiated, incident beam inhomogeneity, absorption by crystal and crystal decay. The program also improves the esds of the measure intensity.[17] The data reduction process includes the merging and averaging of repeated and symmetry-equivalent measurements in order to produce a unique, corrected, and scaled set of data. This calculation affords a numerical measure of the agreement amongst equivalent reflections, which indicates the quality of the data and the appropriateness of the applied corrections.[18]

2.3.2.5 Solving crystal structure

After the measurement and correction of diffraction data, mathematical solution of the structure can be performed. This can be done by summation of the corrected amplitudes and phases of all the diffracted X-ray beams by the following equation:

$$\rho(xyz) = \frac{1}{V}\sum_{h,k,l}|F(h,k,l)|\cdot \exp[i\phi(hkl)]\,)\cdot\exp[-2\pi i(hx+ky+lz)] \qquad (2.8)$$

where $\rho(xyz)$ is electron density at the position *xyz*, *V* is unit cell volume, $|F(h,k,l)|$ is structure factor for the reflection *hkl*, $\phi\ (hkl)$ is intrinsic phase of the diffracted beams, relatives to the incident beam, and $-2\pi i(hx+ky+lz)$ is phase shift relative to the unit cell origin.[18]

The final exponential term can be calculated for the contribution of each reflection *hkl* to each position *xyz*. However, the intrinsic phases, $\phi\ (hkl)$, are unknown. This is called "*phase problem*". Patterson and Direct method are common processes to solve the problem. The Patterson method is appropriate for the structure containing one or small number of heavy atoms, while the Direct method is more suitable for the structures which contain about equal electron densities.[18,19]

2.3.2.5.1 Patterson synthesis

The Patterson method is based on an assumption that all diffracted beams are in phase ($\phi\ (hkl) = 0$). The electron density equation is shorten as expressed below:

$$\rho(xyz) = \frac{1}{V}\sum_{h,k,l}|F(h,k,l)|^2 \cdot \exp[-2\pi i(hx+ky+lz)] \qquad (2.9)$$

The Patterson map shows an arrangement of atoms relative to each other as vector representations between pairs of atoms in the structure. The Patterson peaks' size are proportional to the size of atomic number of the two connected atoms. It shows where the atoms lie relative to each other but not relative to the unit cell origin. Patterson map usually shows large regions of overlapped broad peaks, with significantly intense peaks due to the vectors involved with heavy atoms and inversion centre due to the use of $|F_o(h,k,l)|^2$ term. If the structure contains only a few heavy atoms amongst a lot of lighter atoms, the Patterson map will show a small number of intense peaks standing out clearly above the background level.[18,19]

2.3.2.5.2 Direct method

The Direct method involves selecting the most important reflections, working out the probable relationship amongst their phases, and trying different possible phases to see how well the probability relationship are satisfied. The process can be regarded simply as a sort of trial and error method. When the solving is successful, most or all of non-hydrogen atoms in the structure will be located.[18,19]

2.3.2.6 Structure refinement

The rest of the atoms in asymmetric unit of the proposed structure can be located by using a difference Fourier map ($|F_o|$-$|F_c|$), followed by full-matrix least squares refinement. The process of locating new atoms and refinements are repeated until the best fit of the proposed structure to the experimental data is satisfied. The most widely used assessment is a "*residual factor*" or "*R-factor*", which can be defined as,

$$R = \frac{\sum\left||F_o|-|F_c|\right|}{\sum|F_o|} \qquad (2.10)$$

If the weighting factors (*w*) are multiplied to the different reflections, based on their standard uncertainty, another residual factor is obtained which is more meaningful than the basic *R* factor.

$$wR2 = \sqrt{\frac{\sum w\left(F_o^2 - F_c^2\right)^2}{\sum w\left(F_o^2\right)^2}} \tag{2.11}$$

For a correct and complete crystal structure, R factor is typically between 0.02-0.07. The value of *wR*2 is generally higher.[18,19]

If *n* is a number of reflections and *p* is a total number of parameters refined, corresponding Goodness of Fit (*S*) can be defined as:

$$S = \frac{\sum w\left(F_o^2 - F_c^2\right)^2}{(n-p)^{1/2}} \tag{2.12}$$

where

$$w = \frac{1}{\left[\sigma^2 (F_o)\right]^2} \tag{2.12}$$

2.4 Thermogravimetric analysis

Thermogravimetric analysis (TGA) is used to determine the thermal stability of solid materials and also chemical composition, specifically, solvent(s) and/or guest molecules in porous materials. The TGA involves precise controlled measurement of mass of a solid sample as a function of time and temperature in a flow gas atmosphere. Changes in mass are observed during heating. In porous materials, mass loss is often observed due to removal of adsorbed solvents. The absorption of atmospheric moisture can be also observed by TGA experiments. Furthermore, when considering materials containing both organic and inorganic components, *e.g.* MOFs, metal content can be accurately determined by comparing the ratio between the remaining residue (often a metal-oxide) and the mass of the desolvated compound.

In this thesis, TGA was carried out using a SDT Q600 Thermogravimetric Analyser. In a typical experiment, 5-10 mg of ground sample was placed an alumina pan. The material was then heated to 1,300°C at a rate of 20°C min^{-1} under a 50 cm^3 min^{-1} flow of air, and then cooled back down to room temperature.

2.5 Chemical analysis

2.5.1 Elemental microanalysis

Elemental microanalysis is used to accurately measure the weight percentage of chemical elements within a compound. Generally, C, H and N are the elements measured by this technique as the majority of organic compounds contain these elements.

In this thesis, the elemental microanalyses (C, H, N, and S) were obtained using a Thermo EA1112 Flash CHNS-O Analyser.

2.5.2 Inductively coupled plasma

Inductively coupled plasma atomic emission spectroscopy (ICP-AES), also referred to as inductively coupled plasma optical emission spectrometry (ICP-OES), is an analytical technique used for the detection of trace metals. It is a type of emission spectroscopy that uses the inductively coupled plasma to produce excited atoms and ions that emit electromagnetic radiation at wavelengths characteristic of a particular element. It is a flame technique with a flame temperature in a range from 6000 to 10000 K. The intensity of this emission is indicative of the concentration of the element within the sample.

In this thesis, ICP-OES was employed to analyse chemical compositions *i.e.* Al, Na, S contents in the obtained compounds.

2.6 Spectroscopic methods

2.6.1 Ultraviolet-Visible spectroscopy

Ultraviolet Visible (UV/vis) Spectroscopy is used to measure electronic transitions within a compound. This technique can provide useful information into how a ligand is coordinated and was used to identify the wavelength of maximum absorbance of compound.

In this thesis, a UV/vis spectra was collected in a solution state quartz cuvette at room temperature on a Perkin–Elmer Lambda 650S UV/vis spectrometer equipped with Labsphere integrating over the spectral range 190-900 nm.

2.6.2 ^{27}Al Nuclear Magnetic Resonance (NMR) spectroscopy

^{27}Al is on of the most sensitive nuclei. In contrast to ^{13}C and ^{1}H, the ^{27}Al is a quadrupolar nucleus (I = 5/2; Q = 0.149 ×10^{-28} m^2) ^{27}Al chemical shifts cover a range of 300 ppm and this range can be subdivided grossly into three regions: (i) alkylaluminium compounds resonance at 100 ppm or more (ii) tetrahedrally coordinated aluminium resonance between 140 and 40 ppm; and (iii) octahedrally coordinated aluminium resonance between 40 and −46 ppm. [20]

In this thesis, solution state and solid state (MAS) ^{27}Al NMR spectroscopy were applied to study local structure of aluminium atoms in the obtained compounds. Solid state NMR measurements were performed by Kenneth Kazuya Inglis and Dr Frédéric Blanc at the University of Warwick, Warwickshire.

Bibliography

(1) Rabenau, A. *Angew. Chemie Int. Ed. English* **1985**, *24* (12), 1026–1040.

(2) Chen, H.; Hiller, D.; Hudson, J.; Westenbroek, C. *IEEE Trans. Magn.* **1984**, *20* (1), 24–26.

(3) Rau, H.; Rabenau, A. *Solid State Commun.* **1967**, *5* (5), 331–332.

(4) Rüdiger Kniep, A. R. *Phys. Inorg. Chem.* **1983**, *111*, 145–192.

(5) Demianets, L. N.; Lobachev, A. N. *Krist. und Tech.* **1979**, *14* (5), 509–525.

(6) Laudise, R. A. *Chem. Eng. News* **1987**, *65* (39), 30–43.

(7) Cooper, J. R. *Int. Assoc. Prop. Water Steam* **2007**, 1–49.

(8) Wagner, W. *J. Phys. Chem. Ref. Data* **1999**, *31* (2), 387.

(9) Kestin, J.; Sokolov, M.; Wakeham, W. A. *J. Phys. Chem. Ref. Data* **1978**, *7* (3), 941.

(10) Shechtman, D.; Blech, I.; Gratias, D.; Cahn, J. W. *Phys. Rev. Lett.* **1984**, *53* (20), 1951–1953.

(11) Monroe, D. *Physics (College. Park. Md).* **2011**, *28*.

(12) IUCr. *Acta Crystallogr. Sect. A Found. Crystallogr.* **1992**, *48* (6), 922–946.

(13) *Encyclopedia of Inorganic and Bioinorganic Chemistry*; Scott, R. A., Ed.; John Wiley & Sons, Ltd: Chichester, UK, 2011.

(14) N.V.A. Oosthoek's Uitgeversmaatschappij, U. *50 Years of X-ray Diffraction*; International Union of Crystallography: The Natherland, 1962.

(15) Bragg, W. H.; Bragg, W. L. *Proc. R. Soc. A Math. Phys. Eng. Sci.* **1913**, *88* (605), 428–438.

(16) Nowell, H.; Barnett, S. A.; Christensen, K. E.; Teat, S. J.; Allan, D. R. *J. Synchrotron Radiat.* **2012**, *19* (3), 435–441.

(17) Sheldrick, G. M. University of Göttingen, Germany 1996.

(18) Clegg, W. *Crystal Structure Determination, Oxford Chemistry Primers*; Oxford Science Publications: New York, 1998.

(19) B.D. Cullity. *Elements of X-ray Diffraction*, 3rd ed.; Addison-Wesley Publishing Company, Inc.: California, 1956.

(20) Lars-Olof Öhman, U. E. *Encycl. Magn. Reson.* **2007**, 1–9.

Chapter 3

A New Polyoxocation: Al_{30}-acetate

3.1 Introduction

As described in Chapter 1, dimerisation of *Keggin*-Al_{13} produces two distinct classes of polyoxocation *i.e.* Al_{26} and Al_{30} as illustrated in Figure 3.1. The Al_{26}, formulated $(Al_2(\mu_4\text{-}O)_8(Al_{24}(\mu_2\text{-}OH)_{50}(\eta\text{-}H_2O)_{20}]^{12+}$, contains two *δ-Keggin*-Al_{13} units linked together *via* corner sharing. It was synthesised using partially hydrolysed Al(III) chloride solution (r_{OH} = $[OH^-]/[Al^{3+}]$ = 2.55) and 2,6-naphthalene trisulphonate (2,6-NDS) anion and reported by *T.Z. Frobes et al.* in early 2012.[1] The Al_{30}, $[Al_2(\mu_4\text{-}O)_8(Al_{28}(\mu_2\text{-}OH)_{56}(\eta\text{-}H_2O)_{26}]^{18+}$, was synthesised as sulphate salts and reported by two independent research groups of *J. Rowsell et al.* and *L. Allouche et al*. in 2000.[2,3] Similar to Al_{13}, the Al_{30} plays important roles in water treatments, especially in removal of organic waste as well as toxic contamination *e.g.* organic and inorganic arsenate.[4–6] Surface modifications of the Al_{30} polyoxocation have been recently reported with its potential to adsorb metal cations *i.e.* Zn(II), Pb(II) and Cu(II) as well as Cl^-, SO_4^{2-}.[7–9]

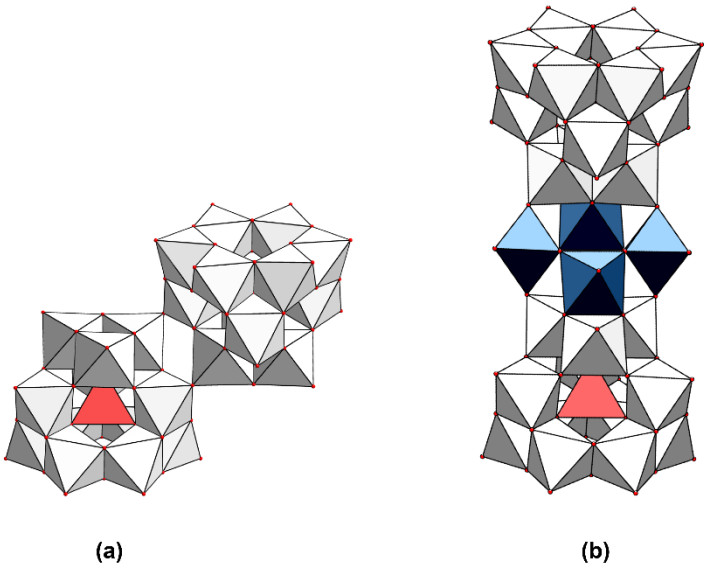

Figure 3.1 Polyhedral representations showing structure of two distinct dimers of Keggin-Al_{13} *i.e.* (a) $(Al_2(\mu_4\text{-}O)_8(Al_{24}(\mu_2\text{-}OH)_{50}(\eta\text{-}H_2O)_{20}]^{12+}(Al_{26})$ and (b) $[Al_2(\mu_4\text{-}O)_8(Al_{28}(\mu_2\text{-}OH)_{56}(\eta\text{-}H_2O)_{26}]^{18+}(Al_{30})$.

In this chapter, the discovery, synthesis and characterisation of a new polyoxocation $[Al_2(\mu_4\text{-}O)_8(Al_{28}(\mu_2\text{-}OH)_{50}(\mu_2\text{-}OH)_6(\eta\text{-}H_2O)_{22}(\eta_2\text{-}CH_3COO)_2]^{16+}$ (Al_{30}-acetate) are described.

3.2 Experimental

3.2.1 Materials and equipment

All chemicals and solvents were purchased from Sigma Aldrich and applied without further purification (*see* Appendix SI0) Glass vials (40 mL) applied as solvothermal vessels were purchased from Fisher Scientific. Carbolite electric ovens coupled with Eurotherm temperature controller were applied for the following syntheses.

3.2.2 Discovery of Al_{30}-acetate

3.2.2.1 Solvothermal synthesis

Single crystals of $[Al_2(\mu_4\text{-}O)_8Al_{26}(\mu_2\text{-}OH)_{56}(\eta\text{-}H_2O)_{22}Al_2(\eta_2\text{-}CH_3COO)_2](2,6\text{-}NDS)_7(CH_3COO)_2{\cdot}2H_2O$ (**Al_{30}-acetate**) were obtained from post-solvothermal solution prepared from partially hydrolysed Al(III) solution ($r_{OH} = [OH^-]/[Al^{3+}] = 1.00$) and 2,6–NDS in 50% MeCN. The partially hydrolysed Al(III) solution (solution **A**) was prepared by drop-wise addition of 500.00 mL 0.125 M NaOH (62.5 mmol) into 350 mL 0.178 M $AlCl_3{\cdot}6H_2O$ (62.5 mmol) at 60°C under fast stirring and the solution were transferred into an 1.00-L Duran® glass bottle, sealed with screw cap and maintained at 80°C for 16 hours. Fifteen millilitre of MeCN was transferred into a 40-mL glass vial, followed by the addition of 5.00 mL of 0.0625 M 2,6-NDS, 5.00 mL of solution **A**, 5.00 mL of deionised water. The pH of pre-solvothermal solution was measured by glass electrode pH meter. The vial was sealed with screw cap and heated at 120°C for 12 hours with heating rate of 10°C min^{-1} and then cooled down to ambient temperature with cooling rate of 0.25°C min^{-1}. The vial was opened, pH of post-solvothermal solution was measured, and the solution was then evaporated naturally in fumehood for 5 days. Colourless block crystals were obtained from the solution with 30% yield based on aluminium precursor. Due to the fact that the bulk product is lack of phase purity, chemical analysis and further characterisation were not possible.

3.2.2.2 Single crystal X-ray structure analysis and refinements

A colourless single crystal was selected to analyse by X-ray diffraction technique at Experimental Hutch (EH1), I19 Beamline, Diamond Light Source, Oxfordshire (Zr *K*-edge, 17.998 keV, λ= 0.6889 Å, CCD area detector (*Rigaku Saturn* 724+), four-circle κ goniometer (ω, κ, φ, θ), at 100 K (*Oxford Cryosystems Cryostream Plus*), *Rigaku ACTOR* robotic sample changer). The diffraction data was processed *CrystalClear* (*Rigaku*, 2010) program and crystal structure was then solved by direct method using SHELX–97 *via* Olex^2 program. Crystallographic parameters and X-ray data for Al_{30}-acetate is listed in Table 3.1. Fractional atomic coordinates and isotropic or equivalent isotropic displacement parameters are shown in Table SI1 (*see* Appendix SI1.1). Selected bond distances and bond lengths are listed in Table SI2 (*see* Appendix SI1.2).

Table 3.1 Crystallographic information of Al_{30}–acetate.

Compound	**Al_{30}–acetate**
Empirical formula	$Al_{7.50}O_{33.89}S_{3.40}C_{18.90}H_{38}$
Formula mass M_r	1119.04
Colour	colourless
Crystal size	0.10 mm × 0.15 mm × 0.05 mm
Space group	$P\bar{1}$
Z	4
Density	1.476 Mg m^{-3}
Radiation	λ = 0.6889 Å (synchrotron)
T	100 K
a	14.1675 (8) Å
b	18.5259 (10) Å
c	20.4693 (11) Å
α	84.849 (2)°
β	74.332 (2)°
γ	76.951 (2)°
Unit cell volume V	5036.9 (5) Å^3
R_{int}	0.0620
Measured reflections	41879
Independent reflections	22065
Reflections with $I > 2\sigma(I)$	14706
$R[F^2 > 2\sigma(F^2)]$	0.0940
$wR(F^2)$	0.3090
S	1.100

$w = 1/[\sigma^2(F_o^2) + (0.1959P)^2]$, where $P = (F_o^2 + 2F_c^2)/3$

3.2.2.3 Protonation state of oxygen atoms

Apart from two ligated acetate anions, there are four different coordination modes of oxygen atoms in Al_{30}-acetate polyoxocation *i.e.* (i) η-H_2O: terminal bound water molecules, (ii) μ_2-OH: bridging hydroxide linking two Al(III) cations, (iii) μ_3-OH:

bridging hydroxide linking three Al(III) cations, and (iv) μ_4-O : oxide linking to four Al(III) cations. Bond Valence Sum (BVS) method was applied to calculate valence and assign protonation state of oxygen atoms. The detailed BVS calculation results and assignment of oxygen atoms in Al_{30}-acetate are shown in Table SI3 (*see* Appendix SI1.3).

3.2.2.3 Assignment of hydrogen bonds

As described in Chapter 1, hydrogen bond has been officially defined as "An attractive interaction between a hydrogen atom from a molecule or a molecular fragment X–H in which X is more electronegative than H, and an atom or a group of atoms in the same or a different molecule, in which there is evidence of bond formation." by IUPAC and can be classified into three class *i.e.* (i) strong, (ii) moderate, and (iii) weak hydrogen bond depending on its physicochemical properties.[10,11] (*see* Table 1.1). The elements X in Al_{30}-acetate are C, S and O, because they are more electronegative than H. In order to identify hydrogen bonds in Al_{30}-acetate, *PLATON* program was applied to calculate and classify hydrogen bond from X-ray crystal structure. According to criteria proposed by *G. Jeffrey* (*see* Table 1.1), there are 44 crystallographically unique hydrogen bonds in Al_{30}-acetate structure which can be classified into two type *i.e.* (i) moderate and (ii) strong hydrogen bonds as listed in Table SI4 (*see* Appendix SI1.4).

3.3 Results and discussion

A new polyoxocation of aluminium, $[Al_2(\mu_4\text{-}O)_8Al_{26}(\mu_2\text{-}OH)_{50}(\mu_3\text{-}OH)_6(\eta\text{-}H_2O)_{22}\,Al_2(\mu_2\text{-}CH_3COO)_2](2,6\text{-}NDS)_7(CH_3COO)_2{\cdot}2H_2O$, is a centrosymmetric structure about a centre of inversion at the tetrameric aluminium linker as shown in Figure 3.2. Its structure is similar to Al_{30} polyoxocation, which has been discovered since 2000, but there are two acetate anions bidentately coordinate to the cluster by replacement of four η-H_2O molecules.[2,3] Each of the acetato groups links between a corner of an octahedral $\{AlO_6\}$ of a corner-sharing $\{Al_3O_{13}\}$ triad (O1E), and a corner of a capping $\{AlO_6\}$ unit (red octahedrons) (O1A) (*see* Figure 3.2 b). Coordination mode of the two acetato ligands is *syn-syn* bridging which is each of the acetates links two Al(III) as observed previously in binuclear $[Al_2(\eta\text{-}H_2O)_6(\mu_2\text{-}OH)_2(\mu_2\text{-}CH_3COO)_2]^{3+}$ complex.[12] Two monomeric $\{AlO_6\}$ units (green octahedra) share their three corners with the corner-

sharing triad and another corner-sharing triad in another δ-Keggin-Al_{13} SBUs resulting a big aluminium polyoxocation $[Al_2(\mu_4\text{-}O)_8Al_{26}(\mu_2\text{-}OH)_{50}(\mu_3\text{-}OH)_6(\eta\text{-}H_2O)_{22}Al_2(\mu_2\text{-}CH_3COO)_2]^{16+}$. Crys-tallographically unique oxygen ligands are shown in Figure 3.3.

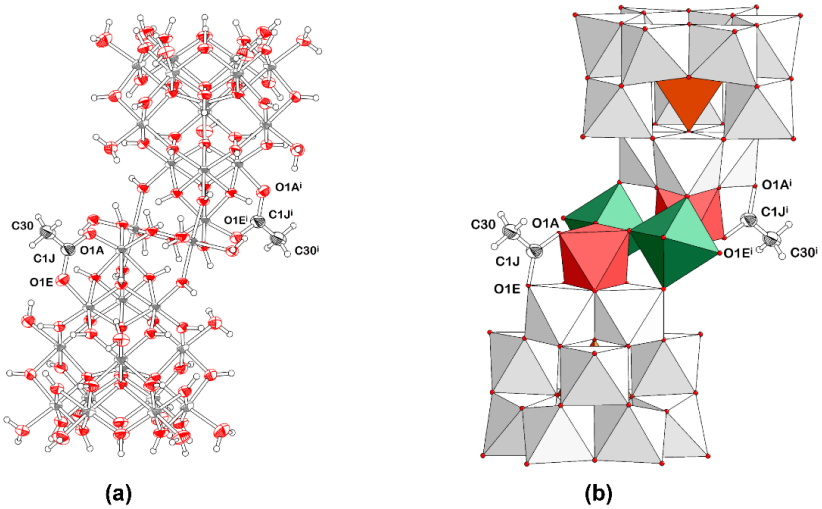

Figure 3.2 Structure of an Al_{30}-acetate polyoxocation, $[Al_2(O)_8Al_{26}(OH)_{56}(H_2O)_{22}Al_2(CH_3COO)_2]^{16+}$: (a) Ellipsoid-stick representation, non-hydrogen atoms are represented with 50% probability thermal ellipsoids. Oxygen, aluminium, carbon, and hydrogen atoms are in red, grey, black, and white, respectively. (b) Polyhedral representation showing two white δ-Keggin-Al_{13} SBUs with orange $\{AlO_4\}$ centres, red capping $\{AlO_6\}$, and green $\{AlO_6\}$ linkers. Acetato ligands are shown by ellipsoid-stick with 50% probability thermal ellipsoids. Only those atom from coordinated acetate anions are labelled. Symmetry code: (i) $1-x, 1-y, 1-z$.

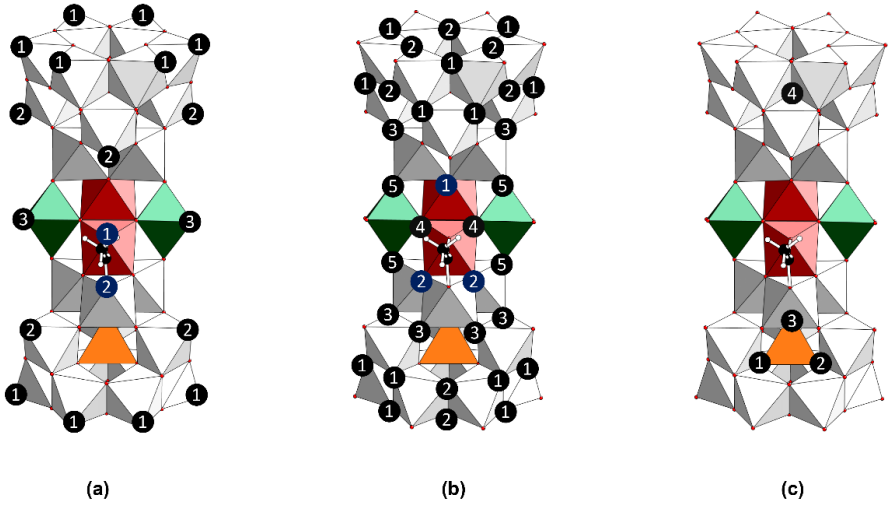

Figure 3.3 (a) Three crystallographically unique bound water molecules, η-H_2O, labelled in black and two oxygen from bridging acetato ligand, μ_2-CH_3COO^-, labelled in blue. (b) Five bidentate bridging hydroxides (μ_2-OH), labelled in black and two tridentate bridging hydroxides (μ_3-OH), labelled in blue. (c) Four tetradentate bridging oxides (μ_2-O).

In the $\{Al_4O_{20}\}$ tetramer which links two δ-Keggin-Al_{13} SBUs in the Al_{30}-acetate polyoxocation, intramolecular hydrogen bonds, O44−H44···O15^{i}, O44−H44···O19^{i}, O44^{i}−H44^{i}···O15 and O44^{i}−H44^{i}···O19, form [$6^4.4^2$] tetraasterane-like cage as shown in Figure 3.4. Inversion centre (*i*) and two-fold rotation, C_2, axis of the structure locate at the centre of this cage.

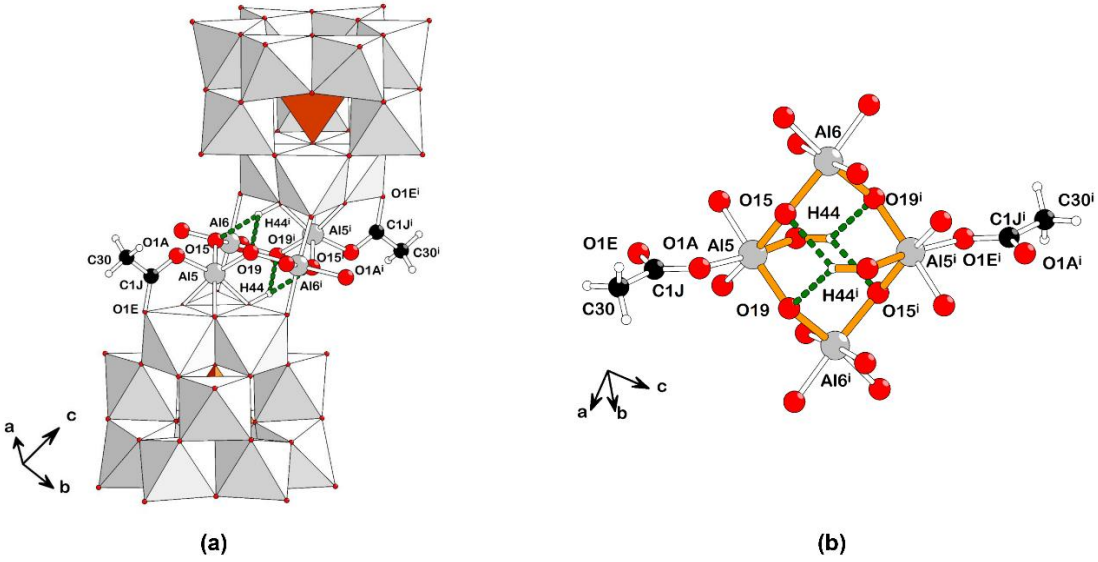

Figure 3.4 Intramolecular hydrogen bonds (green dashed line) inside the tetrameric $\{Al_4O_{20}\}$ linker in Al_{30}-acetate polycation: (a) δ-Keggin-Al_{13} SBUs represented by polyhedrons with ball-and-stick $\{Al_4O_{20}\}$ linker; (b) fragment of Al_{30}-acetate showing a tetrameric $\{Al_4O_{20}\}$ linker with highlighted [$6^4.4^2$] tetraasterane-like cage (yellow solid lines), non-acetate hydrogen atoms were omitted. Symmetry code: (i) 1−*x*, 1−*y*, 1−*z*.

The $[Al_2(\mu_4\text{-}O)_8Al_{26}(\mu_2\text{-}OH)_{50}(\mu_3\text{-}OH)_6(\eta\text{-}H_2O)_{22}Al_2(\mu_2\text{-}CH_3COO)_2]^{16+}$ carries a highly positive charge of 16+ which is compensated by seven 2,6-NDS^{2-} and two uncoordinated acetate anions. Not only ionic or coulombic interactions between the polyoxocation and its counterparts, hydrogen bonding interaction is also important in the supramolecular assemblies. One of the 2,6-NDS^{2-} forms moderate hydrogen bonds to three μ_2-OH at the hexagonal face of polyoxocation as shown in Figure 3.5. An oxygen atom in the sulphonate group of the 2,6-NDS^{2-} (O8) acts as a hydrogen bonds acceptor for three crystallographic unique hydrogen bonds *i.e.* O51—H51···O8, O55—H55···O8, and O58—H58···O8 (*see* Figure 3.5 b). These are four-centre hydrogen bonds. The 2,6-NDS^{2-} links two Al_{30}-acetate polyoxocations together and leads the

formation of an infinite hydrogen-bonded chain (*see* Figure 3.5 a). Other six 2,6-NDS^{2-} anions form moderate hydrogen bonds surrounding the Al_{30}-acetate polyoxocation as illustrated in Figure 3.6. Oxygen atoms in sulphonate group in each of the 2,6-NDS^{2-} acts as a hydrogen bond acceptor for hydroxyl bridges (μ_2-OH) and also terminal water hydrogen (η-H_2O).

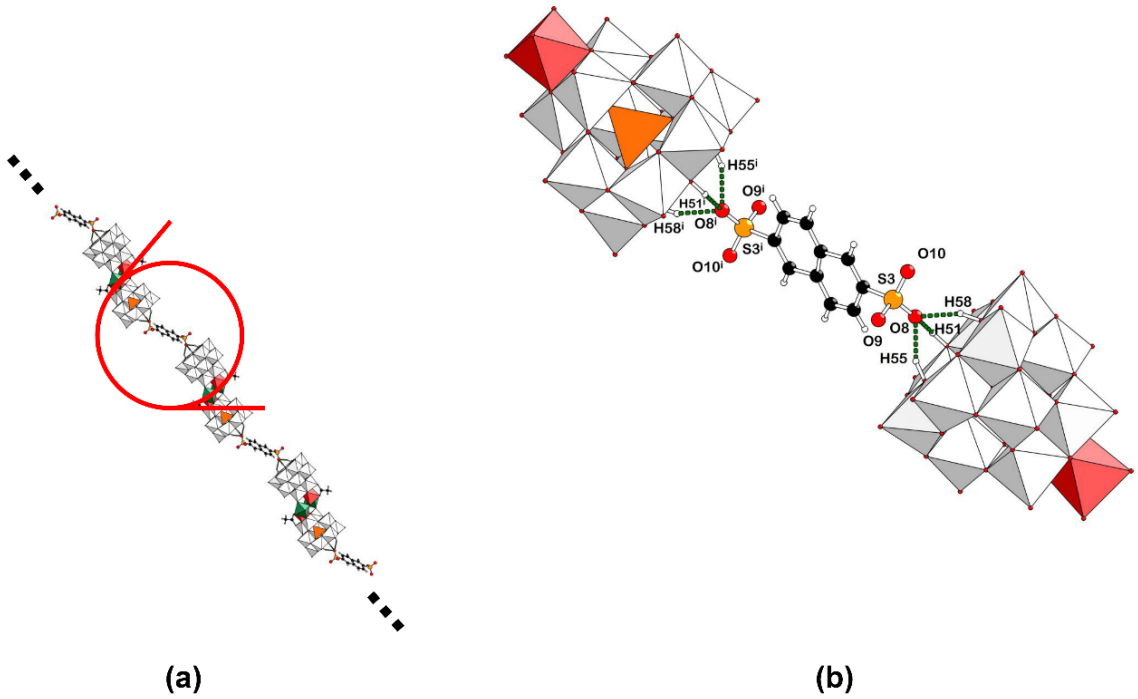

Figure 3.5 Hydrogen bonds (green dashed lines) between Al_{30}-acetate polyoxocation and 2,6-NTS^{2-} anions led the formation of infinite hydrogen-bonded chain (a) with the zoomed in (b) illustrating the intercalating 2,6-NDS^{2-} anion which forms three crystallographically unique hydrogen bonding interactions and links two Al_{30}-acetate polyoxocation into the chain. Symmetry code: (i) 1−*x*, 1−*y*, 1−*z*.

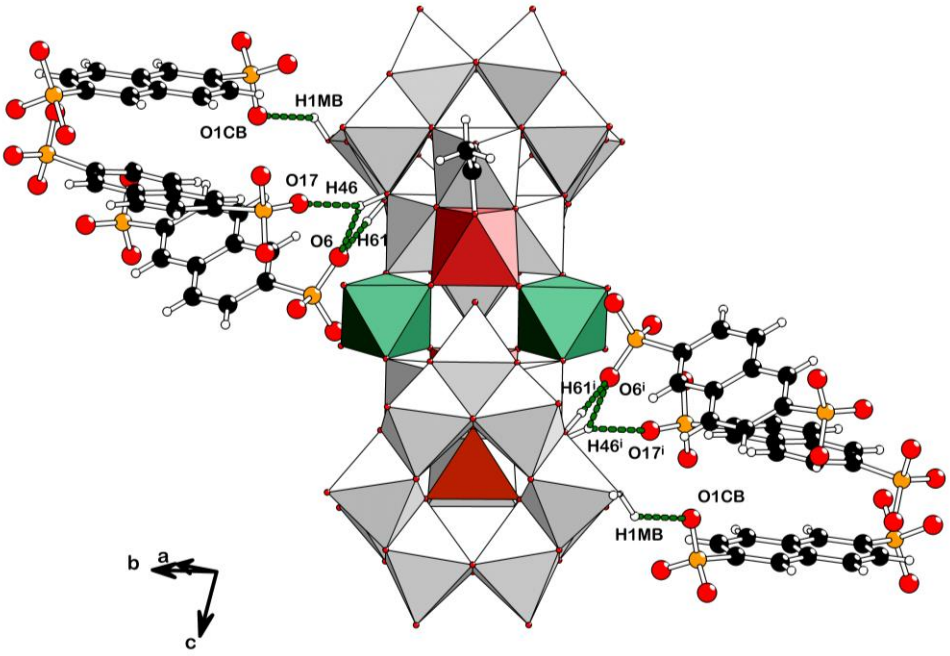

Figure 3.6 Hydrogen bonds (green dashed lines) between Al_{30}-acetate polyoxocation and other six 2,6-NTS^{2-} anions around the cluster. Symmetry code: (i) 1−*x*, 1−*y*, 1−*z*.

As described above, there are two acetate anions bidentately coordinate to the Al_{30}-acetate polyoxocation. Acetate is also present as an uncoordinated anion. In X-ray crystal structure of Al_{30}-acetate, two uncoordinated acetate anions locate close to the polyoxocation and form four crystallographically unique hydrogen bonds with the cluster as illustrated in Figure 3.7. Carboxylate oxygen atoms in the acetate (O11 and O1J) act as three-centre hydrogen bond acceptors *i.e.* O1F—H1FA···O11, O1F—H1FB···O11, O19—H19···O1J, and O1I—H1IA···O1J.

Molecular environment of the Al_{30}-acetate polyoxocation contains two 2,6-NDS^{2-} anions hydrogen-bonded to the two pentagonal faces of the cluster, six 2,6-NDS^{2-} anions hydrogen-bonded to sides of the cluster, and two uncoordinated acetate anions hydrogen-bonded to sides of the polyoxocations as illustrated in Figure 3.8.

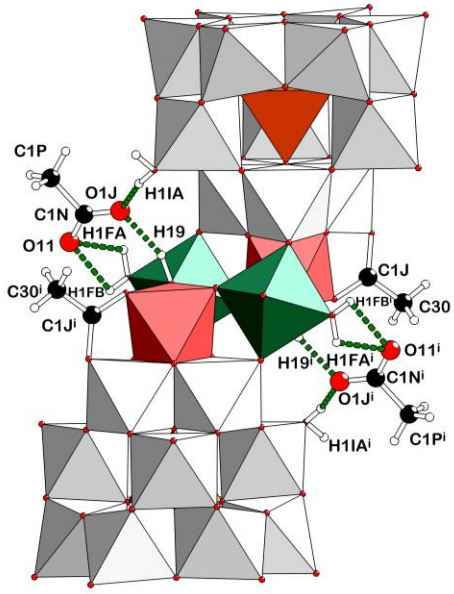

Figure 3.7 Hydrogen bonds (green dashed lines) between uncoordinated acetate anions and Al_{30}-acetate polyoxocations. Symmetry code: (i) 1−*x*, 1−*y*, 1−*z*.

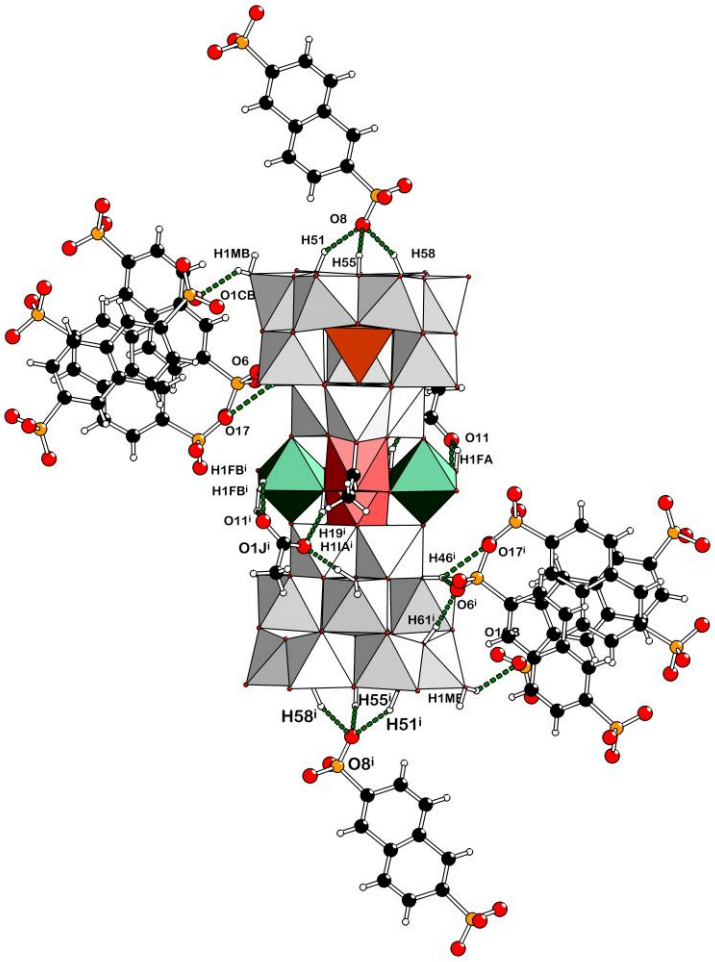

Figure 3.8 Molecular environment of Al_{30}-acetate polyoxocation. Hydrogen bonds are represented by green dashed lines. Non-hydrogen-bond hydrogen atoms on the polyoxocation were omitted.

The hydrogen-bonded assembly between Al_{30}-acetate polyoxocation and its counter anions is illustrated in Figure 3.9. It can be clearly seen that the organic and inorganic moieties are separated. The 2,6-NDS^{2-} anions which form hydrogen bonds to the sides of Al_{30}-acetate polyoxocation are stacked and filled in the space between each polyoxocations. Two of the 2,6-NDS^{2-} anions stack parallel-offset and form π-π interactions with the interatomic distances approximately 3.6 - 3.9 Å as shown in Figure 3.10.

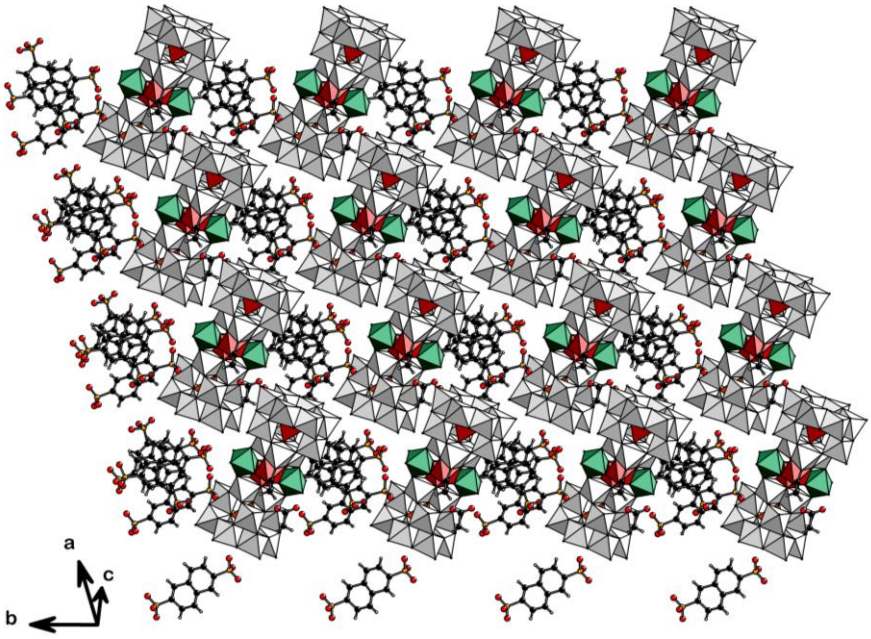

Figure 3.9 Supramolecular assembly of Al_{30}-acetate and its counterparts.

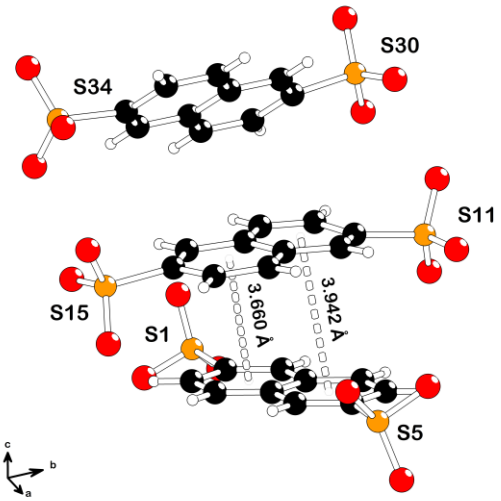

Figure 3.10 Stacking 2,6-NDS^{2-} anions. Interatomic distances between centroids of each naphthalene rings are represented by white dashed lines.

Previously reported surface modified Al_{30} and the Al_{30}-acetate polyoxocations have structural similarity. The surface modified Al_{30} polyoxocations have been synthesised and reported *i.e.* $Al_{32}SO_4$, Cu_2Al_{30}NDS, Al_{32}IDA, Al_{30}TBP, and Zn_2Al_{32}NTA and their structure are illustrated in Figure 3.11.[5,8,9,13] All of these polyoxocations are analogues of Al_{30}-type structure which the same terminal water molecules were replaced.

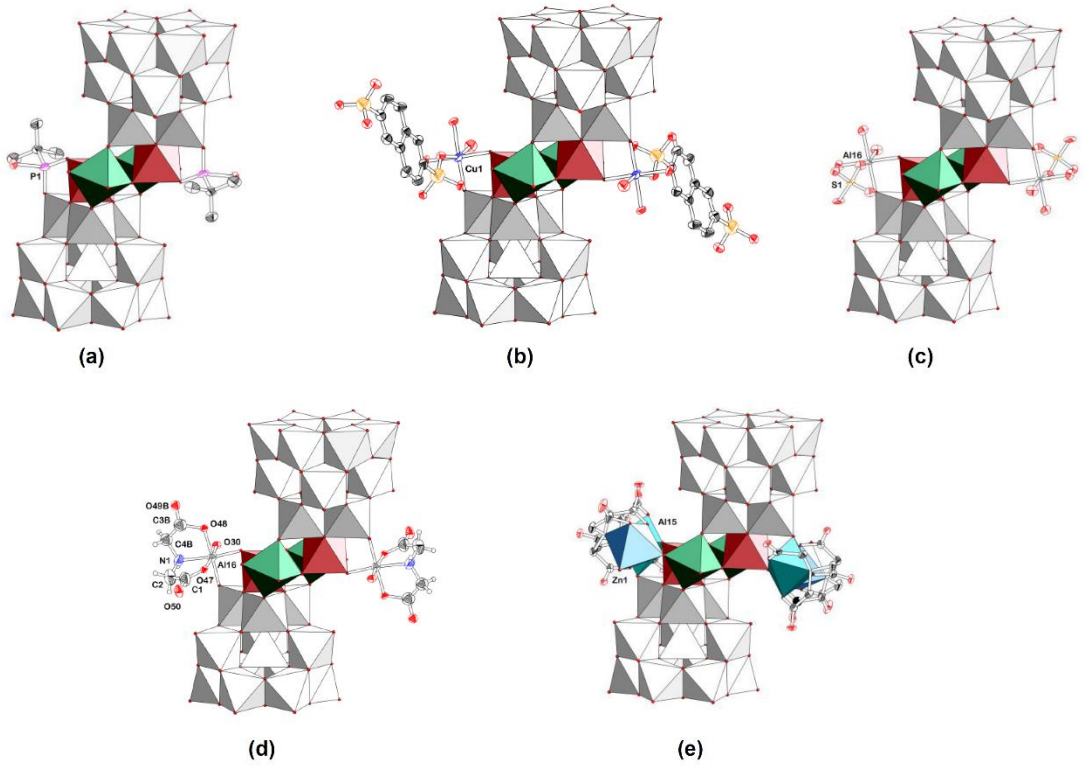

Figure 3.11 Polyhedral representations illustrating structures of modified Al_{30} polyoxocations: (a) $[(TBP)_2\ Al_{30}O_8(OH)_{56}(H_2O)_{22})]^{14+}$ **(Al_{30}TBP)**, (b) $[(Cu(H_2O)_3(2,6\text{-NDS})_2Al_{30}O_8(OH)_{60}(H_2O)_{22}]^{18+}$ **(Cu_2 Al_{30}NDS)**, (c) $[Al_{32}O_8(OH)_{60}(H_2O)_{28}(SO_4)_2]^{16+}$ **($Al_{32}SO_4$)**, (d) $[(Al(IDA)H_2O)_2(Al_{30}O_8(OH)_{60}(H_2O)_{22})]^{16+}$ (**Al_{32}IDA**), (e) $[(Zn(NTA)H_2O)_2(Al(NTA)(OH)_2)_2(Al_{30}O_8(OH)_{60}(H_2O)_{20}]$ **(Zn_2Al_{32}NTA)**. (TBP = *tert*-butylphos-phonate, IDA = iminodiacetate, 2,6-NDS = naphthalene-2,6-disulphonate, NTA = nitrile triacetate)

There are exchangeable oxygen atom in Al_{30} polyoxocation *i.e.* (i) five unique bound water molecules (η-H_2O) (ii) five unique bidentate bridging hydroxide (μ_2-OH) and (iii) three tridentate bridging hydroxide (μ_3-OH) as illustrated in Figure 3.12. Among these oxygens, η-H_2O at position ❸ and ❹ are the most reactive to exchange.[14] This is reflected by the fact that all of the modified Al_{30} structures

including Al_{30}-acetate can be synthesised by replacements of these two η-H_2O molecules.

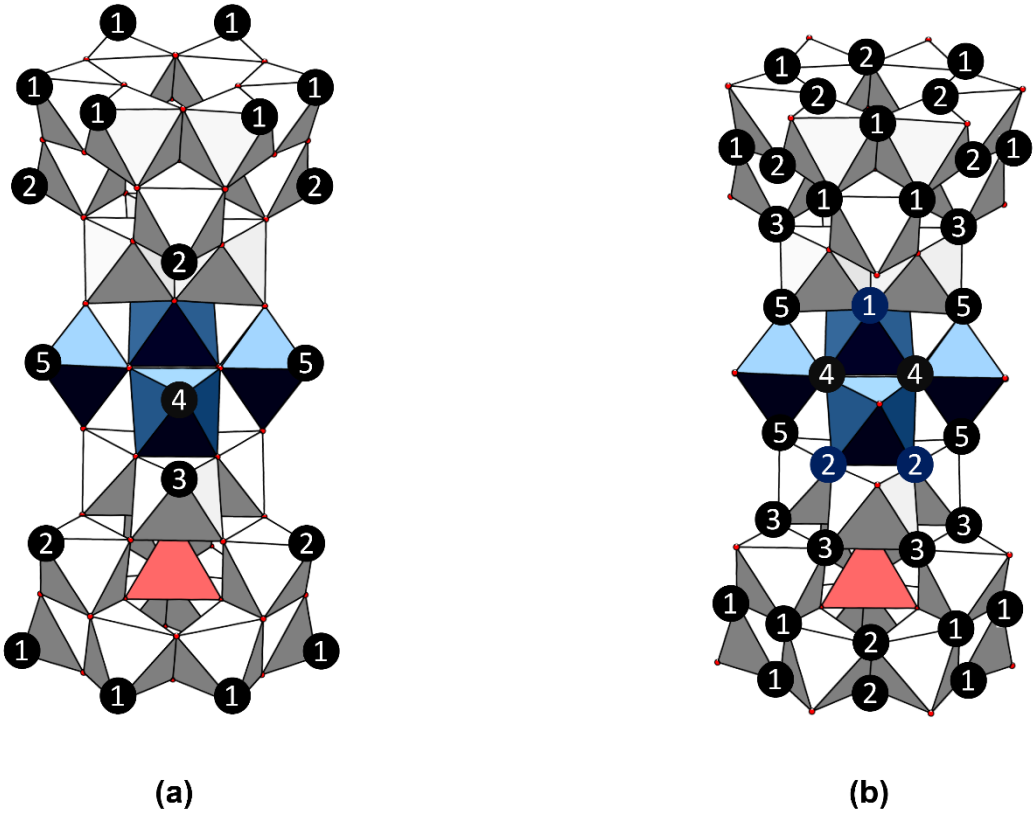

Figure 3.12 Polyhedral representations showing assignments of different oxygen sites in an Al_{30}-type polycation (a) five different terminal ligated water molecules and (b) five different bridging hydroxide ions with doubly-bridging sites (μ_2-OH) shown with black labels and the three different triply bridging sites (μ_3-OH) shown in navy-blue label. (Reprinted with permission from Ref. 8)

As described above, the Al_{30}-acetate contains both coordinated and uncoordinated acetate anions. Because there was no acetate salts as a starting materials, we proposed that hydrolysis of acetonitrile is the origin of acetate anions in the system as depicted in Equation 3.1.[15,16]

$$CH_3C{\equiv}N\ (aq) + 2H_2O\ (l) \longrightarrow CH_3COO^-\ (aq) + NH_4^+\ (aq) \qquad (3.1)$$

The acetate could react with aluminium aqua complex, $[Al(H_2O)_6]^{3+}$, and form a *syn-syn* bridging dimeric polyoxocation, $[Al_2(OH)_2(\mu_2\text{-}CH_3COO)(H_2O)_4]^{3+}$, which is one of building blocks of the Al_{30}-acetate.[17–19]

3.4. Conclusion

A new polyoxocation Al_{30}-acetate has been synthesised and characterised. The compound comprises $[Al_2(\mu_4\text{-}O)_8Al_{26}(\mu_2\text{-}OH)_{50}(\mu_3\text{-}OH)_6(\eta\text{-}H_2O)_{22}Al_2(\mu_2\text{-}CH_3COO)_2]^{16+}$ polyoxocation and its compensating anions *i.e.* 2,6-NDS^{2-} and CH_3COO^-. It crystallises in $P\bar{1}$ and has crystallographic formula $[Al_2(\mu_4\text{-}O)_8Al_{26}(\mu_2\text{-}OH)_{50}(\mu_3\text{-}OH)_6(\eta\text{-}H_2O)_{22}Al_2(\mu_2\text{-}CH_3COO)_2](2,6\text{-}NDS)_7(CH_3COO)_2\cdot 2H_2O$. Ionic interaction, hydrogen bonds and π-π stacking are important intramolecular forces which establish the crystal structure. Further characterisations were precluded due to its low yield, lack of phase purity, and low stability.

Bibliography

(1) Abeysinghe, S.; Unruh, D. K.; Forbes, T. Z. *Cryst. Growth Des.* **2012**, *12* (4), 2044–2051.

(2) Rowsell, J.; Nazar, L. F. *J. Am. Chem. Soc.* **2000**, *122* (15), 3777–3778.

(3) Allouche, L.; Gérardin, C.; Loiseau, T.; Férey, G.; Taulelle, F. *Angew. Chem. Int. Ed. Engl.* **2000**, *39* (3), 511–514.

(4) Mertens, J.; Casentini, B.; Masion, A.; Pöthig, R.; Wehrli, B.; Furrer, G. *Water Res.* **2012**, *46* (1), 53–62.

(5) Corum, K. W.; Fairley, M.; Unruh, D. K.; Payne, M. K.; Forbes, T. Z.; Mason, S. E. *Inorg. Chem.* **2015**, *54* (17), 8367–8374.

(6) Ye, C.; Bi, Z.; Wang, D. *Colloids Surfaces A Physicochem. Eng. Asp.* **2013**, *436*, 782–786.

(7) Corum, K. W.; Mason, S. E. *Mol. Simul.* **2014**, *41* (1-3), 146–155.

(8) Abeysinghe, S.; Unruh, D. K.; Forbes, T. Z. *Inorg. Chem.* **2013**, *52* (10), 5991–5999.

(9) Abeysinghe, S.; Corum, K. W.; Neff, D. L.; Mason, S. E.; Forbes, T. Z. *Langmuir* **2013**, *29* (46), 14124–14134.

(10) Arunan, E.; Desiraju, G. R.; Klein, R. A.; Sadlej, J.; Scheiner, S.; Alkorta, I.;

Clary, D. C.; Crabtree, R. H.; Dannenberg, J. J.; Hobza, P.; Kjaergaard, H. G.; Legon, A. C.; Mennucci, B.; Nesbitt, D. J. *Pure Appl. Chem.* **2011**, *83* (8), 1637–1641.

(11) Arunan, E.; Desiraju, G. R.; Klein, R. A.; Sadlej, J.; Scheiner, S.; Alkorta, I.; Clary, D. C.; Crabtree, R. H.; Dannenberg, J. J.; Hobza, P.; Kjaergaard, H. G.; Legon, A. C.; Mennucci, B.; Nesbitt, D. J. *Pure Appl. Chem.* **2011**, *83* (8), 1619–1636.

(12) Persson, P.; Karlsson, M.; Öhman, L.-O. *Geochim. Cosmochim. Acta* **1998**, *62* (23-24), 3657–3668.

(13) Sun, Z.; Wang, H.; Tong, H.; Sun, S. *Inorg. Chem.* **2011**, *50* (2), 559–564.

(14) Phillips, B. L.; Lee, A.; Casey, W. H. *Geochim. Cosmochim. Acta* **2003**, *67* (15), 2725–2733.

(15) Barbosa, L. A. M. M.; van Santen, R. A. *J. Catal.* **2000**, *191* (1), 200–217.

(16) Venardou, E.; Garcia-Verdugo, E.; Barlow, S. J.; Gorbaty, Y. E.; Poliakoff, M. *Vib. Spectrosc.* **2004**, *35* (1-2), 103–109.

(17) Ohman, L.-O. *Geochim. Cosmochim. Acta* **1995**, *59* (22), 4775–4779.

(18) Palmer, D. A.; Bell, J. L. S. *Geochim. Cosmochim. Acta* **1995**, *59* (22), 4781–4784.

(19) Palmer, D. A.; Bell, J. L. . *Geochim. Cosmochim. Acta* **1994**, *58* (2), 651–659.

Chapter 4

MegaKeggin-Al_{162} Polyoxocation: A Novel Cationic Motif for New Ionic Open Frameworks

4.1 Introduction

As described in Chapter 1, there are only a handful of polycationic species of aluminium (as listed in Figure 4.1) synthesised and characterised by X-ray diffraction over last half century reflecting the difficulty of their isolation and characterization. [1–8] The majority of them relate to a cage-like "*Baker-Figgis-Keggin"* structure, which comprises of a tetrahedral $\{AlO_4\}$ unit surrounded by twelve $\{AlO_6\}$ octahedra with various configurations. These configurations can be classified into five rotational isomers, namely, *α*, *β*, *γ*, *δ*, and *ε*-*Keggin*-Al_{13}. The *α*-*Keggin*-Al_{13}^{7+} can be found in a mineral zunyite, whereas the *δ*-*Keggin*-Al_{13} found in form of Na-Al_{13}^{8+}, Al_{26}^{18+} and Al_{30}^{18+}.[5] The *ε*-*Keggin*-Al_{13}^{7+} is found in aqueous solution and is the origin of flocs in nature.[9,10] In contrary, the *γ*- and *β*-Al_{13} are rare due to their low stability.[11,12] The *Keggin*-Al_{13} polyoxocation plays an important role as secondary building units (SBUs) forming two distinct new classes of *Keggin*-Al_{13}-based materials *i.e.* Al_{26} and Al_{30}.[5–7] Although the fact that the largest polyoxocation, reported up to date, is $[Al_{32}O_8(OH)_{60}(H_2O)_{28}(SO_4)_2]^{16+}$ (Al_{32}-sulphate), it is still an analogue of Al_{30} class.[13] All of the *Keggin*-Al_{13}-containing structures are supramolecular assemblies of Al_{13}^{7+} polycation and its counterpart *via* hydrogen bonding and electrostatic interactions. So far only one *Keggin*-Al_{13}-containing porous structure, the $[\varepsilon\text{-}Al_{13}O_4(OH)_{24}(H_2O)_{12}]_2[V_2W_4O_{19}]_3(OH)_2\cdot 27H_2O$, has being reported by *Son Jung Ho et al.* in 2004.[14] It is an open framework but lacks stability and phase purity.[14] Due to the particular weak ionic and hydrogen bonding interactions, lack of stability at dryness, yields and phase purities have become problematic for this class of structures.[5,11,14]

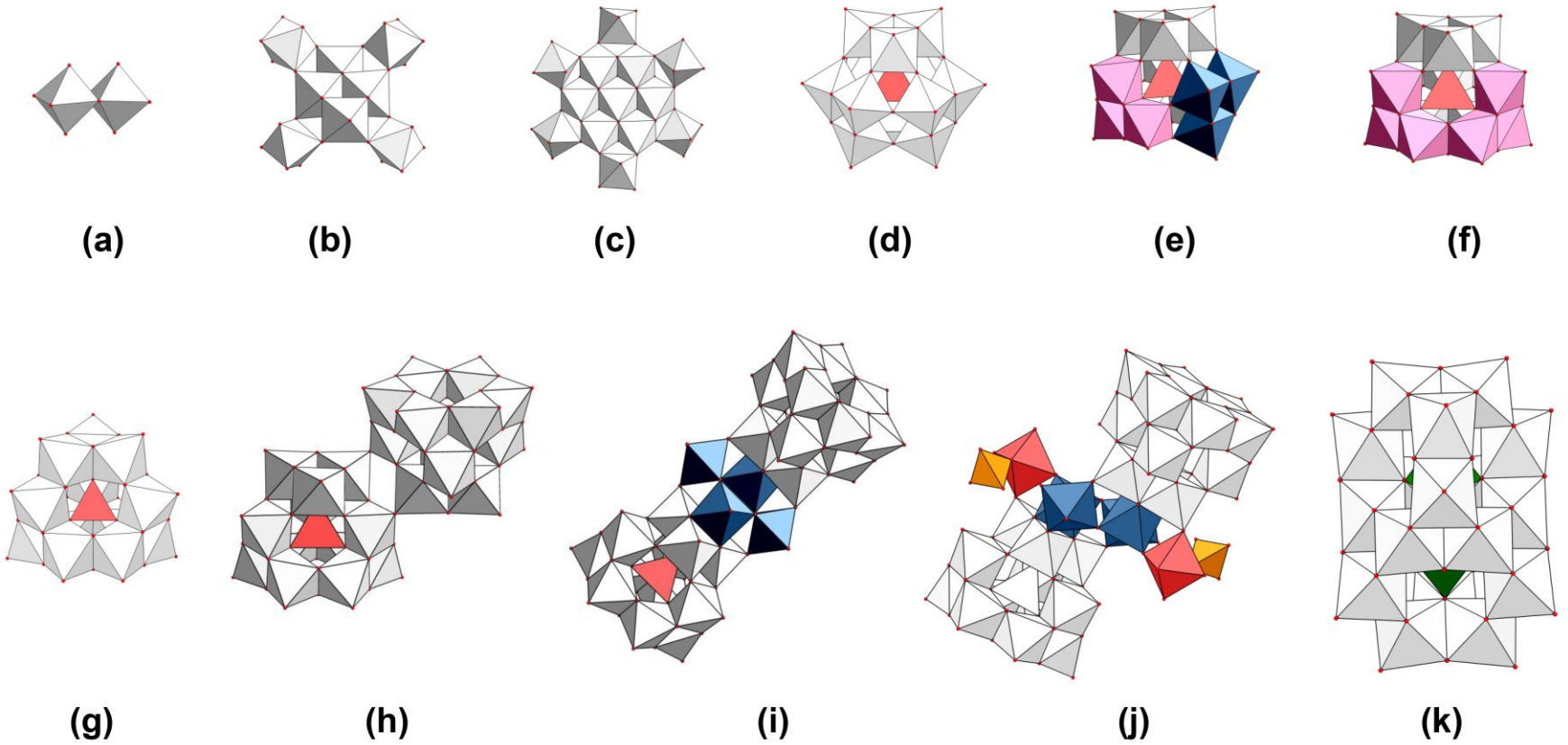

Figure 4.1 Aluminium polyoxocations characterised by X-ray diffraction technique reported until 2015. (a) Al_2: $[Al_2(OH)_2(H_2O)_8]^{4+}$, (b) Al_8: $[Al_8(OH)_{14}(H_2O)_{16}]^{10+}$, (c) *Mögel*-$Al_{13}$: $[Al_{13}(OH)_{24}\ (H_2O)_{24}]^{15+}$, (d) *α-Keggin*-$Al_{13}$: $[AlO_4Al_{12}(OH)_{24}(H_2O)_{12}]^{7+}$, (e) *γ-Keggin*-$Al_{13}$: $[AlO_4Al_{12}(OH)_{25}\ (H_2O)_{11}]^{6+}$, (f) *δ-Keggin*-$Al_{13}$: $[AlO_4Al_{12}(OH)_{24}(H_2O)_{12}]^{7+}$, (g) *ε-Keggin*-$Al_{13}$: $[AlO_4Al_{12}(OH)_{24}(H_2O)_{12}]^{7+}$ (h) Al_{26}: $[Al_{26}O_8(OH)_{50}\ (H_2O)_{20}]^{12+}$, (i) Al_{30}: $[Al_{30}O_8(OH)_{56}(H_2O)_{24}]^{18+}$ and (j) Al_{32}: $[Al_{32}O_8(OH)_{60}(H_2O)_{28}(SO_4)_2]^{16+}$, (k) *Well-Dawson* Al_{20}: $[Al_2Al_{18}O_8(OH)_{36}(H_2O)_{12}]^{8+}$.

As mentioned before, discovery of new aluminium polyoxocations is challenging in both materials and geological chemistry due to its difficulty.[9] From research literatures, *Keggin*-Al_{13}-containing structures were mostly crystallised in form of sulphate and sulphonate salts (*see* Table 1.1 in Chapter 1).[3–8,11,13,15–24] Among the reported structures, only sulphate anion can directly coordinate to *Keggin*-Al_{13} polyoxocation and applications of naphthalene sulphonates as crystallising reagents for *Keggin*-Al_{13}-based structures have been growing since 2012.[5,8,13,22–24] Reaction explorations between partially hydrolysed Al(III) solution and naphthalene sulphonates 1,3,(6,7)-naphthalene trisulphonate (NTS) were studied. Three polymorphs of the novel polyoxocation *megaKeggin*-Al_{162} (**MK-A**, **MK-B** and **MK-C**) have been discovered and synthesised from hydrolysed Al(III) solution and NTS under hydrothermal condition with different crystal growth processes.

This chapter reports the discovery of a novel polyoxocation of aluminium, $[2SO_4 \subset Al_{162}(\mu_4\text{-}O_{44}(\mu_2\text{-}O)_2(\mu_3\text{-}OH)_{32}(\mu_2\text{-}OH)_{276}(\eta\text{-}H_2O)_{100}(\eta\text{-}SO_4)_{16}]^{50+}$, *megaKeggin*-$Al_{162}$. It is the largest aluminium polyoxocationic cluster which has been characterised by X-ray diffraction reported so far. It is the first combination of two different isomers of δ- and γ-*Keggin*-Al_{13} to date according to literatures. Detailed synthetic procedure, crystal growth, crystal structure and polymorphism of this compound are described in this chapter.

4.2 Experimental

4.2.1 Materials and equipment

All of chemicals and solvents have been purchased from *Sigma Aldrich* and used without further purification (*see* list of chemical and purity details in Appendix S0). Glass vials were purchased from *Fisher Scientific*. Ovens for hydrothermal syntheses were from *Carbolite* coupled with *Eurotherm* temperature controller.

4.2.1 Discovery of the novel polyoxocation

4.2.1.1 Original synthesis

The first polymorphic crystals of *megaKeggin*-Al_{162} polyoxocation (**MK-A**), $Na_2[2SO_4{\subset}Al_{162}(\mu_4\text{-}O_{44}(\mu_2\text{-}O)_2(\mu_3\text{-}OH)_{32}(\mu_2\text{-}OH)_{276}(\eta\text{-}H_2O)_{100}(\eta\text{-}SO_4)_{16}][SO_4]_{20}[C_{10}H_5S_3O_9]_4$ *c.a.* $90H_2O$, were originally synthesised from 0.0735 M partially hydrolysed[†] $AlCl_3{\cdot}6H_2O$ and 1.00 M NTS solution under hydrothermal condition, 120°C, 12 hours. The partially hydrolysed Al(III) stock solution (degree of hydrolysis, $r_{OH} = [OH^-]/[Al^{3+}] = 2.40$) was prepared by drop-wise addition of 0.125 M NaOH (500.00 mL) into 350 mL of 0.180 M $AlCl_3{\cdot}6H_2O$. Temperature of the solution was controlled at 60°C by a water bath and the solution was stirred quickly (1,200 rpm, PTFE magnetic bar) by a magnetic stirrer. A white cloudy solution of $Al(OH)_3$ formed immediately when the NaOH solution plunged into the Al(III) solution.[25] These solid were quickly dissolved by stirring resulting in a clear solution with pH of 3.70. The final solution was transferred into a 1.0 L Duran glass bottle, heated at 80°C for 16 hours (heating rate = 10°C min^{-1}) and subsequently cooled down to ambient temperature (cooling rate = 10°C min^{-1}, pH = 3.40). Speciation in aqueous solution were analysed by ^{27}Al NMR as shown in Figure 4.5.

The partially hydrolysed Al(III) stock solution (1.00 mL) was transferred into a 4- mL-glass vial and mixed with 0.25 mL of 1.0 M NTS solution and 1.55 mL deionised H_2O (pH of final solution = 3.74). The vial was sealed with a screw cap and put into an oven at 120°C for 12 hours (heating rate = 10°C min^{-1}). Cooling down to ambient temperature (cooling rate = 0.5°C min^{-1}) leads to a colourless solution. The solution of ten vials were combined into a 50-mL beaker and allowed to evaporate under controlled air-flow at room temperature for 5 days (evaporation rate = 5 g H_2O $days^{-1}$). Pale yellow hexagonal crystals of the first polymorph, MK-A, crystallised during the evaporation (crystallisation occurred after 85% evaporation). This slow evaporation (5 g H_2O day^{-1}) produced large (10-70 μm) single crystals which are suitable for X-ray diffraction as shown in Figure 4.2.

[†] Al(III) can be fully hydrolysed at $r_{OH} > 2.5$ in aqueous solution.[44]

Although the original synthesis can produce good quality of MK-A, it offers very low yields (<0.1% based on $AlCl_3 \cdot 6H_2O$ precursor) and also produces amorphous precipitate as a by-product. This makes difficulty for bulk characterisations including powder X-ray diffraction (PXRD) and its chemical composition analysis. For this reason, we optimized the synthesis using a high-throughput system.

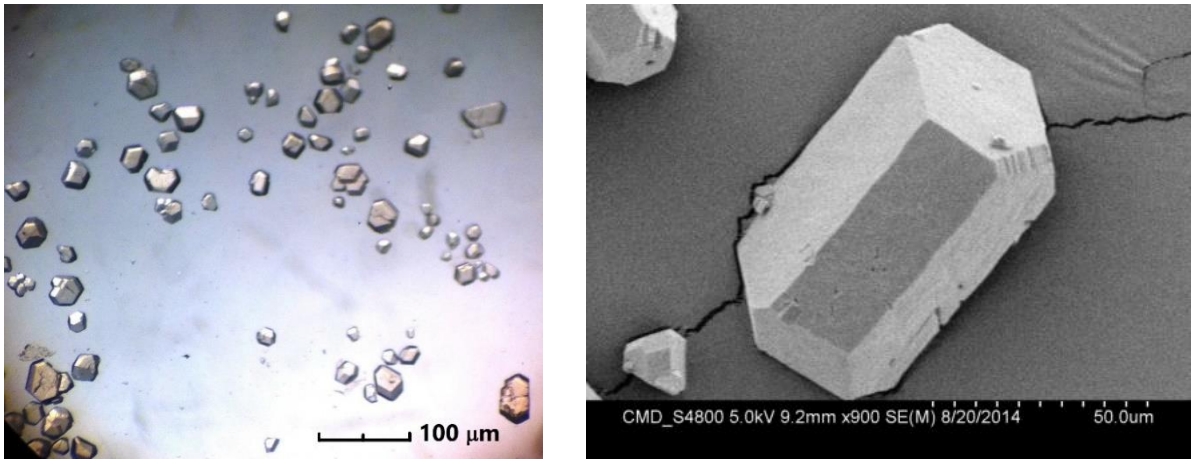

(a) **(b)**

Figure 4.2 Crystals of MK-A obtained from original synthesis under (a) optical stereo microscope and (b) Scanning Electron Microscope (SEM).

4.2.1.1 Optimised synthesis

4.2.1.1.1 Precursor and stoichiometric explorations

The explorations starting with the selection of the best precursors. Several bases *i.e.* NaOH, KOH, NH_4OH and triethylamine (TEA) were applied as bases, as well as, three aluminium salts *i.e.* $AlCl_3 \cdot 6H_2O$, $Al(NO_3)_3 \cdot 9H_2O$ and $Al_2(SO_4)_3 \cdot 16H_2O$ were applied as Al(III) sources. The syntheses were conducted in 40-mL-glass vials and treated under hydrothermal condition (70% filling) at 120°C for 60 hours. Stoichiometric ratios of the starting materials were varied as shown in Figure 4.3. and the Al(III) concentration in each reaction was controlled at 7.35 mM. In order to prevent the formation of amorphous precipitate, the reaction was performed in more acidic conditions than the original synthesis (using r_{OH} = 1.50, 1.00 and 0.50). The pH of the *pre*- and *post*-hydrothermal solutions were measured using glass electrode pH

meter. Post-hydrothermal solutions were transferred to a 50-mL beaker and let naturally evaporate in a fumehood for five days. After crystallization the obtained samples were separated from the supernatant by filtration and washed with deionized water. The wet crystals were re-dispersed in water or other solvents depending on the experimental needs. The optimum reaction is number 32 in the ternary diagram, as shown in Figure 4.3 with the selected Al(III) and OH^- precursors of $Al(NO_3)_3{\cdot}9H_2O$ and NaOH (r_{OH} = 1.0, Al(III):OH^-:1,3,(6,7)-NTS = 1:1:3.4) based on crystal quality, phase purity and yields. These precursors and stoichiometric ratio have been applied to the synthesis for further investigation.

4.2.1.1.2 Hydrothermal heating time and temperature explorations

Hydrothermal reactions at the optimum ratios were conducted at 120 °C for 4, 8, 12, 24, 36, 48, 60 and 90 hours and different heating temperature *i.e.* 80, 100, 120, and 140°C. The optimum hydrothermal condition is 120 °C for 60 hours. Pre- and post-hydrothermal solutions have different degree of acidity reflecting by the reduction of pH from 4.30±0.50 to 3.60±0.50, and also different colours. UV-Visible spectrometer was employed to measure the absorbance of both solutions. It is clearly seen that the post-hydrothermal solution contains coloured species, which absorb(s) at wavelength at 325 nm as illustrated in Figure 4.4.

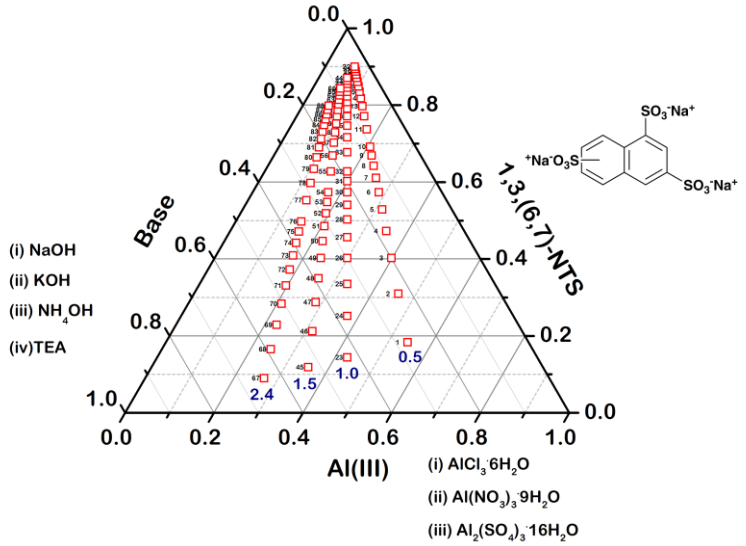

Figure 4.3 Ternary diagram represents the mole fractions of reactants in the high throughput synthetic plan. The amounts of base and Al(III) are dependent on the r_{OH} ratios. There are four series (from left to right) of r_{OH} = 2.40, 1.50, 1.00 and 0.50, respectively. Deionised water was used as reaction media and the concentration of Al(III) in each reaction vessels was controlled at 7.35 mM. The reactions were performed in 40-mL-glass vials filled with 70% filling degree by deionised water.

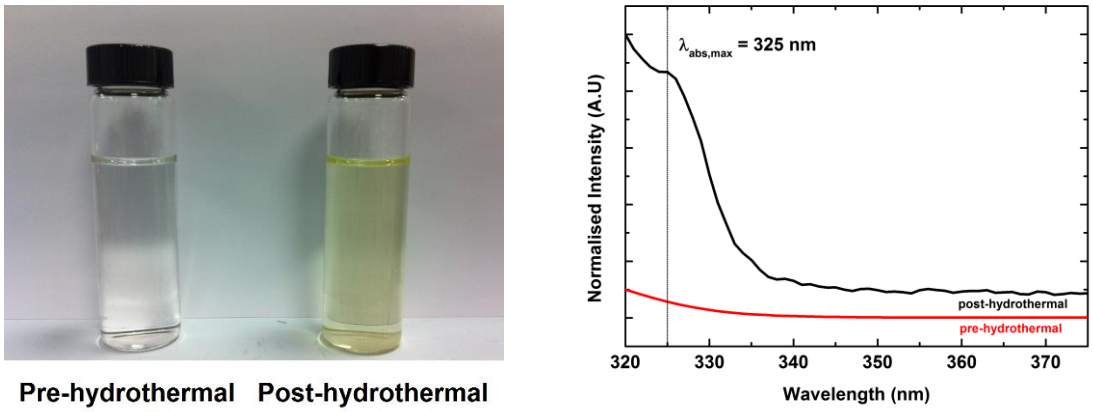

Figure 4.4 (a) Post- and pre-hydrothermal solution in 40-mL glass vials and (a) UV-Visible absorbance spectra of pre- (red) and post-hydrothermal (black) solutions (measure at room temperature in quartz cuvette).

4.3.1.1 Solution state ^{27}Al NMR spectroscopy of partially hydrolysed Al(III) solution

Solution state ^{27}Al NMR spectrum of partially hydrolysed Al(III) stock solution are shown in Figure 4.5. The spectrum show sharp peaks at 0.00, 63.10 ppm are corresponding to the resonances of $[Al(H_2O)_6]^{3+}$ and *ε-Keggin*-$[AlO_4(OH)_{24}(H_2O)_{12}]^{7+}$, respectively.[26] A broad peak at 4.34 ppm is due to the resonance of $[Al_3(OH)_6(H_2O_3)]^{3+}$. Ratios between each species depend on the r_{OH} of the solution as shown in Figure 4.5.

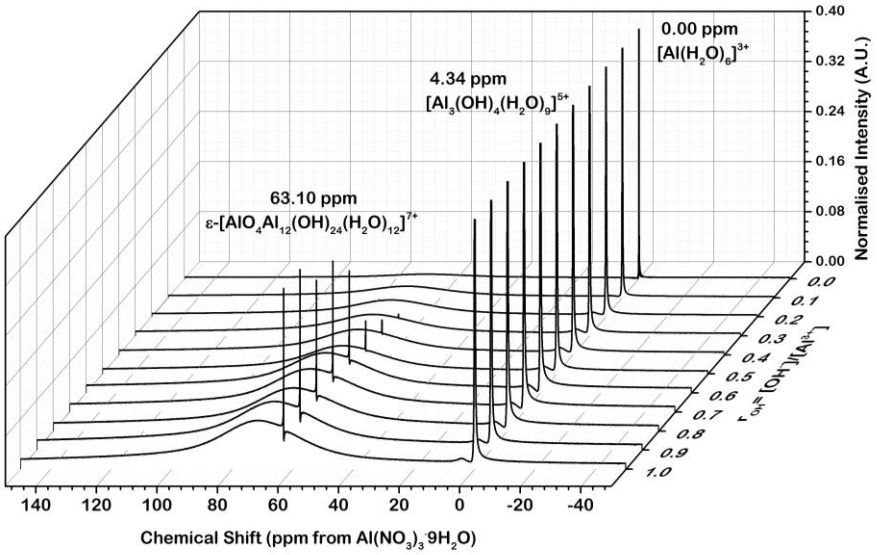

Figure 4.5 Solution state ^{27}Al NMR spectra of partially hydrolysed Al(III) solution with different r_{OH}. Sharp peaks at 0.00, 63.10 ppm are corresponding to the resonances of $[Al(H_2O)_6]^{3+}$ and *ε-Keggin*-$[AlO_4(OH)_{24}(H_2O)_{12}]^{7+}$, respectively. Small broad peak at 4.34 is corresponding to $[Al_3(OH)_6(H_2O_3)]^{3+}$. Broad peak between 40-100 ppm is form probe background.

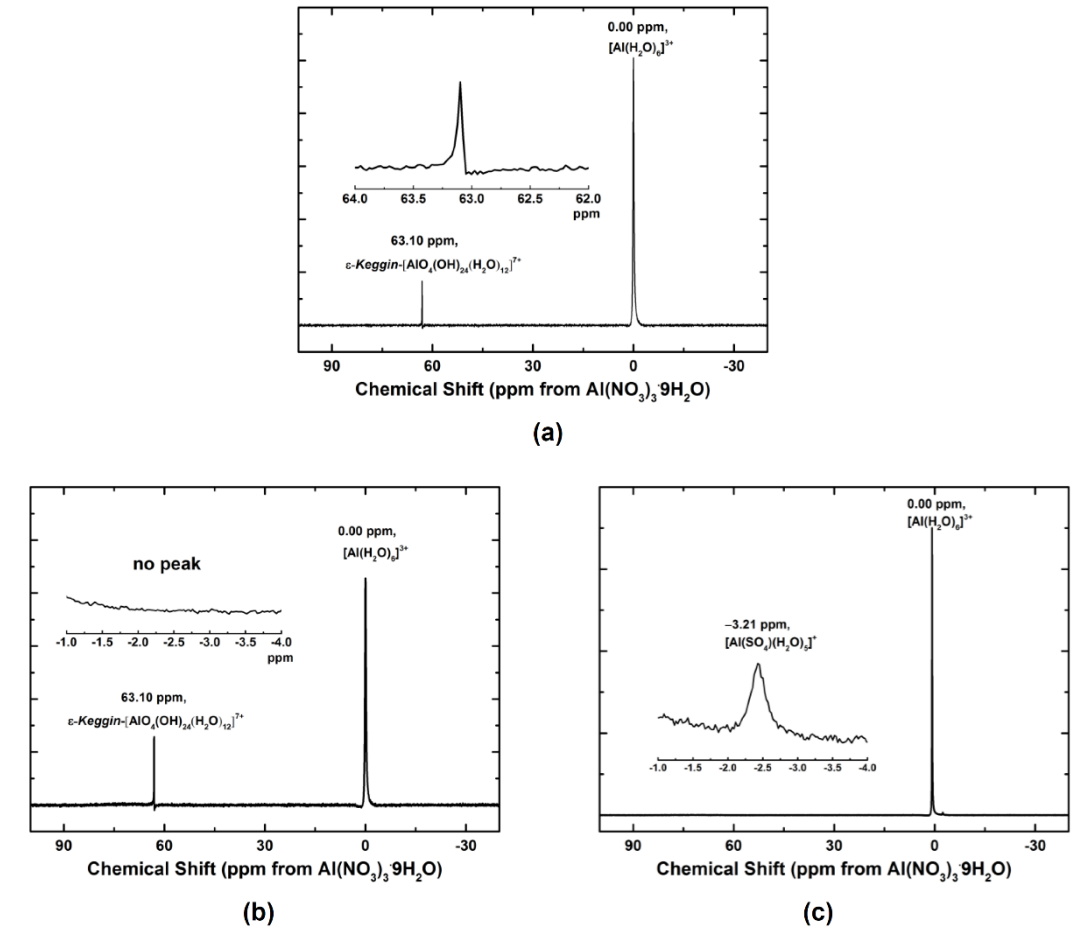

Figure 4.6 ^{27}Al NMR spectra of (a) partially hydrolysed Al(III), r_{OH} 1.00, (b) pre-hydrothermal solution, and (c) post-hydrothermal solution with important regions in zoomed-in. inset (Bruker 400 MHz, number of scan = 2500). Background was removed for clarity.

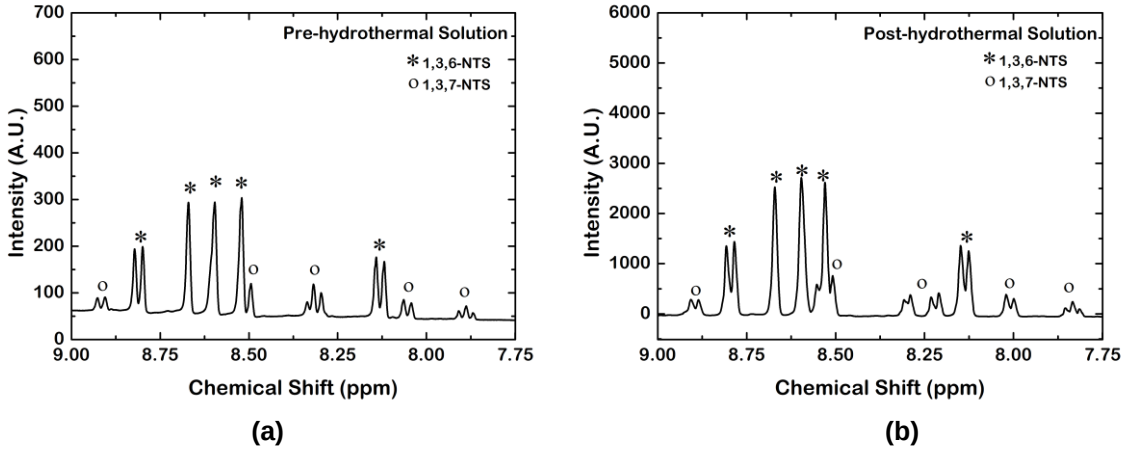

Figure 4.7 (a) ^{1}H NMR spectra of pre-hydrothermal solution (^{1}H NMR (400 MHz, D_2O), 1,3,6-NTS; δ 8.81 (d, J = 9.0 Hz, 1H), 8.67 (s, 1H), 8.59 (s, 1H), 8.52 (s, 1H), 8.13 (d, J = 9.0 Hz, 1H); 1,3,7-NTS; δ 8.92 (d, J = 8.6 Hz, 1H), 8.50 (s, 1H), 8.32 (t, J = 7.8 Hz, 1H), 8.05 (d, J = 8.7 Hz, 1H), 7.89 (t, J = 8.0 Hz, 1H) and (b) ^{1}H NMR spectra of post-hydrothermal solution.

^{27}Al and ^{1}H NMR spectroscopic methods were applied to study the change of cationic aluminium species and NTS during hydrothermal synthesis. ^{27}Al NMR spectrum of partially hydrolysed Al(III) solution and pre-hydrothermal post-hydrothermal solution shows sharp peaks at 0.00, 63.10 ppm and a small broad peak at 4.34 ppm corresponding to $[Al(H_2O)_6]^{3+}$, *ε-Keggin*-$[AlO_4(OH)_{24}(H_2O)_{12}]^{7+}$ and $[Al(OH)_4(H_2O)_9]^{5+}$, respective-ly.[26] Whereas, the peak at 63.10 ppm disappeared from the ^{27}Al NMR spectrum of post-hydrothermal solution, however, a small sharp peak at –3.21 ppm which corresponding to the resonances of $[Al(SO_4)_4(H_2O)_5]^{+}$ species presented.[26] (as illustrated in Figure 4.6). This is an important evidence suggesting that the aluminium sulphate monomer species, $[Al(SO_4)_4(H_2O)_5]^{+}$, was generated and the *ε-Keggin*-$[AlO_4(OH)_{24}(H_2O)_{12}]^{7+}$ polyoxocation was decomposed, transformed, or isomerised to other species in the solution during hydrothermal heating. Thermal decomposition of the NTS generated sulphate anions *in situ*.[27] The ^{1}H NMR spectrum (Figure 4.7) of the post-hydrothermal solution show peaks splitting at 8.13 ppm and 8.38 ppm, indicating product of the NTS decomposition. The optimised hydrothermally synthetic process followed by conventional vaporisation-based crystallisation produces phase-pure, single polymorph, MK-A. Bulk materials were characterised by PXRD and chemical analysis. The PXRD pattern reflects its phase purity as shown in Figure 4.8. Crystal structure determination and structural description are reported in the next section.

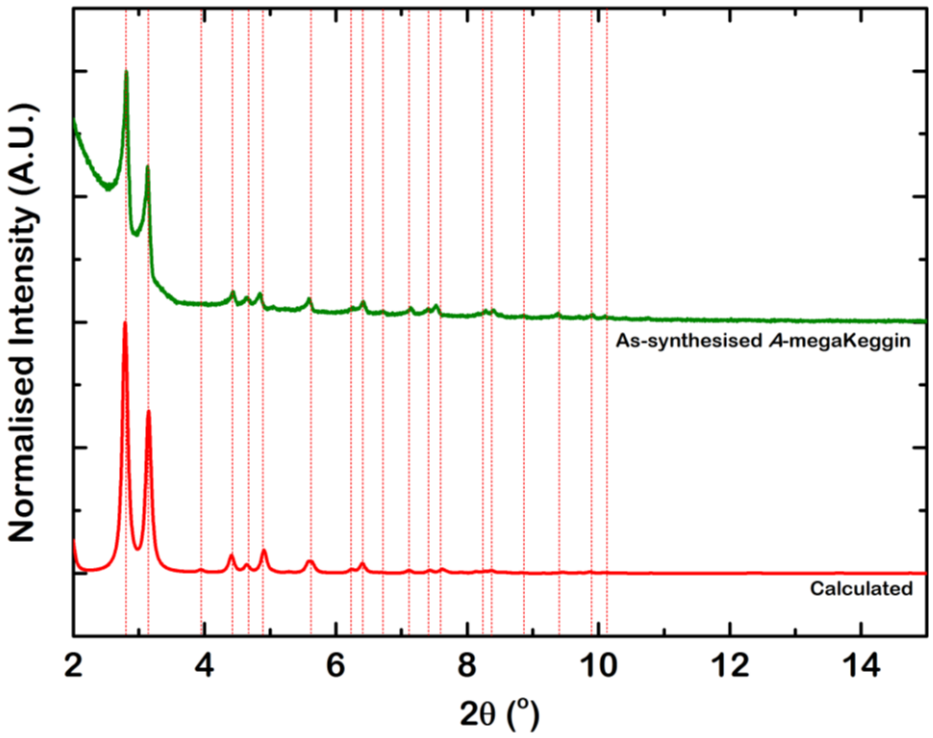

Figure 4.8 PXRD pattern of MK-A synthesised by the optimised procedure (green) compared to the calculated pattern (red, calculated from $P4_2/mmc$, a, b = 44.766(6) Å c = 35.032(4) Å by Mercury 3.3 CCDC, λ = 1.54 Å). The MK-A sample was sealed in capillary (Ø = 0.7 mm) filled with water.

4.2.1.1.3 Optimisation of the crystallisation process

As mentioned above, low yield is problematic for the syntheses of aluminium polyoxocationic materials. The original and the optimised synthetic method with conventional crystallisation protocol, undisturbed evaporation of aqueous solution, offered a yield in the range of ten milligrams per week. This was a time-consuming process. A new crystallisation protocol was proposed and applied for the hundreds-mg-scale crystallisation, which is able to reduce the synthetic procedure from 3.5 weeks to 3 days. The new protocol consists of a controllable air flow through the surface of the solution in 1.0 L conical flask (*see* Figure 4.9). The air flow was controlled and rate of evaporation was tracked from weight changes (20 g H_2O hour^{-1}). Crystals start to be visible to the naked eye after the evaporation reached 85%. Phase-pure MK-A is obtained from this method. This synthetic procedure is reproducible that confirmed by PXRD as shown in Figure 4.10.

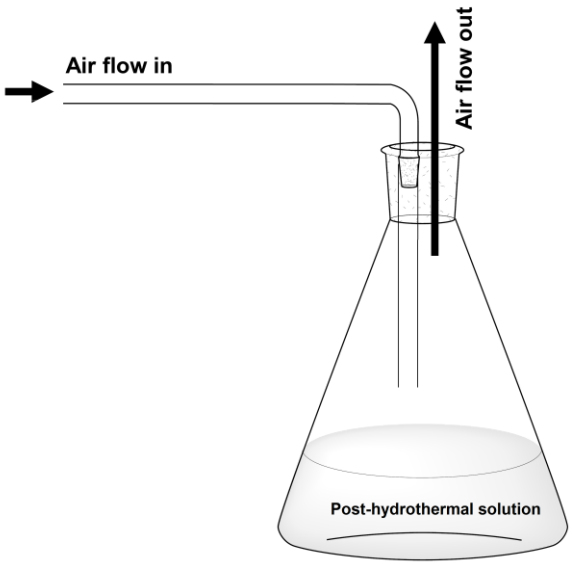

Figure 4.9 New crystallisation method with controlled air flow and rate to evaporation was 20 g H_2O hour^{-1}.

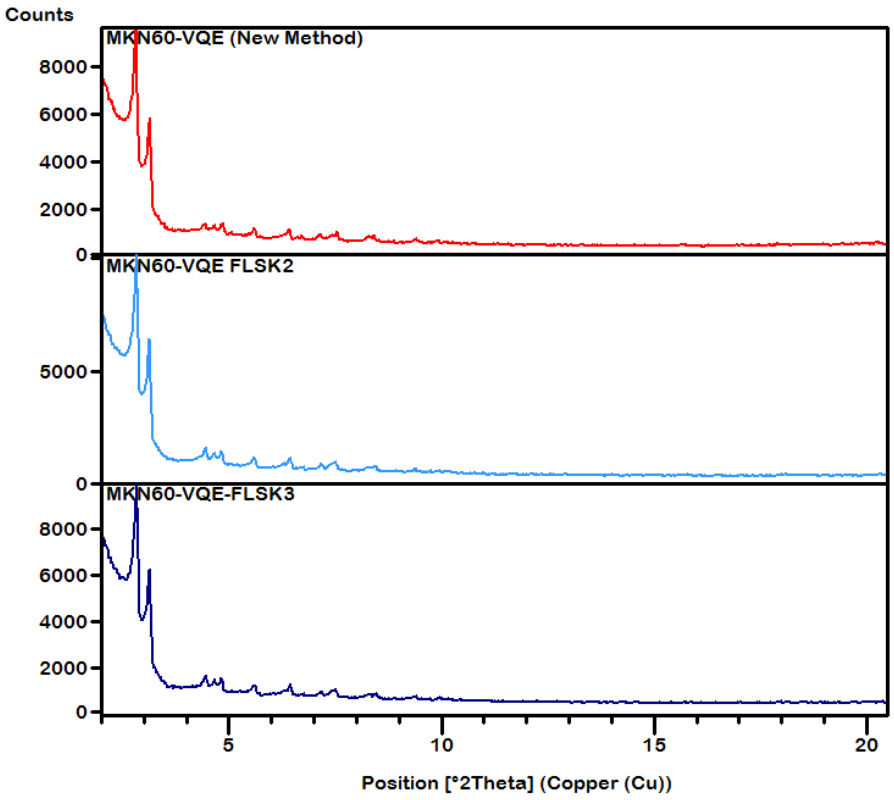

Figure 4.10 PXRD patterns of MK-A from new method of crystallisation from three different batches.

Beyond the crystallization *via* evaporation, which led to the new material, crystallisation *via* organic solvent diffusion was investigated. A beaker containing 30 mL of post-hydrothermal solution was placed in a glass chamber of organic solvent as shown in Figure 4.11 in order to allow the solvent to diffuse into the post-hydrothermal solution. Three different organic solvents were applied *i.e.* acetone, *i*-PrOH, and MeCN, respectively. Colourless crystals were obtained in all beakers. The crystals were separated from the supernatants by filtration, washed by DI water and collected in water. The PXRD pattern shows that the organic solvent diffusion technique promoted the formation of a known smaller polyoxocation, $[Al_{32}O_8(OH)_{60}(H_2O)_{28}(SO_4)_2](SO_4)_7Cl_2{\cdot}30H_2O$ (Al_{32} sulphate), as illustrated in Figure 4.12.

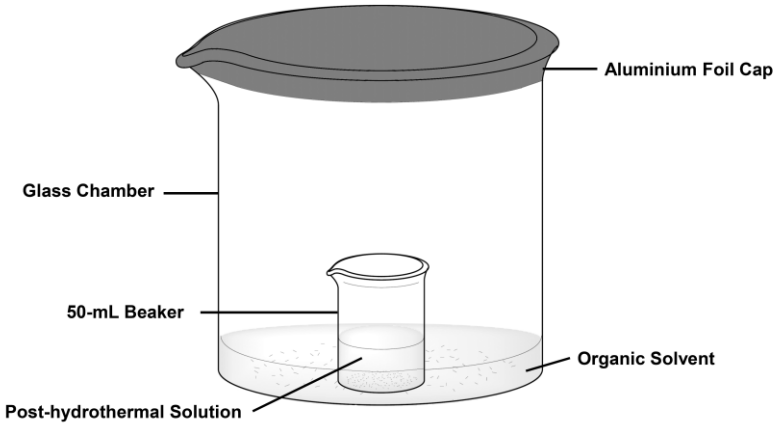

Figure 4.11 Diagram of the solvent diffusion crystallisation. A 50-mL beaker contains 30 mL of post-hydrothermal solution placed in organic solvent in a closed glass chamber.

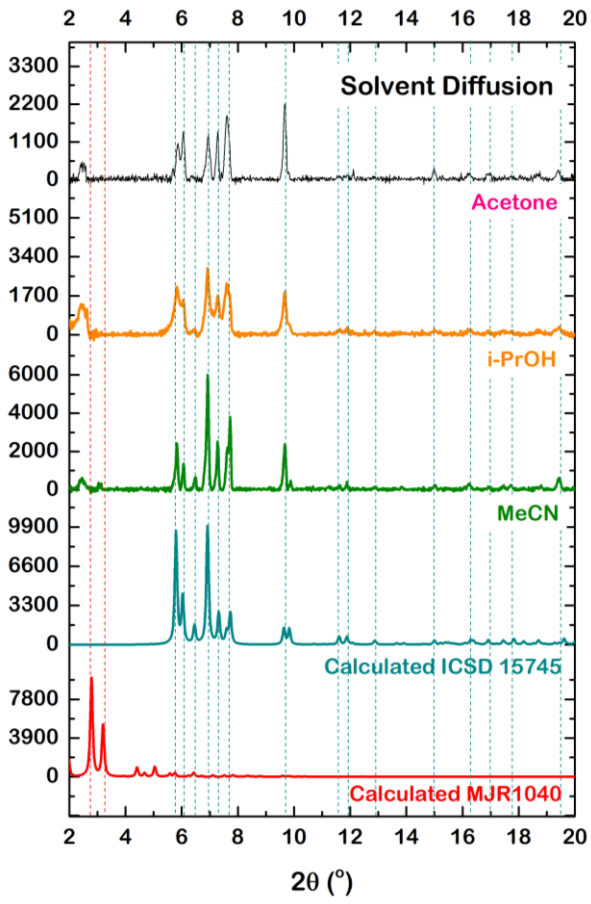

Figure 4.12 PXRD patterns of bulk solids from organic solvent diffusion crystallisation of acetone (black), *i*-PrOH (orange) and MeCN (green), comparing to calculated patterns of Al_{32} sulphate (cyan) and *A-megaKeggin*-Al_{162} sulphate (red).

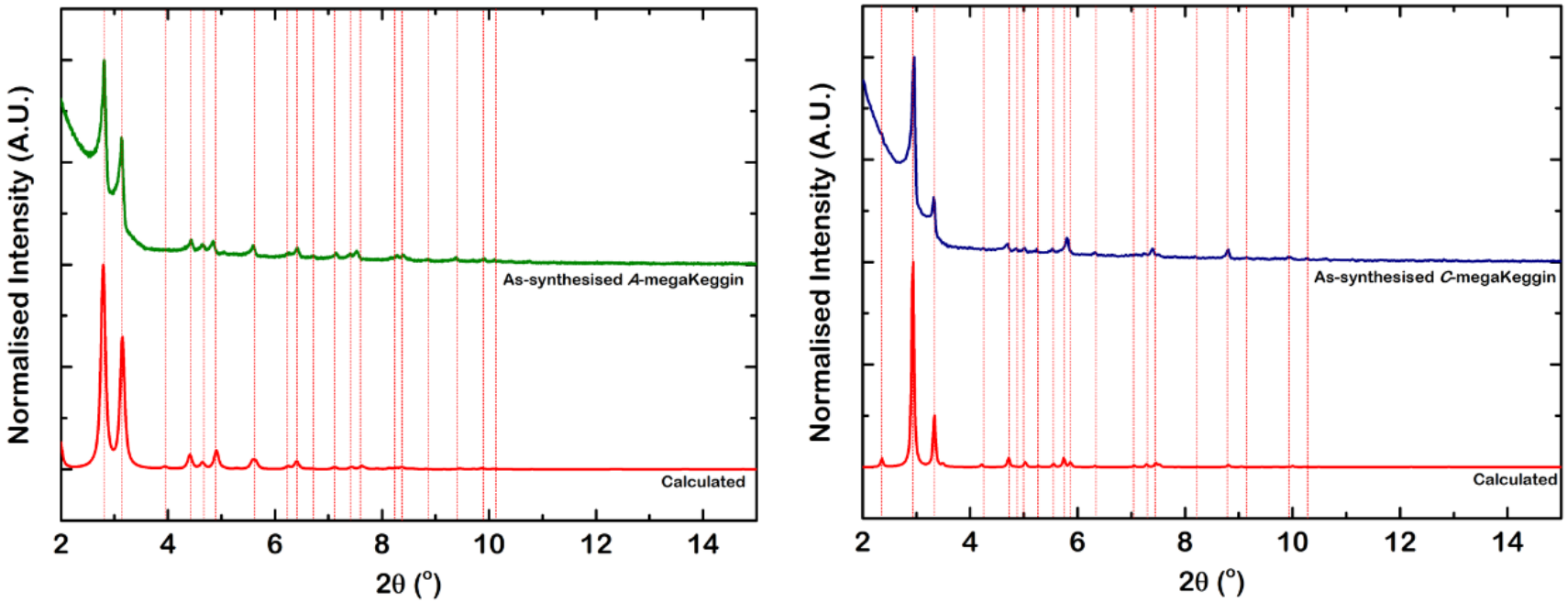

Figure 4.13 PXRD patterns of the bulk materials obtained from three different crystallisation condition *i.e.* (a) conventional evaporation (5 g H_2O day^{-1}) and (b) non-evaporation comparing to the calculated patterns. The PXRD patterns were measured at ambient temperature. The samples were sealed in Ø = 0.70 mm capillary filled with water. (Cu Bruker diffractometer, λ = 1.5406 Å).

4.2.2 *MegaKeggin*-Al_{162} sulphate polymorphism

Pale yellow crystals with different shape and size compared with MK-A crystallised from the 1-month-aged solution (without evaporation). PXRD patterns illustrate new phase with larger unit cell parameters as shown in Figure 4.13. The new phase is a polymorphic structure of the conventional MK-A which we will call **MK-C**. The third polymorph, **MK-B** was then obtained from the synthesis in which the hydrothermal treatment was shorter than 60 hours and the crystallization was performed without evaporation. PXRD of bulk materials containing MK-B polymorph is shown in Figure 4.14.

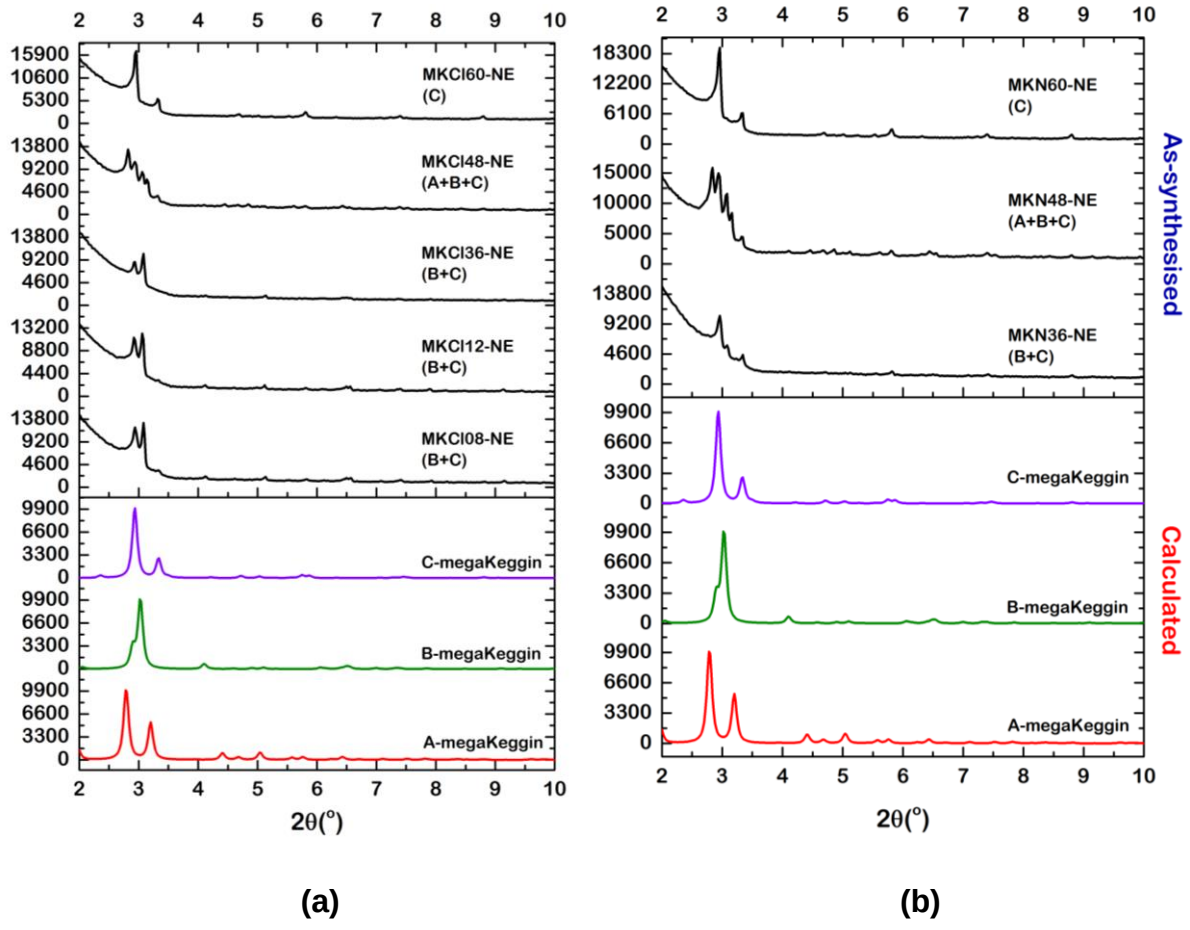

Figure 4.14 PXRD patterns of (a) bulk materials synthesised from $AlCl_3 \cdot 6H_2O$ precursor and (b) bulk materials synthesised from $Al(NO_3)_3 \cdot 9H_2O$ precursor, with different heating hydrothermal times (8, 12, 36, 48, 60 hours), crystallised without evaporation, compared with calculated PXRD patterns of MK-A (red), MK-B (green) and MK-C (purple). The PXRD patterns were measured at ambient temperature. The samples were sealed in Ø = 0.70 mm capillaries filled with water. (Cu Bruker diffractometer, λ = 1.5406 Å).

4.2.3 Chemical Analysis

Crystalline phase pure MK-A materials were synthesised from the optimised hydrothermal synthesis followed by the optimised crystallisation process (as described above). Crystalline phase purity was confirmed by indexed PXRD patterns ($P4_2/mmc$, a,b = 44.769(6) Å, c = 35.032(4) Å). The materials were analysed by ICP-OES, CHNS, and EDX. The MK-A materials were separated from supernatant by Büchner filtration, washed with 50 mL of deionised water five times and kept in a glass vial immediately. Homogeneities of the crystals were observed under an optical stereomicroscope. The materials were weighed by analytical balance, dried under static vacuum for 12 hour, digested in 3.20 M HNO_3 and analysed by ICP-OES (three parts). The other parts were analysed by elemental analyser (CHN microanalysis), TGA and EDX analysis. The results of ICP-OES are listed in Table 4.1 and Table 4.2. TGA and CHN microanalysis results are listed in Table 4.1-4.4 , respectively. The proposed formula is $Na_2[2SO_4{\subset}Al_{162}(\mu_4\text{-}O)_{44}(\mu_2\text{-}O)_2(\mu_3\text{-}OH)_{32}(\mu_2\text{-}OH)_{276}(\eta\text{-}H_2O)_{100}(\eta\text{-}SO_4)_{16}][SO_4]_{20}[C_{10}H_5S_3O_9]_4$ *c.a.* $90H_2O$. Oxygen atoms in MK-A structure were classified into (i) O^{2-}, (ii) OH^- and (iii) H_2O using BVS calculations. The BVS calculation results and oxygen assignment are shown in Table SI2.3 (*see* Appendix SI 2.3). NTS^{3-} anions were not observed in single crystal X-ray structures but were observed by ^1H NMR of the digested MK-A and CHN analysis.

Table 4.1 ICP-OES and EDX analyses results compared with the expected values.

Element Ratios	Al	S	Na	C	H	O
Proposed Formula	162	50	2	30	528	732
ICP1 (x3 analysis)	162±3.56	53.05±0.19	2.06±0.02	N/A	N/A	N/A
ICP2 (x3 analysis)	162±0.77	52.90±0.67	0.99±0.02	N/A	N/A	N/A
ICP3 (x3 analysis)	162±2.31	53.41±0.23	2.18±0.03	N/A	N/A	N/A
EDX (50 crystals)	162±20.52	55.12±11.40	N/A	N/A	N/A	N/A

Table 4.2 Raw data of ICP-OES analyses of MK-A with the expected concentrations in ppm.

Part 1	**Al (ppm)**	**S (ppm)**	**Na (ppm)**
Blank	0.000	0.000	0.000
Analysis 1	63.015	24.995	0.702
Analysis 2	65.850	25.066	0.690
Analysis 3	64.538	25.174	0.699
<x>	64.468	25.078	0.697
Sd	1.418	0.09	0.006
Report	**64.468±1.418**	**25.078±0.09**	**0.697±0.006**
Expected	**64.47**	**23.64**	**0.68**

Part 2	**Al (ppm)**	**S (ppm)**	**Na (ppm)**
Blank	0.000	0.000	0.000
Analysis 1	53.627	20.810	0.280
Analysis 2	54.142	20.693	0.274
Analysis 3	53.881	21.199	0.287
<x>	53.883	20.901	0.280
Sd	0.257	0.264	0.006
Report	**53.883±0.257**	**20.901±0.264**	**0.280±0.006**
Expected	**53.88**	**19.76**	**0.56**

Part 3	**Al (ppm)**	**S (ppm)**	**Na (ppm)**
Blank	0.000	0.000	0.000
Analysis 1	53.420	21.103	0.613
Analysis 2	53.867	21.143	0.620
Analysis 3	54.920	21.277	0.630
<x>	54.069	21.174	0.621
sd	0.770	0.090	0.008
Report	**54.069±0.770**	**21.174±0.090**	**0.621±0.008**
Expected	**54.07**	**19.82**	**0.57**

Table 4.3 TGA results compared with the calculated values.

TGA	**%Calc.**	**%Obs.**
%TGA Residual (Al_2O_3, PXRD)	43.91	42.09
%SO_3	21.28	20.03
%CO_2+H_2O	34.63	37.88

Table 4.4 CHNS analyses results compared with the calculated values.

CHNS Analysis	**C (%)**	**H (%)**	**S (%)**
%Calc.	2.55	2.83	8.52
%Obs.	2.45	3.74	6.78

4.2.4 Crystal structure characterisation

4.2.4.1 Single crystal X-ray diffraction

Three polymorphic crystals were grown from the same post hydrothermal solution with different crystallisation condition (details of the synthesis are described above). To prepare suitable single crystals for X-ray diffraction, single crystals of MK-A were grown slowly from post-hydrothermal solution using a slow evaporation method (5 g H_2O day^{-1}). Single crystals of MK-B and MK-C were grown from post-hydrothermal solution in glass vials without evaporation for two months. MK-A crystal has generally a hexagonal or rectangular shape while MK-B is smaller and has an elongated shape with a higher aspect ratio compared to the one found in MK-A. MK-C is generally larger than the MK-A and MK-B as shown in Figure 4.15. In each case, the crystals were extracted from mother liquor into paratone/flombin Y-1800 on microscope glass slide and then mounted on a 20μm-Mitegen tip. The mounted crystal was immediately placed under 100 K nitrogen flow or 30 K helium flow of an *Oxford Cryosystems Cryostream Plus* on a *CrystalLogic Kappa* (4 circle) on beamline I19, Diamond Light Source, Harwell, Oxfordshire. Diffraction data was collected using a *Saturn* 724+ CCD detector with radiation at λ= 0.6889 Å) from the synchrotron.

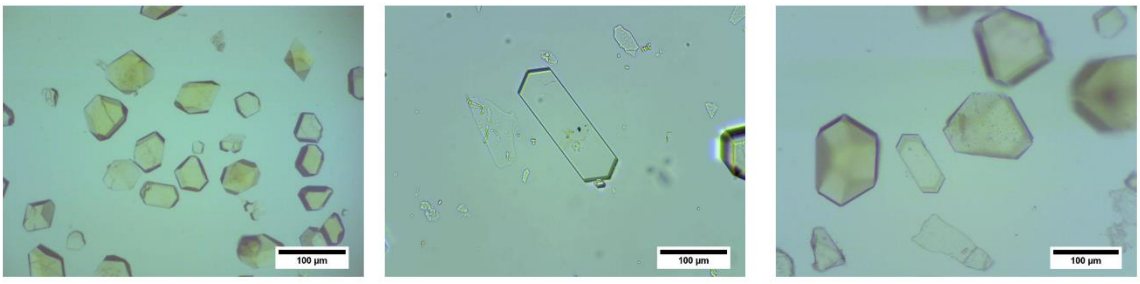

Figure 4.15 Photos taken under optical microscope for (a) MK-A, (b) MK-B and (c) MK-C crystals.

4.2.4.2 Crystal structure refinement

Data were processed and empirical absorption corrections were carried out using *CrysAlis Pro* with the unit cell parameters refined against all data. The structures were solved by direct methods using *SHELXS*.[28] All structures were refined on F_o^2 by full-matrix least squares refinement using *SHELXL*[64] implemented within *Olex2*.[29] The crystallographic information is listed in Table 4.5.

Table 4.5 Crystallographic information for MK-A, MK-B and MK-C.

ID Code			
Polymorphs	***A***	***B***	***C***
Empirical formula	$Al_{162}O_{679}S_{36}$	$Al_{162}O_{679}S_{36}$	$Al_{162}O_{679}S_{36}$
Formula mass M_r	16382.55	16382.55	16382.55
Colour	Pale yellow	Pale yellow	Pale yellow
Density	0.754 Mg m^{-3}	0.754 Mg m^{-3}	0.707 Mg m^{-3}
Radiation	Mo Kα, λ = 0.71073 Å	Mo Kα, λ = 0.71073 Å	Synchrotron, λ = 0.68890 Å
Crystal system	Tetragonal	Tetragonal	Tetragonal
Space group	*P*4$_2$/*mmc*	*P*4$_2$/*mmc*	*P*4$_2$/*mmc*
Z	16	16	16
T	100 K	100 K	100 K
a	44.7647 (3) Å	43.0413 (6) Å	37.4615 (2) Å
b	44.7647 (3) Å	43.0413 (6) Å	37.4615 (2) Å
c	36.0009 (4) Å	39.6119 (4) Å	50.5550 (3) Å
α	90°	90°	90°
β	90°	90°	90°
γ	90°	90°	90°
Unit cell volume *V*	72141.5 (11) Å^3	73383.2(10) Å^3	70947.1 (9) Å^3
R_{int}	0.118	0.060	0.042
θ_{max}, θ_{min}	26.4°, 1.48°	22.5°, 1.48°	26.4°, 1.61°
Measured reflections	585460	124871	273604
Independent reflections	38452	25075	37839
Reflections with $I > 2\sigma(I)$	22868	17958	24844
$R[F^2 > 2\sigma(F^2)]$	0.116	0.293	0.170
$wR(F^2)$	0.386	0.723	0.524
S	1.38	3.56	2.14

PXRD data of bulk materials of two crystalline-phase-pure MK-A and MK-C were measured at ambient temperature in capillary mode of the Cu *Bruker* diffractometer, λ = 1.5406 Å. In order to prevent dehydration, the fresh samples were sealed in glass capillaries (Ø = 0.7 mm) filled with liquid water. The patterns were indexed by *X'pert High Score plus* program. Refinement using the unit cell parameters

from the single crystal data corresponding to MK-A and MK-C polymorph are shown in Figure 4.16.

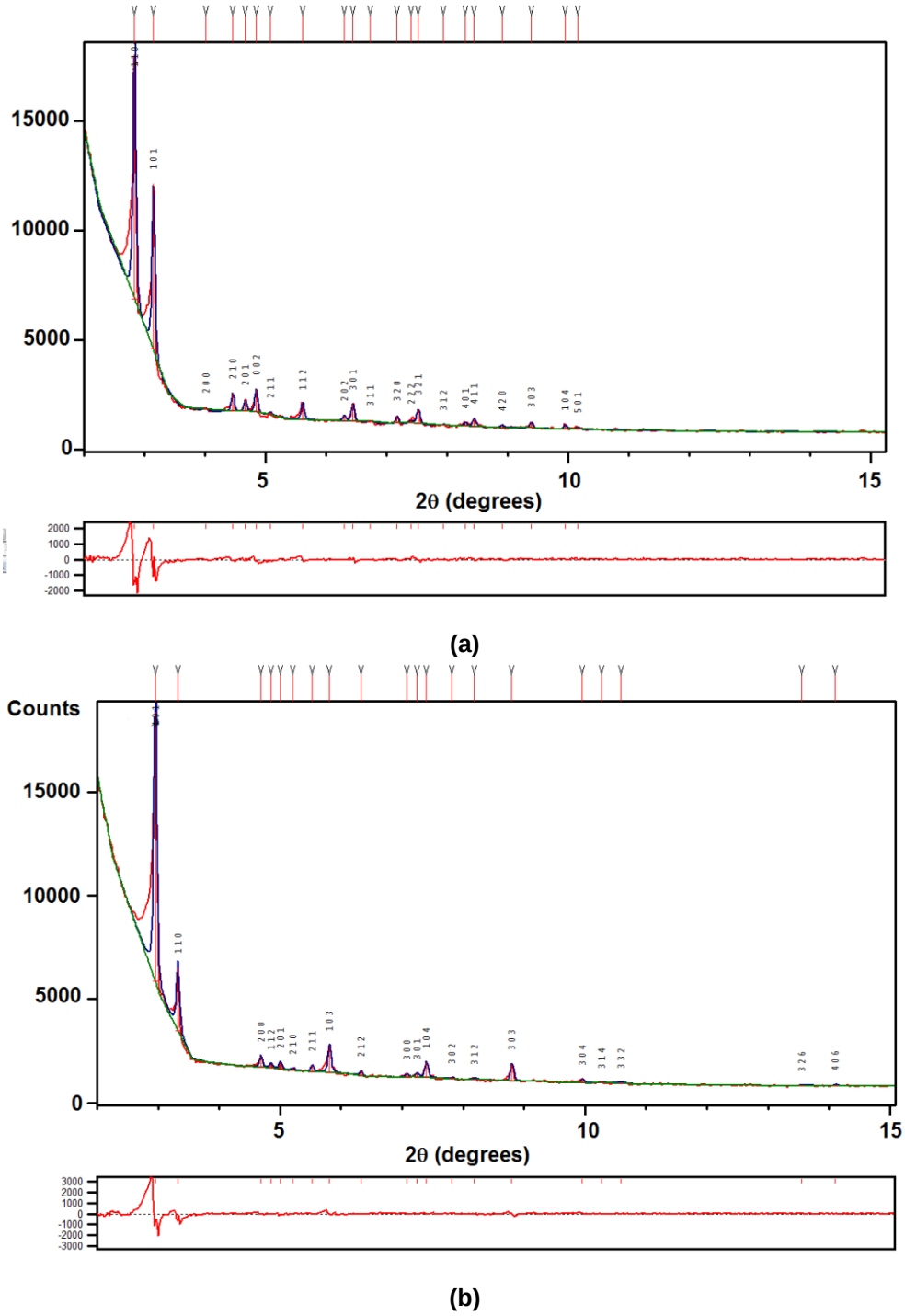

Figure 4.16 PXRD patterns of (a) MK-A and (b) MK-C plotted in red. Refinement against the unit cell calculated from the unit cell parameters. **MK-A**: Tetragonal, $P4_2/mmc$; a = 44.72(1) Å, c = 36.18(4) Å; V = 72357(11) Å^3, $\chi^2 = 8.62 \times 10^{-8}$, Snyder's FOM = 1.65; **MK-C**: Tetragonal, $P4_2/mmc$; a = 37.44(2) Å, c = 50.56(3) Å; V = 70887(10) Å^3, $\chi^2 = 1.21 \times 10^{-7}$, Snyder's FOM = 1.28. The samples were sealed in capillaries (Ø = 0.7 mm) filled with water.

4.2.5 Structural Description

4.2.5.1 MegaKeggin-Al_{162} polycation

The crystal structures of MK-A, MK-B and MK-C polymorphs comprise of a common gigantic *cage-like* polyoxocation which carries a highly positive charge, $[2SO_4{\subset}Al_{162}(\mu_4\text{-}O_{44}(\mu_2\text{-}O)_2(\mu_3\text{-}OH)_{32}(\mu_2\text{-}OH)_{276}(\eta\text{-}H_2O)_{100}(\eta\text{-}SO_4)_{16}]^{50+}$. The positive charge is balance by uncoordinated sulphate and NTS^{3-} anions. MK-A has chemical formula of $Na_2[2SO_4{\subset}Al_{162}(\mu_4\text{-}O_{44}(\mu_2\text{-}O)_2(\mu_3\text{-}OH)_{32}(\mu_2\text{-}OH)_{276}(\eta\text{-}H_2O)_{100}(\eta\text{-}SO_4)_{16}][SO_4]_{20}[C_{10}H_5S_3O_9]_4$ *c.a.* $90H_2O$. The polyoxocation itself comprises eight *δ-Keggin*-Al_{13} and two *γ-Keggin*-Al_{13} SBUs linked together *via* $\{Al(OH)_4(H_2O)(SO_4)\}$ units as shown in Figure 4.17. From reported structures in CDS databases, it is the largest polyaluminiumoxocation and also the first structure which combines two different isomers of *Keggin*-Al_{13} polyoxocation reported to date. [3–8,11,13,15–24]

The *megaKeggin*-Al_{162} polyoxocation has D_{2h} point group symmetry. There are three C_2 axes aligning with *a*-, *b*- and *c*- axes as illustrated in Figure 4.18. A reflection plane, σ_v, has other two reflection planes, σ_v' and σ_v'', perpendicular, and one can be assigned to σ_h. This results D_{2h} point group and is the most symmetrical polycation observed in *Keggin*-Al_{13}-based structures reported so far.

As mentioned above, the *megaKeggin*-Al_{162} cluster comprise of two different isomers of *Keggin*-Al_{13} SBUs. The first isomer is the *δ-Keggin*-Al_{13} which has C_{3v} point group as shown in Figure 4.19. This SBU contains a tetrahedral $\{AlO_4\}$ core surrounded by four $\{Al_3O(OH)_9(H_2O)_3\}$ triads which link together by corner and edge sharings. Each $\{Al_3O(OH)_9(H_2O)_3\}$ triad carries a positive charge of +3, contains three $\{AlO(OH)_4(H_2O)\}$ octahedrons which share their two edges with each other as shown in Figure 4.20. The Al_{13} cluster has a stoichiometric formula of $[AlO_4Al_{12}(OH)_{24}(H_2O)_{12}]^{7+}$.

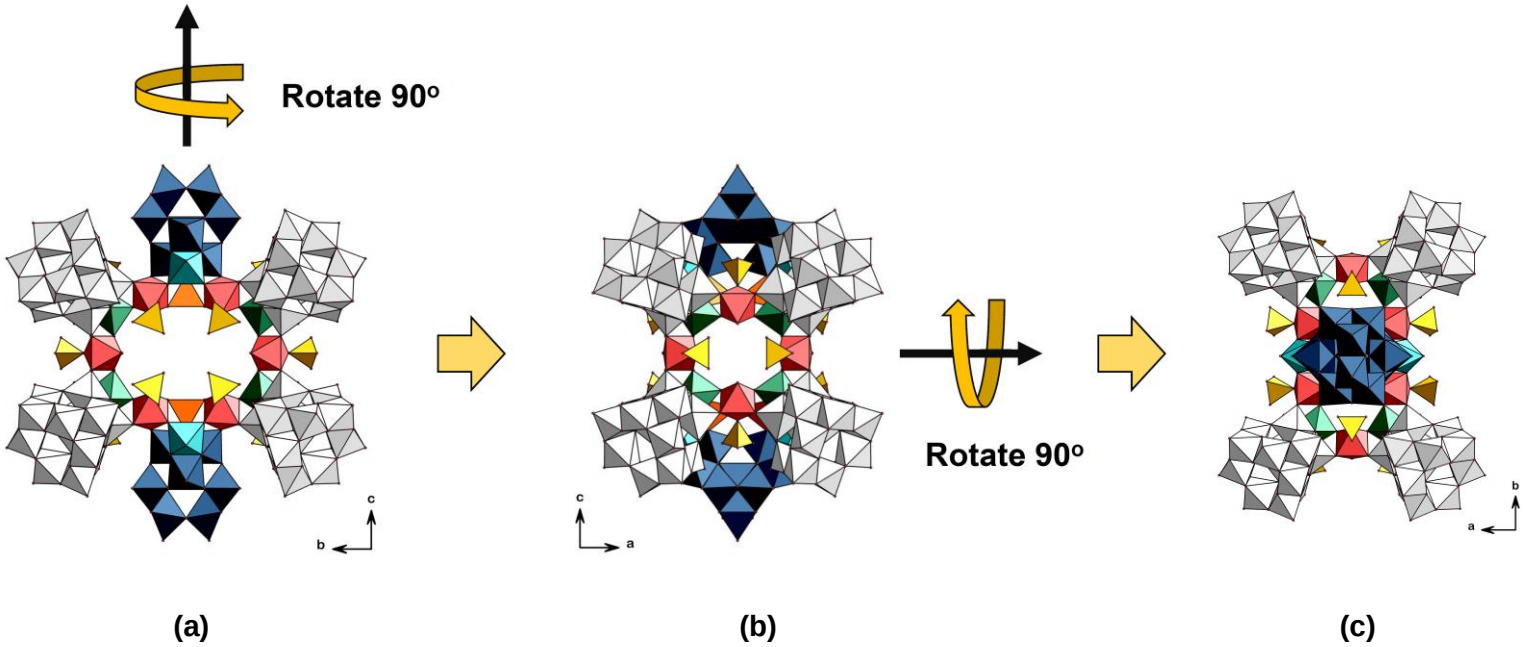

Figure 4.17 Polyhedral representation of a single *megaKeggin*-Al_{162} polyoxocation viewed along (a) *a*-, (b) *b*-, and (c) *c*-axis. The *δ*- and *γ*-*Keggin*-Al_{13} SBUs are in white and blue, respectively. Capping $\{Al(OH)_6\}$, capping $\{AlO_5(OH)_4\}$, $\{Al(OH)_4(H_2O)\}$ linkers and ligating sulphate anions are in green, red, orange and yellow, respectively.

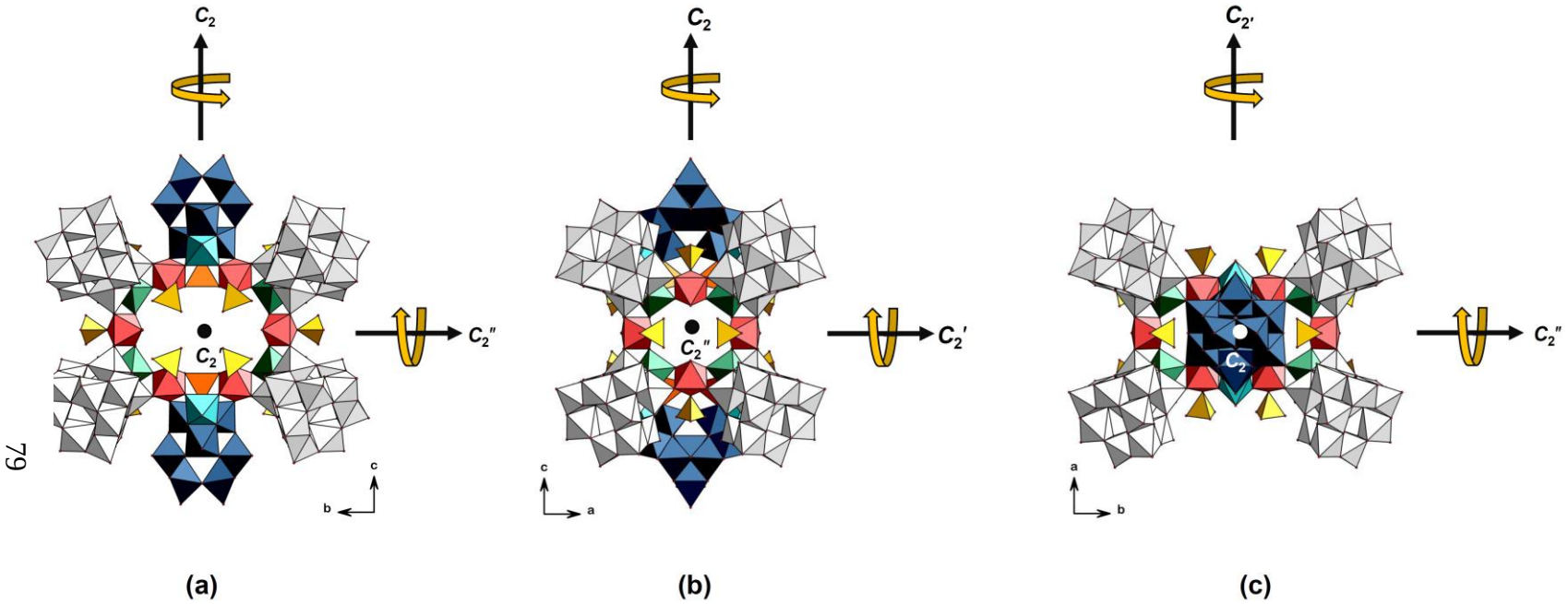

Figure 4.18 Polyhedral representation of *megaKeggin*-Al_{162} showing its C_2 axes viewed along (a) *a*-, (b) *b*-, and (c) *c*-axis.

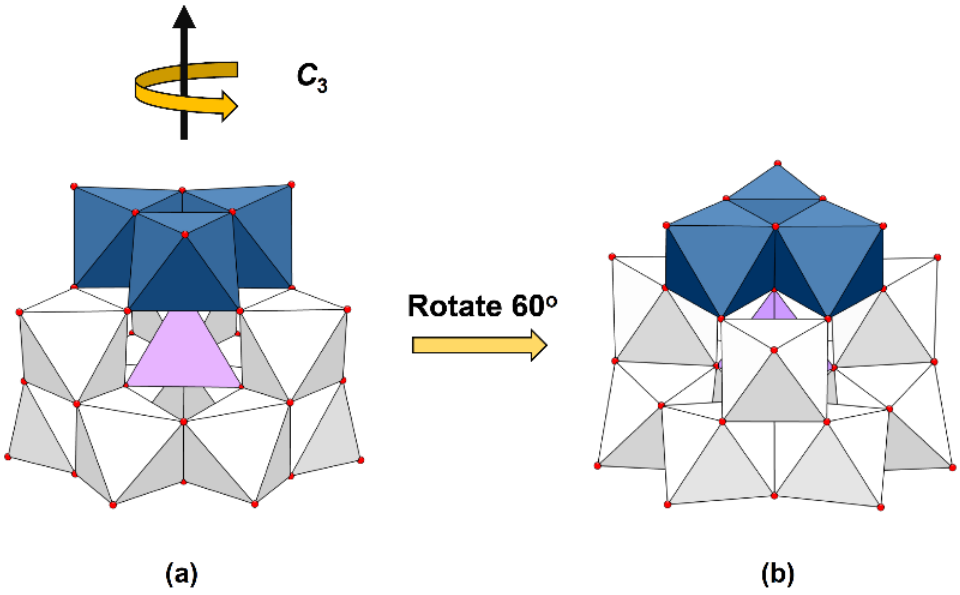

Figure 4.19 Graphical representation of *δ-Keggin*-Al_{13} SBUs. It comprises of tetrahedral $\{AlO_4\}$ core (purple) surrounded by four $\{Al_3O(OH)_9(H_2O)_3\}$ triads which are linked by edge sharing (white) and corner sharing (blue). (a) The principal rotation axis, C_3, is along the oxide centre of the corner sharing triad. The result of 60° rotation about C_3 axis is shown in (b).

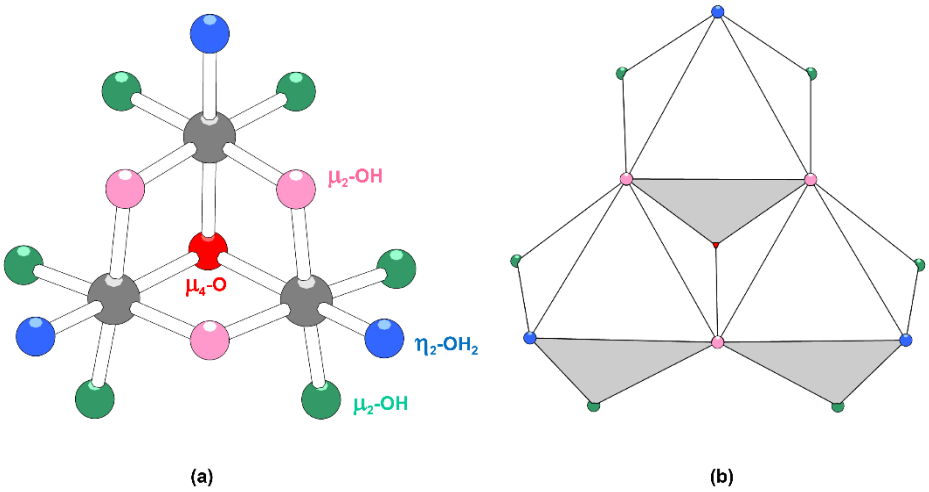

Figure 4.20 Triangle $\{Al_3O(OH)_9(H_2O)_3\}$ triad SBUs represented in (a) ball-and-stick and (b) polyhedral representation. Bridging oxides, μ_4-O, hydroxides, μ_2-OH and terminal ligating water molecules, η-OH_2, are labelled in red, pink and green, respectively.

Another isomer presenting in the *megaKeggin*-Al_{162} is *γ-Keggin*-Al_{13}. It has the same stoichiometric composition formula, $[AlO_4Al_{12}(OH)_{24}(H_2O)_{12}]^{7+}$, but different triad arrangements and point group symmetry. Whereas the *δ* isomer has C_{3v} point group, the *γ* isomer has C_{2v} point group symmetry. In the *γ-Keggin*-Al_{13}, two of the $\{Al_3O(OH)_9(H_2O)_3\}$ triads share an edge to each other, whereas the other two triads share their corners as illustrated in Figure 4.21. Due to its lower symmetry, the stability of the *γ* is lower than the *δ* isomer.[30] This is reflected by the fact that there is only one structure containing this Al_{13} isomer isolated and reported so far.[11]

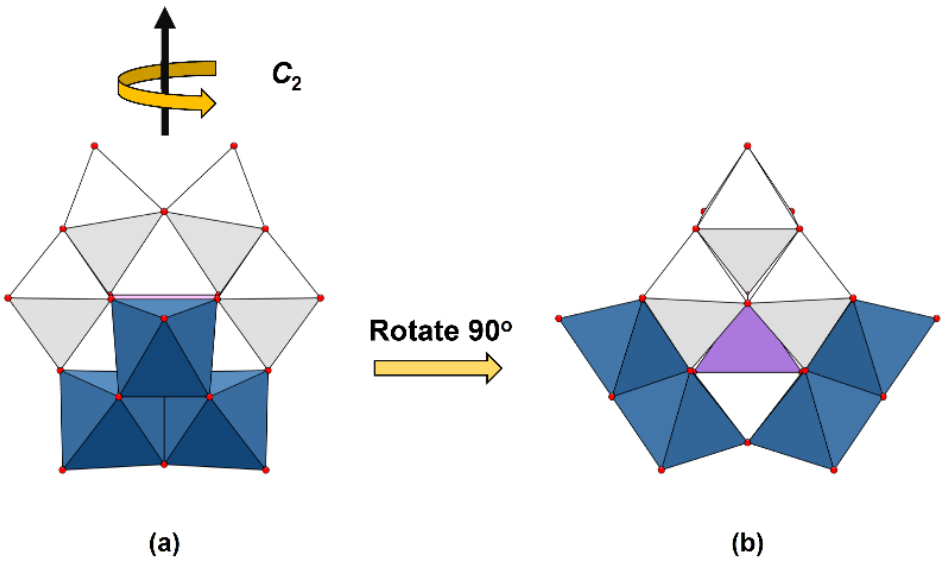

Figure 4.21 Graphical representation of *γ-Keggin*-Al_{13} SBUs. It composes of tetrahedral $\{AlO_4\}$ core (purple) surrounded by four $\{Al_3O(OH)_9(H_2O)_3\}$ triads which are linked by edge sharing (white) and corner sharing (blue). The principal rotation axis, C_2, is shown in (a). The results of 90° rotation about C_2 axis is shown in (b).

The *δ-Keggin*-Al_{13} polyoxocation is found in two forms of capped clusters, *i.e.* (i) sodium capped, $Na[AlO_4Al_{12}(OH)_{24}(H_2O)_{12}]^{8+}$ and aluminium monomer capped $[Al(OH)_3][AlO_4Al_{12}(OH)_{24}(H_2O)_{12}]^{7+}$.[5,7] The triaquasodium cation, $[Na(H_2O)_3]^+$, and the aluminium monomer usually cap on the face of a corner sharing triad as shown in Figure 4.22. In 2003, *Allouche et al.* proposed the role of the capping aluminium monomer in the isomerisation of *Keggin*-Al_{13} to *ε* to *δ* using evidences based on solution state ^{27}Al NMR studies.[31] *Abeysinghe et al.* proposed that sodium, as a heterocation, also exhibits an important role in the isomerisation process of the *Keggin*-Al_{13} polycation from *ε* to *δ*.[5] The Al_{30} and Al_{32} also comprise of $\{AlO_6\}$capped *δ*-

Keggin-Al_{13} as their SBUs.[5,7,13] This capping behaviour is also present in the eight *δ-Keggin*-Al_{13} SBUs of the *megaKeggin*-Al_{162} polyoxocation.

There is an octahedral AlO_6 cap that shares its face with corner-sharing triad and shares its edges with three $\{Al(OH)_4(H_2O)(SO_4)\}$ linker units as shown in Figure 4.23. A couple of these $\{Al(OH)_4(H_2O)(SO_4)\}$ units act as bridges between the *δ-Keggin*-Al_{13} and its two neighbour *δ-Keggin*s. Another unit links to the neighbour *γ-Keggin*. This kind of coordination behaviour of $\{Al(OH)_4(H_2O)(SO_4)\}$ units are found in Al_{32} sulphate which has been reported by *Sun et al*. in 2011.[13]

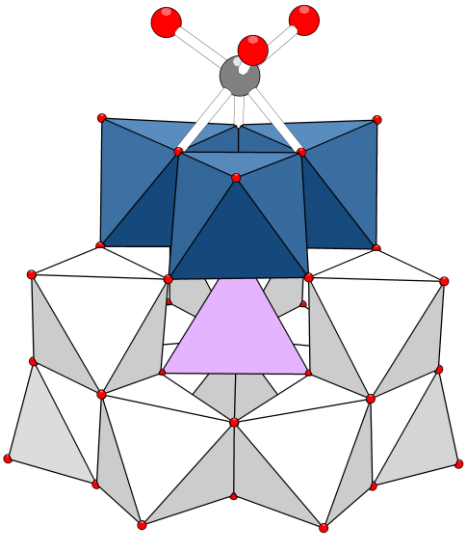

Figure 4.22 Polyhedral representation of *δ-Keggin*-Al_{13} with capping ML_3, where = Na^+ or Al^{3+} and L = H_2O and OH^-. Edge sharing and corner sharing triads are in white and blue, respectively.

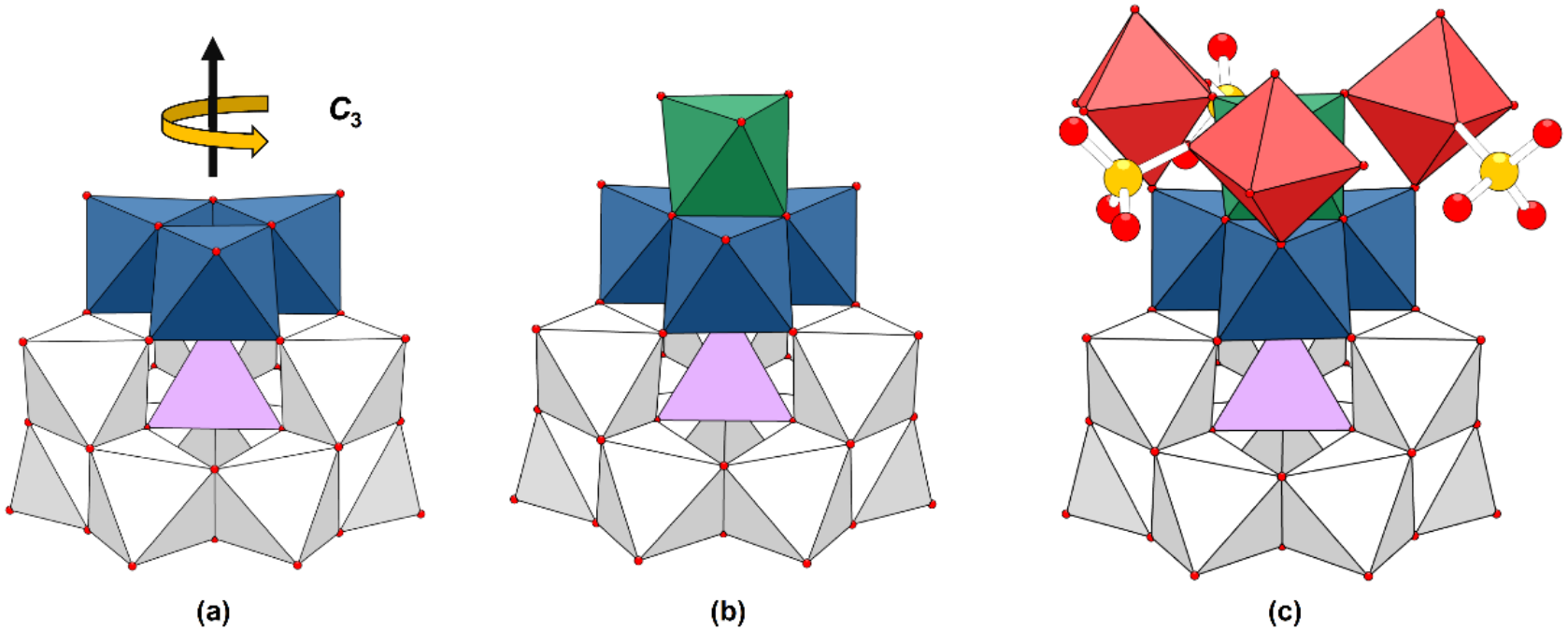

Figure 4.23 Graphical representation of (a) *δ-Keggin*-Al_{13} SBU showing corner-sharing triad (blue) with C_3 rotation axis (b) AlO_6 capped *δ-Keggin*-Al_{13} SBU with capping AlO_6 unit (green) and (c) *δ-Keggin*-Al_{13} SBU with three corner-sharing $\{Al(OH)_4(H_2O)(SO_4)\}$ units (red). Decorating sulphate anions are illustrated with ball-and-stick.

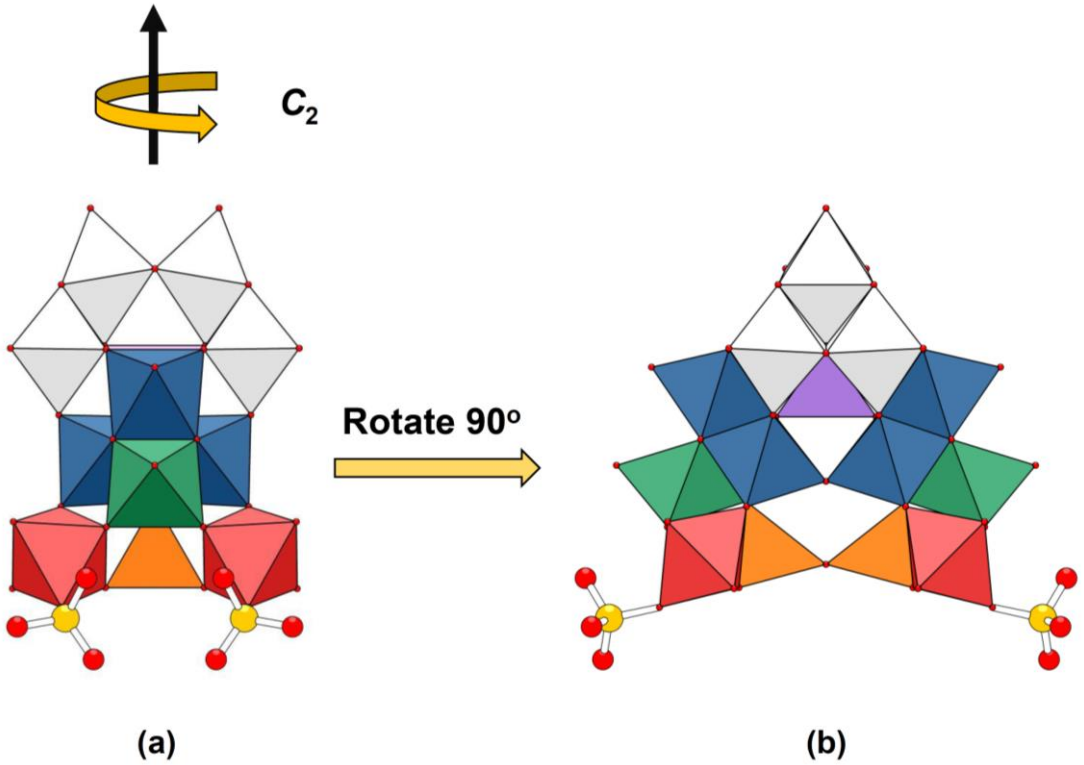

Figure 4.24 Graphical representation of γ-*Keggin*-Al_{13} SBU with octahedral capping AlO_6 (green), capping tetrahedral pyroaluminate, Al_2O_7 (orange) and $\{Al(OH)_4(H_2O)(SO_4)\}$ linkers (red) viewed along a-axis (a). Result of 90° about C_2 rotation axis is shown in (b). Decorating sulphate anions are represented with ball-and-stick.

Similarly, *γ-Keggin*-Al_{13} SBUs in *megaKeggin*-Al_{162} are capped by two octahedral AlO_6, as well as, a capping pyroaluminate $\{Al_2O_7\}$ unit as illustrated in Figure 4.24 and Figure 4.25. The capping $\{Al_2O_7\}$ acts as a bridge between four $\{Al(OH)_4(H_2O)(SO_4)\}$ units by corner sharing. The Al8 and $Al8^{i}$ are linked *via* a bridging oxide (O22). The Al8—O22—$Al8^{i}$ bond angle is close to linear, 174°. The Al8—O22 and $Al8^{i}$—O22 bonds have identical distances, 1.737(2) Å. According to the BVS calculation results O22 is assigned to O^{2-}. All O19, $O19^{i}$, $O19^{ii}$, O^{iii}, O5 and $O5^{i}$ are assigned to OH^{-}.

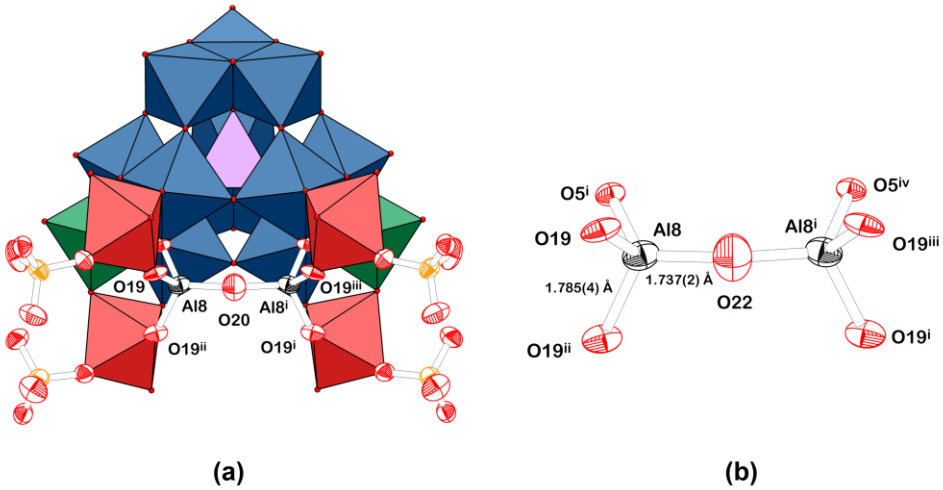

Figure 4.25 Graphical representation of (a) *γ-Keggin*-Al_{13} SBU (blue) with its capping units *i.e.* AlO_6 (green), Al_2O_7 (*ball-and-stick*) and $\{Al(OH)_4(H_2O)(SO_4)\}$ linkers (red). (b) Pyroaluminate $\{Al_2O_7\}$ units with atom and bond labels.

From the SBUs of the *megaKeggin*-Al_{162} polyoxocation, each *δ*- and *γ-Keggin*-Al_{13} SUBs links together *via* an Al_{32}-sulphate cage which are built from corner sharing of capping $\{AlO_6\}$, $\{AlO_5SO_4\}$ and $\{Al_2O_7\}$ SBUs. The Al_{32}-sulphate cage is illustrated in Figure 4.26. The assembly of *δ*- and *γ-Keggin*-Al_{13} SUBs and the Al_{32}-sulphate cage produce the *megaKeggin*-Al_{162} polyoxocation as shown in Figure 4.27.

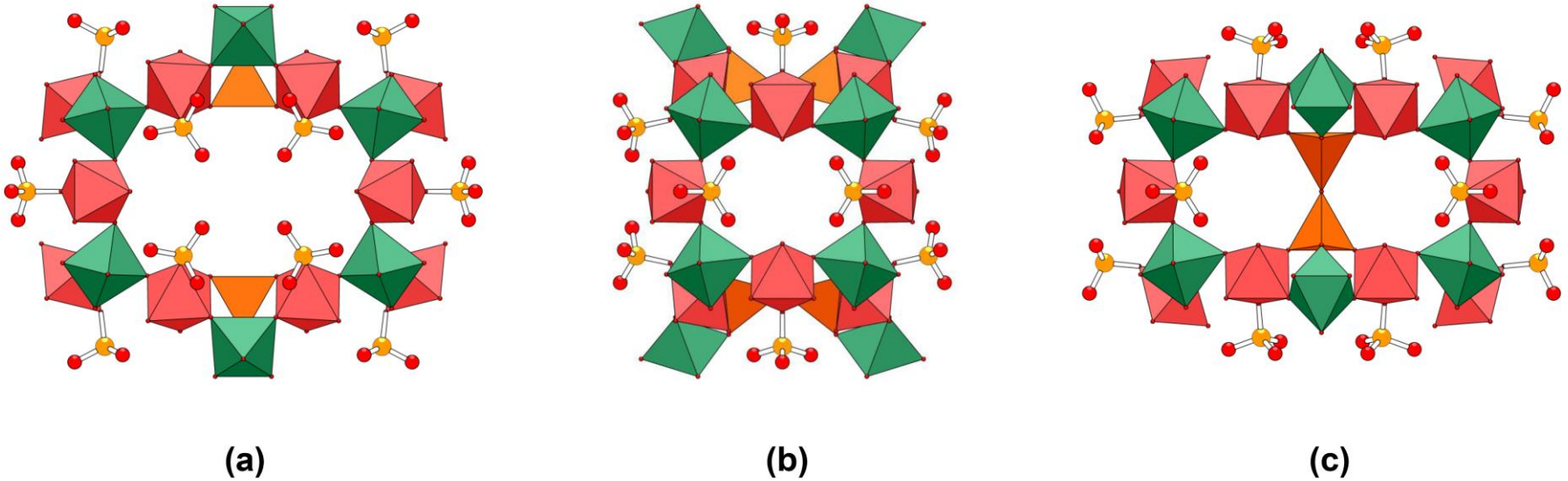

Figure 4.26 Graphical representations of Al_{32}-sulphate cage viewed along (a) *a*-, (b) *b*- and (c) *c*-axis. Capping $\{AlO_6\}$, $\{AlO_5SO_4\}$ and $\{Al_2O_7\}$ are in green, red, and orange, respectively. Coordinated sulphate anions are represented by ball-and-stick.

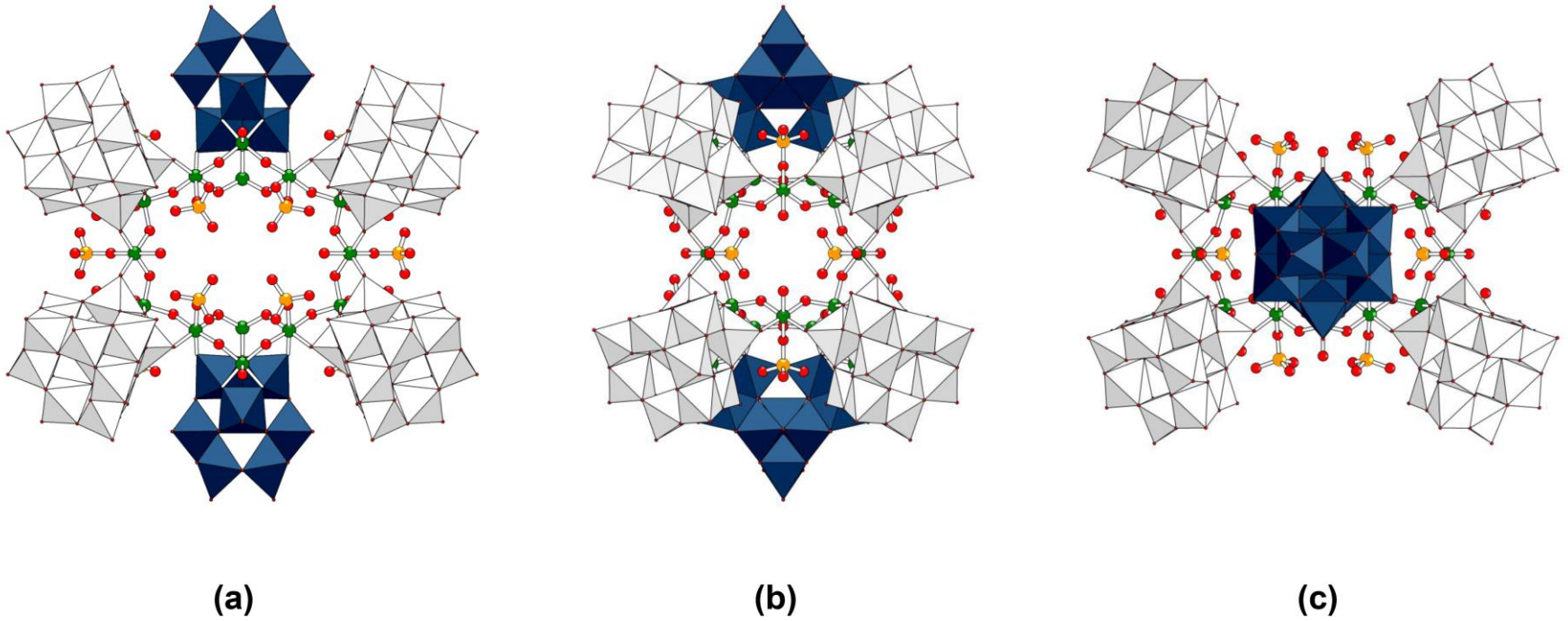

Figure 4.27 Graphical representations of *megaKeggin*-Al_{162} polyoxocation viewed along (a) *a*-, (b) *b*- and (c) *c*-axis. The δ- and γ-Al_{13} SBUs are represented by white and blue polyhedra, respectively. The Al_{32}-sulphate cage is represented by ball-and-stick.

4.2.5.2 Supramolecular assemblies of megaKeggin-Al_{162} polycation and polymorphism

The packing of *megaKeggin*-Al_{162} SBUs produces ionic porous structures. Each *megaKeggin*-Al_{162} polyoxocation in the crystal structure binds to its eight neighbouring clusters by hydrogen bonding and electrostatic interactions with intercalating units *i.e.* water molecules and sulphate anions, called *face-to-face* interaction. [32] This resulting in ionically porous architecture as shown in Figure 4.28. The rigidity of the *megaKeggin*-Al_{162} polyoxocation and the directionality of the *face-to-face* hydrogen bonding and ionic interaction results in the formation of a highly porous hydrogen-bonded extended structure. The contacting hexagonal faces of the *δ-Keggin*-Al_{13} SBUs in a *megaKeggin*-Al_{162} and its neighbour are parallel to each other. Each *megaKeggin*-Al_{162} cluster aligns perpendicularly to its neighbouring clusters. Rotations 90° about different C_2 axis results in different rotational polymorphs as illustrated in Figure 4.29. In MK-A, the neighbouring polyoxocations rotate by 90° about their C_2 axis (*see* Figure 4.18 and Figure 4.29 a). The supramolecular assemblies in MK-A result an open framework structure with mesopores. It contains large solvent accessible voids of 46,991 $Å^3$ (67% of the total unit cell volume). The largest pores are parallel to the *c*-axis and resemble those of the zeolite ACO topology with octagonal walls running the length of the structure (*see* Figure 4.30). The channels allow a penetrating sphere with a radius of 12.6 Å along the *c*-axis. Perpendicular to these, the channels along the *a*- and *b*- axes allow restricted access to these larger channels with non-linear channels allowing a largest penetrating sphere radius of 6 Å.

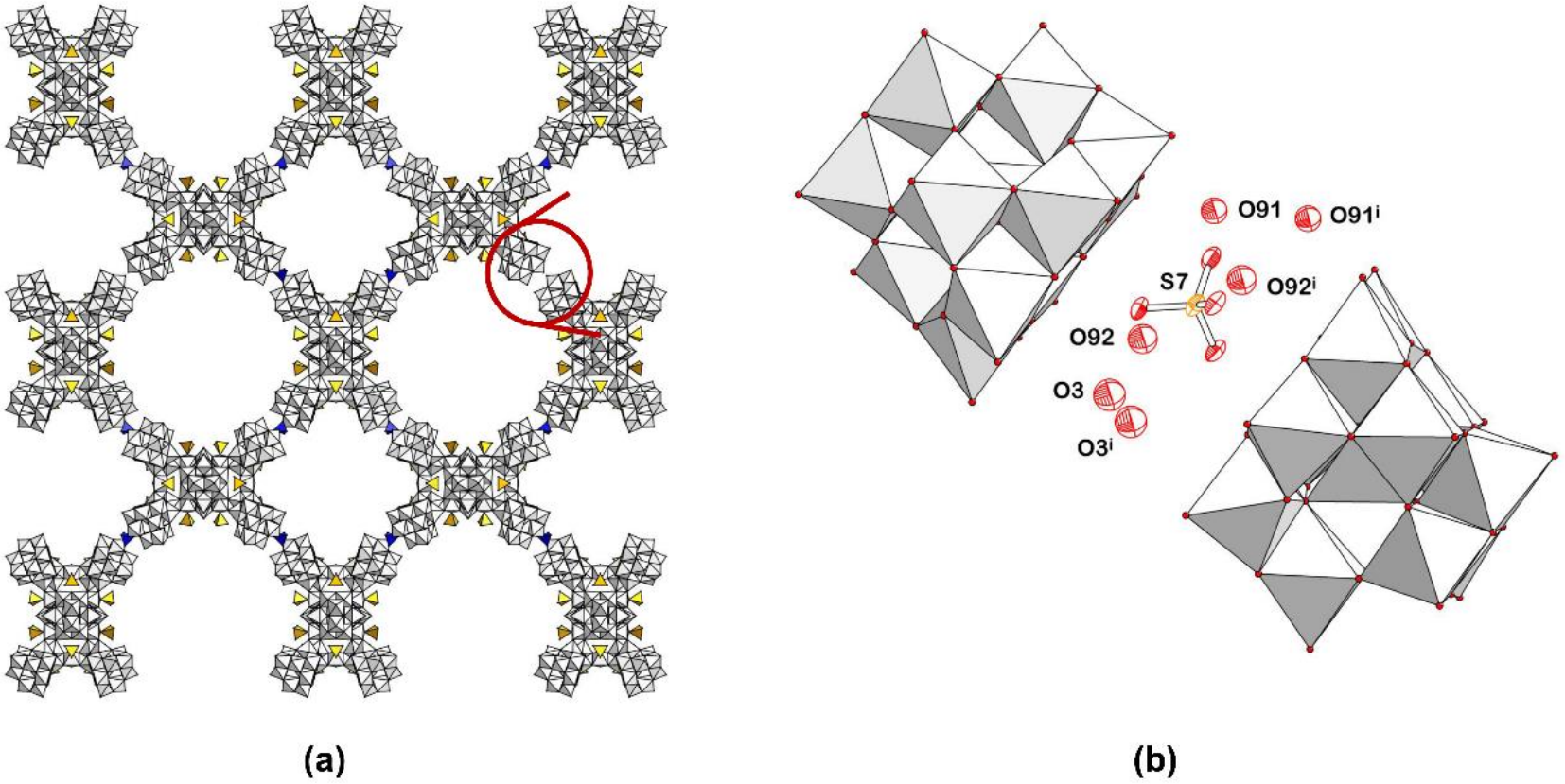

Figure 4.28 Polyhedral representation of (a) packing of *megaKeggin*-Al_{162} in MK-A and (b) zoomed intercalating sulphate anion and water molecule at the gap between each polyoxocation. Decorating and intercalating sulphate in (a) are yellow and blue, respectively. (Symmetry code: i = 1+*x*, 1−*y*, 1+*z*).

In case of MK-B, neighbouring clusters rotate 90° about C_2' (*see* Figure 4.18 and Figure 4.29 a), resulting a new rotational polymorph which also contains large solvent accessible voids of 51,129.3 $Å^3$ (69.7% of the total unit cell volume). The channels allow a penetrating sphere with a radius of 8.0 Å along the *c*-axis. The *a*- and *b*- axes allow restricted access to these larger channels with non-linear channels allowing a largest penetrating sphere radius of 7.4 Å. In MK-C, the neighbouring *megaKeggin*-Al_{162} clusters rotate 90° about the other C_2 axis (C_2'') (*see* Figure 4.18 and Figure 4.29). This results in the formation of the third rotational polymorphism with the largest spherical void radius of 10.80 Å (5276.67 $Å^3$, 70.14%). The largest channels are along *a*- and *b*-axes which allow a sphere of 9.20 Å to penetrate. The perpendicular channels (parallel to the *c*-axis) has radius of 7.00 Å.

The three polymorphic structures have similar tetragonally-distorted zeolite ACO topology.[33,34] As shown in Figure 4.30, we simplified the structural motif by linking each $\{AlO_4\}$ in the centre of each *δ-Keggin*-Al_{13} SBUs, and analyse topology using TOPOS program. Its vertex point symbol is $4^3.8^3$ and extended point symbol is $4.8_2.4.8_2.4.8_2$. Point symbol for net is $4^3.8^3$ and it is classified as 4-*c* uninodal net with ACO zeolite topology.

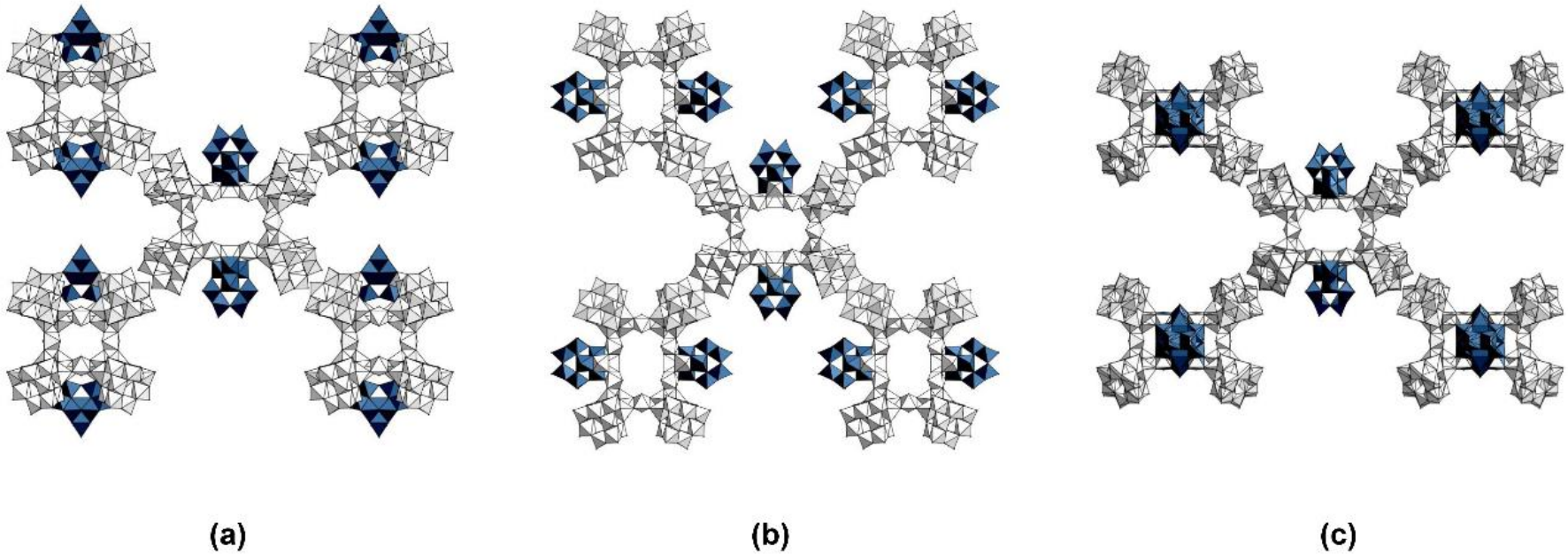

Figure 4.29 Graphical representations show the simplified structures of (a) MK-A (b) MK-B and (c) MK-C. The *γ-Keggin*-Al_{13} SUBs are represented by blue polyhedra. Coordinated and uncoordinated sulphate anions were omitted.

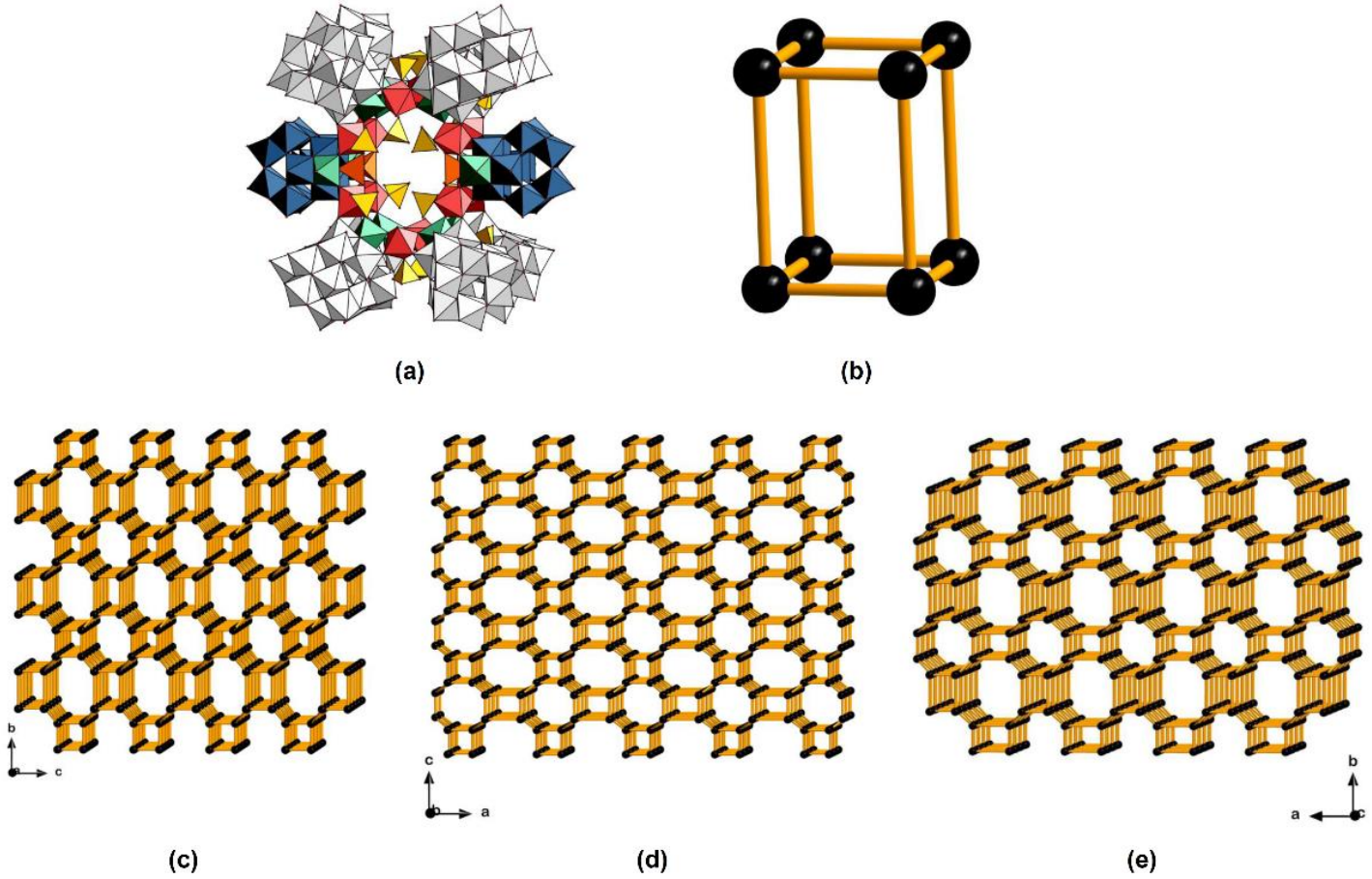

Figure 4.30 (a) A *megaKeggin*-Al_{162} polyoxocation as a structural motif represented by polyhedron, (b) simplified SBUs according to reticular chemistry approach of the *megaKeggin*-Al_{162} cluster, and topological structure of MK-A view along (c), *a*-, (d) *b*- and (e) *c*-axis, respectively.

4.2.6 Local structure analysis: solid state ^{27}Al NMR spectroscopy

Magic Angle Spinning (MAS) ^{27}Al NMR spectroscopic studies provide information about the local structure of the MK-A materials. As described above, X-ray crystal structure analysis, including single crystal and powder X-ray diffraction techniques, give useful information about structural properties of bulk materials of MK-A. A local structure of the MK-A materials was studied by solid state MAS ^{27}Al NMR spectroscopy as the results shown in Figure 4.31. Coordination environments of Al(III) in *megaKeggin*-Al$_{162}$ polyoxocation can be classified as listed in Table 4.6.

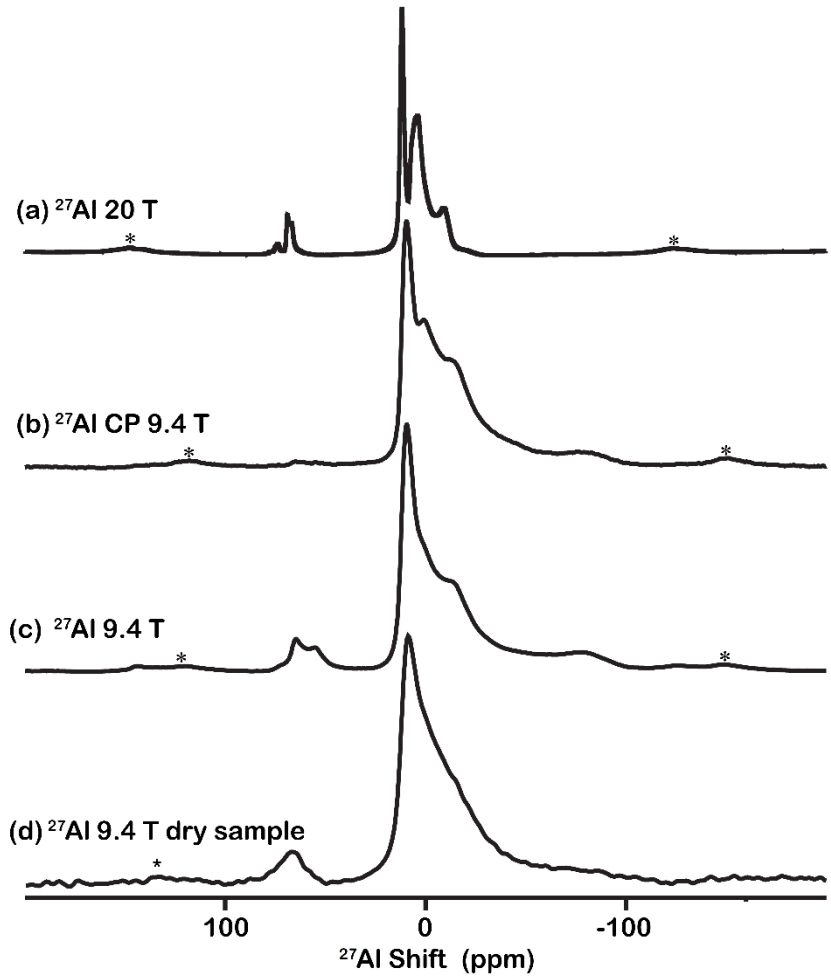

Figure 4.31 A stack plot of (a) 1D ^{27}Al MAS NMR spectra obtained at 20 T (b) 1D cross polarisation (CP) ^{27}Al MAS NMR spectrum at 9.4 T (c) ^{27}Al MAS NMR at 9.4 T on a fresh MK-A sample, (c) ^{27}Al MAS NMR at 9.4 T on a dry sample. The stars indicate spinning sideband from MAS.

Table 4.6 Parts of *megaKeggin*-Al_{162} polyoxocation classified by coordination geometries of aluminium.

Parts of Structure	**Coordination Geometry**	**^{27}Al Shift (ppm)**	**Number**
$\{AlO_4\}$ at the centre of *δ-Keggin*-Al_{13}	Tetrahedral	63	8
$\{AlO_4\}$ at the centre of *γ-Keggin*-Al_{13}	Tetrahedral	75	2
$\{Al_2O_7\}$ capping at *γ-Keggin*-Al_{13}	Tetrahedral	80	4
$\{AlO_6\}$ surrounding the *δ-Keggin*-Al_{13}	Octahedral	0 - 20	96
$\{AlO_6\}$ surrounding the *γ-Keggin*-Al_{13}	Octahedral	0 - 20	24
$\{AlO_6\}$ capping at the *δ-Keggin*-Al_{13}	Octahedral	0 - 20	8
$\{AlO_6\}$ capping at the *γ-Keggin*-Al_{13}	Octahedral	0 - 20	4
$\{AlO_5SO_4\}$ linkers	Octahedral	–20	16
Total			**162**

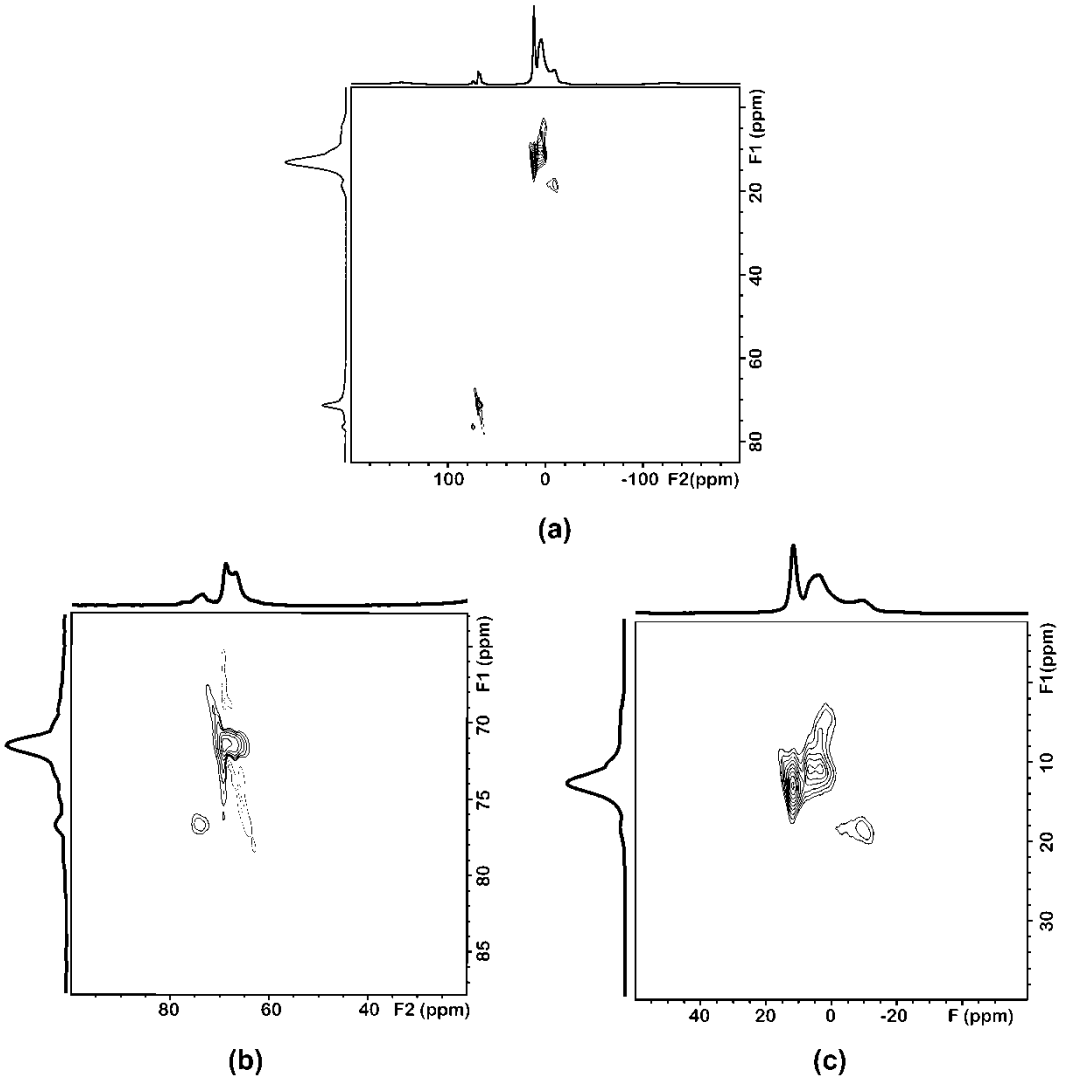

Figure 4.32 2D MAS ^{27}Al NMR spectrum of MK-A (a) full-spectrum (b) tetrahedral region and (c) octahedral region.

Aluminium-27 nuclei has a 5/2 spin number and ^{27}Al NMR spectra exhibit second order quadrupolar broadening. Tetrahedrally coordinated aluminium compounds have chemical shifts between 140 and 40 ppm, whereas octahedrally coordinated aluminium resonance between 40 and −46 ppm.[26] As shown in Figure 4.31, peaks of the resonances of tetrahedral {AlO_4} observed in range of 60 - 80 ppm and peaks of octahedral {AlO_6} are presenting near 0 ppm. Number of signals in each region was observed in 2D MAS ^{27}Al NMR spectrum (see Figure 4.32). Relative intensity and peak area reflects the ratio between each coordination geometries of aluminium. Resonance signals in the spectrum collected at low magnetic field (9.4 T) were improved by the measurement at higher field of 20 T (see Figure 4.31 a and c). PXRD patterns of the materials before and after MAS measurement were collected. The materials were still crystalline after MAS as we can see the indexed characteristic peaks of MK-A comparing with as-synthesised materials as shown in Figure 4.33. As mentioned before, the *megaKeggin*-Al_{162} lost its crystallinity at dryness. However, the characteristic MAS ^{27}Al NMR peaks of *megaKeggin*-Al_{162} were still observed for the dried sample (see Figure 4.31 d). This indicates that the *megaKeggin*-Al_{162} polyoxocation may be still present in the solid even if the supramolecular frameworks, particularly, hydrogen-bonded networks were destroyed by dehydration. Cross polarisation MAS ^{1}H/^{27}Al NMR result indicates the fact that octahedral {AlO_6} coordinate to OH^- and H_2O, while most of {AlO_4} tetrahedrons coordinated by oxides. A small signal in the tetrahedral region indicates that there is an {AlO_4} coordinates to OH^- which is capping the {AlO_4} near *γ-Keggin*-Al_{13} SBUs. These MAS ^{27}Al NMR results confirm the local structure of MK-A deduced by X-ray diffraction method previously.

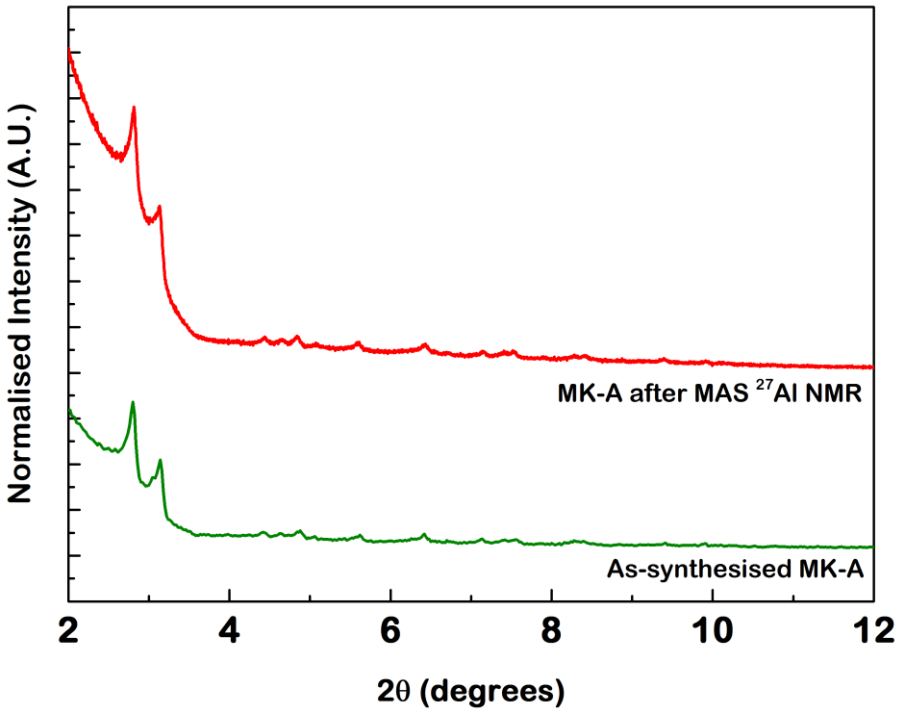

Figure 4.33 Comparison of PXRD patterns between MK-A materials before (green) and after (red) MAS NMR measurements.

4.3 Discussion

MegaKeggin-Al$_{162}$ polyoxocation comprises of two geometries of building blocks *i.e.* (i) tetrahedral {AlO_4} and SO_4^{2-} (ii) octahedral {AlO_6} and {AlO_5SO_4}. There was no sulphate precursor applied in the synthesis. The first part of the discussion will be focused on the generation of SO_4^{2-}. We propose that the desulphonation of NTS followed by the hydrolysis of SO_3 is the source of SO_4^{2-}, as illustrated in Scheme 4.1.

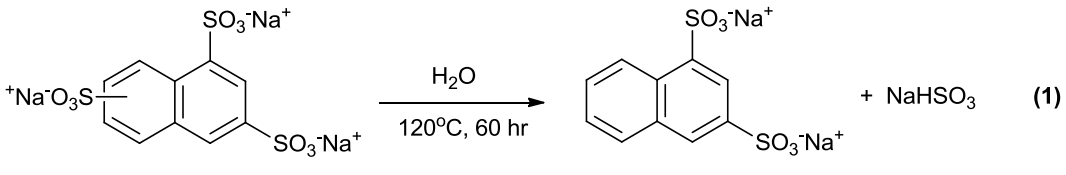

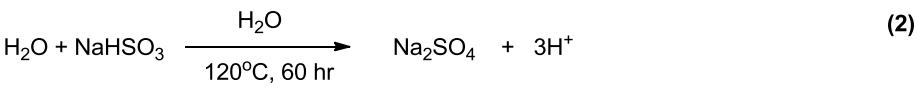

Scheme 4.1

Liquid Chromatography coupled with Mass Spectrometry (LC-MS) and ^{1}H NMR spectroscopy were applied to analyse the post-hydrothermal solution in order to track the reactions. The MS spectrum (*see* Figure 4.34) shows an obvious evidence of naphthalene-1,3-disulphonate anion (m/z = 143) which is a product of desulphonation of NTS (reaction (1) in Scheme 4.1). The ^{1}H NMR spectrum of post-hydrothermal solution shows evidence of naphthalene-1,3-disulphonate anions as shown in Figure 4.7. The desulphonation of NTS could generate SO_3.[27,35] From the studies of reaction between SO_3 and water by *E. R. Lovejoy et al.* and *K. Morokuma et al.*, we propose that the SO_3, an intermediate, rapidly reacts with water to produce H_2SO_4 which dissociates completely and produces SO_4^{2-} in the system (reaction (2) in Scheme 4.1).[36,37]

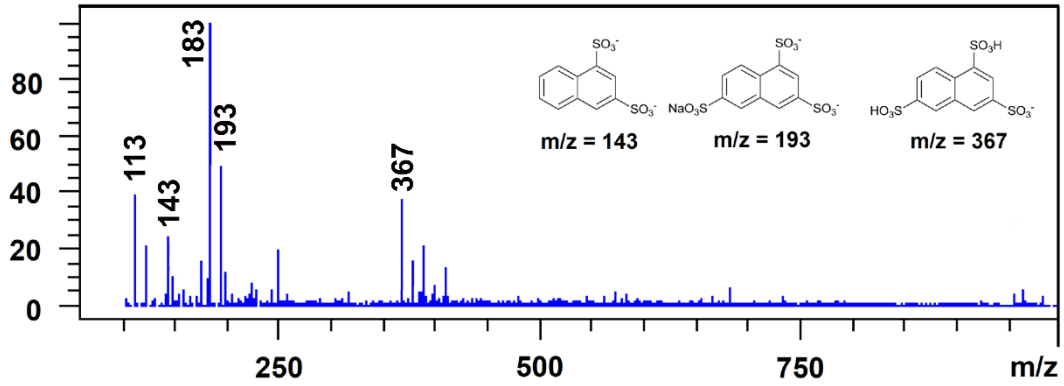

Figure 4.34 Mass spectrum of post-hydrothermal solution showing the presence of several organic species *e.g.* naphthalene-1,3-disulphonate (m/z = 143), 6-sulphonaphthalene-1,3-disulphonate (m/z = 193), 4,7-bis(sulpho)naphthalene-2-sulphonate (m/z = 367), and other unidentified anionic species.

Other tetrahedral building unit is a monomeric aluminium oxide anion, $\{AlO_4\}$. This building block can be formed by direct addition of base to Al(III) solution. $Al(OH)_4^-$ is produced and then links four $\{Al(OH)_6(H_2O)\}_3$ triads as a tetrahedral template to form *cage-like ε-Keggin*-Al_{13} structure.[25] The reaction without base injection, *e.g.* reduction of H^+ using Zn, leads the formation of *flat-like* or *core-link* Mögel-Al_{13} structure instead.[16] At low r_{OH} = 0.0, Al(III) is in form of octahedral $[Al(H_2O)_6]^{3+}$ complex cation in acidic solution. The Al(III) can be partially hydrolysed when base was dropped into the solution and polymerise to bigger species.

Olation is an important process in aluminium oxide and hydroxide chemistry that the Al(III) cations bridge *via* bridging ligands, especially, oxide and hydroxide to

form polymeric species.[38] An olation of Al(III) forming a trimeric $[Al_3(\mu_2\text{-}OH)_3(\mu_3\text{-}OH)(H_2O)_9]^{5+}$ cation in the partially hydrolysed Al(III) solution was observed by ^{27}Al NMR at $r_{OH} > 0.2$ (*see* Figure 4.5). This triad is an important building block for the formation of the ε-*Keggin*-Al_{13} SBUs. The ^{27}Al NMR of partially hydrolysed Al(III) shows a sharp peak at 63.5 ppm corresponding to ε-$[AlO_4Al_{12}(\mu_2\text{-}OH)_{24}(\eta\text{-}H_2O)_{12}]^{7+}$ as shown in the following olation reactions.

$$3[Al(H_2O)_6]^{3+} \rightleftharpoons [Al_3(OH)_4(H_2O)_9]^{5+} + 5H_2O + 4H^+ \quad (4.1)$$

$$4[Al_3(OH)_4(H_2O)_9]^{5+} + [Al(OH)_4]^- \rightleftharpoons \varepsilon\text{-}[AlO_4Al_{12}(OH)_{24}(H_2O)_{12}]^{7+} + 16H_2O + 12H^+ \quad (4.2)$$

The structure of trimeric $[Al_3(\mu_2\text{-}OH)_3(\mu_3\text{-}OH)(H_2O)_9]^{5+}$ is shown in Figure 4.35. The triad has a C_{3v} point-group symmetry. Three octahedra $\{AlO_6\}$ have the same coordination environment and resonance at the same chemical shift in ^{27}Al NMR spectrum, at 4.34 ppm. The olation processes (equation 4.1 and 4.2) releases H^+ into the solution. This causes the reduction of pH from 4.30 (pre-hydrothermal) to 3.60 (post-hydrothermal)

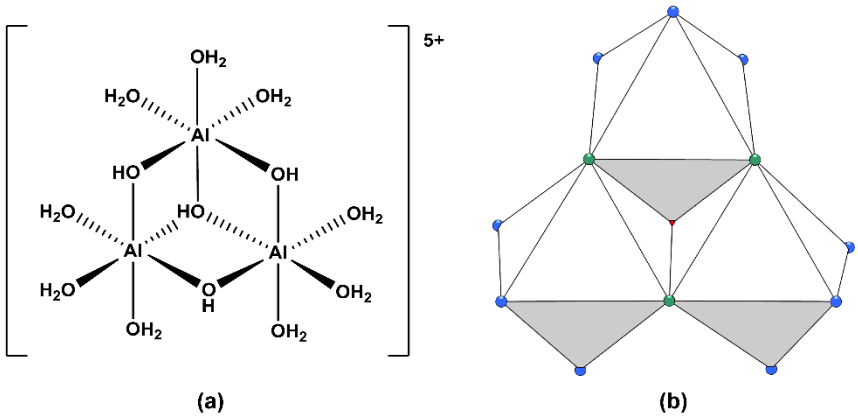

Figure 4.35 Trimeric $[Al_3(\mu_2\text{-}OH)_3(\mu_3\text{-}OH)(H_2O)_9]^{5+}$represented by (a) structural formula and (b) polyhedral representation.

Other important SBUs, which bridge each *Keggin*-Al_{13} to form the *megaKeggin*-Al_{162} polyoxocation, is an octahedrally monomeric $[Al(H_2O)_5(SO_4)]^+$ cation (denoted $\{AlO_5SO_4\}$. The presence of this monomeric species in post-hydrothermal solution was

confirmed by ^{27}Al NMR spectroscopy as shown in Figure 4.6. It could be generated from the reaction between $[Al(H_2O)_6]^{3+}$ and SO_4^{2-} as shown in the following equation.

$$[Al(H_2O)_6]^{3+} + SO_4^{2-} \rightleftharpoons [Al(H_2O)_5(SO_4)]^{+} + H_2O \qquad (4.3)$$

The presence of monomeric the $[Al(H_2O)_5(SO_4)]^{+}$ species was confirmed by a small peak at –3.21 ppm (*see* Figure 4.6).

There are two different bridging modes of $\{AlO_5SO_4\}$ linkers in *megaKeggin*-Al$_{162}$ *i.e.* (i) tetrakis(monodentate) and (ii) pentakis(monodentate) as illustrated in Figure 4.36. The tetrakis(monodentate) AlO_5SO_4 linkers, *i.e.* Al11 and Al12, share their equatorial edges with four neighbour octahedral AlO_6. The formula of this kind of linker is $[Al(\mu_2\text{-}OH)_4(\eta\text{-}H_2O)(\eta\text{-}SO_4)]^{3-}$. The Al—$OH_2$ bond, which is in *trans* position of Al—OSO_3 bond, has a longer distance. This can be explained by an inductive effect that the electronegative sulphate group has its ability to withdraw electrons in the molecule by induction effect and weaken the opposite Al—OH_2 bond.[39] In contrast, the pentakis(monodentate) $\{AlO_5SO_4\}$ has no ligated H_2O, but OH links to another AlO_4. The $\{AlO_4\}$ is more electronegative than SO_4^{2-}. This makes the Al—OSO_3 (1.924(5) Å) weak and has a longer distance than the opposite Al—OH bond (1.900(4) Å) (see Figure 4.36).

As described above, there was some direct evidence (from ^{27}Al NMR) for the presence of small building blocks of the *megaKeggin*-Al$_{162}$ cluster but we could not observe any direct evidence of the cluster in solution state. The isomerisation of *Keggin*-Al$_{13}$ from ε-isomer to *δ*- and *γ*-isomers occurred during the formation of *megaKeggin*-Al$_{162}$ polyoxocation. However, the isomerised polyoxocations were only observed in its solid state, by ^{27}Al MAS NMR and X-ray crystal structure.

The chemical formula of the MK-A materials elucidated by the X-ray crystal structure, local structure analysis and its chemical composition is $Na_2[2SO_4{\subset}Al_{162}(\mu_4\text{-}O_{44})(\mu_2\text{-}O)_2(\mu_3\text{-}OH)_{32}(\mu_2\text{-}OH)_{276}(\eta\text{-}H_2O)_{100}(\eta\text{-}SO_4)_{16}][SO_4]_{20}[C_{10}H_5S_3O_9]_4$ *c.a.* $90H_2O$. The high-ly positive charge of the *megaKeggin*-Al$_{162}$ polyoxocation was balanced by uncoordinated SO_4^{2-} and NTS^{3-}, which are closely positioned to the polyoxocation by electrostatic and hydrogen bonding interactions. Two sulphate anions were encapsulated in the polyoxocation. These could act as anionic templates for the polyoxocation as previously observed in spherical polyoxometalates.[40–42] Because of

these weak non-covalent networks and huge amount of solvent molecules in its mesopore, the structure collapses easily when dehydrated or desolvated. The crystal structure lost its crystallinity when it is dried. However, these open the opportunities for solvent and ion sorption and/or exchanges. Due to its stabilities in water and various organic solvents, potential applications of the MK-A are promising and described in the following chapters.

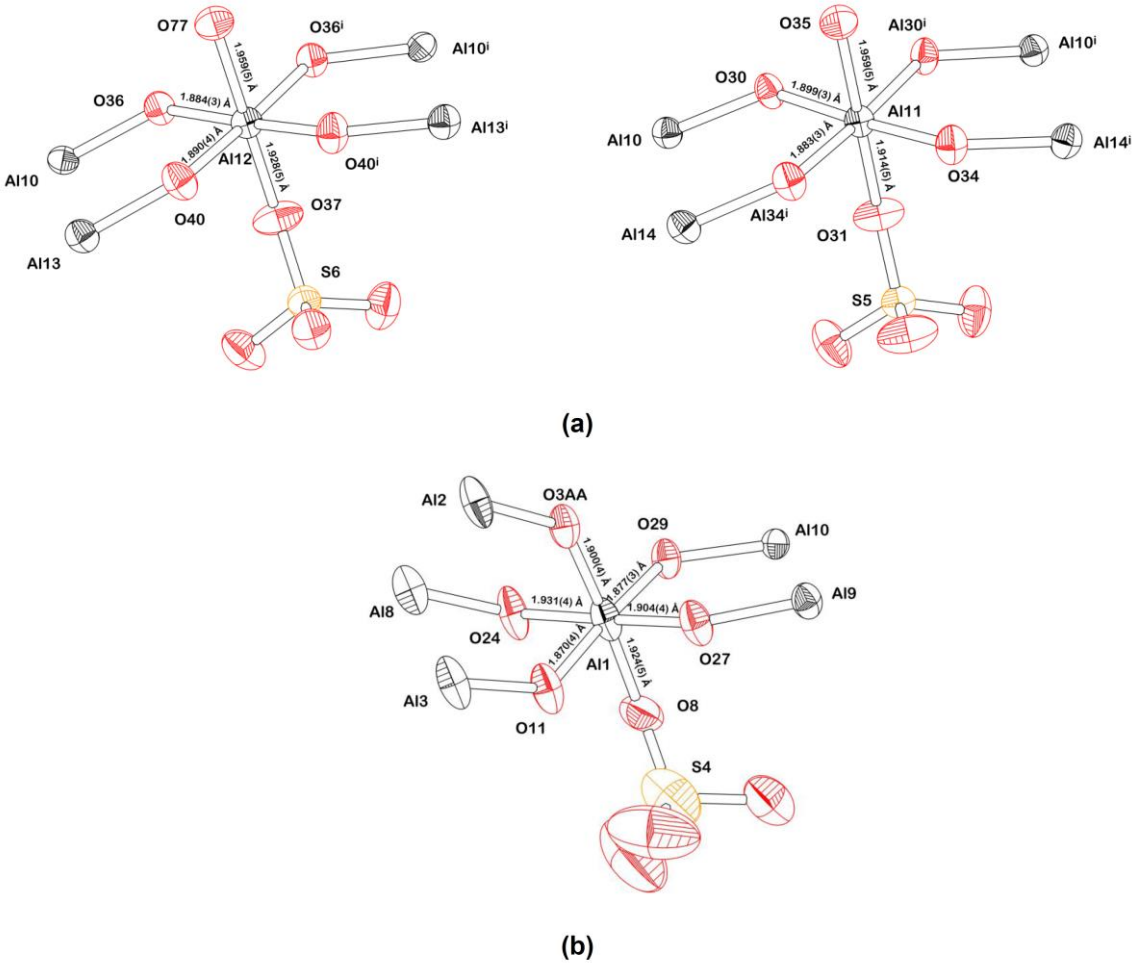

Figure 4.36 Thermal ellipsoids represent three crystallographically unique AlO_5SO_4 bridging units with two different modes of bridging *i.e.* (a) tetrakis(monodentate) and (b) pentakis(monodentate).

4.4 Conclusion

In summary, the work described in this chapter illustrates the discovery, synthesis and characterisation of a novel cage-like polyoxocation of aluminium containing two different isomers of *Keggin*-Al_{13}. The polyoxocation, formula $[2SO_4{\subset}Al_{162}(\mu_4\text{-}O_{44})(\mu_2\text{-}O)_2(\mu_3\text{-}OH)_{32}(\mu_2\text{-}OH)_{276}(\eta\text{-}H_2O)_{100}(\eta\text{-}SO_4)_{16}]^{50+}$, crystallises in three polymorphic structures. Among the three polymorphs, MK-A can be reproduced and scaled-up successfully. PXRD shows that there is no crystalline impurity in MK-A production. New ionic open framework architectures were obtained from supramolecular assemblies of cationic and anionic moieties. The topology of the open framework structure is similar to ACO zeotype-topology. The potential application studies of the MK-A are described in the following chapter.

Future work on *megaKeggin*-Al_{162} could include be the computational calculations of polymorphic structural landscape including energetic. Due to its exchangeable hydroxyl surface, solvent exchange rate could be another interesting area to study.

Bibliography

(1) Johansson, G. *Acta Chem. Scand.* **1960**, *14* (3), 771–773.

(2) Johansson, Georg; Lundgren, Georg; Sillén, Lars Gunnar; Söderquist, R. *Acta Chem. Scand.* **1960**, *14* (3), 769–771.

(3) Drljaca, A.; Hardie, M. J.; Raston, C. L. *J. Chem. Soc. Dalt. Trans.* **1999**, No. 20, 3639–3642.

(4) Mainicheva, E. A.; Gerasko, O. A.; Sheludyakova, L. A.; Naumov, D. Y.; Naumova, M. I.; Fedin, V. P. *Russ. Chem. Bull.* **2006**, *55* (2), 267–275.

(5) Abeysinghe, S.; Unruh, D. K.; Forbes, T. Z. *Cryst. Growth Des.* **2012**, *12* (4), 2044–2051.

(6) Allouche, L.; Gérardin, C.; Loiseau, T.; Férey, G.; Taulelle, F. *Angew. Chem. Int. Ed. Engl.* **2000**, *39* (3), 511–514.

(7) Rowsell, J.; Nazar, L. F. *J. Am. Chem. Soc.* **2000**, *122* (15), 3777–3778.

(8) Fairley, M.; Corum, K. W.; Johns, A.; Unruh, D. K.; Basile, M.; de Groot, J.; Mason, S. E.; Forbes, T. Z. *Chem. Commun. (Camb).* **2015**, *51* (62), 12467–12469.

(9) Casey, W. H. *Chem. Rev.* **2006**, *106* (1), 1–16.

(10) Furrer, G.; Phillips, B. L.; Ulrich, K.-U.; Pöthig, R.; Casey, W. H. *Science* **2002**, *297* (5590), 2245–2247.

(11) Smart, S. E.; Vaughn, J.; Pappas, I.; Pan, L. *Chem. Commun. (Camb).* **2013**, *49* (97), 11352–11354.

(12) André Ohlin, C.; Rustad, J. R.; Casey, W. H. *Dalton Trans.* **2014**, *43* (39), 14533–14536.

(13) Sun, Z.; Wang, H.; Tong, H.; Sun, S. *Inorg. Chem.* **2011**, *50* (2), 559–564.

(14) Son, J.-H.; Kwon, Y.-U. *Inorg. Chem.* **2004**, *43* (6), 1929–1932.

(15) Seichter, W.; Mögel, H.-J.; Brand, P.; Salah, D. *Eur. J. Inorg. Chem.* **1998**, *1998* (6), 795–797.

(16) Gatlin, J. T.; Mensinger, Z. L.; Zakharov, L. N.; Macinnes, D.; Johnson, D. W. *Inorg. Chem.* **2008**, *47* (4), 1267–1269.

(17) Icente, M.A., Lambert, J.-F. *Phys. Chem. Chem. Phys.* **1999**, *1* (7), 1633–1639.

(18) Schmitt, W.; Baissa, E.; Mandel, A.; Anson, C. E.; Powell, A. K. *Angew. Chem. Int. Ed. Engl.* **2001**, *40* (19), 3577–3581.

(19) Reinsch, H.; Marszałek, B.; Wack, J.; Senker, J.; Gil, B.; Stock, N. *Chem. Commun. (Camb).* **2012**, *48* (76), 9486–9488.

(20) Son, J.-H.; Kwon, Y.-U. *Inorg. Chem.* **2004**, *43* (6), 1929–1932.

(21) Son, J. H.; Kwon, Y.-U.; Han, O. H. *Inorg. Chem.* **2003**, *42* (13), 4153–4159.

(22) Abeysinghe, S.; Unruh, D. K.; Forbes, T. Z. *Inorg. Chem.* **2013**, *52* (10), 5991–5999.

(23) Corum, K. W.; Fairley, M.; Unruh, D. K.; Payne, M. K.; Forbes, T. Z.; Mason, S. E. *Inorg. Chem.* **2015**, *54* (17), 8367–8374.

(24) Abeysinghe, S.; Corum, K. W.; Neff, D. L.; Mason, S. E.; Forbes, T. Z. *Langmuir* **2013**, *29* (46), 14124–14134.

(25) Bi, S. *Coord. Chem. Rev.* **2004**, *248* (5-6), 441–455.

(26) Lars-Olof Öhman, U. E. *Encycl. Magn. Reson.* **2007**, 1–9.

(27) Rose, P. E.; Benoit, W. R.; Kilbourn, P. M. *Geothermics* **2001**, *30* (6), 617–640.

(28) Sheldrick, G. M. *Acta Crystallogr. A.* **2008**, *64* (Pt 1), 112–122.

(29) Dolomanov, O. V.; Bourhis, L. J.; Gildea, R. J.; Howard, J. A. K.; Puschmann, H. *J. Appl. Crystallogr.* **2009**, *42* (2), 339–341.

(30) Armstrong, C. R.; Casey, W. H.; Navrotsky, A. *Proc. Natl. Acad. Sci. U. S. A.* **2011**, *108* (36), 14775–14779.

(31) Allouche, L.; Taulelle, F. *Inorg. Chem. Commun.* **2003**, *6* (9), 1167–1170.

(32) Byrappa, K.; Keerthiraj, N.; Byrappa, S. M. *Handbook of Crystal Growth*; Elsevier, 2015.

(33) Baerlocher, C.; McCusker, L. B.; Olson, D. H. *Atlas of Zeolite Framework Types*; Elsevier, 2007.

(34) *Zeolite Structure Codes ABW to CZP*; Baur, W. H., Fischer, R. X., Eds.; Landolt-Börnstein - Group IV Physical Chemistry; Springer-Verlag: Berlin/Heidelberg, 2000; Vol. 14B.

(35) Rivera-Utrilla, J.; Sánchez-Polo, M.; Zaror, C. A. *Phys. Chem. Chem. Phys.* **2002**, *4* (7), 1129–1134.

(36) Lovejoy, E. R.; Hanson, D. R.; Huey, L. G. *J. Phys. Chem.* **1996**, *100* (51), 19911–19916.

(37) Morokuma, K.; Muguruma, C. *J. Am. Chem. Soc.* **1994**, *116* (22), 10316–10317.

(38) Jolivet, J.-P.; Chanéac, C.; Chiche, D.; Cassaignon, S.; Durupthy, O.; Hernandez, J. *Comptes Rendus Geosci.* **2011**, *343* (2-3), 113–122.

(39) Gineityte, V. *J. Mol. Struct. THEOCHEM* **2000**, *532* (1-3), 257–267.

(40) Miras, H. N.; Sorus, M.; Hawkett, J.; Sells, D. O.; McInnes, E. J. L.; Cronin, L. *J. Am. Chem. Soc.* **2012**, *134* (16), 6980–6983.

(41) Monakhov, K. Y.; Bensch, W.; Kögerler, P. *Chem. Soc. Rev.* **2015**, *44* (23), 8443–8483.

(42) Hutin, M.; Rosnes, M. H.; Long, D.-L.; Cronin, L. *Comprehensive Inorganic Chemistry II*; Elsevier, 2013.

(43) Ag, A.; Ix, T.; Hg, H.; Xi, T.; Xii, T.; Xiii, T. **1916**, *1448* (1913), 762–785.

(44) Akitt, J. W.; Elders, J. M.; Fontaine, X. L. R.; Kundu, A. K. *J. Chem. Soc. Dalt. Trans.* **1989**, No. 10, 1889–1895.

Chapter 5

Ion Exchange and Sorption Properties of MK-A Materials

5.1 Introduction

A porous solid is defined by IUPAC as a solid with pores, *i.e.* cavities, channels or interstices, which are deeper than they are wide.[1] Its pores can be classified into three categories depending on its size *i.e.* (i) Macropores: Pores with widths exceeding about 50 nm; (ii) Micropores: pores with widths not exceeding 2 nm; and (iii) Mesopores: pores of intermediate size.[2–4]According to this international criterion, MK-A, MK-B and MK-C are open framework with mesopores as described previously in Chapter 4. The three polymorphs comprise identical Al_{162} polyoxocations, which carry high positive charge of +50. The cationic building blocks are compensated by small counter anions *i.e.* SO_4^{2-} and NTS^{3-} and filled with neutral solvent molecules. Some of the SO_4^{2-} anions, particularly, the SO_4^{2-} intercalated between the inter-polycation gaps, and water molecules are key scaffolds of the porous architectures. The particular intercalating species provide a *face-to-face* hydrogen-bonded network between each polyoxocations and are not able to be exchanged or removed from the molecular structures. The rest of the anions are in the pore. These species could not be observed by diffraction technique but hinted by chemical analysis and fitted with charge-balance approximations. These anions and space-filling water molecules have potential properties in both cationic and neutral guest-exchanges and adsorptions *i.e.* SO_4^{2-}, $HAsO_4^{2-}$, and $C_{33}H_{38}N_2O_8S_2^{2-}$ ($Chromis^{2-}$).

Sixteen triangles hydroxyl faces of $\{Al_3O_{13}\}$ triads in the *δ-Keggin*-Al_{13} SUBs also offer positions for cations *i.e.* Na^+ and K^+ to bind. This interesting structure opens up challenging studies on cationic adsorption and exchange across the periodic table, especially, alkali metal cations.

In this chapter, the studies of potential properties in adsorption and ion exchange are described. Among the three polymorphs of megaKeggin-Al_{162}, MK-A has been synthesised and scaled-up successfully, whereas the other two polymorphs are obtained with time-consuming crystallising processes and with lower yields. So, the study detailed in this chapter focuses on MK-A.

5.2 Experimental

5.2.1 Materials and equipment

Most of chemicals were purchased from *Sigma Aldrich* and used without further purification (*see* Appendix SI0) Potassium 2-((1*E*,3*E*,5*E*)-5-(1-(5-carboxypentyl)-3,3-dimethyl-5-sulphonatoindolin-2-ylidene)penta-1,3-dienyl)-1-ethyl-3,3-dim-ethyl-3*H*-indolium-5-sulphonate (Chromis-645-A-*acid*, $KC_{33}H_{39}N_2O_8S_2$, ≥95%)) was purchased from Cyanagen Srl. Structural formula of Chromis-645-A-*acid* is shown in Scheme 5.1. It was selected to be an anionic dye in ion-exchange/sorption experiments due to the fact that it has sulphonate group which similar to NTS^{3-} in the pores.

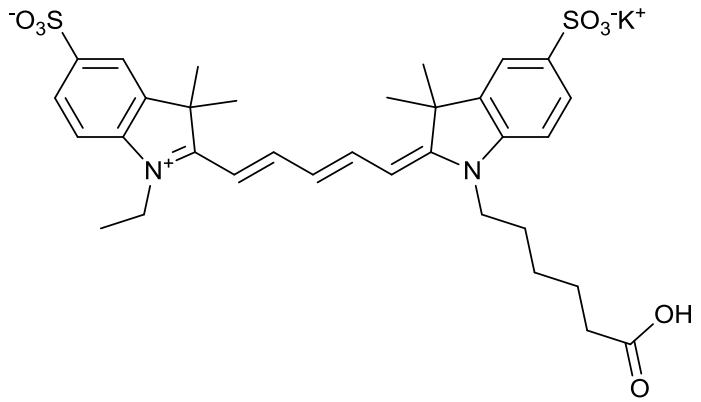

Scheme 5.1 Structural formula of Chromis-645-A-*Acid*

5.2.2 Ion exchange and/or sorption

The first experiment focuses on the sorption of alkali metal sulphates *i.e.* Na_2SO_4, K_2SO_4, Rb_2SO_4, and Cs_2SO_4. This allows the study of cation adsorption or exchange with $\{Na(H_2O)_3\}^+$, anion exchange of SO_4^{2-} with NTS^{3-}, and ionic salts adsorption. The second type of exchange is performed with an organic anionic dye, $Chromis^{2-}$. The third experiment studies the adsorption of a toxic As(V) compound, Na_2HAsO_4, by MK-A.

5.2.1.1 Alkali metal sulphates

Four 4-mL-glass vials containing freshly well-washed MK-A (5 mg each) and 1.00 mL of four sulphate salt solutions *i.e.* 0.10 M Na_2SO_4 (aq), 0.10 M K_2SO_4 (aq) and 0.10 M Rb_2SO_4 (aq) and 0.10 M Cs_2SO_4 (aq) were prepared. The solutions were transferred into the vials, 2.00 mL each, and left at room temperature for three days. ^1H

NMR and ICP (Al, S) of the supernatant were measured. Crystallinity of the final solids was confirmed by PXRD and single crystal X-ray diffraction was employed to elucidate the *post*-sorption/exchange crystal structures.

5.2.1.2 Anionic dye

Chromis 645-A-*acid*, a single negatively charged organic sulphonate dye was selected as a guest for sorption/exchange (structure as shown in Scheme 5.1). The experiments were designed to be static and dynamic solution as following.

5.2.1.2.1 Static Chromis 645-A-acid adsorption

A quartz cuvette containing freshly synthesised MK-A (50 mg) and 3 mL of 0.20 mg mL^{-1} Chromis-645-A-*acid* (aq) solution was prepared. UV-visible absorbance intensity at 647 nm of the solution was recorded every minute for 24 hours. ^{1}H NMR and ICP-OES (Al, S) of the supernatant were measured. Chromis-645-A-*acid* adsorption was quantified using a concentration *vs* absorbance calibration curve. CHN microanalysis and TGA of the final solid were used to estimate the chemical formula of the final solid. Crystallinity of the final solids was confirmed by powder and single crystal XRD.

2.2.1.2.2 Chromis 645-A-acid adsorption under gentle stirring

A glass vial containing MK-A (50 mg) and 10 mL of 0.20 mg mL^{-1} Chromis 645-A-*acid* (aq) solution was prepared and gently stirred by overhead stirrer (250 rpm). Absorbance spectra of 200 µL aliquots diluted by deionised water, in 5.00 mL volumetric flask, were collected at 30, 60, 90, 120, 150, 180 minutes, and 24 hours and then plotted. ^{1}H NMR and ICP-OES (Al, S) of the supernatant were measured at the end of the experiment in order to quantify NTS^{3-} and leaching Al, respectively. Chromis 645-A-*acid* adsorption was quantified using a concentration *vs* absorbance calibration curve. CHNS analysis and TGA of the final solid were used to estimate the formula of the final product. Crystallinity of the final solids was confirmed by PXRD and single crystal XRD.

5.2.1.3 Arsenate

Five, 12-mL, glass vial containing freshly MK-A (20 mg) and 5.00 mL of 5 ppm As(V) from Na_2HAsO_4 (aq) were prepared. Every 5-20 min the solid of one of the vials was separated from the supernatant *via* centrifugation (10,000 rpm for 1 min) and washed with deionised water. Aluminium, sulphur and arsenic content of the precipitates and supernatants were quantified *via* ICP-OES. Crystal stability of the final solid, after the anion exchange, was confirmed by PXRD and single crystal XRD using powder gently separated from the supernatant and washed with deionised water.

5.3 Results

5.3.1 Ion exchange and/or sorption

5.3.1.1 Alkali metal sulphates

Single crystal X-ray diffraction data of Na_2SO_4@MK-A, K_2SO_4@MK-A, Rb_2SO_4@MK-A, and Cs_2SO_4@MK-A were collected by Rigaku diffractometer (Mo K_α, λ = 0.71073 Å) at the University of Liverpool. The crystal structures were solved and refined by direct method in space group $P4_2/mmc$ using *SHLEXS* and *SHELXL via* Olex^2 program. Crystallographic information of the crystals compared with the as-synthesised MK-A is illustrated in Table 5.1. Selected bond distances and bond angles of Na_2SO_4@MK-A, K_2SO_4@MK-A, Rb_2SO_4@MK-A, and Cs_2SO_4@MK-A are listed in the Appendix. Samples for Na_2SO_4@MK-A, K_2SO_4@MK-A, Rb_2SO_4@MK-A, and Cs_2SO_4@MK-A were packed in glass capillaries (Ø = 0.7 mm) with their supernatant solutions. PXRD data were then collected by Cu Bruker (Cu K_α, λ =1.5406 Å) diffractometer in transmission geometry. The obtained PXRD patterns were indexed by X'pert High Score plus program using the unit cell parameters from the single crystal XRD analysis. The PXRD patterns comparison with as-synthesised MK-A are shown in Figure 5.1.

Table 5.1 Crystallographic information of MK-A, Na_2SO_4@MK-A, K_2SO_4@MK-A, Rb_2SO_4@MK-A, and Cs_2SO_4@MK-A.

Compounds	**MK-A**	**Na_2SO_4@MK-A**	**K_2SO_4@MK-A**
Empirical formula	$Al_{162}O_{666.01}S_{38}$	$Al_{162}Na_{11.46}O_{686.38}S_{38}$	$Al_{162}K_{14.57}O_{758.94}S_{41.31}$
Formula mass M_r	16382.55	16834.50	18408.24
Colour	Pale yellow	Colourless	Colourless
Crystal size	0.6 × 0.6 × 0.4 mm	0.6 × 0.6 × 0.4 mm	1.0 × 0.9 × 0.8 mm
Radiation	Mo Kα, λ = 0.71073 Å	Mo Kα, λ = 0.71073 Å	Mo Kα, λ = 0.71073 Å
T	100 K	100 K	100 K
Space group	$P4_2/mmc$	$P4_2/mmc$	$P4_2/mmc$
Z	16	16	16
a	44.8162 (3) Å	44.7329 (2) Å	45.0656 (3) Å
c	36.0041 (9) Å	34.8472 (4) Å	35.5632 (4) Å
Unit cell volume V	72394.3 (9) Å^3	69730.4(9) Å^3	72226.0 (1) Å^3
R_{int}	0.097	0.060	0.118
θ_{max}, θ_{min}	26.4°, 1.48°	26.4°, 1.90°	23.3°, 1.50°
Measured reflections	502330	347767	474141
Independent reflections	38378	36946	27202
Reflections with $I > 2\sigma(I)$	22299	26750	18235
$R[F^2 > 2\sigma(F^2)]$	0.112[*]	0.078[†]	0.126[‡]
$wR(F^2)$	0.380	0.263	0.417
S	1.29	1.07	1.66
Compounds	**Rb_2SO_4@MK-A**	**Cs_2SO_4@MK-A**	
Empirical formula	$Al_{162}O_{582.05}Rb_{10.14}S_{20.53}$	$Al_{162}Cs_{6.75}O_{585.58}S_{24.915}$	
Formula mass M_r	15208.06	16834.50	
Colour	Colourless	Colourless	
Crystal size	0.6 × 0.6 × 0.4 mm	0.6 × 0.6 × 0.4 mm	
Radiation	Mo Kα, λ = 0.71073 Å	Mo Kα, λ = 0.71073 Å	
T	100 K	100 K	
Space group	$P4_2/mmc$	$P4_2/mmc$	
Z	16	16	
a	44.6837 (2) Å	44.8747 (2) Å	
c	35.7450 (3) Å	35.9390 (3) Å	
Unit cell volume V	71369.9 (10) Å^3	72371.8 (8) Å^3	
R_{int}	0.105	0.088	
θ_{max}, θ_{min}	23.3°, 1.5°	20.4°, 1.50°	
Measured reflections	78327	80369	
Independent reflections	26888	18793	
Reflections with $I > 2\sigma(I)$	17966	14921	
$R[F^2 > 2\sigma(F^2)]$	0.161[ζ]	0.109[*]	
$wR(F^2)$	0.473	0.263	
S	1.34	1.07	

[*] $w = 1/[\sigma^2(F_o^2) + (0.2P)^2]$ where $P = (F_o^2 + 2F_c^2)/3$, [†] $w = 1/[\sigma^2(F_o^2) + (0.168P)^2 + 59.4312P]$, where $P = (F_o^2 + 2F_c^2)/3$,
[‡] $w = 1/[\sigma^2(F_o^2) + (0.2P)^2]$, where $P = (F_o^2 + 2F_c^2)/3$, [ζ] $w = 1/[\sigma^2(F_o^2) + (0.1P)^2]$, where $P = (F_o^2 + 2F_c^2)/3$

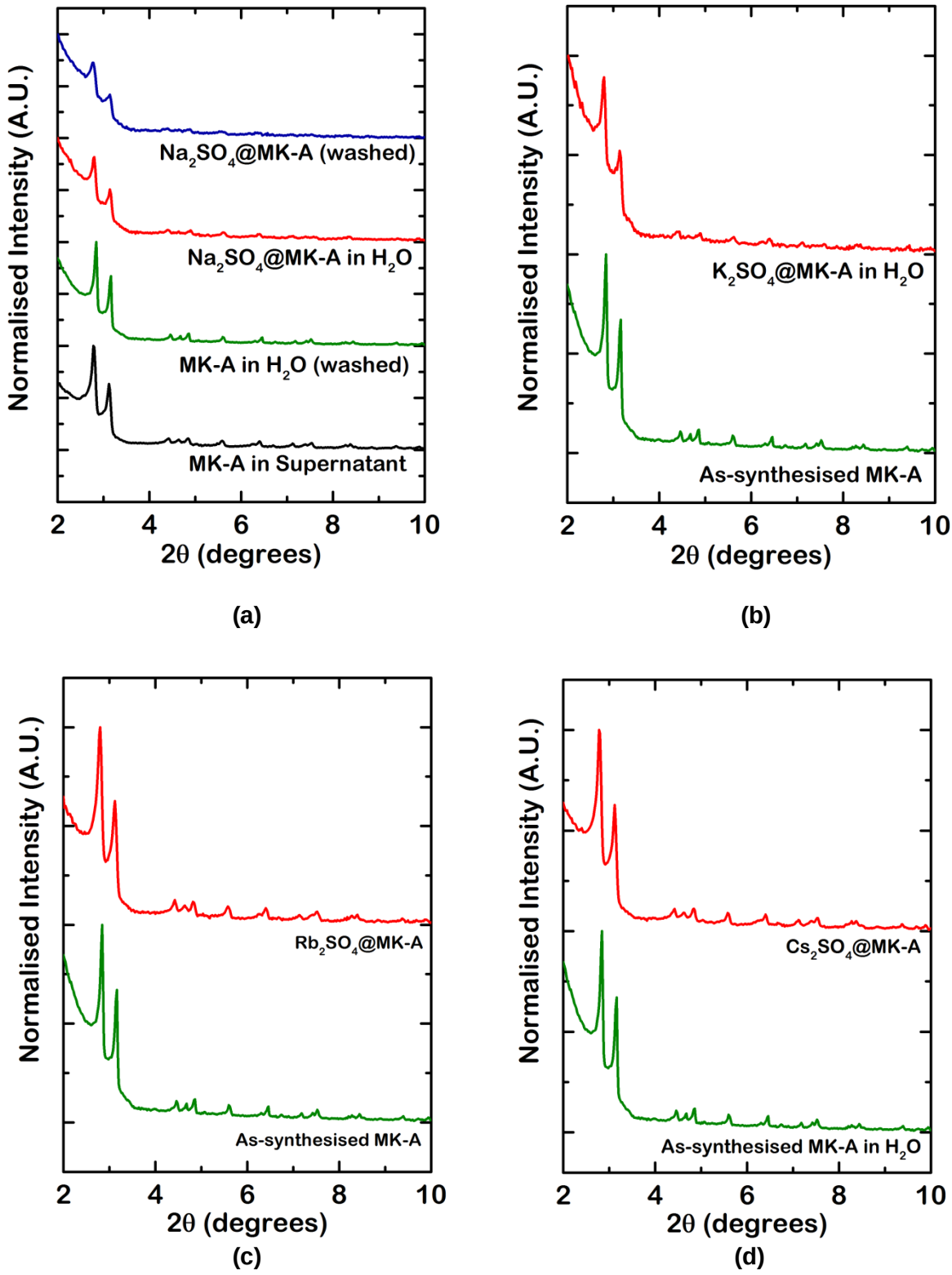

Figure 5.1 (a) Comparison between the PXRD patterns of fresh as-synthesised MK-A in the supernatant (black), as-synthesised MK-A in water (green), Na_2SO_4@MK-A (red) and washed Na_2SO_4@MK-A (blue). (b) Comparison between the PXRD patterns of fresh as-synthesised MK-A in water (green) and K_2SO_4@MK-A (red) (c) fresh as-synthesised MK-A in water (green) and Rb_2SO_4@MK-A (red), and (d) fresh as-synthesised MK-A in water (green) and Cs_2SO_4@MK-A (red) .

^{1}H NMR spectroscopy was applied to quantify NTS^{3-} anions in the supernatants of Na_2SO_4@MK-A and K_2SO_4@MK-A by standard calibration curve. The ^{1}H-NMR spectrum are illustrated in Figure 5.2.

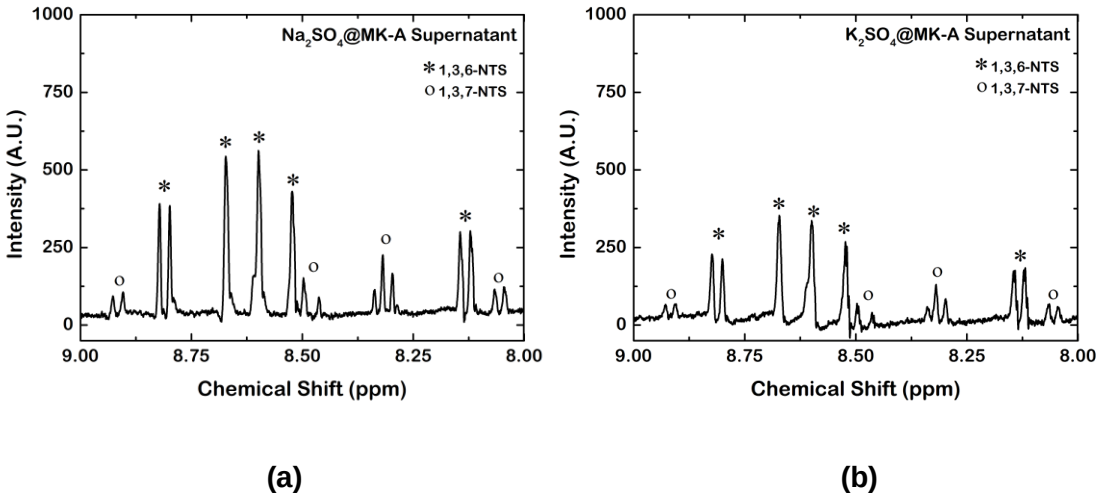

(a) **(b)**

Figure 5.2 ^{1}H NMR spectrum of (a) Na_2SO_4@MK-A supernatant and (b) K_2SO_4@MK-A supernatan. Peaks which corresponds to the resonance of 1,3,6-and 1,3,7-NTS are indexed by * and o, respectively.

5.3.1.2 Anionic dye

Reduction of an anionic dye, Chromis-645-A-*acid*, concentration in the supernatant of Chromis@MK-A were tracked by UV-visible absorption spectroscopic method as shown in Figure 5.3.

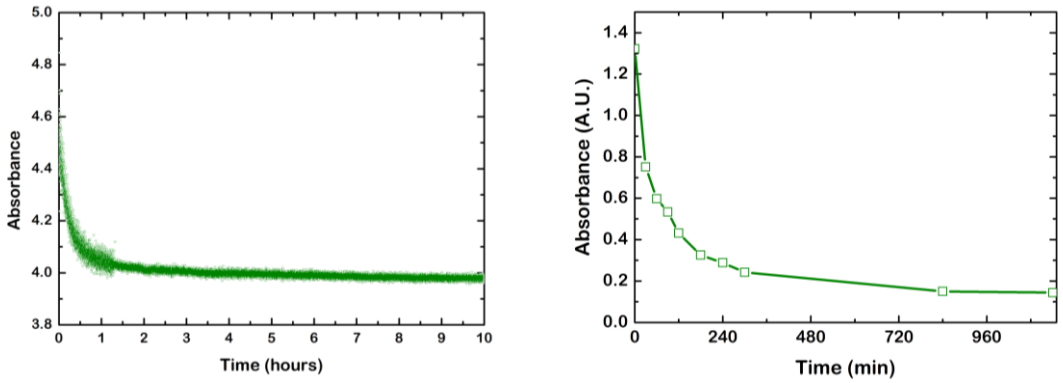

(a) **(b)**

Figure 5.3 Plot of UV-Visible absorbance at λ = 654 nm of the supernatant of chromis-645-A-acid (a) static and (b) dynamic adsorption experiment.

Degree of exchange/sorption for Chromis^{2-} was determined by chemical composition CHN microanalysis, TGA/DTA and ^{1}H NMR quantification. The TGA/DTA results, as shown in Figure 5.5. Final product of the combustion at 1300°C is alumina, Al_2O_3, confirmed by PXRD and EDX (*see* Figure 5.5 c and d).

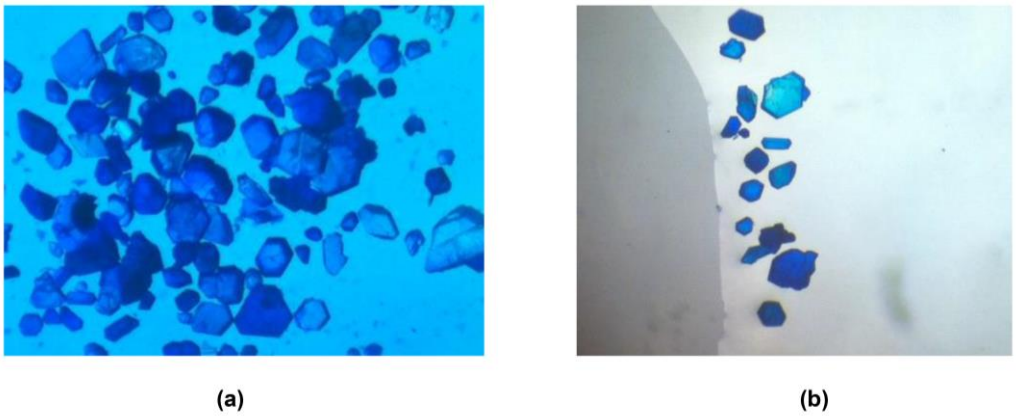

Figure 5.4 (a) Chromis@MK-A in its supernatant and (b) Chromis@MK-A after washed by deionised water.

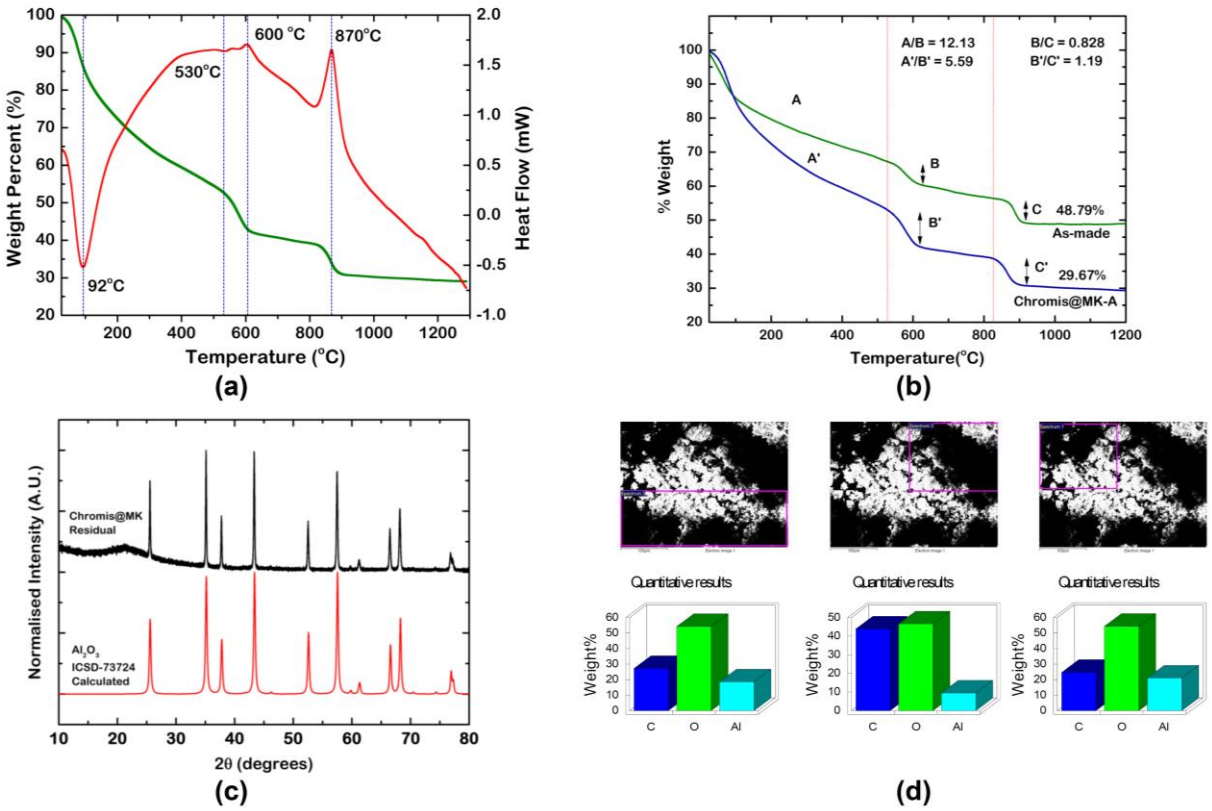

Figure 5.5 (a) TGA/DTA of Chromis@MK-A from static exchange/sorption experiment (b) comparison of TGA of Chromis@MK-A (blue) and as-made MK-A (green) (c) comparison of PXRD patterns of TGA residual solid of Chromis@MK-A (black) and the calculated pattern of Al_2O_3 (ICSD-73724, red)

and (d) EDX results showing the areas of elemental analysis (above) with quantitative result histogram (below).

^{1}H NMR was applied to analyse the presence of NTS^{2-} in the supernatant as shown in Figure 5.6. Crystallinity of the materials was checked by PXRD. The PXRD pattern is shown in Figure 5.7.

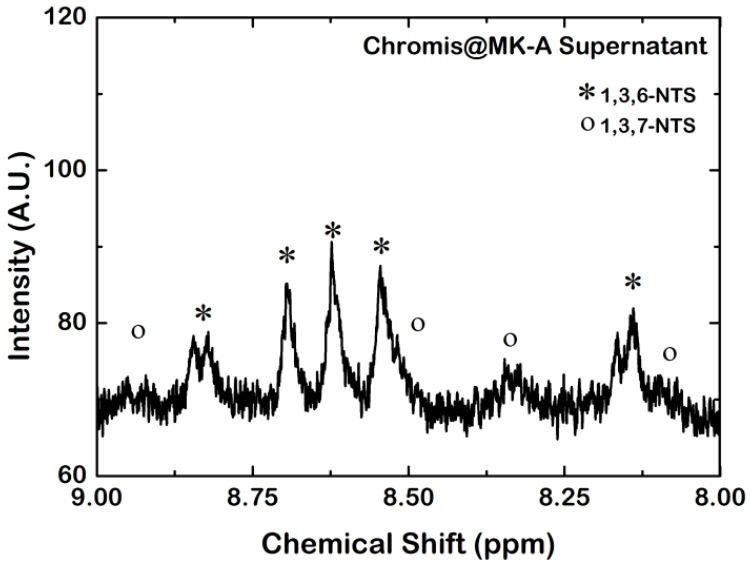

Figure 5.6 ^{1}H NMR of Chromis@MK-A supernatant showing the presence of (i) 1,3,6-NTS (*) and (ii) 1,3,7-NTS (o).

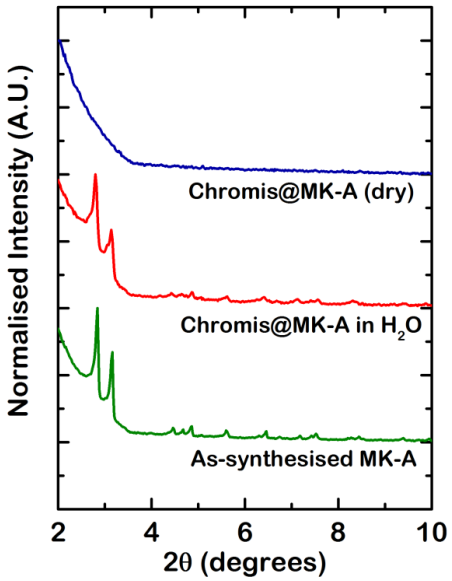

Figure 5.7 Comparison of PXRD patterns of fresh as-synthesised MK-A (green) in water, Chromis @MK-A in water (red) and dry Chromis@ MK-A (blue).

5.3.1.3 Na_2HAsO_4@MK-A

ICP-OES was used to quantify As(V) concentration in solution as a function of time. The plot of As(V) concentration is shown in Figure 5.8. Crystallinity of the solid was measured by PXRD. The PXRD pattern comparison with as-synthesised MK-A is shown in Figure 5.9. Comparison of As(V) removal capacity in milligrams of As(V) per grams of materials between the MK-A, commercial active carbon, ZIF-8 and ZIF-8-MeOH is illustrated in Figure 5.10.[5]

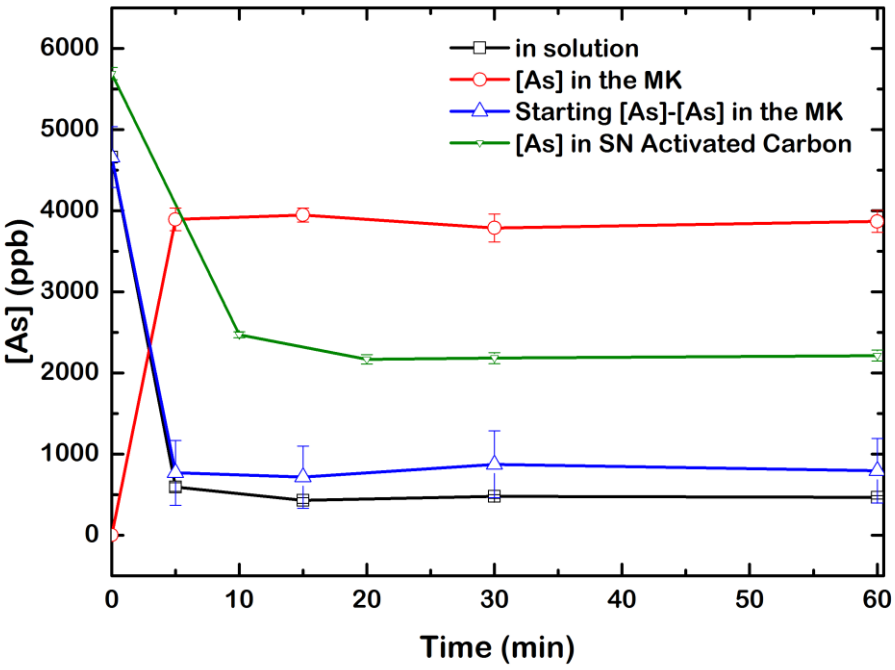

Figure 5.8 Plot of As concentration in ppm (analysed by ICP) of supernatant (green), digested As@MK-A solids (red), and the difference between starting As concentration and concentration of As presented As@MK-A.

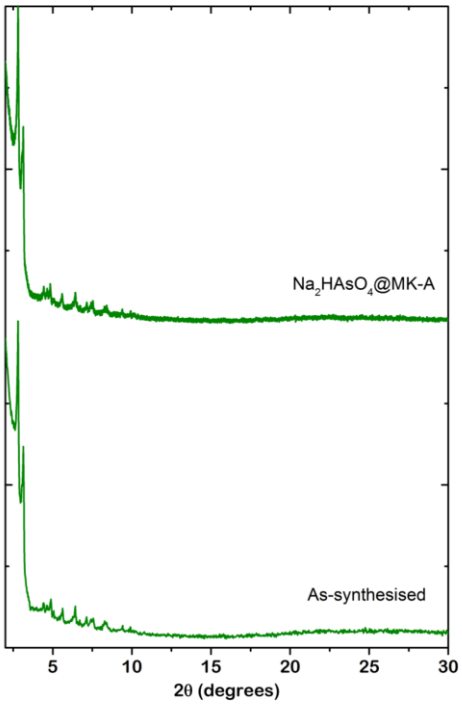

Figure 5.9 Comparison of PXRD of (i) As@MK-A (above) in its supernatant and (ii) as-synthesised MK-A in water.

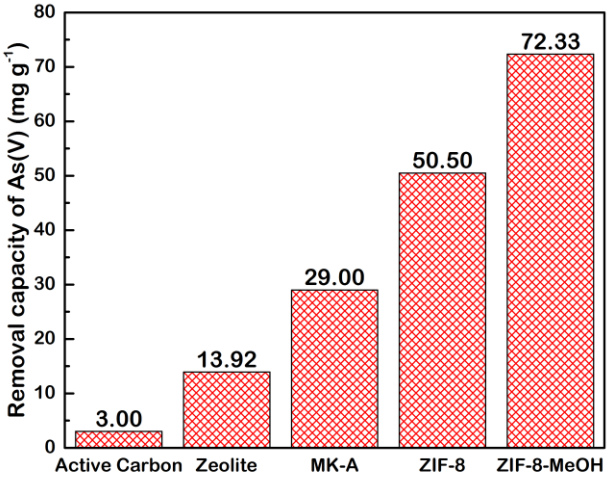

Figure 5.10 Comparison of the removal capacity of As (V) by commercial active carbon, zeolite, MK-A, normal ZIF-8 synthesized in water, ZIF-8 synthesised in methanol. The histogram was adapted from Ref. 5.

5.4 Discussion

As mentioned before, the megaKeggin-Al_{162} polycation provides many positions for $\{M(H_2O)_n\}^+$ cations, where M = alkali metals, to bind on its surface. From the single crystal X-ray structural analyses, MK-A soaked in four alkali metal sulphate solutions *i.e.* Na_2SO_4, K_2SO_4, Rb_2SO_4, Cs_2SO_4, for three days, show that the hydrated complexes of the cations attach on the surface of MK-A cluster.

In case of Na_2SO_4@MK-A, there are eighteen coordination sites for $\{Na(H_2O)_n\}^+$ on megaKeggin-Al_{162} cluster observed in single crystal X-ray structure as illustrated in Figure 5.11. List of all crystallographically unique Na—O bond distances and O—Na—O bond angles is in the Appendix (*see* Table SI3.2). The bond distances and bond angles are corresponding to coordination properties of Na—O.[6–9] Coordination environments of $\{Na(H_2O)_n\}^+$ can be classified into two types. First, $\{Na(H_2O)_n\}^+$ units cap onto sixteen $\{Al_3O_9\}$ triads on the eight δ-Keggin-Al_{13} parts of the cluster. These Na^+ cations have coordination number of six with distorted triangular antiprism geometry as represented by green atoms in Figure 5.12. This kind of capping $\{Na(H_2O)_n\}^+$ cation was previously found in two reported δ-Keggin-Al_{13}-based structures *i.e.* δ-Keggin-Al_{13} sulphate (*Rowsell et al.* in 2000) and δ-Keggin-Al_{13} naphthalene-2,6-disulphonate (*Frobes et al.* in 2012).[10,11] The Na—O bonds in the distorted triangular antiprism $\{NaO_6\}$ falls in range of 2.299 (10)-2.610 (5) Å which agree with previously reported structures, [6–9] however, there is no significant difference in bond length between Na—OH_2 (η-H_2O molecules) and Na—OH (μ_2-OH in $\{Al_3O_{13}\}$ moieties). However, bond angles are more different. The O—Na—O bond angles between μ_2-OH of the triads and Na^+ are in range of 63.03(12)° - 64.59 (14)°, which are much smaller angles comparing to those bonds between η-OH_2 molecules and Na^+ (101.3(6)° - 109.2(6)°) (*see* Figure 5.12 a). The second type of $\{Na(H_2O)_n\}^+$ has augmented triangular prism geometry as shown in Figure 5.12 b. The Na^+ cations are chelated by four decorating sulphate anions. Since the coordination number of Na^+ is seven, the rest of coordination sites are filled with three ligated H_2O molecules. The Na—O bond lengths in this augmented triangular prism $\{NaO_7\}^+$ are in a range of 2.384 (4) - 2.468 (13) Å. Three coordinated H_2O ligands arrange in triangle plane perpendicular with the square planar $\{Na(SO_4)_4\}$ as shown in Figure 5.12 b.

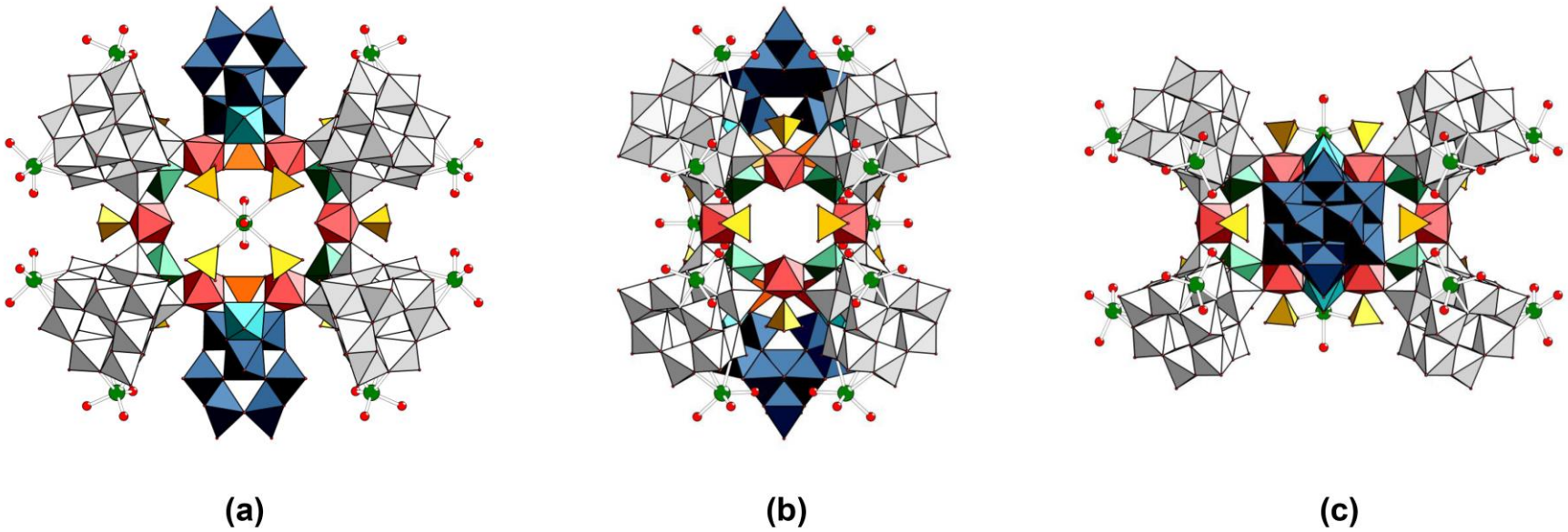

Figure 5.11 Polyhedral representation of megaKeggin-Al_{162} polyoxocation after soaked in 0.10 M Na_2SO_4 for three days viewed along (a) *a*- (b) *b*- and (c) *c*-axis. $\{Na(H_2O)_3\}^+$ represented by ball-and-stick style. Oxygen and sodium atoms are in red and green, respectively.

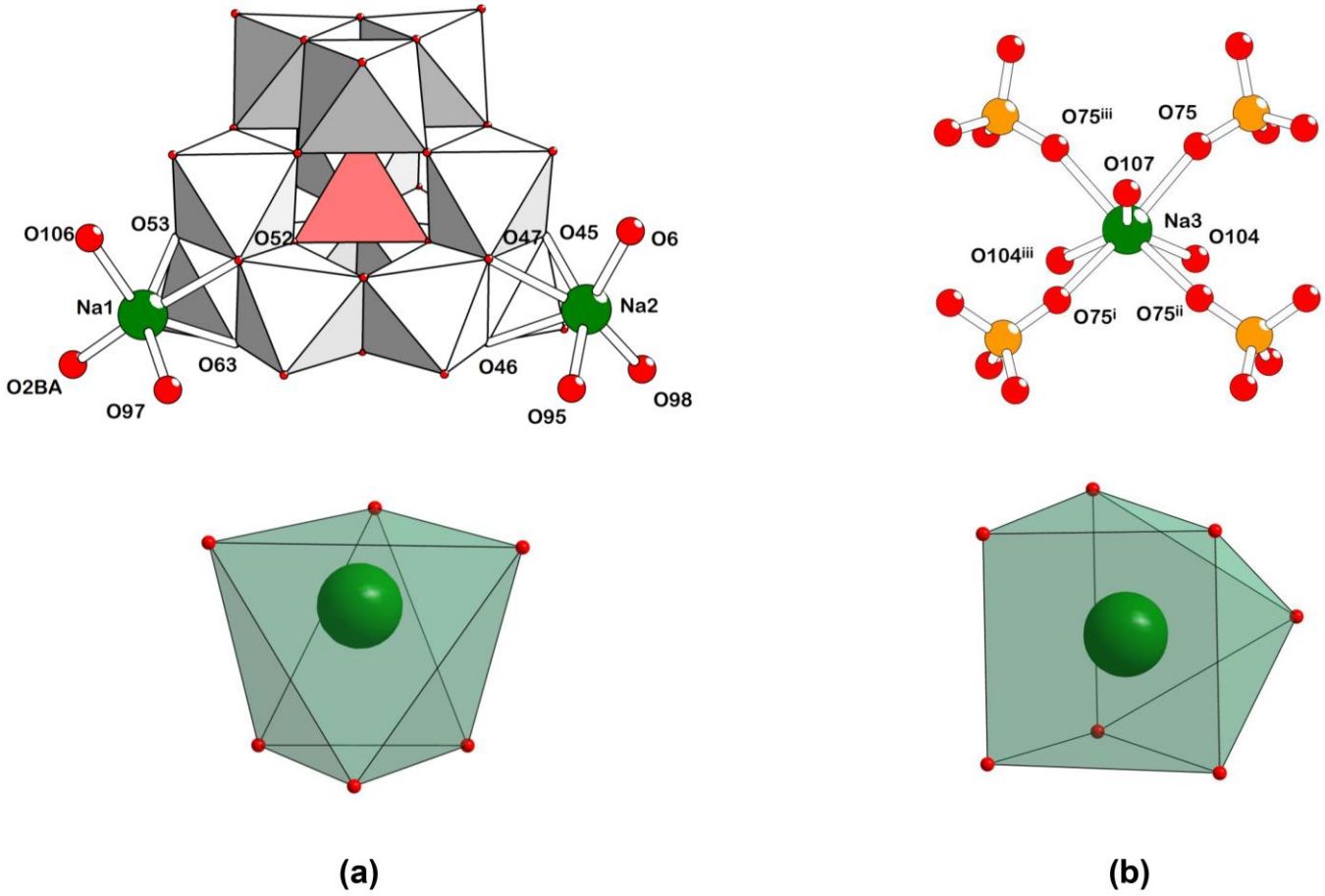

Figure 5.12 Graphical representation of $\{Na(H_2O)_3\}^+$ (a) bound to δ-Keggin-Al_{13} moieties with distorted triangular antiprism geometry and (b) bound to decorating sulphates in augmented triangular prism geometry.

PXRD indicate that the solid state framework of MK-A remains stable after the cations sorption (*see* Figure 5.1). The conservation of crystallinity after cation adsorption reflects the strong ionic hydrogen bonds which provide strong *face-to-face* interactions. The intercalating SO_4^{2-} anions are not able to be exchanged with other SO_4^{2-}, since it might cause a collapse of the hydrogen-bonded networks.

Along group 1 of the periodic table of elements, the next sulphate salt, K_2SO_4, was applied as source of an alternative alkali metal cation guest to adsorb on the MK-A structure. Single crystal X-ray crystallographic details are listed in **Table 5.1**. As observed in Na^+, there are eighteen K^+ cation observed in X-ray structure, as shown in Figure 5.13. List of K—O bond distances and O—K—O angles are listed in the Appendix (*see* Table SI3.4). The K—O bond lengths are in range of 2.52(3) – 3.200(15) Å which fall into the range of reported K—O bond lengths in hydrated potassium structures.[12–14]

There are three different potassium appearing in the asymmetric unit of the K_2SO_4@MK-A structure (*see* Figure 5.14). Two of them, like Na^+, cap on two edge sharing $\{Al_3O_{13}\}$ triads of the δ-Keggin-Al_{13}. The other is captured by four decorating SO_4^{2-}, like Na^+ but with different geometry. Looking into the first two K^+ cations, there are two kinds of the hydrated complexes as depicted in Figure 5.15. First, potassium cation (K2) is simply coordinating to $\{Al_3O_{13}\}$ triad with coordination number equal to nine (*see* Figure 5.15 a). The second potassium cation, K1, coordinates to the other $\{Al_3O_{13}\}$ triad with coordination number of ten, and a sulphate anion (S9) bidentately chelates. Interestingly, this sulphate has never been observed in any of the previous X-ray structures including MK-A and Na_2SO_4@MK-A. The rest of K1 and K2 coordination sites are filled by water molecules. The sulphate chelating to K1 is disordered. The disordered bonds K1—O118 and S9—O118 are represented in dashed lines as shown in Figure 5.15 b.

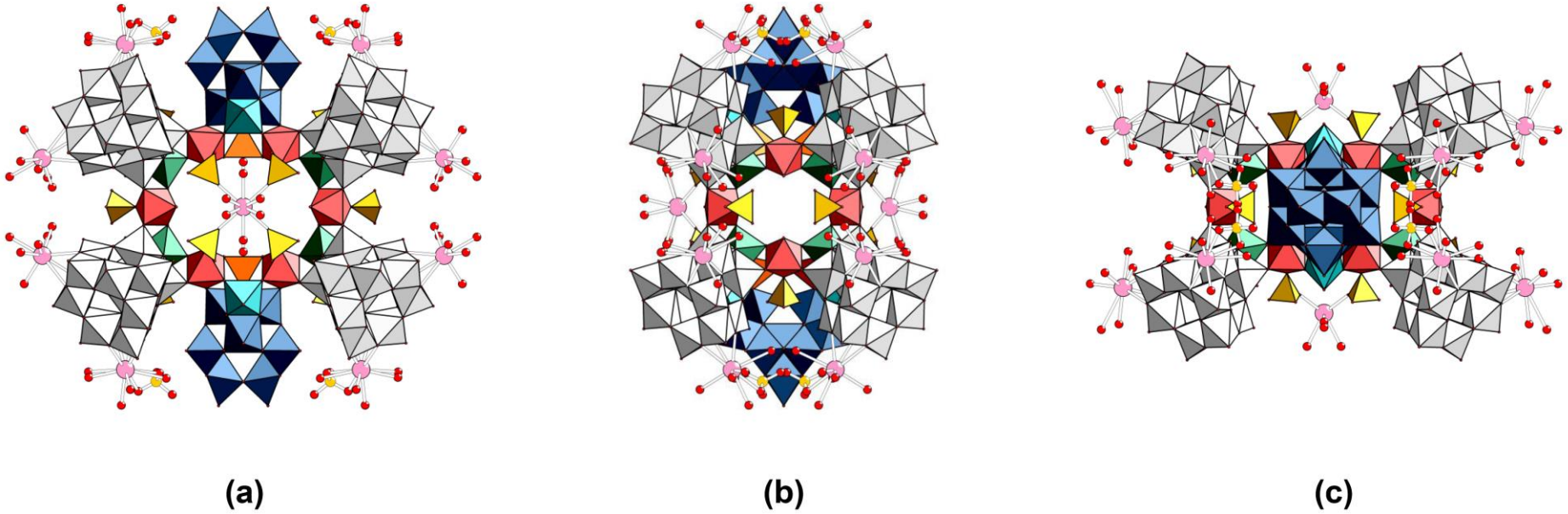

Figure 5.13 Polyhedral representation of megaKeggin-Al_{162} polyoxocation after soaking in 0.10 M K_2SO_4 for three days viewed along (a) *a*- (b) *b*- and (c) *c*-axis. $\{K(H_2O)_n\}^+$ represented by *ball-and-stick* style. Oxygen, sulphur and potassium atoms are in red, yellow and pink, respectively.

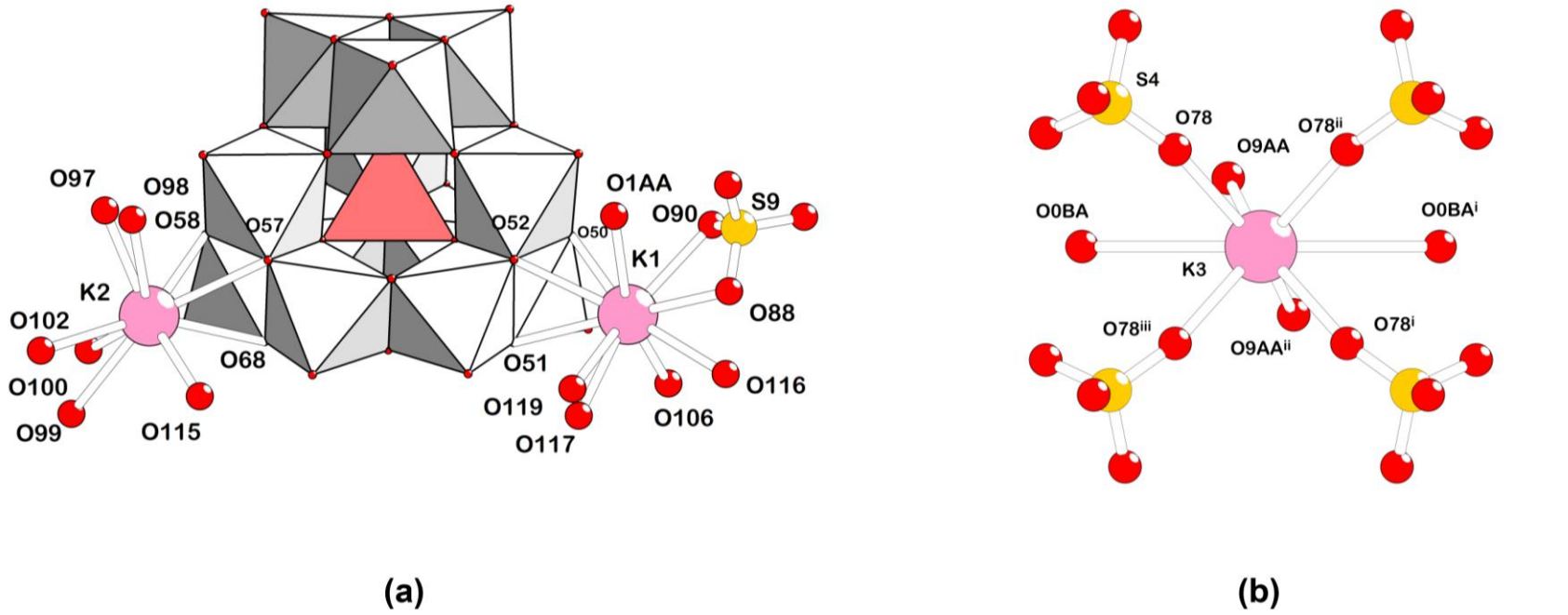

Figure 5.14 Graphical representation illustrating three different K^+ cations presenting in asymmetric unit of K_2SO_4@MK-A (a) two K^+ cations (K1 and K2) adsorbed on the triangle face of edge sharing $\{Al_3O_{13}\}$ triads of the δ-Keggin-Al_{13} SBUs and (b) another K^+ cation (K3) is captured by decorating SO_4^{2-} anions.

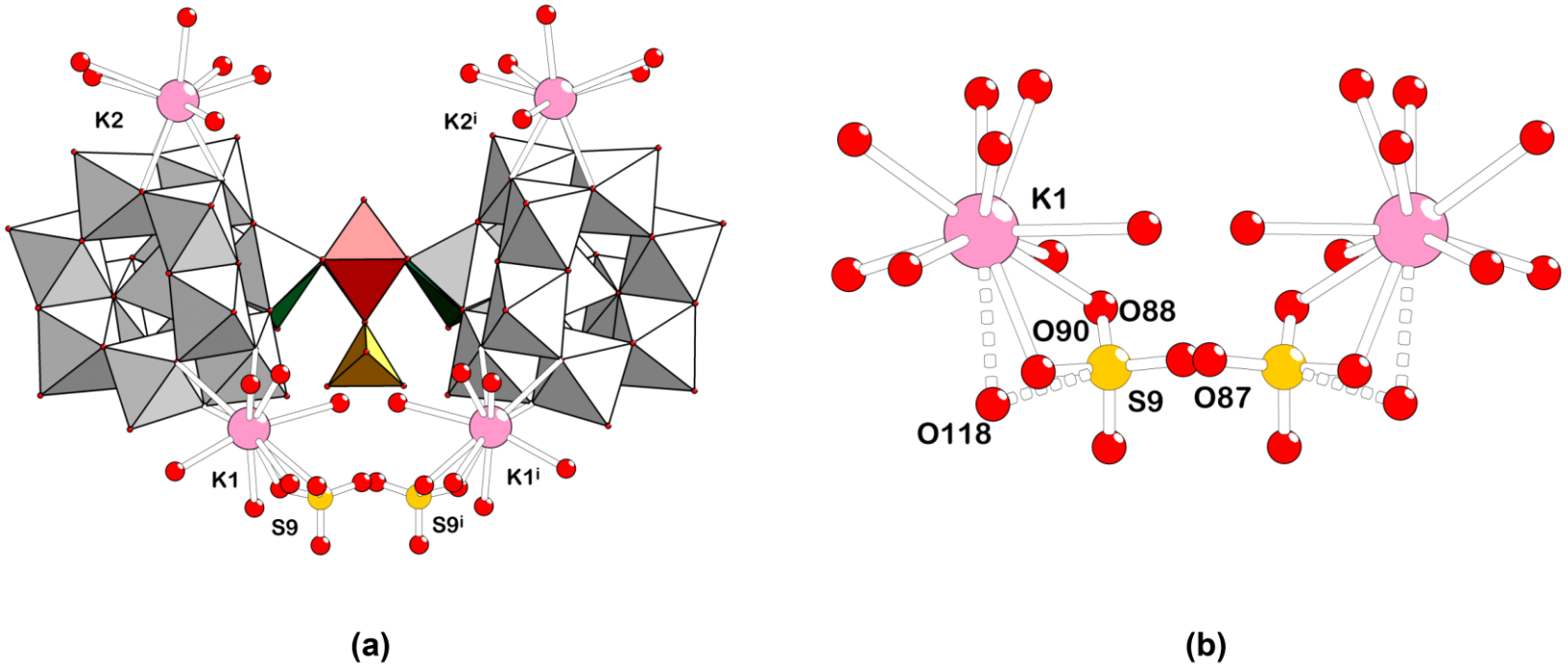

Figure 5.15 (a) Two kind of face-adsorbed K^+ represented in ball-and-stick style. (b) Coordination environment of K1. Potassium, oxygens, and sulphurs are in pink, red and yellow, respectively. Bonds of disordered atom are represented by dashed line.

According to PXRD patterns, the bulk materials of K_2SO_4@MK-A is also crystalline. The PXRD patterns are illustrated in Figure 5.1. Similarly to the Na_2SO_4 case, K_2SO_4 does not affect the *face-to-face* hydrogen-bonded scaffold and let the framework too remain stable.

^{1}H NMR quantification of the supernatant shows that 48.41% (calc. 50%) or two of NTS^{3-} anions in Na_2SO_4@MK-A and 49.25% (calc. 50%) of NTS^{3-} in K_2SO_4@MK-A were exchanged with SO_4^{2-} anions (*see* Figure 5.2).

Similar to its alkali metal congeners, rubidium and caesium cations can also be adsorbed as hydrated complexes ($\{Rb(H_2O)_n\}^+$, $\{Cs(H_2O)_n\}^+$) on the surface of megaKeggin-Al_{162} polyoxocation. The single crystal X-ray structure of Rb_2SO_4@MK-A and Cs_2SO_4@MK-A exhibit that the positions of the absorbed cations are different from those observed in Na_2SO_4@MK-A and K_2SO_4@MK-A as illustrated in Figure 5.16. and Figure 5.17. Due to their large ionic radii (Rb 142 pm and Cs 174 pm), the cations adsorb on the surfaces of megaKeggin-Al_{162} polyoxocation at different sites with different bond distances. Selected bond lengths and bond angles are listed in Table SI8 (*see* Appendix)

There are three crystallographically unique rubidium atoms in the asymmetric unit of the Rb_2SO_4@MK-A structure (*see* Figure 5.18). Similar to Na^+ and K^+, two of them cap on two edge sharing $\{Al_3O_{13}\}$ triads of the δ-Keggin-Al_{13} but at different distances. Coordination environments of the rubidium ion are also different from Na^+ and K^+ (*see* Figure 5.18). Another Rb^+ is captured by four decorating SO_4^{2-}, similar to Na^+ and K^+ but with different coordination geometry (*see* Figure 5.18 b). In the first two Rb^+ cations, there are two kinds of the $[Rb(H_2O)_n]^+$ complexes. First, rubidium cation (Rb95) is directly attached to $\{Al_3O_{13}\}$ triad with coordination number equal to nine (*see* Figure 5.18 a). The second rubidium cation, Rb0A, coordinates to the other $\{Al_3O_{13}\}$ triad with coordination number of eight, and one sulphato ligand (S14) bidentately chelates to the rubidium. As mentioned before, this sulphate was not observed in any of the previous X-ray structures including MK-A and Na_2SO_4@MK-A but presents in K_2SO_4@MK-A. Rb—O bond in Rb_2SO_4@MK-A structure are listed in the Appendix (*see* Table SI3.6)

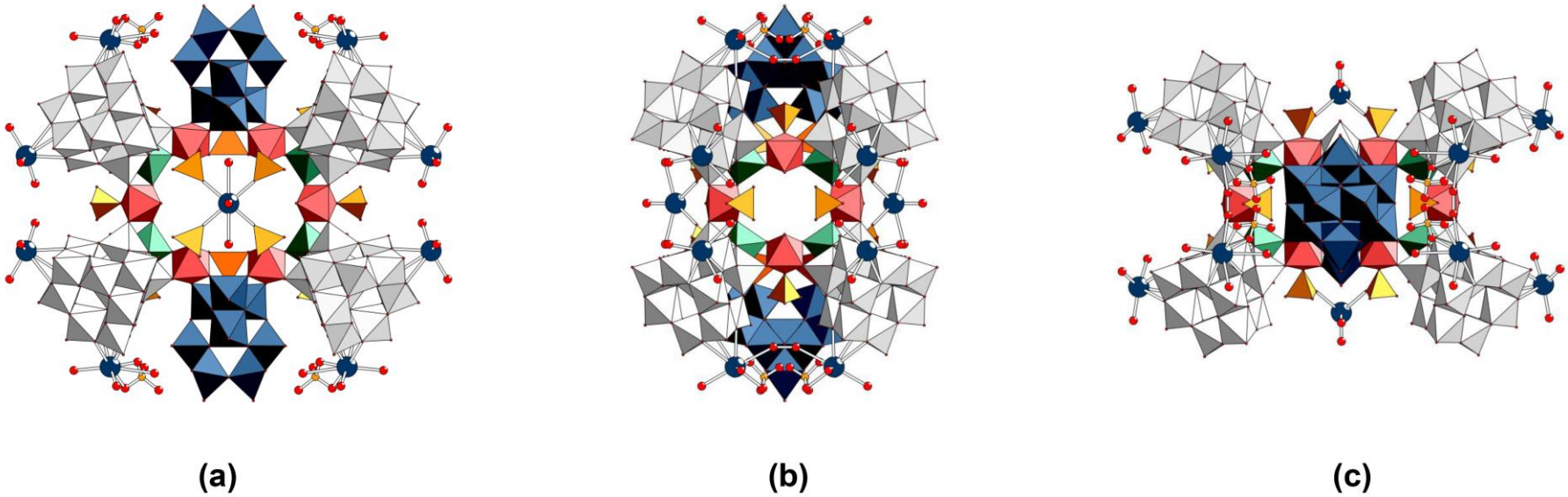

Figure 5.16 Polyhedral representation of megaKeggin-Al_{162} polyoxocation after soaking in 0.10 M Rb_2SO_4 for three days viewed along (a) *a*-, (b) *b*-, and (c) *c*-axis. $\{Rb(H_2O)_n\}^+$ represented by *ball-and-stick* style. Oxygen, sulphur, and rubidium atoms are in red, yellow and blue, respectively.

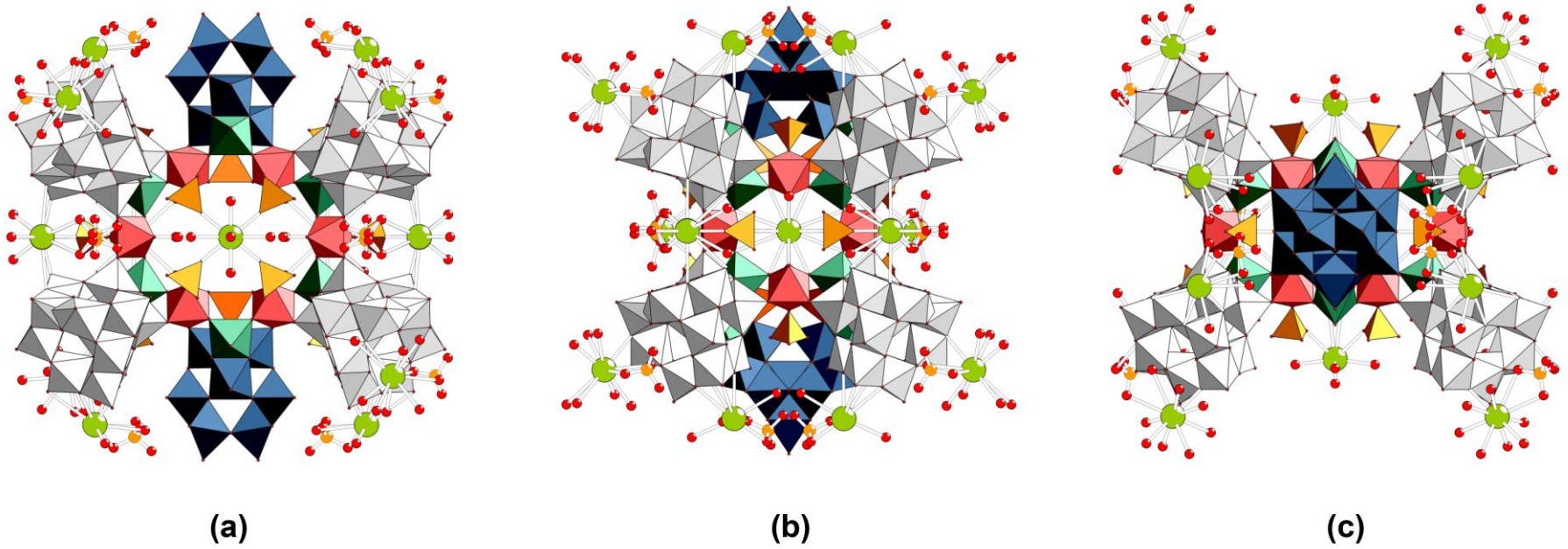

Figure 5.17 Polyhedral representation of megaKeggin-Al_{162} polyoxocation after soaking in 0.10 M Cs_2SO_4 for 3 days viewed along (a) *a*- (b) *b*- and (c) *c*-axis. $\{Cs(H_2O)_n\}^+$ represented by ball-and-stick style. Oxygen sulphur and caesium atoms are in red, yellow and green, respectively.

Similar to the previous alkali metal cations, $[Cs(H_2O)_n]^+$ complexe can be adsorbed on megaKeggin-Al_{162} surface as they are observed in single crystal X-ray structure (see Figure 5.17). Interestingly, there are five crystallographically unique Cs^+ in the asymmetric unit of Rb_2SO_4@MK-A. Three of them adsorbed on the faces of *δ*-Keggin-Al_{13} SBUs as illustrated in Figure 5.19 a. Cs1 is bidentately chelated by a sulphato ligand (S1) and monodentately ligated by another sulphato group (S7). Cs3 is also bidentately coordinated by a sulphato ligand (S13), while another Cs^+ (Cs2) is intercalating as a pillar between each megaKeggin-Al_{162} polyoxocation. The latter Cs^+ is chelated by the intercalating SO_4^{2-}. Cs0A is trapped by four decorating sulphate and Cs97 is trapped in a 16-membered $\{AlO_6\}$ ring as illustrated in Figure 5.19. Cs—O bond lengths are listed in the Appendix (*see* Table SI3.8) PXRD patterns of both Rb_2SO_4@MK-A and Cs_2SO_4@MK-A show that the materials are crystalline (*see* Figure 5.1). Chemical analysis results for all cationic adsorbed MK-A indicate that the MK-A may also uptake the sulphate as salts into its pores.

A part of the anionic adsorption studies, MK-A exhibits potential properties with organic anionic dye such as Chromis-645-A-*acid* (Chromis). The Chromis is normally a potassium salt of monovalent sulphonate anion which contains a dissociable carboxylic group (RCOOH, pK_a = 5.6) as its structural formula shown in Scheme 5.1. The exchange properties of MK-A were studied by two independent experiments, performed in (i) static and (ii) gently stirred solution. According to the UV-Vis absorbance results for both static and gently stirred experiments (*see* Figure 5.3), the absorbance of the solutions decrease exponentially to a stable level within *c.a.* six hours. This reflects that the $Chromis^{2-}$ anion in the solution was exchanged with anionic species in the MK-A pores till an equilibrium. As the pH of starting solution is 6.30 ± 0.50, the carboxylic acid group in chromis molecule was deprotonated and the Chromis was predominantly present as a divalent anion ($Chromis^{2-}$). The amount of exchanged $Chromis^{2-}$ was estimated from the absorbance spectra using a calibration curve and the Beer-Lambert's law. Solution state ^{1}H NMR indicates the presence of NTS^{3-} in the supernatant and the ^{1}H NMR quantification results indicate that two NTS^{3-} were exchanged by one $Chromis^{2-}$ (*see* Figure 5.6). The number of exchanged NTS^{3-} is the same as the one observed in alkali metal cation adsorptions. Solid materials after exchanged (Chromis@MK-A) is blue (*see* Figure 5.4). This reflects the presence of the $Chromis^{2-}$ in the solids. Chromis@MK-A in water is crystalline as shown in Figure 5.7,

but the presence of Chromis^{2-} is not visible in single crystal X-ray structure. The crystalline structure collapses when the sample is dried due to the destruction of hydrogen-bonded molecular assemblies (*see* Figure 5.7). TGA/DTA results indicate that the organic contents in Chromis@MK-A is higher than in the as-synthesised MK-A materials (*see* Figure 5.5). The first step of weight loss (A, 92°C) is endothermic, corresponding to the dehydration process. Exothermic combustion of carbon in organic moieties to carbon dioxide occurs at around 600°C (B). Another exothermic combustion at 870°C corresponding to the combustion of sulphur to sulphur trioxide.

As described above, MK-A has the ability to exchange/adsorb anionic and cationic species. This includes a toxic compound arsenic (V) such as Na_2HAsO_4. Concentration of As(V) rapidly reduced *c.a.* 90% (from 5 ppm to 0.50 ppm) within five minutes after the addition of MK-A as illustrated in Figure 5.8. It is a short time comparing to reported method which are in scale of hours.[5,15–19] Removal capacity of As(V) by MK-A is 29.0 mg g^{-1}. This capacity is higher than the capacity of commercial active carbon and higher than zeolite as shown in Figure 5.10.[5]

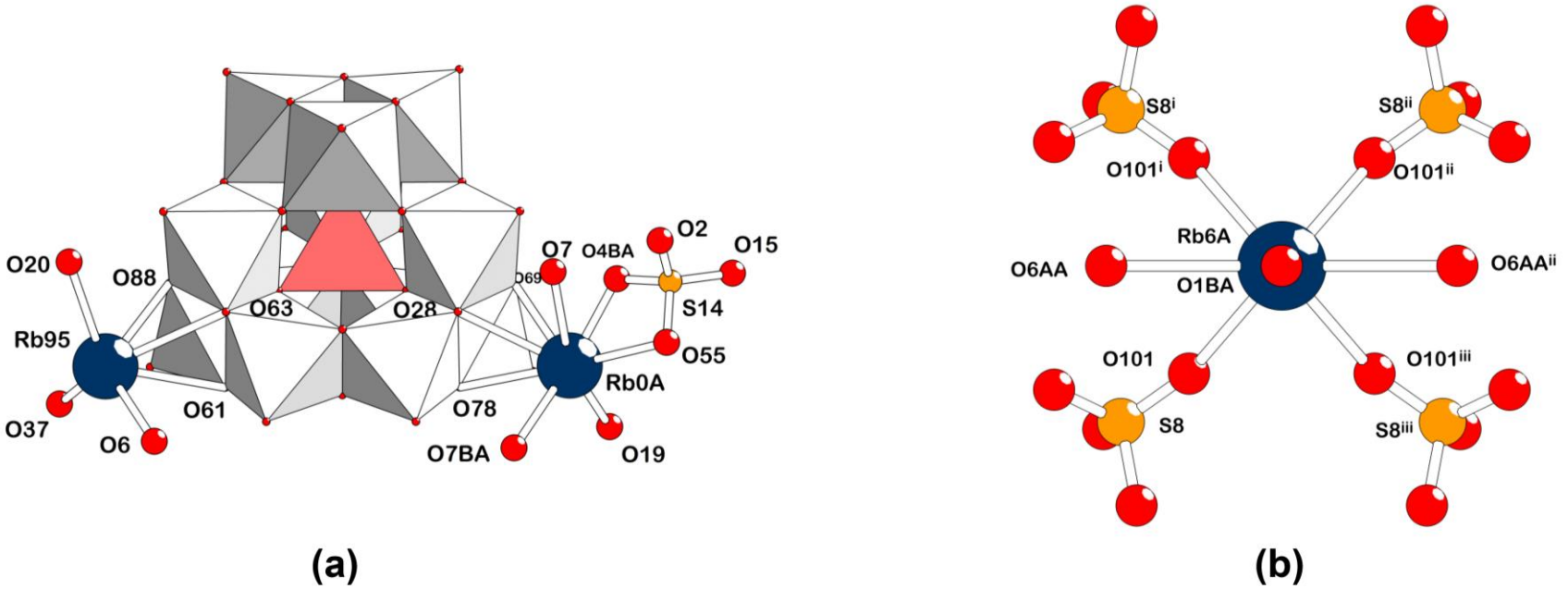

Figure 5.18 Graphical representation illustrating three different Rb^{+} cations presenting in asymmetric unit of Rb_2SO_4@MK-A (a) two Rb^{+} cations (Rb0A and Rb95) adsorbed on the triangle face of edge sharing $\{Al_3O_{13}\}$ triads of the δ-Keggin-Al_{13} SBUs and (b) another Rb^{+} cation (Rb6A) is captured by decorating SO_4^{2-} anions

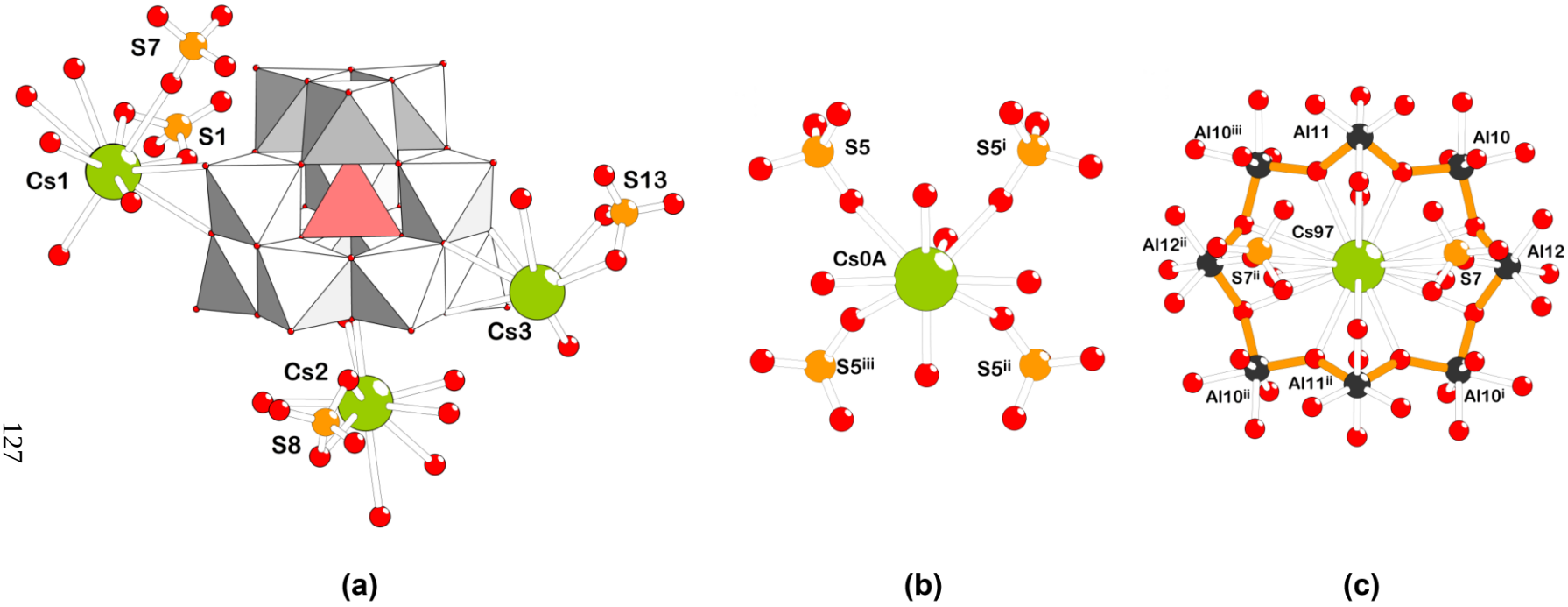

Figure 5.19 Graphical representation illustrating five different Cs^+ cations presented in asymmetric unit of Cs_2SO_4@MK-A (a) three Cs^+ cations (Cs1, Cs2 and Cs3) adsorbed on the triangle face of edge sharing $\{Al_3O_{13}\}$ triads and also the hexagonal face of the δ-Keggin-Al_{13} SBUs (b) Cs^+ cation (Rb0A) is captured by decorating SO_4^{2-} anions, and (c) Cs^+ cation (Cs97) is captured in a 16-membered ring of $\{AlO_6\}$. Oxygen sulphur and caesium atoms are in red, yellow and green, respectively. The 16-membered ring is highlighted by orange solid line.

5.4 Conclusion

In this chapter, the studies of potential properties of ion exchange and/or sorption of MK-A were described. The MK-A exhibits the abilities of alkali metal sulphate (*i.e.* Na_2SO_4, K_2SO_4, Rb_2SO_4 and Cs_2SO_4) uptakes. The alkali metal cations were observed in single crystal X-ray structures. Sulphate anions were exchanged with NTS^{3-} anions confirmed by ^1H NMR. The MK-A exhibits its ability to uptake organically anionic dye *i.e.* $Chromis^{2-}$ and also shows its potential application to removal of a toxic As(V) compound such as Na_2HAsO_4.

Bibliography

(1) Rouquerol, J.; Avnir, D.; Fairbridge, C. W.; Everett, D. H.; Haynes, J. M.; Pernicone, N.; Ramsay, J. D. F.; Sing, K. S. W.; Unger, K. K. *Pure Appl. Chem.* **1994**, *66* (8), 1739–1758.

(2) Zdravkov, B. D.; Čermák, J. J.; Šefara, M.; Janků, J. *Cent. Eur. J. Chem.* **2007**, *5* (2), 385–395.

(3) Rouquerol, J.; Avnir, D.; Fairbridge, C. W.; Everett, D. H.; Haynes, J. M.; Pernicone, N.; Ramsay, J. D. F.; Sing, K. S. W.; Unger, K. K. *Pure Appl. Chem.* **1994**, *66* (8), 1739–1758.

(4) Haber, J. *Pure Appl. Chem.* **1991**, *63* (9), 1227–1246.

(5) Wu, Y.; Zhou, M.; Zhang, B.; Wu, B.; Li, J.; Qiao, J.; Guan, X.; Li, F. *Nanoscale* **2014**, *6* (2), 1105–1112.

(6) Tomoyuki Higami, M. H. and S. O. *Acta Crystallogr. Sect. C* **2002**, *C58* (10), i144–i146.

(7) A, R. O. A. A. T. B. E. B. M. L. *Acta Crystallogr. Sect. E* **2002**, *E58*, i23–i25.

(8) Angeli, F.; Delaye, J.-M.; Charpentier, T.; Petit, J.-C.; Ghaleb, D.; Faucon, P. *J. Non. Cryst. Solids* **2000**, *276* (1-3), 132–144.

(9) Olga V. Yakubovich, Ian M. Steele, E. V. Y. and O. V. D. *Acta Crystallogr. Sect. C* **2015**, *71* (6), 465–473.

(10) Rowsell, J.; Nazar, L. F. *J. Am. Chem. Soc.* **2000**, *122* (15), 3777–3778.

(11) Abeysinghe, S.; Unruh, D. K.; Forbes, T. Z. *Cryst. Growth Des.* **2012**, *12* (4), 2044–2051.

(12) Bush, M. A.; Truter, M. R. *J. Chem. Soc. Perkin Trans. 2* **1972**, No. 3, 345.

(13) Okaya, Y. *Acta Crystallogr.* **1965**, *19* (6), 879–882.

(14) Angeles, J. N. L. P. A. J. C. M. *Acta Crystallogr. Sect. C* **2011**, *57* (5), 534–537.

(15) Choong, T. S. Y.; Chuah, T. G.; Robiah, Y.; Gregory Koay, F. L.; Azni, I. *Desalination* **2007**, *217* (1-3), 139–166.

(16) Wang, C.; Liu, X.; Chen, J. P.; Li, K. *Sci. Rep.* **2015**, *5*, 16613.

(17) Li, S.; Chen, Y.; Pei, X.; Zhang, S.; Feng, X.; Zhou, J.; Wang, B. *Chinese J. Chem.* **2016**, *34* (2), 175–185.

(18) Li, J.; Wu, Y.; Li, Z.; Zhang, B.; Zhu, M.; Hu, X.; Zhang, Y.; Li, F. *J. Phys. Chem. C* **2014**, *118* (47), 27382–27387.

(19) Wu, C.; Xiong, Z.; Li, C.; Zhang, J. *RSC Adv.* **2015**, *5* (100), 82127–82137.

Chapter 6

Summary and Future Work

This thesis presented the discovery, synthesis and characterisation of novel polyoxocations of aluminium *i.e.* (i) Al_{30}-acetate, $[Al_2(\mu_4\text{-}O)_8(Al_{28}(\mu_2\text{-}OH)_{50}\ (\mu_2\text{-}OH)_6(\eta\text{-}H_2O)_{22}(\eta_2\text{-}CH_3COO)_2]^{16+}$ and (ii) *megaKeggin*-Al_{162}, $[2SO_4{\subset}Al_{162}(\mu_4\text{-}O_{44})(\mu_2\text{-}O)_2(\mu_3\text{-}OH)_{32}\ (\mu_2\text{-}OH)_{276}(\eta\text{-}H_2O)_{100}(\eta\text{-}SO_4)_{16}]^{50+}$. Studies of potential application of the polyoxocation were described.

The Al_{30}-acetate crystals, $[Al_2(\mu_4\text{-}O)_8Al_{26}(\mu_2\text{-}OH)_{56}(\eta\text{-}H_2O)_{22}Al_2(\eta_2\text{-}CH_3COO)_2](2,6\text{-}NDS)_7(CH_3COO)_2{\cdot}2H_2O$, were crystallised and refined in space group $P\bar{1}$. Its crystal structure comprises of coordinated and uncoordinated acetate anions generated *in situ* by hydrolysis of acetonitrile. Hydrogen bonding and π-π interactions were calculated and described as the main intermolecular interaction for supramolecular assemblies. Due to its lack of purity and low yield, chemical analysis and further characterisation were not possible.

The *megaKeggin*-Al_{162} was reported as the largest polyoxocation based on research literatures reported up to date. It is the first structure which combine two different isomers of *Keggin*-Al_{13} polyoxocation *i.e.* δ- and γ-isomers. MAS ^{27}Al NMR was applied to investigate its local structure. The supramolecular assemblies of the *megaKeggin*-Al_{162} generate three rotational polymorphs (MK-A, MK-B and MK-C). Every polymorph are open frameworks with large pores in their crystal structures. Amongst the three polymorphs, MK-A has been successfully synthesised and investigated the potential applications as a sorbent for alkali metal cations and also anions *i.e.* sulphate, arsenate and Chromis-A^{2-}.

Due to the novelty of megaKeggin-Al_{162} structure and its interesting polymorphism, manuscript preparation for publication is in progress. Future work on computational study is also considered.

Appendix

Table of Contents

SI0 List of Chemicals

1. Aluminium nitrate nonahydrate ($Al(NO_3)_3 \cdot 9H_2O$, puriss. *p.a.*, ACS reagent, ≥98.5%)
2. Aluminium chloride hexahydrate ($AlCl_3 \cdot 6H_2O$, purum *p.a.*, crystallised, ≥99.0%)
3. Aluminum sulphate hexadecahydrate ($Al_2(SO_4)_3 \cdot 16H_2O$, purum p.a., ≥95.0%)
4. Sodium hydroxide (NaOH, reagent grade, ≥98%, pellets (anhydrous))
5. Potassium hydroxide (KOH, ≥85% KOH basis, pellets, white)
6. Triethylamine ($N(C_2H_5)_3$, BioUltra, ≥99.5% (GC)
7. Ammonium hydroxide solution (28% NH_3 in H_2O, ≥99.99% trace metals basis)
8. 1,3,(6,7)-Naphthalenetrisulphonic acid trisodium salt trihydrate, ($C_{10}H_5(SO_3Na)_3 \cdot 3H_2O$, 98%)
9. 2,6-naphthalenedisulphonic acid disodium salt ($C_{10}H_6(SO_3Na)_2$, powder, Sigma Aldrich, ≥97%)
10. Sodium sulphate (Na_2SO_4, ACS reagent, ≥99.0%, anhydrous, granular)
11. Potassium sulphate (K_2SO_4, ReagentPlus®, ≥99.0%)
12. Rubidium sulphate (Rb_2SO_4, 99.99%, trace metals basis)
13. Caesium sulphate, Cs_2SO_4, 99.99%, trace metals basis)
14. Sodium arsenate dibasic heptahydrate (Na_2HAsO_4, ≥98.0%).
15. Acetonitrile (CH_3CN, CHROMASOLV® Plus, for HPLC, ≥99.9%)
16. Ethanol (C_2H_5OH, 200 proof, ACS reagent, ≥99.5%)
17. Methanol, (CH_3OH, CHROMA-SOLV®, for HPLC, ≥99.9%)
18. Nitric acid (HNO_3, puriss. p.a., ACS reagent, reag. ISO, ≥69%).

SI1 Supplementary Information for Chapter 3

SI1.1 Fractional atomic coordinates and isotropic or equivalent isotropic displacement parameters of Al_{30}-acetate structure

Table SI1.1 Fractional atomic coordinates and isotropic or equivalent isotropic displacement parameters of Al_{30}-acetate structure, Space group $P\bar{1}$

Atom	***x***	***y***	***z***	U_{iso}/U_{eq} **(Å^2)**	**Occupancy**
Al1	0.56897 (10)	0.53443 (7)	0.25479 (7)	0.0291 (3)	1.00
Al2	0.35067 (10)	0.64008 (7)	0.24858 (6)	0.0289 (3)	1.00
Al3	0.17460 (12)	0.79200 (8)	0.31308 (8)	0.0391 (4)	1.00
Al4	0.40259 (11)	0.47243 (8)	0.19360 (7)	0.0320 (3)	1.00
Al5	0.59083 (11)	0.48636 (7)	0.39443 (6)	0.0287 (3)	1.00
Al6	0.43022 (11)	0.38034 (7)	0.49300 (6)	0.0283 (3)	1.00
Al7	0.37673 (11)	0.58920 (8)	0.09002 (7)	0.0349 (3)	1.00
Al8	0.21270 (11)	0.66247 (8)	0.40328 (7)	0.0322 (3)	1.00
Al9	0.10388 (11)	0.65534 (8)	0.30389 (8)	0.0364 (3)	1.00
Al10	0.39277 (10)	0.50215 (7)	0.35937 (6)	0.0279 (3)	1.00
Al11	0.47056 (11)	0.63722 (7)	0.36816 (7)	0.0289 (3)	1.00
Al12	0.44929 (12)	0.72082 (9)	0.10019 (7)	0.0375 (3)	1.00
Al13	0.34909 (12)	0.82262 (8)	0.21207 (8)	0.0390 (4)	1.00
Al14	0.54103 (11)	0.71983 (8)	0.21065 (7)	0.0338 (3)	1.00
Al17	0.20053 (12)	0.55488 (8)	0.19396 (7)	0.0358 (3)	1.00
C0AA	0.6680 (11)	1.0090 (7)	0.1377 (7)	0.0528 (9)	0.50
C1	0.7286 (4)	0.9029 (3)	0.3508 (3)	0.0385 (11)	1.00
C10	0.8070 (4)	0.9329 (3)	0.3614 (3)	0.0454 (12)	1.00
C11	0.2550 (3)	1.09032 (15)	0.32598 (18)	0.093 (3)	1.00
C12	0.7511 (10)	1.1040 (7)	0.1371 (6)	0.0528 (9)	0.50
C13	0.8348 (10)	1.0513 (7)	0.1569 (6)	0.0528 (9)	0.50
C14	0.9099 (10)	0.9273 (7)	0.1856 (6)	0.0528 (9)	0.50
C15	−0.0209 (6)	0.9002 (4)	0.0153 (4)	0.0687 (9)	1.00
C16	0.0624 (6)	0.8690 (4)	0.0353 (4)	0.0687 (9)	1.00
C17	0.9842 (5)	1.0622 (4)	0.1855 (4)	0.0593 (11)	0.50
C18	0.8326 (10)	0.9758 (7)	0.1655 (6)	0.0528 (9)	0.50
C19	0.1344 (6)	0.9132 (4)	0.0388 (4)	0.0687 (9)	1.00
C1A	0.6761 (10)	1.0797 (7)	0.1273 (6)	0.0528 (9)	0.50
C1B	0.7441 (10)	0.9549 (8)	0.1528 (6)	0.0528 (9)	0.50
C1C	0.7228 (5)	1.0512 (4)	0.1336 (4)	0.0593 (11)	0.50
C1D	0.1216 (6)	0.9849 (4)	0.0225 (4)	0.0687 (9)	1.00
C1E	0.9864 (10)	0.9507 (7)	0.1965 (6)	0.0528 (9)	0.50
C1F	0.7495 (6)	0.9205 (4)	0.1623 (4)	0.0593 (11)	0.50
C1G	0.9908 (11)	1.0253 (8)	0.1911 (6)	0.0528 (9)	0.50
C1H	0.0378 (6)	1.0150 (4)	0.0038 (4)	0.0687 (9)	1.00
C1I	0.8099 (4)	1.0549 (3)	0.1509 (3)	0.0593 (11)	0.50
C1J	0.7553 (8)	0.4472 (5)	0.2809 (4)	0.049 (3)	0.65
C1N	0.1192 (5)	0.4876 (3)	0.5682 (4)	0.057 (3)	1.00
C1P	0.0033 (8)	0.5231 (6)	0.5787 (7)	0.071 (5)	0.67

Table SI1.1 Fractional atomic coordinates and isotropic or equivalent isotropic displacement parameters of Al_{30}-acetate structure, Space group $P\bar{1}$ (Continued)

Atom	***x***	***y***	***z***	U_{iso}/U_{eq} **(Å^2)**	**Occupancy**
C2	0.6479 (4)	0.9466 (3)	0.3331 (3)	0.0413 (11)	1.00
C20	0.3629 (3)	0.95557 (10)	0.44337 (17)	0.0469 (13)	1.00
C21	0.3859 (2)	1.00249 (13)	0.48340 (14)	0.0357 (10)	1.00
C22	0.3652 (2)	1.07868 (13)	0.47095 (13)	0.0385 (11)	1.00
C23	0.32162 (15)	1.10796 (10)	0.41847 (10)	0.0365 (10)	1.00
C24	0.3010 (2)	1.18415 (10)	0.40602 (15)	0.0406 (11)	1.00
C25	0.2574 (3)	1.21343 (12)	0.35355 (17)	0.0471 (13)	1.00
C26	0.2344 (3)	1.16651 (16)	0.31353 (18)	0.077 (2)	1.00
C28	0.2986 (2)	1.06105 (11)	0.37845 (13)	0.0565 (16)	1.00
C29	0.3193 (3)	0.98485 (11)	0.39090 (18)	0.066 (2)	1.00
C3	0.6423 (4)	1.0263 (3)	0.3227 (3)	0.0391 (11)	1.00
C30	0.8608 (9)	0.4145 (8)	0.2561 (6)	0.055 (3)	0.50
C4	0.5618 (4)	1.0728 (3)	0.3006 (3)	0.0489 (13)	1.00
C5	0.5615 (4)	1.1462 (3)	0.2869 (3)	0.0444 (12)	1.00
C6	0.6440 (4)	1.1738 (3)	0.2932 (2)	0.0385 (11)	1.00
C7	0.7203 (4)	1.1316 (3)	0.3168 (2)	0.0375 (11)	1.00
C8	0.7213 (4)	1.0545 (3)	0.3311 (2)	0.0362 (10)	1.00
C82	0.8668 (4)	0.9914 (3)	0.1739 (3)	0.0593 (11)	0.50
C83	0.9272 (6)	1.1257 (4)	0.1624 (4)	0.0593 (11)	0.50
C84	0.8401 (5)	1.1220 (3)	0.1452 (4)	0.0593 (11)	0.50
C86	0.8366 (5)	0.9242 (3)	0.1796 (4)	0.0593 (11)	0.50
C87	0.6926 (5)	0.9840 (4)	0.1393 (4)	0.0593 (11)	0.50
C88	0.9540 (5)	0.9951 (4)	0.1912 (4)	0.0593 (11)	0.50
C9	0.8021 (4)	1.0085 (3)	0.3526 (3)	0.0424 (12)	1.00
C999	0.9122 (10)	1.0770 (7)	0.1700 (6)	0.0528 (9)	0.50
O0AA	1.1774 (14)	1.0232 (14)	0.1655 (11)	0.073 (6)	0.25
O1	0.4644 (4)	0.8387 (2)	0.4931 (2)	0.0577 (11)	1.00
O10	0.0029 (5)	0.7471 (3)	0.0766 (4)	0.0934 (19)	1.00
O11	0.1360 (4)	0.4231 (3)	0.5929 (3)	0.058 (2)	0.77
O12	0.7389 (3)	1.2816 (2)	0.2777 (3)	0.0602 (11)	1.00
O13	0.6379 (5)	1.2767 (3)	0.1988 (2)	0.0735 (15)	1.00
O14	0.5596 (3)	1.3126 (2)	0.3116 (2)	0.0501 (10)	1.00
O15	0.5545 (2)	0.40803 (17)	0.45170 (15)	0.0292 (6)	1.00
O16	0.8426 (3)	0.7788 (2)	0.3058 (2)	0.0561 (11)	1.00
O17	0.6629 (3)	0.7867 (2)	0.3361 (2)	0.0566 (11)	1.00
O18	0.7487 (3)	0.7814 (2)	0.4237 (2)	0.0479 (9)	1.00
O19	0.6255 (2)	0.53107 (17)	0.45903 (15)	0.0293 (6)	1.00
O1A	0.7179 (3)	0.44002 (19)	0.34821 (17)	0.0362 (7)	1.00
O1AA	1.102 (2)	1.0195 (11)	0.2672 (16)	0.107 (16)	0.25
O1B	0.5190 (3)	0.66876 (17)	0.43479 (15)	0.0313 (7)	1.00
O1C	0.3764 (2)	0.42244 (17)	0.41966 (15)	0.0304 (7)	1.00
O1CB	0.4991 (7)	0.9816 (5)	0.1844 (5)	0.112 (3)	0.85
O1D	0.0897 (3)	0.5200 (2)	0.1811 (2)	0.0485 (9)	1.00

Table SI1.1 Fractional atomic coordinates and isotropic or equivalent isotropic displacement parameters of Al_{30}-acetate structure, Space group $P\bar{1}$ (Continued)

Atom	***x***	***y***	***z***	U_{iso}/U_{eq} **(Å^2)**	**Occupancy**
O1DA	0.5955 (8)	0.9050 (6)	0.1065 (6)	0.135 (3)	0.85
O1E	0.7028 (3)	0.47868 (19)	0.23404 (19)	0.0394 (8)	1.00
O1F	0.3059 (3)	0.34688 (19)	0.53186 (18)	0.0379 (8)	1.00
O1FB	0.5482 (9)	1.0205 (7)	0.0689 (6)	0.143 (4)	0.85
O1G	0.4588 (3)	0.3678 (2)	0.18256 (18)	0.0437 (9)	1.00
O1H	0.4050 (3)	0.5860 (2)	−0.00740 (17)	0.0444 (9)	1.00
O1I	0.1712 (3)	0.6559 (2)	0.50112 (17)	0.0422 (8)	1.00
O1J	0.1795 (4)	0.5172 (3)	0.5328 (3)	0.0479(19)	0.81
O1K	0.6671 (3)	0.7413 (2)	0.2111 (2)	0.0477 (9)	1.00
O1L	0.4952 (3)	0.7430 (2)	0.00446 (18)	0.0503 (10)	1.00
O1M	0.3219 (3)	0.9303 (2)	0.2087 (2)	0.0549 (10)	1.00
O1N	−0.0316 (3)	0.6471 (2)	0.3137 (2)	0.0497 (9)	1.00
O1O	0.0955 (4)	0.8896 (2)	0.3361 (2)	0.0603 (11)	1.00
O1Q	1.1268 (17)	1.0030 (10)	0.2448 (13)	0.111 (3)	0.50
O1R	1.0626 (8)	1.1399 (5)	0.2250 (7)	0.070 (3)	0.50
O1T	1.1150 (13)	1.1210 (9)	0.1874 (9)	0.111 (3)	0.50
O1V	1.0156 (12)	1.1095 (8)	0.2893 (8)	0.111 (3)	0.50
O2	0.2854 (4)	0.8482 (2)	0.5149 (3)	0.0655 (12)	1.00
O21	1.1798 (14)	1.0669 (11)	0.1376 (11)	0.070 (3)	0.25
O24	0.1558 (3)	0.55415 (19)	0.28852 (17)	0.0366 (7)	1.00
O26	0.5346 (2)	0.46032 (16)	0.32536 (15)	0.0292 (6)	1.00
O27	0.4340 (3)	0.48686 (18)	0.09644 (16)	0.0352 (7)	1.00
O28	0.4975 (3)	0.6168 (2)	0.08751 (17)	0.0391 (8)	1.00
O2AA	0.7231 (3)	0.2904 (2)	0.42789 (19)	0.0425 (8)	1.00
O3	0.2496 (3)	0.5729 (2)	0.10187 (17)	0.0383 (8)	1.00
O30	0.3388 (2)	0.57603 (17)	0.19231 (15)	0.0311 (7)	1.00
O31	0.5964 (2)	0.57137 (17)	0.33084 (15)	0.0290 (6)	1.00
O31A	0.2084 (7)	1.3241 (4)	0.2718 (5)	0.053 (2)	0.50
O31B	0.2875 (8)	1.3345 (7)	0.2883 (5)	0.078 (3)	0.50
O32A	0.2864 (8)	1.3423 (4)	0.3547 (4)	0.058 (3)	0.50
O32B	0.2163 (7)	1.3499 (4)	0.4060 (5)	0.053 (2)	0.50
O33	0.3375 (3)	0.67958 (17)	0.40411 (16)	0.0320 (7)	1.00
O33A	0.1200 (9)	1.3281 (6)	0.3903 (6)	0.087 (4)	0.50
O33B	0.1207 (7)	1.3232 (5)	0.3320 (6)	0.059 (2)	0.50
O34	0.0922 (3)	0.64173 (19)	0.39746 (18)	0.0375 (7)	1.00
O35	0.2340 (2)	0.67907 (17)	0.30534 (16)	0.0329 (7)	1.00
O36	0.2691 (2)	0.55989 (17)	0.39611 (15)	0.0292 (6)	1.00
O38	0.3657 (2)	0.46185 (17)	0.28937 (15)	0.0297 (7)	1.00
O4	0.0649 (3)	0.7582 (2)	0.30546 (19)	0.0431 (8)	1.00
O40	0.1606 (3)	0.76464 (19)	0.40465 (18)	0.0401 (8)	1.00
O41	0.5708 (3)	0.7298 (2)	0.11585 (17)	0.0400 (8)	1.00
O43	0.2774 (3)	0.45761 (19)	0.19140 (17)	0.0362 (7)	1.00

Table SI1.1 Fractional atomic coordinates and isotropic or equivalent isotropic displacement parameters of Al_{30}-acetate structure, Space group $P\bar{1}$ (Continued)

Atom	***x***	***y***	***z***	U_{iso}/U_{eq} **(Å^2)**	**Occupancy**
O44	0.4538 (2)	0.54465 (16)	0.41874 (15)	0.0286 (6)	1.00
O45	0.4115 (2)	0.71003 (17)	0.20124 (16)	0.0316 (7)	1.00
O46	0.5060 (3)	0.70984 (17)	0.30550 (16)	0.0323 (7)	1.00
O5	0.4331 (2)	0.58559 (17)	0.29898 (15)	0.0290 (6)	1.00
O51	0.2165 (3)	0.8157 (2)	0.22086 (18)	0.0406 (8)	1.00
O53	0.5959 (2)	0.61711 (18)	0.20245 (16)	0.0327 (7)	1.00
O54	0.4773 (3)	0.8199 (2)	0.22074 (19)	0.0412 (8)	1.00
O55	0.3394 (3)	0.69107 (19)	0.08828 (16)	0.0357 (7)	1.00
O58	0.1323 (3)	0.6518 (2)	0.21011 (17)	0.0397 (8)	1.00
O59	0.5286 (2)	0.48978 (18)	0.19356 (16)	0.0322 (7)	1.00
O6	0.3938 (4)	0.8221 (2)	0.4021 (2)	0.0519 (10)	1.00
O61	0.2959 (3)	0.81558 (18)	0.30398 (17)	0.0380 (8)	1.00
O65	0.3845 (3)	0.8168 (2)	0.11923 (19)	0.0456 (9)	1.00
O7	0.4751 (3)	0.28729 (17)	0.44525 (17)	0.0349 (7)	1.00
O8	0.1392 (3)	0.7717 (2)	0.1122 (2)	0.0559 (11)	1.00
O9	0.1635 (4)	0.7396 (3)	−0.0032 (2)	0.0666 (13)	1.00
S0AA	1.0677 (8)	1.0691 (5)	0.2300 (7)	0.052 (2)	0.40
S1	0.5695 (2)	0.97802 (16)	0.12363 (14)	0.0800 (7)	0.85
S11	0.64745 (11)	1.26729 (7)	0.26754 (6)	0.0400 (3)	1.00
S15	0.74615 (10)	0.80562 (7)	0.35423 (7)	0.0404 (3)	1.00
S3	0.09335 (12)	0.77480 (8)	0.05682 (8)	0.0502 (4)	1.00
S30	0.21627 (13)	1.31118 (8)	0.34368 (8)	0.0523 (4)	1.00
S34	0.37880 (11)	0.85901 (7)	0.46433 (7)	0.0425 (3)	1.00
S5	1.0963 (7)	1.0616 (3)	0.2024 (6)	0.059 (2)	0.55

SI1.2 Selected bond distances and bond angles in Al_{30}-acetate structure

Table SI1.2 Selected bond distances and bond angles in Al_{30}-acetate structure

Bonds	**Distance (Å)**	**Bonds**	**Distance (Å)**
Al1—O59	1.836 (3)	C1—S15	1.761 (5)
Al1—O53	1.841 (3)	C2—C3	1.461 (7)
Al1—O1E	1.898 (4)	C3—C8	1.391 (8)
Al1—O31	1.918 (3)	C3—C4	1.419 (7)
Al1—O26	1.943 (3)	C4—C5	1.362 (8)
Al1—O5	1.953 (3)	C5—C6	1.417 (8)
Al1—Al10	2.955 (2)	C6—C7	1.358 (7)
Al1—Al11	2.9668 (19)	C7—C8	1.429 (7)
Al1—Al5	2.9925 (17)	C8—C9	1.413 (7)
Al2—O35	1.783 (4)	C9—C10	1.384 (8)

Table SI1.2 Selected bond distances and bond angles in Al_{30}-acetate structure (Continued)

Bonds	**Distance (Å)**	**Bonds**	**Distance (Å)**
Al2—O45	1.785 (4)	S15—O17	1.449 (4)
Al2—O30	1.790 (3)	S15—O18	1.459 (4)
Al2—O5	1.838 (3)	S15—O16	1.464 (5)
Al3—O61	1.825 (4)	S3—O10	1.431 (6)
Al3—O4	1.849 (4)	S3—O8	1.442 (4)
Al3—O51	1.863 (4)	S3—O9	1.454 (5)
Al3—O40	1.866 (4)	S3—C16	1.746 (8)
Al3—O1O	1.924 (4)	C1D—C19	1.325 (11)
Al3—O35	2.074 (3)	C1D—C1H	1.333 (10)
Al3—Al13	2.893 (2)	C1H—C1H^{i}	1.361 (16)
Al3—Al8	2.935 (2)	C1H—C15^{i}	1.565 (11)
Al4—O43	1.868 (4)	C15—C16	1.344 (10)
Al4—O59	1.883 (4)	C15—C1H^{i}	1.565 (11)
Al4—O38	1.892 (3)	C16—C19	1.464 (12)
Al4—O27	1.925 (3)	O1J—C1N	1.166 (8)
Al4—O30	1.929 (3)	O11—C1N	1.252 (9)
Al4—O1G	1.931 (4)	C1N—C1P	1.589 (12)
Al7—O55	1.841 (4)	C1B—C0AA	1.377 (18)
Al7—O3	1.842 (4)	C1B—C18	1.485 (19)
Al7—O28	1.880 (4)	C17—S5	1.713 (8)
Al7—O27	1.894 (4)	C1A—C12	1.312 (19)
Al7—O1H	1.929 (4)	C1A—C0AA	1.334 (18)
Al7—O30	2.023 (3)	C12—C13	1.479 (18)
Al8—O34	1.868 (4)	C13—C999	1.386 (19)
Al8—O40	1.870 (4)	C13—C18	1.399 (19)
Al8—O33	1.870 (4)	C18—C14	1.382 (18)
Al8—O36	1.890 (3)	C14—C1E	1.329 (19)
Al8—O1I	1.930 (4)	C1E—C1G	1.392 (18)
Al8—O35	1.952 (3)	C999—C1G	1.432 (18)
Al9—O58	1.856 (4)	S34—O1	1.448 (4)
Al9—O4	1.862 (4)	S34—O2	1.484 (5)
Al9—O24	1.874 (4)	S34—C20	1.780 (2)
Al9—O34	1.876 (4)	S11—O13	1.442 (4)
Al9—O1N	1.915 (4)	S11—O12	1.450 (5)
Al9—O35	1.998 (4)	S11—O14	1.458 (4)
Al9—Al17	2.888 (2)	S11—C6	1.772 (5)
Al9—Al8	2.893 (2)	C1—C2	1.359 (7)
Al9—Al3	2.963 (2)	C1—C10	1.421 (8)
Al10—O36	1.835 (3)	O1CB—S1	1.365 (9)
Al10—O38	1.838 (3)	O1FB—S1	1.371 (12)
Al10—O1C	1.852 (3)	C1G—S0AA	1.859 (17)
Al10—O26	1.939 (3)	O1DA—S1	1.370 (11)
Al10—O44	1.973 (3)	Al5—O1A	1.844 (4)
Al10—O5	1.979 (3)	Al5—O19	1.846 (3)
Al10—Al11	2.9901 (19)	Al5—O15	1.857 (3)
Al11—O46	1.832 (3)	O15—Al6	1.899 (4)

Table SI1.2 Selected bond distances and bond angles in Al_{30}-acetate structure (Continued)

Bonds	**Distance (Å)**	**Bonds**	**Distance (Å)**
Al11—O33	1.844 (4)	O19—Al6^{ii}	1.888 (3)
Al11—O1B	1.871 (3)	O1A—C1J	1.343 (10)
Al11—O31	1.923 (3)	Al6—O19^{ii}	1.889 (3)
Al11—O44	1.950 (3)	Al6—O1B^{ii}	1.889 (3)
Al11—O5	2.020 (3)	Al6—O1C	1.893 (3)
Al12—O65	1.831 (4)	Al6—O1F	1.940 (4)
Al12—O55	1.845 (4)	Al6—O7	1.950 (3)
Al12—O41	1.879 (4)	O1B—Al6^{ii}	1.889 (3)
Al12—O28	1.910 (4)	O1E—C1J	1.378 (9)
Al12—O1L	1.929 (4)	C1J—C30	1.447 (16)
Al12—O45	1.995 (3)	O1Q—S0AA	1.378 (15)
Al13—O61	1.833 (4)	O1Q—S5	1.39 (2)
Al13—O65	1.836 (4)	O1R—S5	1.495 (11)
Al13—O54	1.861 (4)	O21—S5	1.532 (17)
Al13—O51	1.871 (4)	C0AA—S1	1.724 (14)
Al13—O1M	1.942 (4)	S0AA—O1AA	1.236 (16)
Al13—O45	2.080 (3)	S0AA—O1T	1.400 (14)
Al14—O46	1.872 (3)	S0AA—O1V	1.418 (16)
Al14—O41	1.873 (4)	S0AA—O0AA	1.84 (3)
Al14—O54	1.873 (4)	S5—O0AA	1.29 (3)
Al14—O53	1.890 (4)	S5—O1AA	1.49 (2)
Al14—O1K	1.917 (4)	S30—O32A	1.333 (8)
Al14—O45	1.946 (4)	S30—O33B	1.403 (9)
Al17—O58	1.848 (4)	S30—O31B	1.408 (12)
Al17—O3	1.853 (4)	S30—O33A	1.424 (11)
O26—Al5	1.942 (3)	S30—O31A	1.499 (8)
O31—Al5	1.953 (3)	S30—O32B	1.519 (9)
O44—Al5	1.952 (3)	S30—C25	1.784 (2)
S34—O6	1.443 (4)		
O58—Al9—O4	94.44 (17)	O41—Al14—O53	89.11 (16)
O58—Al9—O24	77.50 (16)	O54—Al14—O53	175.78 (18)
O4—Al9—O24	170.93 (18)	O46—Al14—O1K	90.91 (17)
O58—Al9—O34	169.22 (17)	O41—Al14—O1K	91.30 (18)
O4—Al9—O34	95.38 (17)	O54—Al14—O1K	91.62 (18)
O24—Al9—O34	92.36 (16)	O53—Al14—O1K	92.42 (17)
O58—Al9—O1N	91.45 (18)	O46—Al14—O45	94.69 (15)
O4—Al9—O1N	90.70 (18)	O41—Al14—O45	83.07 (15)
O24—Al9—O1N	93.64 (18)	O54—Al14—O45	82.76 (16)
O34—Al9—O1N	92.85 (18)	O53—Al14—O45	93.34 (15)
O58—Al9—O35	95.56 (16)	O1K—Al14—O45	171.87 (17)
O4—Al9—O35	81.07 (16)	O58—Al17—O3	93.78 (16)
O24—Al9—O35	95.43 (15)	O58—Al17—O24	77.89 (16)
O34—Al9—O35	81.62 (15)	O3—Al17—O24	169.22 (18)
O1N—Al9—O35	169.55 (18)	O58—Al17—O43	169.83 (16)
O59—Al1—O53	97.97 (15)	O3—Al17—O43	93.43 (16)
O59—Al1—O1E	95.74 (16)	O24—Al17—O43	94.05 (16)

Table SI1.2 Selected bond distances and bond angles in Al_{30}-acetate structure (Continued)

Bond Angle	Angle (°)	Bond Angle	Angle (°)
O53—Al1—O1E	96.37 (16)	O58—Al17—O1D	95.82 (18)
O59—Al1—O31	169.70 (17)	O3—Al17—O1D	92.88 (17)
O53—Al1—O31	91.33 (15)	O24—Al17—O1D	94.75 (18)
O1E—Al1—O31	87.59 (15)	O43—Al17—O1D	90.96 (18)
O59—Al1—O26	92.24 (15)	O58—Al17—O30	94.53 (16)
O53—Al1—O26	168.36 (15)	O3—Al17—O30	79.60 (15)
O1E—Al1—O26	88.13 (15)	O24—Al17—O30	94.11 (15)
O31—Al1—O26	78.11 (14)	O43—Al17—O30	79.74 (15)
O59—Al1—O5	93.84 (15)	O1D—Al17—O30	167.59 (18)
O53—Al1—O5	92.44 (15)	Al7—O3—Al17	106.54 (17)
O1E—Al1—O5	165.96 (15)	Al3—O4—Al	105.99 (18)
O31—Al1—O5	81.28 (14)	Al2—O5—Al1	120.63 (17)
O26—Al1—O5	81.25 (14)	Al2—O5—Al10	120.89 (18)
O35—Al2—O45	111.79 (16)	Al1—O5—Al10	97.43 (14)
O35—Al2—O30	112.84 (17)	Al2—O5—Al11	119.02 (17)
O45—Al2—O30	110.16 (16)	Al1—O5—Al11	96.61 (14)
O35—Al2—O5	108.25 (15)	Al10—O5—Al11	96.77 (13)
O45—Al2—O5	108.01 (16)	Al17—O24—Al	101.06 (17)
O30—Al2—O5	105.46 (15)	Al10—O26—Al5	102.44 (15)
O61—Al3—O4	168.05 (19)	Al10—O26—Al1	99.12 (14)
O61—Al3—O51	76.30 (17)	Al5—O26—Al1	100.77 (16)
O4—Al3—O51	94.56 (18)	Al7—O27—Al4	99.90 (16)
O61—Al3—O40	92.78 (17)	Al7—O28—Al12	99.64 (17)
O4—Al3—O40	95.63 (18)	Al2—O30—Al4	122.18 (16)
O51—Al3—O40	168.22 (19)	Al2—O30—Al7	123.61 (18)
O61—Al3—O1O	96.1 (2)	Al4—O30—Al7	95.39 (15)
O4—Al3—O1O	92.3 (2)	Al2—O30—Al17	121.52 (18)
O51—Al3—O1O	94.33 (19)	Al4—O30—Al17	93.75 (15)
O40—Al3—O1O	91.17 (19)	Al7—O30—Al17	92.57 (13)
O61—Al3—O35	93.85 (15)	Al1—O31—Al11	101.12 (15)
O4—Al3—O35	79.33 (15)	Al1—O31—Al5	101.26 (15)
O51—Al3—O35	96.29 (15)	Al11—O31—Al5	102.03 (15)
O40—Al3—O35	79.83 (15)	Al11—O33—Al8	137.18 (19)
O1O—Al3—O35	166.9 (2)	Al8—O34—Al	101.16 (18)
O43—Al4—O59	178.13 (16)	Al2—O35—Al8	120.76 (17)
O43—Al4—O38	89.60 (15)	Al2—O35—Al	123.12 (18)
O59—Al4—O38	91.83 (14)	Al8—O35—Al	94.18 (16)
O43—Al4—O27	88.61 (15)	Al2—O35—Al3	123.89 (19)
O59—Al4—O27	89.91 (16)	Al8—O35—Al3	93.57 (14)
O38—Al4—O27	177.12 (16)	Al—O35—Al3	93.38 (14)
O43—Al4—O30	83.92 (15)	Al10—O36—Al8	136.3 (2)
O59—Al4—O30	94.77 (15)	Al10—O38—Al4	135.12 (19)
O38—Al4—O30	94.37 (14)	Al3—O40—Al8	103.56 (18)
O27—Al4—O30	83.19 (14)	Al14—O41—Al12	100.91 (18)
O43—Al4—O1G	90.47 (17)	Al4—O43—Al17	102.49 (18)
O59—Al4—O1G	90.65 (16)	Al11—O44—Al5	101.11 (16)

Table SI1.2 Selected bond distances and bond angles in Al_{30}-acetate structure (Continued)

Bond Angle	Angle (°)	Bond Angle	Angle (°)
O38—Al4—O1G	92.66 (15)	Al11—O44—Al10	99.34 (13)
O27—Al4—O1G	89.62 (16)	Al5—O44—Al10	100.87 (14)
O30—Al4—O1G	170.97 (15)	Al2—O45—Al14	120.69 (16)
O55—Al7—O3	95.62 (17)	Al2—O45—Al12	124.96 (19)
O55—Al7—O28	78.15 (16)	Al14—O45—Al12	94.45 (16)
O3—Al7—O28	171.48 (17)	Al2—O45—Al13	122.61 (18)
O55—Al7—O27	170.30 (17)	Al14—O45—Al13	93.81 (15)
O3—Al7—O27	93.25 (17)	Al12—O45—Al13	92.21 (14)
O28—Al7—O27	92.61 (16)	Al11—O46—Al14	136.04 (19)
O55—Al7—O1H	92.10 (16)	Al3—O51—Al13	101.57 (18)
O3—Al7—O1H	92.27 (17)	Al1—O53—Al14	133.97 (19)
O28—Al7—O1H	93.76 (17)	Al13—O54—Al14	103.94 (19)
O27—Al7—O1H	91.45 (16)	Al7—O55—Al12	103.55 (17)
O55—Al7—O30	96.00 (15)	Al17—O58—Al	102.45 (17)
O3—Al7—O30	81.20 (15)	Al1—O59—Al4	131.73 (19)
O28—Al7—O30	93.56 (15)	Al3—O61—Al13	104.54 (18)
O27—Al7—O30	81.49 (14)	Al12—O65—Al13	106.45 (19)
O34—Al8—O40	92.41 (17)	O32A—S30—O33B	146.1 (6)
O34—Al8—O33	176.29 (17)	O32A—S30—O31B	60.2 (6)
O40—Al8—O33	89.79 (16)	O33B—S30—O31B	112.7 (6)
O34—Al8—O36	88.14 (16)	O32A—S30—O33A	116.1 (8)
O40—Al8—O36	176.46 (16)	O33B—S30—O33A	50.4 (7)
O33—Al8—O36	89.47 (15)	O31B—S30—O33A	148.1 (6)
O34—Al8—O1I	90.98 (17)	O32A—S30—O31A	111.7 (5)
O40—Al8—O1I	90.57 (16)	O33B—S30—O31A	62.0 (6)
O33—Al8—O1I	91.98 (16)	O31B—S30—O31A	53.5 (5)
O36—Al8—O1I	92.91 (15)	O33A—S30—O31A	111.1 (7)
O34—Al8—O35	83.05 (16)	O32A—S30—O32B	50.5 (5)
O40—Al8—O35	83.03 (15)	O33B—S30—O32B	112.7 (6)
O33—Al8—O35	94.27 (15)	O31B—S30—O32B	107.7 (6)
O36—Al8—O35	93.57 (14)	O33A—S30—O32B	66.9 (7)
O1I—Al8—O35	171.03 (16)	O31A—S30—O32B	143.5 (4)
O36—Al10—O38	100.05 (15)	O32A—S30—C25	106.8 (4)
O36—Al10—O1C	95.54 (15)	O33B—S30—C25	106.8 (4)
O38—Al10—O1C	95.73 (15)	O31B—S30—C25	106.4 (5)
O36—Al10—O26	166.73 (16)	O33A—S30—C25	104.7 (5)
O38—Al10—O26	90.42 (14)	O31A—S30—C25	105.5 (3)
O1C—Al10—O26	91.46 (14)	O32B—S30—C25	110.3 (3)
O36—Al10—O44	91.46 (14)	O6—S34—O1	113.0 (3)
O38—Al10—O44	166.08 (16)	O6—S34—O2	111.7 (3)
O1C—Al10—O44	90.88 (14)	O1—S34—O2	111.3 (3)
O26—Al10—O44	77.15 (14)	O6—S34—C20	106.5 (2)
O36—Al10—O5	91.00 (14)	O1—S34—C20	107.1 (2)
O38—Al10—O5	90.64 (14)	O2—S34—C20	106.8 (2)
O1C—Al10—O5	169.92 (15)	C20—C29—C28	120
O26—Al10—O5	80.67 (14)	C21—C20—C29	120

Table SI1.2 Selected bond distances and bond angles in Al_{30}-acetate structure (Continued)

Bond Angle	Angle (°)	Bond Angle	Angle (°)
O44—Al10—O5	81.28 (13)	C21—C20—S34	119.75 (15)
O46—Al11—O33	99.68 (15)	C29—C20—S34	120.00 (14)
O46—Al11—O1B	95.00 (15)	C20—C21—C22	120 (14)
O33—Al11—O1B	96.35 (15)	C21—C22—C23	120 (14)
O46—Al11—O31	90.58 (15)	C28—C23—C22	120 (14)
O33—Al11—O31	165.75 (16)	C28—C23—C24	120 (14)
O1B—Al11—O31	92.55 (15)	C22—C23—C24	120 (14)
O46—Al11—O44	166.73 (16)	C23—C28—C11	120 (14)
O33—Al11—O44	91.01 (15)	C23—C28—C29	120 (14)
O1B—Al11—O44	91.58 (14)	C11—C28—C29	120 (14)
O31—Al11—O44	77.60 (14)	C26—C11—C28	120 (14)
O46—Al11—O5	91.18 (14)	C11—C26—C25	120 (14)
O33—Al11—O5	90.40 (14)	C24—C25—C26	120 (14)
O1B—Al11—O5	169.94 (14)	C24—C25—S30	120.37 (15)
O31—Al11—O5	79.45 (13)	C26—C25—S30	119.17 (15)
O44—Al11—O5	80.82 (13)	C25—C24—C23	120 (14)
O65—Al12—O55	95.41 (18)	O13—S11—O12	115.8 (3)
O65—Al12—O41	95.74 (19)	O13—S11—O14	109.0 (3)
O55—Al12—O41	167.96 (17)	O12—S11—O14	110.8 (3)
O65—Al12—O28	171.1 (2)	O13—S11—C6	107.2 (3)
O55—Al12—O28	77.31 (16)	O12—S11—C6	107.2 (3)
O41—Al12—O28	91.17 (17)	O14—S11—C6	106.4 (2)
O65—Al12—O1L	93.22 (18)	C2—C1—C10	121.8 (5)
O55—Al12—O1L	91.91 (18)	C2—C1—S15	121.2 (4)
O41—Al12—O1L	92.00 (18)	C10—C1—S15	116.8 (4)
O28—Al12—O1L	92.12 (17)	C1—C2—C3	119.4 (5)
O65—Al12—O45	81.77 (16)	C8—C3—C4	121.0 (5)
O55—Al12—O45	95.54 (16)	C8—C3—C2	118.1 (5)
O41—Al12—O45	81.57 (15)	C4—C3—C2	120.8 (5)
O28—Al12—O45	93.76 (15)	C5—C4—C3	119.9 (5)
O1L—Al12—O45	171.37 (19)	C4—C5—C6	118.6 (5)
O61—Al13—O65	167.8 (2)	C7—C6—C5	123.0 (5)
O61—Al13—O54	93.31 (17)	C7—C6—S11	119.3 (4)
O65—Al13—O54	96.25 (19)	C5—C6—S11	117.7 (4)
O61—Al13—O51	75.94 (17)	C6—C7—C8	118.5 (5)
O65—Al13—O51	93.84 (18)	C3—C8—C9	121.4 (5)
O54—Al13—O51	168.30 (17)	C3—C8—C7	118.8 (4)
O61—Al13—O1M	94.36 (19)	C9—C8—C7	119.8 (5)
O65—Al13—O1M	93.12 (19)	C10—C9—C8	119.9 (5)
O54—Al13—O1M	90.14 (18)	C9—C10—C1	119.3 (5)
O51—Al13—O1M	95.22 (18)	O17—S15—O18	111.8 (3)
O61—Al13—O45	95.08 (15)	O17—S15—O16	112.7 (3)
O65—Al13—O45	79.35 (16)	O18—S15—O16	111.6 (3)
O54—Al13—O45	79.48 (15)	O17—S15—C1	107.9 (3)
O51—Al13—O45	96.64 (16)	O18—S15—C1	106.8 (2)
O1M—Al13—O45	166.34 (19)	O16—S15—C1	105.7 (3)

Table SI1.2 Selected bond distances and bond angles in Al_{30}-acetate structure (Continued)

Bond Angle	Angle (°)	Bond Angle	Angle (°)
O46—Al14—O41	177.74 (18)	O10—S3—O8	112.2 (4)
O46—Al14—O54	87.48 (16)	O10—S3—O9	112.5 (4)
O41—Al14—O54	92.00 (17)	O8—S3—O9	112.1 (3)
O46—Al14—O53	91.25 (15)	O10—S3—C16	108.1 (4)
O8—S3—C16	105.0 (3)	C1J—O1E—Al1	125.5 (5)
O9—S3—C16	106.3 (3)	O1A—C1J—O1E	126.8 (8)
C19—C1D—C1H	115.8 (8)	O1A—C1J—C30	115.0 (8)
C1D—C1H—C1H^{i}	131.7 (10)	O1E—C1J—C30	118.1 (8)
C1D—C1H—C15^{i}	116.6 (7)	O1AA—O1Q—S5	88 (3)
C1H^{i}—C1H—C15^{i}	111.7 (8)	O1AA—O1Q—O0AA	135 (4)
C16—C15—C1H^{i}	117.6 (8)	C1A—C0AA—C1B	121.5 (13)
C15—C16—C19	120.8 (7)	C1A—C0AA—S1	122.3 (11)
C15—C16—S3	123.2 (7)	C1B—C0AA—S1	115.8 (10)
C19—C16—S3	116.0 (6)	O1AA—S0AA—O1T	129.4 (15)
C1D—C19—C16	122.5 (7)	O1Q—S0AA—O1T	118.0 (15)
O1J—C1N—O11	125.4 (6)	O1Q—S0AA—O1V	111.6 (14)
O1J—C1N—C1P	120.4 (7)	O1T—S0AA—O1V	102.8 (11)
O11—C1N—C1P	113.4 (7)	O1Q—S0AA—O0AA	59.1 (14)
C0AA—C1B—C18	120.0 (12)	O1T—S0AA—O0AA	68.8 (11)
C87—C1C—C1I	120 (12)	O1V—S0AA—O0AA	156.6 (10)
C1F—C87—C1C	120 (12)	O1AA—S0AA—C1G	104.2 (10)
C87—C1F—C86	120 (12)	O1Q—S0AA—C1G	94.9 (11)
C82—C86—C1F	120 (12)	O1T—S0AA—C1G	114.3 (10)
C86—C82—C1I	120 (12)	O1V—S0AA—C1G	116.0 (10)
C86—C82—C88	120 (12)	O0AA—S5—O1R	135.1 (13)
C1I—C82—C88	120 (12)	O1Q—S5—O1R	122.3 (12)
C84—C1I—C82	120 (12)	O1AA—S5—O1R	102.1 (14)
C84—C1I—C1C	120 (12)	O1Q—S5—O21	111.1 (14)
C82—C1I—C1C	120 (12)	O1AA—S5—O21	129.5 (15)
C1I—C84—C83	120 (12)	O1R—S5—O21	102.8 (10)
C17—C83—C84	120 (12)	O0AA—S5—C17	119.2 (11)
C88—C17—C83	120 (12)	O1Q—S5—C17	114.4 (12)
C88—C17—S5	117.5 (4)	O1AA—S5—C17	109.7 (11)
C83—C17—S5	122.4 (4)	O21—S5—C17	112.3 (11)
C17—C88—C82	120	O1CB—S1—O1DA	106.1 (6)
C12—C1A—C0AA	123.0 (13)	O1CB—S1—O1FB	120.2 (7)
C1A—C12—C13	119.9 (12)	O1DA—S1—O1FB	108.5 (7)
C999—C13—C18	120.3 (12)	O1CB—S1—C0AA	105.9 (6)
C999—C13—C12	120.1 (12)	O1DA—S1—C0AA	112.3 (7)
C18—C13—C12	119.5 (13)	O1FB—S1—C0AA	103.9 (7)
C14—C18—C13	119.0 (13)	O19^{ii}—Al6—O1B^{ii}	92.70 (14)
C14—C18—C1B	125.3 (12)	O19^{ii}—Al6—O1C	90.76 (14)
C13—C18—C1B	115.7 (12)	O1B^{ii}—Al6—O1C	175.42 (16)
C1E—C14—C18	121.5 (13)	O19^{ii}—Al6—O15	94.00 (15)
C14—C1E—C1G	122.1 (13)	O1B^{ii}—Al6—O15	90.82 (15)
C13—C999—C1G	119.2 (12)	O1C—Al6—O15	91.93 (14)

Table SI1.2 Selected bond distances and bond angles in Al_{30}-acetate structure (Continued)

Bond Angle	Angle (°)	Bond Angle	Angle (°)
C1E—C1G—C999	117.8 (13)	O19^{ii}—Al6—O1F	89.40 (16)
C1E—C1G—S0AA	126.2 (10)	O1B^{ii}—Al6—O1F	89.41 (15)
C999—C1G—S0AA	113.9 (10)	O1C—Al6—O1F	87.62 (15)
O1A—Al5—O19	98.29 (16)	O15—Al6—O1F	176.58 (16)
O1A—Al5—O15	99.15 (16)	O19^{ii}—Al6—O7	174.65 (17)
O19—Al5—O15	94.60 (14)	O1B^{ii}—Al6—O7	88.68 (14)
O1A—Al5—O26	90.93 (15)	O1C—Al6—O7	87.60 (14)
O19—Al5—O26	167.36 (15)	O15—Al6—O7	91.15 (15)
O15—Al5—O26	92.43 (14)	O1F—Al6—O7	85.44 (16)
O1A—Al5—O44	164.54 (15)	Al11—O1B—Al6^{ii}	133.60 (18)
O19—Al5—O44	91.70 (14)	Al10—O1C—Al6	135.20 (19)
O15—Al5—O44	91.74 (15)	O19—Al5—Al1	132.76 (11)
O26—Al5—O44	77.59 (13)	O15—Al5—Al1	132.01 (11)
O1A—Al5—O31	90.65 (15)	O26—Al5—Al1	39.63 (10)
O19—Al5—O31	93.87 (14)	O44—Al5—Al1	81.19 (9)
O15—Al5—O31	165.98 (15)	O31—Al5—Al1	38.96 (10)
O26—Al5—O31	77.32 (13)	Al5—O15—Al6	133.74 (17)
O44—Al5—O31	76.86 (14)	Al5—O19—Al6^{ii}	133.97 (18)
O1A—Al5—Al1	83.36 (11)	C1J—O1A—Al5	124.0 (5)

Symmetry codes: (i) $-x, -y+2, -z$; (ii) $-x+1, -y+1, -z+1$.

SI1.3 BVS calculation parameters and assignments of oxygen atoms in Al_{30}-acetate polyoxocation

Table SI1.3 BVS calculation parameters and assignments of oxygen atoms in Al_{30}-acetate polyoxocation

Atoms	Bonds	R_i	R_0-R_i		v_i (v.u.)	Assignment
O1F	Al6—O1F	1.94	-0.32		0.42	
				Σv_i =	**0.42**	H_2O
O1G	Al4—O1G	1.931	-0.311		0.43	
				Σv_i =	**0.43**	η-H_2O
O1H	Al7—O1H	1.929	-0.309		0.43	
				Σv_i =	**0.43**	η-H_2O
O1I	Al8—O1I	1.93	-0.31		0.43	
				Σv_i =	**0.43**	η-H_2O
O1K	Al14—O1K	1.917	-0.297		0.45	
				Σv_i =	**0.45**	η-H2O
O1L	Al12—O1L	1.929	-0.309		0.43	
				Σv_i =	**0.43**	η-H2O
O1M	Al13—O1M	1.942	-0.322		0.42	
				Σv_i =	**0.42**	η-H2O
O1N	O1N—Al0	1.915	-0.295		0.45	
				Σv_i =	0.45	η-H2O
O1O	Al3—O1O	1.924	-0.304		0.44	
				Σv_i =	**0.44**	H_2O

Table SI1.3 BVS calculation parameters and assignments of oxygen atoms in Al_{30}-acetate polyoxocation (Continued)

Atoms	**Bonds**	R_i	R_0-R_i		v_i **(v.u.)**	**Assignment**
O24	Al17—O24	1.867	-0.247		0.51	
	Al0—O24	1.874	-0.254		0.50	
				Σv_i =	**1.02**	μ^2-OH
O26	Al10—O26	1.939	-0.319		0.42	
	Al1—O26	1.943	-0.323		0.42	
	O26—Al5	1.942	-0.322		0.42	
				Σv_i =	**1.26**	μ^3-OH
O27	Al4—O27	1.925	-0.305		0.44	
	Al7—O27	1.894	-0.274		0.48	
				Σv_i =	**0.92**	μ^2-OH
O28	Al12—O28	1.91	-0.29		0.46	
	Al7—O28	1.88	-0.26		0.50	
				Σv_i =	**0.95**	μ^2-OH
O3	Al17—O3	1.853	-0.233		0.53	
	Al7—O3	1.842	-0.222		0.55	
				Σv_i =	**1.08**	μ^2-OH
O30	Al17—O30	2.074	-0.454		0.29	
	Al2—O30	1.79	-0.17		0.63	
	Al4—O30	1.929	-0.309		0.43	
	Al7—O30	2.023	-0.403		0.34	
				Σv_i =	**1.70**	μ^4-O
O31	Al11—O31	1.923	-0.303		0.44	
	Al1—O31	1.918	-0.298		0.45	
	O31—Al5	1.953	-0.333		0.41	
				Σv_i =	**1.29**	μ^3-OH
O33	Al11—O33	1.844	-0.224		0.55	
	Al8—O33	1.87	-0.25		0.51	
				Σv_i =	**1.05**	μ^2-OH
O34	Al8—O34	1.868	-0.248		0.51	
	Al0—O34	1.876	-0.256		0.50	
				Σv_i =	**1.01**	μ^2-OH
O35	Al2—O35	1.783	-0.163		0.64	
	Al3—O35	2.074	-0.454		0.29	
	Al0—O35	1.998	-0.378		0.36	
	Al8—O35	1.952	-0.332		0.41	
				Σv_i =	1.70	μ^4-O
O36	Al10—O36	1.835	-0.215		0.56	
	Al8—O36	1.89	-0.27		0.48	
				Σv_i =	**1.04**	μ^2-OH
O38	Al10—O38	1.838	-0.218		0.55	
	Al4—O38	1.892	-0.272		0.48	
					1.03	μ^2-OH
O4	Al3—O4	1.849	-0.229		0.54	
	Al0—O4	1.862	-0.242		0.52	
				Σv_i =	**1.06**	μ^2-OH

Table SI1.3 BVS calculation parameters and assignments of oxygen atoms in Al_{30}-acetate polyoxocation (Continued)

Atoms	**Bonds**	R_i	R_0-R_i		v_i (v.u.)	**Assignment**
O40	Al3—O40	1.866	-0.246		0.51	
	Al8—O40	1.87	-0.25		0.51	
				Σv_i =	**1.02**	μ^2-OH
O41	Al12—O41	1.879	-0.259		0.50	
	Al14—O41	1.873	-0.253		0.50	
				Σv_i =	**1.00**	μ^2-OH
	Al4—O43	1.868	-0.248		0.51	
				Σv_i =	**1.01**	μ^2-OH
O44	Al10—O44	1.973	-0.353		0.39	
	Al11—O44	1.95	-0.33		0.41	
	O44—Al5	1.952	-0.332		0.41	
				Σv_i =	**1.20**	μ^3-OH
O45	Al12—O45	1.995	-0.375		0.36	
	Al13—O45	2.08	-0.46		0.29	
	Al14—O45	1.946	-0.326		0.41	
	Al2—O45	1.785	-0.165		0.64	
				Σv_i =	**1.71**	μ^4-O
O46	Al11—O46	1.832	-0.212		0.56	
	Al14—O46	1.872	-0.252		0.51	
				Σv_i =	**1.07**	μ^2-OH
O5	Al10—O5	1.979	-0.359		0.38	
	Al11—O5	2.02	-0.4		0.34	
	Al1—O5	1.953	-0.333		0.41	
	Al2—O5	1.838	-0.218		0.55	
				Σv_i =	**1.68**	μ^4-O
O51	Al13—O51	1.871	-0.251		0.51	
	Al3—O51	1.863	-0.243		0.52	
				Σv_i =	**1.03**	μ^2-OH
O53	Al14—O53	1.89	-0.27		0.48	
	Al1—O53	1.841	-0.221		0.55	
				Σv_i =	**1.03**	μ^2-OH
O54	Al13—O54	1.861	-0.241		0.52	
	Al14—O54	1.873	-0.253		0.50	
				Σv_i =	**1.03**	μ^2-OH
O55	Al12—O55	1.845	-0.225		0.54	
	Al7—O55	1.841	-0.221		0.55	
				Σv_i =	**1.09**	μ^2-OH
O58	Al17—O58	1.848	-0.228		0.54	
	Al0—O58	1.856	-0.236		0.53	
				Σv_i =	**1.07**	μ^2-OH
O59	Al1—O59	1.836	-0.216		0.56	
	Al4—O59	1.883	-0.263		0.49	
				Σv_i =	**1.05**	μ^2-OH

Table SI1.3 BVS calculation parameters and assignments of oxygen atoms in Al_{30}-acetate polyoxocation (Continued)

Atoms	**Bonds**	R_i	R_0-R_i		v_i **(v.u.)**	**Assignment**
O61	Al13—O61	1.833	-0.213		0.56	
	Al3—O61	1.825	-0.205		0.57	
				Σv_i =	**1.14**	μ^2-OH
O65	Al12—O65	1.831	-0.211		0.57	
	Al13—O65	1.836	-0.216		0.56	
				Σv_i =	**1.12**	μ^2-OH
O7	Al6—O7	1.95	-0.33		0.41	
				Σv_i =	**0.41**	η-H_2O
O05	Al8—O35	1.952	-0.332		0.41	
				Σv_i =	**0.41**	η-H_2O
O15	Al5—O15	1.857	-0.237		0.53	
	O15—Al6	1.899	-0.279		0.47	
				Σv_i =	**1.00**	μ^2-OH
O19	Al5—O19	1.846	-0.226		0.54	
	Al6—O19^{ii}	1.889	-0.269		0.48	
	O19—Al6^{ii}	1.888	-0.268		0.48	
				Σv_i =	**1.51**	μ^3-OH
O1B	Al11—O1B	1.871	-0.251		0.51	
	Al6—O1B^{ii}	1.889	-0.269		0.48	
				Σv_i =	**0.99**	μ^2-OH
O1C	Al10—O1C	1.852	-0.232		0.53	
	Al6—O1C	1.893	-0.273		0.48	
				Σv_i =	**1.01**	μ^2-OH
O1D	Al17—O1D	1.915	-0.295		0.45	
					0.45	H_2O

Symmetry codes: (i) −*x*, −*y*+2, −*z*; (ii) −*x*+1, −*y*+1, −*z*+1.

SI1.4 Hydrogen bonds in Al_{30}−acetate

Table SI1.4 Hydrogen bonds in Al_{30}−acetate

A–H···A	**A–H (Å)**	**H···B (Å)**	**A···B (Å)**	**∠ A–H···B (°)**
Moderate hydrogen bonds				
O1B–H1B···O1	0.93	2.50	3.318(5)	146
O1B–H1B···O6	0.93	2.44	3.113(5)	130
O1C–H1C···O32A	0.93	1.93	2.779(10)	151
O1C–H1C···O32B	0.93	2.04	2.969(10)	172
O4–H4···O16	0.93	2.29	3.084(6)	143
O7–H7A···O14	0.86	1.88	2.719(5)	165
O1F–H1FA···O11	0.86	2.16	2.551(7)	107
O1F–H1FA···O32B	0.86	2.51	3.156(11)	143
O1F–H1FB···O11	0.86	2.17	2.551(7)	106
O1G–H1GA···O31B	0.87	2.25	2.925(12)	135
O1G–H1GB···O13	0.87	2.10	2.796(8)	136

Table SI1.4 Hydrogen bonds in Al_{30}−acetate (Continued)

A–H···A	**A–H (Å)**	**H···B (Å)**	**A···B (Å)**	**∠ A–H···B (°)**
Moderate hydrogen bonds				
O1G–H1GB···O14	0.87	2.49	3.310(6)	159
O1H–H1HB···O27	0.86	1.90	2.674(5)	149
O1I–H1IA···O1J	0.89	1.70	2.577(7)	168
O15–H15···O2AA	0.93	2.01	2.811(5)	144
O19–H19···O1J	0.93	1.88	2.751(7)	154
O1M–H1MA···O1Q	0.85	1.99	2.72(2)	144
O1M–H1MB···O1CB	0.85	2.19	2.788(11)	127
O1N–H1NA….O16	0.87	1.84	2.698(5)	171
O1N–H1NB···O11	0.86	1.76	2.536(7)	148
O1O–H1OB···O1Q	0.87	1.99	2.72(2)	139
O26–H26···O14	0.98	1.76	2.709(5)	163
O27–H27···O1H	0.93	1.87	2.674(5)	143
O33–H33···O6	0.93	2.23	2.919(5)	131
O36–H36···O1J	0.93	2.30	2.864(7)	119
O38–H38···O31B	0.93	2.00	2.828(13)	147
O38–H38···O32A	0.93	1.91	2.781(9)	154
O43–H43···O31A	0.93	2.33	3.045(9)	133
O43–H43···O31B	0.93	2.46	2.890(12)	108
O44–H44···O15	0.98	2.07	2.832(4)	133
O44–H44···O19	0.98	2.08	2.838(4)	133
O46–H46···O6	0.93	2.18	2.883(5)	132
O46–H46···O17	0.93	2.50	3.115(6)	124
O51–H51···O8	0.93	2.15	2.976(6)	147
O54–H54···O1CB	0.93	2.36	3.085(10)	135
O55–H55···O8	0.93	1.95	2.826(6)	155
O58–H58···O8	0.93	1.98	2.855(5)	156
O61–H61···O6	0.93	1.83	2.756(6)	171
Weak hydrogen bonds				
C2–H2···O17	0.93	2.55	2.918	104
C7–H7···O12	0.93	2.48	2.872(7)	106
C19–H19A···O8	0.93	2.57	2.899(8)	101
C26–H26A···O31A	0.93	2.56	2.937(8)	105

SI2 Supplementary Information for Chapter 4

SI2.1 Fractional atomic coordinates and isotropic or equivalent isotropic displacement parameters of MK-A structure

Table SI2.1 Fractional atomic coordinates and isotropic or equivalent isotropic displacement parameters of MK-A structure, Space group $P4_2/mmc$.

Atom	*x*	*y*	*z*	U_{iso}/U_{eq} (Å^2)	Occupancy
S5	0.5	0.86865 (3)	0.31603 (4)	0.0466 (4)	1.00
S6	0.43402 (4)	0.79182 (4)	0.5	0.0520 (4)	1.00
S4	0.35983 (9)	0.94102 (7)	0.42374 (10)	0.1645 (12)	1.00
Al11	0.5	0.83572 (4)	0.39509 (5)	0.0415 (4)	1.00
Al10	0.43219 (3)	0.86971 (3)	0.41394 (3)	0.0413 (3)	1.00
Al12	0.40056 (4)	0.85567 (4)	0.5	0.0437 (4)	1.00
Al9	0.38960 (3)	0.86860 (3)	0.34881 (4)	0.0514 (4)	1.00
Al14	0.42919 (3)	0.81596 (3)	0.36288 (4)	0.0473 (3)	1.00
Al16	0.36115 (3)	0.80144 (3)	0.33056 (4)	0.0534 (4)	1.00
Al13	0.37831 (3)	0.82885 (3)	0.41311 (4)	0.0502 (3)	1.00
Al20	0.38917 (4)	0.76739 (4)	0.25526 (5)	0.0697 (5)	1.00
Al1	0.41979 (4)	0.93831 (3)	0.37429 (4)	0.0611 (4)	1.00
Al3	0.40529 (7)	1	0.32029 (7)	0.0782 (8)	1.00
Al22	0.38804 (4)	0.75497 (3)	0.39103 (5)	0.0644 (4)	1.00
Al21	0.37799 (4)	0.72929 (4)	0.31830 (5)	0.0725 (5)	1.00
Al15	0.40927 (4)	0.82780 (4)	0.27157 (4)	0.0627 (4)	1.00
Al19	0.34959 (4)	0.81793 (4)	0.24046 (5)	0.0736 (5)	1.00
Al2	0.46072 (5)	0.96673 (3)	0.29995 (4)	0.0728 (5)	1.00
Al17	0.31591 (4)	0.85085 (4)	0.36417 (6)	0.0773 (5)	1.00
Al8	0.46078 (7)	1	0.37976 (7)	0.0742 (7)	1.00
Al18	0.30000 (4)	0.83016 (4)	0.28959 (6)	0.0818 (6)	1.00
Al23	0.32696 (5)	0.74121 (4)	0.36806 (5)	0.0807 (6)	1.00
Al24	0.28913 (4)	0.79164 (5)	0.35434 (6)	0.0862 (6)	1.00
Al4	0.42839 (10)	1	0.24097 (7)	0.1072 (13)	1.00
Al5	0.5	1	0.23487 (9)	0.1010 (17)	1.00
Al6	0.46744 (8)	0.93801 (4)	0.21140 (5)	0.1220 (11)	1.00
Al7	0.5	0.96771 (7)	0.15112 (7)	0.152 (2)	1.00
O43	0.42088 (6)	0.82754 (6)	0.41449 (8)	0.0451 (7)	1.00
O36	0.42311 (7)	0.87554 (7)	0.46345 (8)	0.0477 (7)	1.00
O78	0.3541 (3)	0.96126 (18)	0.4578 (3)	0.235 (5)	1.00
O28	0.43126 (7)	0.85919 (6)	0.36136 (8)	0.0459 (7)	1.00
O29	0.43976 (7)	0.90878 (7)	0.40160 (8)	0.0522 (8)	1.00
O30	0.47127 (6)	0.85909 (6)	0.42068 (8)	0.0472 (7)	1.00
O34	0.53007 (7)	0.81289 (7)	0.37217 (9)	0.0532 (8)	1.00
O42	0.38572 (7)	0.82477 (7)	0.35920 (8)	0.0498 (7)	1.00
O41	0.38927 (6)	0.87024 (6)	0.40190 (9)	0.0480 (7)	1.00
O3AA	0.44875 (8)	0.93983 (7)	0.33582 (9)	0.0587 (9)	1.00
O35	0.5	0.80764 (10)	0.43673 (13)	0.0571 (12)	1.00
O44	0.43262 (7)	0.81350 (8)	0.31207 (9)	0.0593 (9)	1.00

Table SI2.1 Fractional atomic coordinates and isotropic or equivalent isotropic displacement parameters of MK-A structure, Space group $P4_2/mmc$. (Continued)

Atom	***x***	***y***	***z***	U_{iso}/U_{eq} **(Å^2)**	**Occupancy**
O57	0.42135 (8)	0.77673 (7)	0.37335 (9)	0.0585 (9)	1.00
O10	0.44845 (13)	1	0.33155 (13)	0.0665 (14)	1.00
O26	0.5	0.96641 (10)	0.31655 (13)	0.0660 (14)	1.00
O46	0.37476 (8)	0.80363 (7)	0.28428 (9)	0.0594 (9)	1.00
O56	0.36356 (8)	0.76407 (7)	0.34855 (9)	0.0592 (9)	1.00
O31	0.5	0.86467 (10)	0.35604 (13)	0.0692 (15)	1.00
O40	0.37672 (7)	0.83721 (8)	0.46333 (9)	0.0594 (9)	1.00
O58	0.37576 (8)	0.78800 (7)	0.41891 (9)	0.0601 (9)	1.00
O45	0.39740 (8)	0.86145 (7)	0.29890 (9)	0.0608 (9)	1.00
O27	0.39782 (9)	0.90908 (7)	0.34741 (10)	0.0681 (10)	1.00
O24	0.44279 (10)	0.96820 (7)	0.40022 (10)	0.0766 (12)	1.00
O49	0.33876 (7)	0.83743 (8)	0.40476 (10)	0.0663 (10)	1.00
O77	0.37243 (10)	0.88913 (10)	0.5	0.0597 (12)	1.00
O48	0.34883 (8)	0.87174 (8)	0.34596 (11)	0.0663 (10)	1.00
O55	0.40907 (8)	0.75006 (8)	0.29581 (11)	0.0715 (10)	1.00
O47	0.32395 (7)	0.81534 (8)	0.33433 (11)	0.0667 (10)	1.00
O69	0.36044 (9)	0.74140 (8)	0.27376 (11)	0.0718 (10)	1.00
O11	0.39765 (9)	0.96868 (7)	0.35173 (10)	0.0743 (11)	1.00
O76	0.44303 (9)	0.84959 (10)	0.25227 (10)	0.0789 (12)	1.00
O13	0.46775 (16)	1	0.26415 (13)	0.0811 (18)	1.00
O12	0.41984 (10)	0.97304 (8)	0.28247 (10)	0.0769 (12)	1.00
O54	0.42052 (8)	0.79315 (9)	0.24365 (10)	0.0727 (11)	1.00
O38	0.40571 (12)	0.77517 (11)	0.5	0.0714 (14)	1.00
O37	0.42973 (12)	0.82405 (11)	0.5	0.0773 (16)	1.00
O53	0.36446 (9)	0.78375 (9)	0.21969 (10)	0.0759 (11)	1.00
O52	0.38505 (9)	0.83926 (9)	0.23205 (10)	0.0790 (11)	1.00
O15	0.46578 (11)	0.93863 (8)	0.26356 (10)	0.0837 (13)	1.00
O32	0.47357 (8)	0.88608 (8)	0.30685 (13)	0.0788 (12)	1.00
O66	0.34322 (10)	0.71200 (8)	0.33730 (11)	0.0836 (12)	1.00
O33	0.5	0.84108 (12)	0.29699 (15)	0.095 (2)	1.00
O51	0.31444 (9)	0.80032 (8)	0.25803 (11)	0.0755 (11)	1.00
O39	0.44998 (9)	0.78491 (9)	0.46656 (11)	0.0821 (12)	1.00
O72	0.33198 (9)	0.84878 (9)	0.26589 (12)	0.0810 (12)	1.00
O61	0.30076 (9)	0.75636 (10)	0.33329 (12)	0.0827 (12)	1.00
O59	0.39905 (10)	0.72207 (8)	0.36164 (12)	0.0851 (13)	1.00
O8	0.39188 (10)	0.93908 (9)	0.41482 (12)	0.0841 (12)	1.00
O64	0.30970 (9)	0.77358 (10)	0.39221 (11)	0.0836 (12)	1.00
O63	0.27103 (8)	0.80605 (9)	0.31147 (13)	0.0852 (13)	1.00
O68	0.41136 (11)	0.74010 (8)	0.43220 (11)	0.0909 (14)	1.00
O60	0.35400 (10)	0.73384 (8)	0.40590 (11)	0.0874 (13)	1.00
O62	0.28376 (9)	0.82718 (11)	0.38128 (13)	0.0967 (15)	1.00
O23	0.36595 (15)	1	0.30203 (16)	0.091 (2)	1.00
O17	0.5	0.91164 (12)	0.21420 (15)	0.110 (3)	1.00
O70	0.39057 (11)	0.69177 (9)	0.29732 (13)	0.0965 (15)	1.00
O50	0.29397 (9)	0.86197 (10)	0.32263 (14)	0.0946 (15)	1.00

Table SI2.1 Fractional atomic coordinates and isotropic or equivalent isotropic displacement parameters of MK-A structure, Space group $P4_2/mmc$. (Continued)

Atom	***x***	***y***	***z***	U_{iso}/U_{eq} **(Å^2)**	**Occupancy**
O71	0.40414 (10)	0.73726 (11)	0.22121 (13)	0.0979 (14)	1.00
O73	0.33254 (11)	0.83004 (11)	0.19340 (12)	0.1036 (16)	1.00
O14	0.5	0.96733 (11)	0.20784 (15)	0.104 (3)	1.00
O74	0.27077 (10)	0.84569 (11)	0.25486 (14)	0.1070 (17)	1.00
O75	0.30204 (9)	0.88495 (11)	0.39237 (14)	0.1011 (16)	1.00
O25	0.5	1	0.3832 (2)	0.108 (3)	1.00
O16	0.43846 (15)	0.96890 (9)	0.21086 (11)	0.120 (2)	1.00
O65	0.25132 (10)	0.77633 (13)	0.37117 (15)	0.1174 (19)	1.00
O67	0.29780 (12)	0.71373 (12)	0.38840 (14)	0.1190 (19)	1.00
O18	0.43909 (15)	0.90753 (9)	0.21044 (12)	0.125 (2)	1.00
O22	0.3879 (2)	1	0.2256 (2)	0.139 (4)	1.00
O2AA	0.53138 (17)	0.93972 (10)	0.15959 (12)	0.149 (3)	1.00
O79	0.34681 (12)	0.90824 (11)	0.43303 (15)	0.1149 (18)	1.00
O21	0.5	0.96027 (18)	0.09852 (18)	0.183 (5)	1.00
O80	0.3407 (2)	0.9526 (2)	0.3893 (2)	0.233 (5)	1.00
S1	0.5	0.93731 (18)	0.4660 (2)	0.063 (2)	0.251
O1	0.5	0.9211 (3)	0.5	0.127 (4)	0.503
O1AA	0.4720 (2)	0.9571 (3)	0.4662 (3)	0.118 (3)	0.251
O4A	0.5	0.9267 (4)	0.4088 (5)	0.034 (4)	0.249
O3A	0.4448 (4)	0.9257 (4)	0.5	0.036 (4)	0.249
S2	0.46795 (18)	0.94228 (18)	0.5	0.063 (2)	0.249
O1A	0.5	0.9211 (3)	0.5	0.127 (4)	0.497
O2A	0.4720 (2)	0.9571 (3)	0.4662 (3)	0.118 (3)	0.249
O4AA	0.4303 (3)	0.9311 (3)	0.5	0.084 (4)	0.503
O4	0.5	0.9230 (3)	0.4248 (4)	0.071 (3)	0.503
S3	0.49384 (12)	0.76315 (9)	0.28084 (11)	0.1162 (14)	0.5
O5	0.4788 (2)	0.7782 (2)	0.2495 (3)	0.113 (3)	0.5
O6	0.4923 (3)	0.73091 (19)	0.2698 (3)	0.137 (4)	0.5
O7	0.4797 (2)	0.7662 (3)	0.3169 (3)	0.129 (4)	0.5
O7A	0.5257 (2)	0.7733 (2)	0.2849 (3)	0.107 (3)	0.5
S7	0.29474 (4)	0.70526 (4)	0.25	0.0765 (6)	1.00
O81	0.29937 (9)	0.73709 (9)	0.25818 (12)	0.0816 (12)	1.00
O82	0.31269 (9)	0.69602 (10)	0.21707 (12)	0.0860 (12)	1.00
S8	0.36610 (9)	0.92191 (6)	0.24867 (9)	0.1716 (16)	1.00
O83	0.39481 (13)	0.91958 (9)	0.26445 (12)	0.1131 (19)	1.00
O84	0.34528 (17)	0.90986 (17)	0.2760 (3)	0.189 (3)	1.00
O85	0.3590 (2)	0.95190 (16)	0.2374 (3)	0.252 (6)	1.00
O86	0.3649 (3)	0.9032 (2)	0.2150 (2)	0.302 (7)	1.00
S9	0.31566 (15)	0.7874 (2)	0.4953 (3)	0.056 (3)	0.176
O87	0.3331 (6)	0.7624 (6)	0.4784 (9)	0.112 (13)	0.176
O87A	0.3277 (5)	0.7880 (5)	0.5326 (4)	0.046 (6)	0.176
O88	0.2837 (3)	0.7809 (5)	0.4938 (7)	0.061 (6)	0.176
O88A	0.3176 (4)	0.8153 (4)	0.4744 (5)	0.059 (6)	0.176
S9A	0.30934 (16)	0.8018 (2)	0.4943 (3)	0.053 (3)	0.16
O87B	0.3259 (9)	0.7800 (8)	0.4723 (9)	0.160 (18)	0.16

Table SI2.1 Fractional atomic coordinates and isotropic or equivalent isotropic displacement parameters of MK-A structure, Space group $P4_2/mmc$. (Continued)

Atom	*x*	*y*	*z*	U_{iso}/U_{eq} (Å^2)	Occupancy
O87C	0.3213 (5)	0.8001 (6)	0.5319 (4)	0.043 (5)	0.16
O88B	0.2771 (3)	0.7957 (5)	0.4938 (9)	0.078 (8)	0.16
O88C	0.3118 (7)	0.8323 (5)	0.4792 (8)	0.118 (12)	0.16
S9B	0.3213 (3)	0.7666 (4)	0.4955 (7)	0.143 (6)	0.164
O87D	0.3357 (6)	0.7390 (6)	0.4826 (8)	0.124 (12)	0.164
O87E	0.3345 (7)	0.7699 (8)	0.5324 (7)	0.086 (10)	0.164
O88D	0.2891 (3)	0.7676 (5)	0.4942 (9)	0.070 (7)	0.164
O88E	0.3297 (10)	0.7921 (8)	0.4719 (11)	0.160 (18)	0.164
O90	0.5	0.8610 (2)	0.5	0.092 (3)	1.00
O91	0.37285 (12)	0.68307 (12)	0.22637 (15)	0.1119 (16)	1.00
O92	0.33034 (14)	0.74559 (15)	0.17392 (19)	0.143 (2)	1.00
O93	0.41834 (19)	0.81219 (19)	0.1662 (2)	0.192 (3)	1.00
O0AA	0.4744 (2)	1	0.14668 (17)	0.147 (4)	1.00
O9	0.3998 (5)	1	0.4558 (6)	0.176 (8)	0.5
O19	0.2652 (6)	1	0.4134 (7)	0.202 (10)	0.5
O2	0.4863 (2)	0.8174 (2)	0.2097 (3)	0.116 (3)	0.5
O3	0.2407 (3)	0.7658 (3)	0.2636 (4)	0.168 (6)	0.5
O5AA	0.4745 (3)	0.7444 (3)	0.3773 (4)	0.152 (5)	0.5
O6AA	0.4567 (3)	0.7011 (3)	0.2866 (4)	0.152 (5)	0.5
O7AA	0.2268 (4)	0.7194 (4)	0.3531 (5)	0.186 (6)	0.5
O8AA	0.2735 (5)	1	0.2606 (6)	0.168 (8)	0.5
O9AA	0.3293 (3)	0.9563 (3)	0.3138 (4)	0.167 (5)	0.5
O0BA	0.2672 (5)	0.7745 (5)	0.1770 (8)	0.254 (10)	0.5

SI2.2 Selected bond distances and bond angles in Al_{30}-acetate structure

Table SI2.2 Selected bond distances and bond angles in MK-A structure

Bonds	Distance (Å)	Bonds	Distance (Å)
S5—O31	1.453 (5)	Al2—O12	1.958 (5)
S5—O32^{i}	1.457 (4)	Al2—O15	1.833 (4)
S5—O32	1.457 (4)	Al17—O49	1.884 (4)
S5—O33	1.413 (5)	Al17—O48	1.867 (4)
S6—O38	1.472 (5)	Al17—O47	1.955 (4)
S6—O37	1.457 (5)	Al17—O62	1.892 (5)
S6—O39^{ii}	1.435 (4)	Al17—O50	1.859 (5)
S6—O39	1.435 (4)	Al17—O75	1.938 (4)
S4—O78	1.548 (9)	Al8—O10	1.823 (5)
S4—O8	1.474 (5)	Al8—O24^{iii}	1.796 (4)
S4—O79	1.616 (6)	Al8—O24	1.796 (4)
S4—O80	1.595 (7)	Al8—O25	1.762 (3)
Al11—O30^{i}	1.899 (3)	Al18—O47	2.048 (4)
Al11—O30	1.899 (3)	Al18—O51	1.871 (4)

Table SI2.2 Selected bond distances and bond angles in MK-A structure (Continued)

Bonds	**Distance (Å)**	**Bonds**	**Distance (Å)**
Al11—O34^{i}	1.883 (3)	Al18—O72	1.865 (5)
Al11—O34	1.883 (3)	Al18—O63	1.864 (5)
Al11—O35	1.959 (5)	Al18—O50	1.877 (4)
Al11—O31	1.914 (5)	Al18—O74	1.941 (4)
Al10—O43	1.957 (3)	Al23—O56	2.058 (4)
Al10—O36	1.849 (3)	Al23—O66	1.864 (5)
Al10—O28	1.953 (3)	Al23—O61	1.847 (5)
Al10—O29	1.838 (3)	Al23—O64	1.860 (5)
Al10—O30	1.831 (3)	Al23—O60	1.854 (4)
Al10—O41	1.972 (3)	Al23—O67	1.939 (5)
Al12—O36	1.884 (3)	Al24—O47	2.021 (4)
Al12—O36^{ii}	1.884 (3)	Al24—O61	1.830 (5)
Al12—O40^{ii}	1.890 (3)	Al24—O64	1.835 (5)
Al12—O40	1.890 (3)	Al24—O63	1.861 (5)
Al12—O77	1.959 (5)	Al24—O62	1.881 (5)
Al12—O37	1.928 (5)	Al24—O65	1.926 (5)
Al9—O28	1.967 (3)	Al4—O13	1.952 (7)
Al9—O42	2.007 (3)	Al4—O12	1.960 (4)
Al9—O41	1.915 (3)	Al4—O12^{iii}	1.960 (4)
Al9—O45	1.861 (4)	Al4—O16^{iii}	1.823 (5)
Al9—O27	1.852 (3)	Al4—O16	1.823 (5)
Al9—O48	1.836 (4)	Al4—O22	1.899 (10)
Al14—O43	1.967 (3)	Al5—O13	1.790 (7)
Al14—O28	1.940 (3)	Al5—O13^{iv}	1.790 (7)
Al14—O34^{i}	1.861 (3)	Al5—O14^{iv}	1.759 (5)
Al14—O42	1.992 (3)	Al5—O14	1.759 (5)
Al14—O44	1.841 (3)	Al6—Al6^{i}	2.918 (7)
Al14—O57	1.832 (3)	Al6—O15	1.882 (4)
Al16—O42	1.836 (3)	Al6—O17	1.881 (4)
Al16—O46	1.779 (4)	Al6—O14	1.968 (5)
Al16—O56	1.799 (4)	Al6—O16	1.898 (6)
Al16—O47	1.785 (4)	Al6—O18	1.866 (6)
Al13—O43	1.910 (3)	Al6—O2AA^{i}	1.870 (5)
Al13—O42	1.980 (3)	Al7—O14	2.045 (6)
Al13—O41	1.961 (3)	Al7—O2AA^{i}	1.909 (7)
Al13—O40	1.850 (3)	Al7—O2AA	1.909 (7)
Al13—O58	1.846 (3)	Al7—O21	1.925 (7)
Al13—O49	1.838 (4)	Al7—O0AA^{iv}	1.854 (7)
Al20—O46	2.037 (4)	Al7—O0AA	1.854 (7)
Al20—O55	1.880 (4)	O34—Al14^{i}	1.861 (3)
Al20—O69	1.860 (4)	O10—Al2^{iii}	1.955 (4)
Al20—O54	1.866 (4)	O26—Al2^{i}	1.859 (3)
Al20—O53	1.846 (4)	O13—Al2^{iii}	1.997 (4)
Al20—O71	1.944 (4)	O17—Al6^{i}	1.881 (4)
Al1—O29	1.877 (3)	O14—Al6^{i}	1.968 (5)
Al1—O3AA	1.900 (4)	O25—Al8^{iv}	1.762 (3)

Table SI2.2 Selected bond distances and bond angles in MK-A structure (Continued)

Bonds	**Distance (Å)**	**Bonds**	**Distance (Å)**
Al1—O27	1.904 (3)	O2AA—Al6^{i}	1.870 (5)
Al1—O24	1.931 (4)	S1—O1	1.423 (10)
Al1—O11	1.870 (4)	S1—O1AA	1.537 (12)
Al1—O8	1.924 (5)	S1—O1AA^{i}	1.537 (12)
Al3—O10	1.976 (6)	S1—O4	1.620 (15)
Al3—O11^{iii}	1.836 (4)	O1—S1^{ii}	1.423 (10)
Al3—O11	1.836 (4)	O3A—S2	1.276 (18)
Al3—O12	1.935 (5)	S2—O1A	1.721 (10)
Al3—O12^{iii}	1.935 (5)	S2—O2A^{ii}	1.397 (12)
Al3—O23	1.882 (7)	S2—O2A	1.397 (12)
Al22—O57	1.893 (4)	O1A—S2^{i}	1.721 (10)
Al22—O56	1.927 (4)	S3—O5	1.479 (9)
Al22—O58	1.872 (4)	S3—O6	1.500 (8)
Al22—O59	1.881 (4)	S3—O7	1.454 (9)
Al22—O68	1.934 (4)	S3—O7A	1.505 (10)
Al22—O60	1.874 (4)	S7—O81	1.472 (4)
Al21—O56	2.009 (4)	S7—O81^{v}	1.472 (4)
Al21—O55	1.861 (4)	S7—O82^{v}	1.493 (4)
Al21—O69	1.868 (4)	S7—O82	1.493 (4)
Al21—O66	1.870 (5)	S8—O83	1.411 (5)
Al21—O59	1.853 (4)	S8—O84	1.461 (7)
Al21—O70	1.928 (4)	S8—O85	1.440 (7)
Al15—O44	1.907 (4)	S8—O86	1.475 (8)
Al15—O46	1.943 (4)	S9—O87	1.494 (13)
Al15—O45	1.878 (4)	S9—O87A	1.449 (12)
Al15—O76	1.930 (4)	S9—O88	1.461 (11)
Al15—O54	1.918 (4)	S9—O88A	1.465 (12)
Al15—O52	1.863 (4)	S9A—O87B	1.460 (13)
Al19—O46	2.044 (4)	S9A—O87C	1.460 (12)
Al19—O53	1.831 (4)	S9A—O88B	1.470 (12)
Al19—O52	1.879 (4)	S9A—O88C	1.472 (13)
Al19—O51	1.872 (4)	S9B—O87D	1.471 (13)
Al19—O72	1.837 (5)	S9B—O87E	1.463 (14)
Al19—O73	1.938 (4)	S9B—O88D	1.446 (12)
Al2—O3AA	1.847 (4)	S9B—O88E	1.476 (14)
Al2—O10	1.955 (4)	O0AA—Al7^{iv}	1.854 (7)
Al2—O26	1.859 (3)	O0AA—Al7^{iii}	1.854 (7)
Al2—O13	1.997 (4)		
Bonds	**Angle (°)**	**Bonds**	**Angle (°)**
O31—S5—O32	106.9 (2)	O25—Al8—O24^{iii}	114.8 (2)
O31—S5—O32^{i}	106.9 (2)	O51—Al18—O47	93.76 (17)
O32—S5—O32^{i}	108.8 (3)	O51—Al18—O50	168.0 (2)
O33—S5—O31	112.0 (3)	O51—Al18—O74	95.6 (2)
O33—S5—O32	111.0 (2)	O72—Al18—O47	95.91 (17)
O33—S5—O32^{i}	111.0 (2)	O72—Al18—O51	77.0 (2)
O37—S6—O38	112.9 (3)	O72—Al18—O50	93.5 (2)

Table SI2.2 Selected bond distances and bond angles in MK-A structure (Continued)

Bonds	**Angle (°)**	**Bonds**	**Angle (°)**
O39—S6—O38	108.7 (2)	O72—Al18—O74	93.6 (2)
O39^{ii}—S6—O38	108.7 (2)	O63—Al18—O47	81.01 (18)
O39—S6—O37	106.2 (2)	O63—Al18—O51	94.8 (2)
O39^{ii}—S6—O37	106.2 (2)	O63—Al18—O72	171.1 (2)
O39^{ii}—S6—O39	114.2 (4)	O63—Al18—O50	94.1 (2)
O78—S4—O79	108.0 (5)	O63—Al18—O74	90.6 (2)
O78—S4—O80	109.7 (5)	O50—Al18—O47	79.76 (18)
O8—S4—O78	111.6 (5)	O50—Al18—O74	92.3 (2)
O8—S4—O79	110.1 (3)	O74—Al18—O47	167.9 (2)
O8—S4—O80	111.9 (4)	O66—Al23—O56	80.49 (17)
O80—S4—O79	105.2 (5)	O66—Al23—O67	92.4 (2)
O30^{i}—Al11—O30	85.39 (18)	O61—Al23—O56	95.26 (18)
O30—Al11—O35	88.97 (15)	O61—Al23—O66	95.9 (2)
O30^{i}—Al11—O35	88.97 (15)	O61—Al23—O64	76.5 (2)
O30^{i}—Al11—O31	89.05 (15)	O61—Al23—O60	168.6 (2)
O30—Al11—O31	89.05 (15)	O61—Al23—O67	93.5 (2)
O34^{i}—Al11—O30	91.58 (12)	O64—Al23—O56	95.91 (17)
O34—Al11—O30^{i}	91.58 (12)	O64—Al23—O66	171.4 (2)
O34^{i}—Al11—O30^{i}	176.51 (16)	O64—Al23—O67	92.2 (2)
O34—Al11—O30	176.51 (16)	O60—Al23—O56	79.58 (17)
O34—Al11—O34^{i}	91.4 (2)	O60—Al23—O66	93.3 (2)
O34—Al11—O35	89.25 (15)	O60—Al23—O64	93.8 (2)
O34^{i}—Al11—O35	89.25 (15)	O60—Al23—O67	92.8 (2)
O34^{i}—Al11—O31	92.63 (15)	O67—Al23—O56	169.2 (3)
O34—Al11—O31	92.63 (15)	O61—Al24—O47	94.93 (19)
O31—Al11—O35	177.3 (2)	O61—Al24—O64	77.5 (2)
O43—Al10—O41	76.18 (13)	O61—Al24—O63	94.6 (2)
O36—Al10—O43	93.99 (14)	O61—Al24—O62	169.2 (2)
O36—Al10—O28	164.97 (15)	O61—Al24—O65	94.2 (2)
O36—Al10—O41	89.77 (14)	O64—Al24—O47	96.27 (17)
O28—Al10—O43	76.78 (13)	O64—Al24—O63	171.7 (2)
O28—Al10—O41	76.61 (13)	O64—Al24—O62	93.1 (2)
O29—Al10—O43	166.00 (14)	O64—Al24—O65	92.9 (2)
O29—Al10—O36	98.02 (14)	O63—Al24—O47	81.82 (19)
O29—Al10—O28	89.95 (14)	O63—Al24—O62	94.5 (2)
O29—Al10—O41	96.62 (14)	O63—Al24—O65	90.1 (2)
O30—Al10—O43	89.73 (14)	O62—Al24—O47	80.68 (19)
O30—Al10—O36	96.85 (15)	O62—Al24—O65	91.5 (2)
O30—Al10—O28	94.96 (14)	O65—Al24—O47	168.2 (3)
O30—Al10—O29	95.93 (15)	O13—Al4—O12^{iii}	81.38 (19)
O30—Al10—O41	164.85 (14)	O13—Al4—O12	81.39 (19)
O36^{ii}—Al12—O36	88.72 (19)	O12^{iii}—Al4—O12	76.1 (2)
O36—Al12—O40	91.21 (13)	O16—Al4—O13	91.8 (3)
O36^{ii}—Al12—O40^{ii}	91.21 (13)	O16^{iii}—Al4—O13	91.8 (3)
O36^{ii}—Al12—O40	177.39 (19)	O16—Al4—O12^{iii}	166.81 (19)
O36—Al12—O40^{ii}	177.40 (19)	O16^{iii}—Al4—O12	166.81 (19)

Table SI2.2 Selected bond distances and bond angles in MK-A structure (Continued)

Bonds	**Angle (°)**	**Bonds**	**Angle (°)**
O36—Al12—O77	89.04 (15)	O16^{iii}—Al4—O12^{iii}	91.80 (18)
O36^{ii}—Al12—O77	89.04 (15)	O16—Al4—O12	91.80 (18)
O36^{ii}—Al12—O37	89.07 (16)	O16—Al4—O16^{iii}	99.7 (3)
O36—Al12—O37	89.07 (16)	O16—Al4—O22	93.6 (3)
O40^{ii}—Al12—O40	88.7 (2)	O16^{iii}—Al4—O22	93.6 (3)
O40^{ii}—Al12—O77	88.35 (16)	O22—Al4—O13	171.6 (4)
O40—Al12—O77	88.36 (16)	O22—Al4—O12^{iii}	92.0 (3)
O40^{ii}—Al12—O37	93.53 (17)	O22—Al4—O12	92.0 (3)
O40—Al12—O37	93.53 (17)	O13^{iv}—Al5—O13	107.7 (4)
O37—Al12—O77	177.4 (2)	O14^{iv}—Al5—O13	109.07 (12)
O28—Al9—O42	80.19 (13)	O14—Al5—O13	109.06 (12)
O41—Al9—O28	77.62 (13)	O14—Al5—O13^{iv}	109.07 (12)
O41—Al9—O42	81.40 (13)	O14^{iv}—Al5—O13^{iv}	109.07 (12)
O45—Al9—O28	90.41 (15)	O14^{iv}—Al5—O14	112.7 (4)
O45—Al9—O42	91.62 (15)	O15—Al6—Al6^{i}	92.27 (19)
O45—Al9—O41	166.98 (17)	O15—Al6—O14	94.9 (2)
O27—Al9—O28	91.57 (15)	O15—Al6—O16	88.4 (2)
O27—Al9—O42	168.81 (15)	O17—Al6—Al6^{i}	39.12 (15)
O27—Al9—O41	89.49 (15)	O17—Al6—O15	89.2 (2)
O27—Al9—O45	96.03 (17)	O17—Al6—O14	81.2 (2)
O48—Al9—O28	166.99 (18)	O17—Al6—O16	171.8 (3)
O48—Al9—O42	89.96 (15)	O14—Al6—Al6^{i}	42.13 (14)
O48—Al9—O41	92.60 (16)	O16—Al6—Al6^{i}	133.18 (19)
O48—Al9—O45	98.40 (17)	O16—Al6—O14	91.1 (2)
O48—Al9—O27	96.96 (17)	O18—Al6—Al6^{i}	132.9 (2)
O43—Al14—O42	79.95 (13)	O18—Al6—O15	90.1 (2)
O28—Al14—O43	76.85 (13)	O18—Al6—O17	94.0 (2)
O28—Al14—O42	81.20 (13)	O18—Al6—O14	173.0 (3)
O34^{i}—Al14—O43	92.01 (14)	O18—Al6—O16	93.9 (3)
O34^{i}—Al14—O28	91.84 (14)	O18—Al6—O2AA^{i}	91.8 (3)
O34^{i}—Al14—O42	170.35 (14)	O2AA^{i}—Al6—Al6^{i}	88.4 (3)
O44—Al14—O43	166.52 (16)	O2AA^{i}—Al6—O15	176.7 (2)
O44—Al14—O28	91.60 (15)	O2AA^{i}—Al6—O17	93.3 (3)
O44—Al14—O34^{i}	95.32 (16)	O2AA^{i}—Al6—O14	83.5 (3)
O44—Al14—O42	91.57 (15)	O2AA^{i}—Al6—O16	88.8 (3)
O57—Al14—O43	91.26 (15)	O2AA^{i}—Al7—O14	80.47 (18)
O57—Al14—O28	166.68 (17)	O2AA—Al7—O14	80.47 (18)
O57—Al14—O34^{i}	94.58 (15)	O2AA—Al7—O2AA^{i}	94.9 (4)
O57—Al14—O42	90.94 (15)	O2AA^{i}—Al7—O21	92.5 (2)
O57—Al14—O44	99.39 (16)	O2AA—Al7—O21	92.5 (2)
O46—Al16—O42	106.86 (16)	O21—Al7—O14	169.5 (3)
O46—Al16—O56	111.64 (17)	O0AA^{iv}—Al7—O14	95.3 (2)
O46—Al16—O47	111.87 (18)	O0AA—Al7—O14	95.3 (2)
O56—Al16—O42	106.94 (16)	O0AA^{iv}—Al7—O2AA	94.0 (3)
O47—Al16—O42	108.58 (16)	O0AA—Al7—O2AA	169.4 (3)
O47—Al16—O56	110.70 (18)	O0AA^{iv}—Al7—O2AA^{i}	169.4 (3)

Table SI2.2 Selected bond distances and bond angles in MK-A structure (Continued)

Bonds	**Angle (°)**	**Bonds**	**Angle (°)**
O43—Al13—O42	81.66 (13)	O0AA—Al7—O2AAi	94.0 (3)
O43—Al13—O41	77.54 (13)	O0AA—Al7—O21	92.9 (3)
O41—Al13—O42	80.97 (13)	O0AA^{iv}—Al7—O21	92.9 (3)
O40—Al13—O43	91.09 (15)	O0AA—Al7—O0AA^{iv}	76.5 (5)
O40—Al13—O42	170.25 (15)	Al10—O43—Al14	101.30 (14)
O40—Al13—O41	91.14 (15)	Al13—O43—Al10	103.22 (15)
O58—Al13—O43	91.61 (15)	Al13—O43—Al14	99.95 (14)
O58—Al13—O42	91.71 (15)	Al10—O36—Al12	136.56 (17)
O58—Al13—O41	167.63 (17)	Al10—O28—Al9	101.05 (14)
O58—Al13—O40	95.02 (16)	Al14—O28—Al10	102.40 (15)
O49—Al13—O43	166.92 (17)	Al14—O28—Al9	100.08 (14)
O49—Al13—O42	91.17 (15)	Al10—O29—Al1	135.30 (19)
O49—Al13—O41	90.58 (16)	Al10—O30—Al11	136.68 (17)
O49—Al13—O40	94.65 (17)	Al14^{i}—O34—Al11	137.79 (17)
O49—Al13—O58	99.57 (17)	Al14—O42—Al9	96.99 (14)
O55—Al20—O46	94.63 (15)	Al16—O42—Al9	120.29 (17)
O55—Al20—O71	92.3 (2)	Al16—O42—Al14	120.73 (17)
O69—Al20—O46	95.49 (17)	Al16—O42—Al13	120.25 (17)
O69—Al20—O55	77.93 (18)	Al13—O42—Al9	96.16 (14)
O69—Al20—O54	171.54 (19)	Al13—O42—Al14	96.73 (14)
O69—Al20—O71	91.73 (19)	Al9—O41—Al10	102.24 (15)
O54—Al20—O46	81.99 (16)	Al9—O41—Al13	99.88 (14)
O54—Al20—O55	94.17 (18)	Al13—O41—Al10	100.82 (15)
O54—Al20—O71	91.63 (19)	Al2—O3AA—Al1	137.1 (2)
O53—Al20—O46	81.36 (17)	Al14—O44—Al15	134.1 (2)
O53—Al20—O55	171.3 (2)	Al14—O57—Al22	135.6 (2)
O53—Al20—O69	94.73 (19)	Al2^{iii}—O10—Al3	98.95 (19)
O53—Al20—O54	92.88 (19)	Al2—O10—Al3	98.95 (19)
O53—Al20—O71	92.5 (2)	Al2—O10—Al2^{iii}	99.4 (3)
O71—Al20—O46	170.9 (2)	Al8—O10—Al3	119.5 (3)
O29—Al1—O3AA	94.74 (16)	Al8—O10—Al2	118.03 (19)
O29—Al1—O27	91.62 (15)	Al8—O10—Al2^{iii}	118.03 (19)
O29—Al1—O24	88.90 (15)	Al2^{i}—O26—Al2	142.5 (3)
O29—Al1—O8	85.66 (17)	Al16—O46—Al20	123.11 (19)
O3AA—Al1—O27	90.39 (17)	Al16—O46—Al15	121.66 (17)
O3AA—Al1—O24	87.93 (18)	Al16—O46—Al19	123.5 (2)
O3AA—Al1—O8	176.01 (19)	Al20—O46—Al19	91.62 (14)
O27—Al1—O24	178.3 (2)	Al15—O46—Al20	94.08 (17)
O27—Al1—O8	93.6 (2)	Al15—O46—Al19	94.72 (16)
O11—Al1—O29	173.9 (2)	Al16—O56—Al22	121.16 (17)
O11—Al1—O3AA	91.09 (18)	Al16—O56—Al21	123.1 (2)
O11—Al1—O27	90.29 (16)	Al16—O56—Al23	122.6 (2)
O11—Al1—O24	89.36 (16)	Al22—O56—Al21	94.79 (17)
O11—Al1—O8	88.40 (19)	Al22—O56—Al23	94.42 (16)
O8—Al1—O24	88.1 (2)	Al21—O56—Al23	93.20 (15)

Table SI2.2 Selected bond distances and bond angles in MK-A structure (Continued)

Bonds	**Angle (°)**	**Bonds**	**Angle (°)**
O11—Al3—O10	93.19 (18)	S5—O31—Al11	144.4 (3)
O11^{iii}—Al3—O10	93.19 (18)	Al13—O40—Al12	138.69 (19)
O11—Al3—O11^{iii}	99.7 (3)	Al13—O58—Al22	134.8 (2)
O11^{iii}—Al3—O12^{iii}	91.16 (17)	Al9—O45—Al15	134.3 (2)
O11—Al3—O12^{iii}	167.2 (2)	Al9—O27—Al1	139.7 (2)
O11—Al3—O12	91.16 (16)	Al8—O24—Al1	126.3 (2)
O11^{iii}—Al3—O12	167.2 (2)	Al13—O49—Al17	135.9 (2)
O11—Al3—O23	92.4 (2)	Al9—O48—Al17	136.8 (2)
O11^{iii}—Al3—O23	92.4 (2)	Al21—O55—Al20	100.97 (18)
O12—Al3—O10	79.3 (2)	Al16—O47—Al17	119.89 (18)
O12^{iii}—Al3—O10	79.3 (2)	Al16—O47—Al18	122.9 (2)
O12^{iii}—Al3—O12	77.3 (2)	Al16—O47—Al24	124.4 (2)
O23—Al3—O10	171.4 (3)	Al17—O47—Al18	94.16 (17)
O23—Al3—O12	94.0 (2)	Al17—O47—Al24	95.11 (18)
O23—Al3—O12^{iii}	94.0 (2)	Al24—O47—Al18	92.69 (15)
O57—Al22—O56	94.17 (16)	Al20—O69—Al21	101.45 (19)
O57—Al22—O68	90.56 (18)	Al3—O11—Al1	136.5 (3)
O56—Al22—O68	172.03 (16)	Al2^{iii}—O13—Al2	96.6 (2)
O58—Al22—O57	90.31 (15)	Al4—O13—Al2	97.7 (3)
O58—Al22—O56	95.26 (16)	Al4—O13—Al2^{iii}	97.7 (3)
O58—Al22—O59	177.60 (19)	Al5—O13—Al2^{iii}	120.6 (2)
O58—Al22—O68	91.11 (18)	Al5—O13—Al2	120.6 (2)
O59—Al22—O57	90.42 (19)	Al5—O13—Al4	118.5 (3)
O59—Al22—O56	82.40 (17)	Al3—O12—Al2	100.28 (17)
O59—Al22—O68	91.16 (19)	Al3—O12—Al4	102.62 (18)
O60—Al22—O57	176.70 (19)	Al2—O12—Al4	98.7 (2)
O60—Al22—O56	82.56 (17)	Al20—O54—Al15	100.68 (19)
O60—Al22—O58	90.38 (18)	S6—O37—Al12	144.9 (3)
O60—Al22—O59	88.8 (2)	Al19—O53—Al20	105.47 (18)
O60—Al22—O68	92.7 (2)	Al15—O52—Al19	103.3 (2)
O55—Al21—O56	95.13 (16)	Al2—O15—Al6	136.9 (2)
O55—Al21—O69	78.20 (18)	Al23—O66—Al21	104.63 (18)
O55—Al21—O66	172.0 (2)	Al18—O51—Al19	101.26 (19)
O55—Al21—O70	92.7 (2)	Al19—O72—Al18	102.8 (2)
O69—Al21—O56	96.04 (17)	Al24—O61—Al23	102.6 (2)
O69—Al21—O66	94.83 (19)	Al21—O59—Al22	101.8 (2)
O69—Al21—O70	92.26 (19)	S4—O8—Al1	143.1 (3)
O66—Al21—O56	81.63 (17)	Al24—O64—Al23	101.8 (2)
O66—Al21—O70	91.5 (2)	Al24—O63—Al18	104.42 (19)
O59—Al21—O56	80.91 (17)	Al23—O60—Al22	103.4 (2)
O59—Al21—O55	94.2 (2)	Al24—O62—Al17	102.1 (2)
O59—Al21—O69	171.6 (2)	Al6^{i}—O17—Al6	101.8 (3)
O59—Al21—O66	92.5 (2)	Al17—O50—Al18	103.4 (2)
O59—Al21—O70	91.70 (19)	Al5—O14—Al6	121.3 (2)

Table SI2.2 Selected bond distances and bond angles in MK-A structure (Continued)

Bonds	**Angle (°)**	**Bonds**	**Angle (°)**
O11—Al3—O10	93.19 (18)	S5—O31—Al11	144.4 (3)
O70—Al21—O56	169.6 (2)	Al5—O14—Al6^{i}	121.3 (2)
O44—Al15—O46	93.94 (16)	Al5—O14—Al7	123.1 (3)
O44—Al15—O76	90.91 (17)	Al6—O14—Al6^{i}	95.7 (3)
O44—Al15—O54	89.15 (17)	Al6^{i}—O14—Al7	94.1 (2)
O45—Al15—O44	91.37 (15)	Al6—O14—Al7	94.1 (2)
O45—Al15—O46	95.65 (16)	Al8—O25—Al8^{iv}	172.0 (5)
O45—Al15—O76	90.28 (18)	Al4—O16—Al6	136.1 (3)
O45—Al15—O54	178.77 (18)	Al6^{i}—O2AA—Al7	102.0 (3)
O76—Al15—O46	172.24 (16)	O1—S1—S1^{ii}	30.6 (5)
O54—Al15—O46	83.19 (16)	O1—S1—O1AA	106.8 (6)
O54—Al15—O76	90.83 (18)	O1—S1—O1AA^{i}	106.8 (6)
O52—Al15—O44	176.02 (19)	O1—S1—O4	126.0 (8)
O52—Al15—O46	82.54 (17)	O1AA—S1—S1^{ii}	89.7 (5)
O52—Al15—O45	90.84 (18)	O1AA^{i}—S1—S1^{ii}	89.7 (5)
O52—Al15—O76	92.39 (19)	O1AA—S1—O1AA^{i}	109.7 (10)
O52—Al15—O54	88.58 (18)	O1AA^{i}—S1—O4	103.5 (6)
O53—Al19—O46	81.52 (16)	O1AA—S1—O4	103.5 (6)
O53—Al19—O52	93.0 (2)	O4—S1—S1^{ii}	156.6 (5)
O53—Al19—O51	95.27 (19)	S1^{ii}—O1—S1	118.8 (11)
O53—Al19—O72	172.0 (2)	O3A—S2—O1A	111.1 (10)
O53—Al19—O73	91.1 (2)	O3A—S2—O2A	112.3 (6)
O52—Al19—O46	79.47 (16)	O3A—S2—O2A^{ii}	112.3 (6)
O52—Al19—O73	92.9 (2)	O2A—S2—O1A	98.8 (6)
O51—Al19—O46	94.05 (17)	O2A^{ii}—S2—O1A	98.8 (6)
O51—Al19—O52	168.7 (2)	O2A^{ii}—S2—O2A	121.1 (11)
O51—Al19—O73	94.7 (2)	S2—O1A—S2^{i}	113.2 (9)
O72—Al19—O46	95.02 (17)	O5—S3—O6	102.4 (6)
O72—Al19—O52	93.5 (2)	O5—S3—O7A	111.7 (7)
O72—Al19—O51	77.71 (19)	O6—S3—O7A	111.2 (7)
O72—Al19—O73	93.3 (2)	O7—S3—O5	116.2 (7)
O73—Al19—O46	169.0 (2)	O7—S3—O6	107.8 (7)
O3AA—Al2—O10	90.48 (18)	O7—S3—O7A	107.3 (7)
O3AA—Al2—O26	92.56 (19)	O81—S7—O81^{v}	108.3 (4)
O3AA—Al2—O13	170.2 (2)	O81—S7—O82	110.6 (2)
O3AA—Al2—O12	92.74 (18)	O81^{v}—S7—O82^{v}	110.6 (2)
O10—Al2—O13	81.46 (18)	O81^{v}—S7—O82	108.9 (2)
O10—Al2—O12	79.3 (2)	O81—S7—O82^{v}	108.9 (2)
O26—Al2—O10	94.9 (2)	O82—S7—O82^{v}	109.5 (4)
O26—Al2—O13	93.7 (3)	O83—S8—O84	106.4 (4)
O26—Al2—O12	172.15 (19)	O83—S8—O85	112.6 (4)
O12—Al2—O13	80.3 (2)	O83—S8—O86	108.9 (6)
O15—Al2—O3AA	95.06 (17)	O84—S8—O86	108.8 (6)
O15—Al2—O10	167.4 (2)	O85—S8—O84	113.2 (7)
O15—Al2—O26	96.2 (2)	O85—S8—O86	106.8 (6)
O15—Al2—O13	91.78 (17)	O87A—S9—O87	101.5 (15)

Table SI2.2 Selected bond distances and bond angles in MK-A structure (Continued)

Bonds	**Angle (°)**	**Bonds**	**Angle (°)**
O15—Al2—O12	89.1 (2)	O87A—S9—O88	113.7 (13)
O49—Al17—O47	93.84 (17)	O87A—S9—O88A	116.1 (13)
O49—Al17—O62	89.0 (2)	O88—S9—O87	110.3 (15)
O49—Al17—O75	91.08 (19)	O88—S9—O88A	102.0 (12)
O48—Al17—O49	90.20 (16)	O88A—S9—O87	113.5 (15)
O48—Al17—O47	93.96 (17)	O87B—S9A—O87C	106.3 (18)
O48—Al17—O62	175.9 (2)	O87B—S9A—O88B	111.5 (18)
O48—Al17—O75	92.4 (2)	O87B—S9A—O88C	112.5 (18)
O62—Al17—O47	82.13 (18)	O87C—S9A—O88B	111.2 (14)
O62—Al17—O75	91.6 (2)	O87C—S9A—O88C	111.4 (15)
O50—Al17—O49	176.5 (2)	O88B—S9A—O88C	104.1 (14)
O50—Al17—O48	90.0 (2)	O87D—S9B—O88E	111.0 (19)
O50—Al17—O47	82.68 (18)	O87E—S9B—O87D	101.3 (17)
O50—Al17—O62	90.6 (2)	O87E—S9B—O88E	109.9 (19)
O50—Al17—O75	92.4 (2)	O88D—S9B—O87D	117.0 (16)
O75—Al17—O47	171.91 (18)	O88D—S9B—O87E	115.7 (18)
O24—Al8—O10	104.79 (18)	O88D—S9B—O88E	102.2 (18)
O24^{iii}—Al8—O10	104.79 (18)	Al7^{iii}—O0AA—Al7	102.6 (5)
O24^{iii}—Al8—O24	105.1 (3)	Al7^{iv}—O0AA—Al7	102.6 (5)
O25—Al8—O10	111.7 (3)		
O25—Al8—O24	114.8 (2)		

Symmetry codes: (i) −*x*+1, *y*, *z*; (ii) *x*, *y*, −*z*+1; (iii) *x*, −*y*+2, *z*; (iv) −*x*+1, −*y*+2, *z*; (v) −*y*+1, −*x*+1, −*z*+ ½.

SI2.3 BVS calculation parameters and assignments of oxygen atoms in megaKeggin-Al_{162} polyoxocation

Table SI2.3 BVS calculation parameters and assignments of oxygen atoms in megaKeggin-Al_{162} polyoxocation

Atoms	**Bonds**	R_i	R_0-R_i		v_i (v.u.)	**Assignment**
O24	Al8—O24	1.796	-0.176		0.62	
				Σv_i =	**0.62**	η-H_2O
O0AA	Al7—O0AA	1.854	-0.234		0.53	
	O0AA—Al7^{iii}	1.854	-0.234		0.53	
				Σv_i =	**1.06**	μ^2-OH
O10	O10—Al2^{iii}	1.955	-0.335		0.40	
	Al3—O10	1.976	-0.356		0.38	
	Al2—O10	1.955	-0.335		0.40	
	Al8—O10	1.823	-0.203		0.58	
				Σv_i =	**1.77**	μ^4-O
O11	Al1—O11	1.87	-0.25		0.51	
	Al3—O11	1.836	-0.216		0.56	
				Σv_i =	**1.07**	μ^2-OH

Table SI2.3 BVS calculation parameters and assignments of oxygen atoms in megaKeggin-Al_{162} polyoxocation (Continued)

Atoms	**Bonds**	R_i	R_0-R_i		v_i (v.u.)	**Assignment**
O12	Al3—O12	1.935	-0.315		0.43	
	Al2—O12	1.958	-0.338		0.40	
	Al4—O12	1.96	-0.34		0.40	
				Σv_i =	1.23	μ^3-OH
O13	O13—Al2^{iii}	1.997	-0.377		0.36	
	Al2—O13	1.997	-0.377		0.36	
	Al4—O13	1.952	-0.332		0.41	
	Al5—O13	1.79	-0.17		0.63	
				Σv_i =	1.76	μ^4-O
O14	O14—Al6^{i}	1.968	-0.348		0.39	
	Al5—O14	1.759	-0.139		0.69	
	Al6—O14	1.968	-0.348		0.39	
	Al7—O14	2.045	-0.425		0.32	
				Σv_i =	1.78	μ^4-O
O15	Al2—O15	1.833	-0.213		0.56	
	Al6—O15	1.882	-0.262		0.49	
				Σv_i =	1.05	μ^2-OH
O16	Al4—O16	1.823	-0.203		0.58	
	Al6—O16	1.898	-0.278		0.47	
				Σv_i =	1.05	μ^4-O
O17	O17—Al6^{i}	1.881	-0.261		0.49	
	Al6—O17	1.881	-0.261		0.49	
				Σv_i =	0.99	μ^4-O
O18	Al6—O18	1.866	-0.246		0.51	
				Σv_i =	0.51	η-H_2O
O21	Al7—O21	1.925	-0.305		0.44	
				Σv_i =	0.44	η-H_2O
O22	Al4—O22	1.899	-0.279		0.47	
				Σv_i =	0.47	η-H_2O
O23	Al3—O23	1.882	-0.262		0.49	
				Σv_i =	0.49	η-H_2O
O24	Al1—O24	1.931	-0.311		0.43	
	Al8—O24^{iii}	1.796	-0.176		0.62	
				Σv_i =	1.05	μ^2-OH
O25	O25—Al8^{iv}	1.762	-0.142		0.68	
	Al8—O25	1.762	-0.142		0.68	
				Σv_i =	1.36	μ^2-OH
O26	O26—Al2i	1.859	-0.239		0.52	
O26	Al2—O26	1.859	-0.239		0.52	
				Σv_i =	1.05	μ^2-OH
O27	Al9—O27	1.852	-0.232		0.53	
O27	Al1—O27	1.904	-0.284		0.46	
				Σv_i =	1.00	μ^2-OH

Table SI2.3 BVS calculation parameters and assignments of oxygen atoms in megaKeggin-Al_{162} polyoxocation (Continued)

Atoms	**Bonds**	R_i	R_0-R_i		v_i (v.u.)	**Assignment**
O28	Al14—O28	1.94	-0.32		0.42	
O28	O28—Al10	1.953	-0.333		0.41	
O28	O28—Al9	1.967	-0.347		0.39	
				Σv_i =	1.22	μ^3-OH
O29	Al1—O29	1.877	-0.257		0.50	
O29	O29—Al10	1.838	-0.218		0.55	
				Σv_i =	1.05	μ^2-OH
O2AA	Al7—O2AA	1.909	-0.289		0.46	
O2AA	O2AA—Al6i	1.87	-0.25		0.51	
				Σv_i =	0.97	μ^2-OH
O30	O30—Al11	1.899	-0.279		0.47	
O30	O30—Al10	1.831	-0.211		0.57	
$O30^i$	O30—Al11	1.899	-0.279		0.47	
				Σv_i =	1.51	μ^2-OH
O31	O31—Al11	1.914	-0.294		0.45	
				Σv_i =	0.45	η-H_2O
O34	O34—Al14i	1.861	-0.241		0.52	
O34	O34—Al11	1.883	-0.263		0.49	
				Σv_i =	1.01	μ^2-OH
O35	O35—Al11	1.959	-0.339		0.40	
				Σv_i =	0.40	μ^2-OH
O36	O36—Al10	1.849	-0.229		0.54	
O36	O36—Al12	1.884	-0.264		0.49	
				Σv_i =	1.03	μ^2-OH
O37	O37—Al12	1.928	-0.308		0.43	
				Σv_i =	0.43	η-H_2O
O3AA	Al1—O3AA	1.9	-0.28		0.47	
O3AA	Al2—O3AA	1.847	-0.227		0.54	
				Σv_i =	1.01	μ^2-OH
O40	Al13—O40	1.85	-0.23		0.54	
O40	O40—Al12	1.89	-0.27		0.48	
				Σv_i =	1.02	μ^2-OH
O41	Al9—O41	1.915	-0.295		0.45	
O41	Al13—O41	1.961	-0.341		0.40	
O41	O41—Al10	1.972	-0.352		0.39	
				Σv_i =	1.23	μ^3-OH
O42	Al9—O42	2.007	-0.387		0.35	
O42	Al14—O42	1.992	-0.372		0.37	
O42	Al16—O42	1.836	-0.216		0.56	
O42	Al13—O42	1.98	-0.36		0.38	
				Σv_i =	1.65	μ^4-O

Table SI2.3 BVS calculation parameters and assignments of oxygen atoms in megaKeggin-Al_{162} polyoxocation (Continued)

Atoms	**Bonds**	R_i	R_0-R_i		v_i (v.u.)	**Assignment**
O43	Al14—O43	1.967	-0.347		0.39	
	Al13—O43	1.91	-0.29		0.46	
	O43—Al10	1.957	-0.337		0.40	
				Σv_i =	1.25	μ^3-OH
O44	Al14—O44	1.841	-0.221		0.55	
	Al15—O44	1.907	-0.287		0.46	
				Σv_i =	1.01	μ^2-OH
O45	Al9—O45	1.861	-0.241		0.52	
	Al15—O45	1.878	-0.258		0.50	
				Σv_i =	1.02	μ^2-OH
O46	Al16—O46	1.779	-0.159		0.65	
	Al20—O46	2.037	-0.417		0.32	
	Al15—O46	1.943	-0.323		0.42	
	Al19—O46	2.044	-0.424		0.32	
				Σv_i =	1.71	μ^4-O
O47	Al16—O47	1.785	-0.165		0.64	
	Al17—O47	1.955	-0.335		0.40	
	Al18—O47	2.048	-0.428		0.31	
	Al24—O47	2.021	-0.401		0.34	
				Σv_i =	1.70	μ^4-O
O48	Al9—O48	1.836	-0.216		0.56	
	Al17—O48	1.867	-0.247		0.51	
				Σv_i =	1.07	μ^2-OH
O49	Al13—O49	1.838	-0.218		0.55	
	Al17—O49	1.884	-0.264		0.49	
				Σv_i =	1.04	μ^2-OH
O50	Al17—O50	1.859	-0.239		0.52	
	Al18—O50	1.877	-0.257		0.50	
				Σv_i =	1.02	μ^2-OH
O51	Al19—O51	1.872	-0.252		0.51	
	Al18—O51	1.871	-0.251		0.51	
				Σv_i =	1.01	μ^2-OH
O52	Al15—O52	1.863	-0.243		0.52	
	Al19—O52	1.879	-0.259		0.50	
				Σv_i =	1.02	μ^2-OH
O53	Al20—O53	1.846	-0.226		0.54	
	Al19—O53	1.831	-0.211		0.57	
				Σv_i =	1.11	μ^2-OH
O54	Al20—O54	1.866	-0.246		0.51	
	Al15—O54	1.918	-0.298		0.45	
				Σv_i =	0.96	μ^2-OH
O55	Al20—O55	1.88	-0.26		0.50	
	Al21—O55	1.861	-0.241		0.52	
				Σv_i =	1.02	μ^2-OH

Table SI2.3 BVS calculation parameters and assignments of oxygen atoms in megaKeggin-Al_{162} polyoxocation (Continued)

Atoms	**Bonds**	R_i	R_0-R_i		v_i (v.u.)	**Assignment**
O56	Al16—O56	1.799	-0.179		0.62	
	Al22—O56	1.927	-0.307		0.44	
	Al21—O56	2.009	-0.389		0.35	
	Al23—O56	2.058	-0.438		0.31	
				Σv_i =	1.71	μ^4-O
O57	Al14—O57	1.832	-0.212		0.56	
	Al22—O57	1.893	-0.273		0.48	
				Σv_i =	1.04	μ^2-OH
O58	Al13—O58	1.846	-0.226		0.54	
	Al22—O58	1.872	-0.252		0.51	
				Σv_i =	1.05	μ^2-OH
O59	Al22—O59	1.881	-0.261		0.49	
	Al21—O59	1.853	-0.233		0.53	
				Σv_i =	1.03	μ^2-OH
O60	Al22—O60	1.874	-0.254		0.50	
	Al23—O60	1.854	-0.234		0.53	
				Σv_i =	1.03	μ^2-OH
O61	Al23—O61	1.847	-0.227		0.54	
	Al24—O61	1.83	-0.21		0.57	
				Σv_i =	1.11	μ^2-OH
O62	Al17—O62	1.892	-0.272		0.48	
	Al24—O62	1.881	-0.261		0.49	
				Σv_i =	0.97	μ^2-OH
O63	Al18—O63	1.864	-0.244		0.52	
	Al24—O63	1.861	-0.241		0.52	
				Σv_i =	1.04	μ^2-OH
O64	Al23—O64	1.86	-0.24		0.52	
	Al24—O64	1.835	-0.215		0.56	
				Σv_i =	1.08	μ^2-OH
O65	Al24—O65	1.926	-0.306		0.44	
				Σv_i =	0.44	η-H_2O
O66	Al21—O66	1.87	-0.25		0.51	
	Al23—O66	1.864	-0.244		0.52	
				Σv_i =	1.03	μ^2-OH
O67	Al23—O67	1.939	-0.319		0.42	
				Σv_i =	0.42	η-H_2O
O68	Al22—O68	1.934	-0.314		0.43	
				Σv_i =	0.43	η-H_2O
O69	Al20—O69	1.86	-0.24		0.52	
	Al21—O69	1.868	-0.248		0.51	
				Σv_i =	1.03	μ^2-OH
O70	Al21—O70	1.928	-0.308		0.43	
				Σv_i =	0.43	η-H_2O

Table SI2.3 BVS calculation parameters and assignments of oxygen atoms in megaKeggin-Al_{162} polyoxocation (Continued)

Atoms	**Bonds**	R_i	R_0-R_i		v_i **(v.u.)**	**Assignment**
O71	Al20—O71	1.944	-0.324		0.42	
				Σv_i =	0.42	η-H_2O
O72	Al19—O72	1.837	-0.217		0.56	
	Al18—O72	1.865	-0.245		0.52	
				Σv_i =	1.07	μ^2-OH
O73	Al19—O73	1.938	-0.318		0.42	
				Σv_i =	0.42	η-H_2O
O74	Al18—O74	1.941	-0.321		0.42	
				Σv_i =	0.42	η-H_2O
O75	Al17—O75	1.938	-0.318		0.42	
				Σv_i =	0.42	η-H_2O
O76	Al15—O76	1.93	-0.31		0.43	
				Σv_i =	0.43	η-H_2O
O77	O77—Al12	1.959	-0.339		0.40	
				Σv_i =	0.40	η-H_2O
O8	Al1—O8	1.924	-0.304		0.44	
				Σv_i =	0.44	η-H_2O

Symmetry codes: (i) −*x*+1, *y*, *z*; (ii) *x*, *y*, −*z*+1; (iii) *x*, −*y*+2, *z*; (iv) −*x*+1, −*y*+2, *z*; (v) −*y*+1, −*x*+1, −*z*+ ½.

SI3 Supplementary Information for Chapter 3

SI3.1 Fractional atomic coordinates and isotropic or equivalent isotropic displacement parameters of Na_2SO_4@MK-A structure

Table SI3.1 Fractional atomic coordinates and isotropic or equivalent isotropic displacement parameters of Na_2SO_4@MK-A, Space group $P4_2/mmc$.

Atom	*x*	*y*	*z*	U_{iso}/U_{eq} (Å^2)	Occupancy
S3	0.36125 (3)	0.05731 (2)	0.07853 (3)	0.0421 (3)	1.00
S4	0.5	0.13164 (3)	0.18900 (3)	0.0224 (2)	1.00
S5	0.43211 (3)	0.20577 (3)	0	0.0254 (3)	1.00
Al1	0.42070 (2)	0.06161 (2)	0.13027 (3)	0.0253 (2)	1.00
Al2	0.46090 (3)	0.03333 (2)	0.20780 (3)	0.0257 (2)	1.00
Al3	0.40573 (4)	0	0.18608 (4)	0.0268 (3)	1.00
Al4	0.42842 (4)	0	0.26832 (5)	0.0317 (4)	1.00
Al5	0.5	0	0.27481 (6)	0.0318 (5)	1.00
Al6	0.46743 (3)	0.06156 (3)	0.29928 (3)	0.0345 (3)	1.00
Al7	0.5	0.03254 (4)	0.36203 (5)	0.0439 (5)	1.00
Al8	0.46124 (5)	0	0.12587 (5)	0.0392 (4)	1.00
Al9	0.39006 (2)	0.13105 (2)	0.15588 (3)	0.0239 (2)	1.00
Al10	0.43242 (2)	0.12943 (2)	0.08833 (3)	0.0193 (2)	1.00
Al11	0.5	0.16372 (3)	0.10667 (4)	0.0203 (3)	1.00
Al12	0.42930 (2)	0.18367 (2)	0.14010 (3)	0.0235 (2)	1.00
Al13	0.37823 (2)	0.16967 (2)	0.08877 (3)	0.0237 (2)	1.00
Al14	0.40025 (3)	0.14161 (3)	0	0.0213 (3)	1.00
Al15	0.31618 (2)	0.14763 (3)	0.13973 (4)	0.0336 (3)	1.00
Al16	0.36101 (2)	0.19800 (2)	0.17286 (3)	0.0278 (2)	1.00
Al17	0.40943 (3)	0.17286 (3)	0.23419 (3)	0.0306 (3)	1.00
Al18	0.34939 (3)	0.18270 (3)	0.26603 (4)	0.0367 (3)	1.00
Al19	0.38909 (3)	0.23351 (3)	0.24938 (4)	0.0370 (3)	1.00
Al20	0.37750 (3)	0.27042 (3)	0.18364 (4)	0.0390 (3)	1.00
Al21	0.38809 (3)	0.24380 (3)	0.10929 (4)	0.0339 (3)	1.00
Al22	0.32665 (3)	0.25730 (3)	0.13213 (4)	0.0409 (3)	1.00
Al23	0.28899 (3)	0.20658 (3)	0.14776 (4)	0.0412 (3)	1.00
Al24	0.29993 (3)	0.16962 (3)	0.21580 (4)	0.0392 (3)	1.00
O4AA	0.39342 (7)	0.05980 (7)	0.08745 (8)	0.0398 (7)	1.00
O1AA	0.44899 (6)	0.06011 (5)	0.17029 (7)	0.0265 (5)	1.00
O5	0.44894 (8)	0	0.17459 (9)	0.0240 (7)	1.00
O8AA	0.39846 (6)	0.03102 (5)	0.15353 (7)	0.0292 (5)	1.00
O2AA	0.41981 (6)	0.02681 (5)	0.22571 (7)	0.0282 (5)	1.00
O5AA	0.46786 (9)	0	0.24431 (10)	0.0290 (8)	1.00
O9	0.5	0.03244 (8)	0.30307 (10)	0.0328 (8)	1.00
O0AA	0.46600 (6)	0.06142 (5)	0.24585 (7)	0.0306 (6)	1.00
O11	0.43780 (7)	0.03125 (6)	0.29977 (7)	0.0355 (6)	1.00
O12	0.5	0.08800 (9)	0.29663 (11)	0.0380 (9)	1.00
O13	0.46928 (8)	0.05987 (7)	0.35294 (8)	0.0456 (8)	1.00
O14	0.52584 (11)	0	0.36619 (12)	0.0456 (11)	1.00
O9AA	0.5	0.04123 (11)	0.41588 (12)	0.0549 (13)	1.00

Table SI3.1 Fractional atomic coordinates and isotropic or equivalent isotropic displacement parameters of Na_2SO_4@MK-A, Space group $P4_2/mmc$.(Continued)

Atom	***x***	***y***	***z***	U_{iso}/U_{eq} **(Å^2)**	**Occupancy**
O16	0.43771 (8)	0.09246 (6)	0.30074 (9)	0.0444 (7)	1.00
O5BA	0.38831 (10)	0	0.28512 (11)	0.0388 (9)	1.00
O18	0.36585 (9)	0	0.20436 (11)	0.0364 (9)	1.00
O19	0.44420 (7)	0.03167 (6)	0.10366 (8)	0.0377 (7)	1.00
O20	0.5	0	0.12288 (19)	0.074 (2)	1.00
O21	0.5	0.03370 (7)	0.19113 (10)	0.0270 (7)	1.00
O22	0.39849 (6)	0.09058 (5)	0.15794 (7)	0.0276 (5)	1.00
O23	0.43174 (5)	0.14085 (5)	0.14269 (7)	0.0227 (5)	1.00
O24	0.44111 (5)	0.09116 (5)	0.10292 (7)	0.0238 (5)	1.00
O25	0.47092 (5)	0.14104 (5)	0.08024 (7)	0.0246 (5)	1.00
O26	0.5	0.13527 (8)	0.14673 (10)	0.0366 (9)	1.00
O27	0.47300 (6)	0.11470 (6)	0.19945 (9)	0.0393 (7)	1.00
O28	0.5	0.16025 (9)	0.20810 (12)	0.0462 (11)	1.00
O29	0.47019 (5)	0.18683 (5)	0.13054 (7)	0.0275 (5)	1.00
O30	0.38603 (5)	0.17481 (5)	0.14424 (7)	0.0235 (5)	1.00
O31	0.37635 (5)	0.16026 (6)	0.03716 (7)	0.0277 (5)	1.00
O32	0.42893 (8)	0.17303 (8)	0	0.0337 (9)	1.00
O33	0.44843 (6)	0.21386 (6)	0.03469 (8)	0.0381 (6)	1.00
O34	0.40318 (10)	0.22027 (10)	0	0.0464 (11)	1.00
O35	0.42258 (5)	0.12209 (5)	0.03804 (7)	0.0218 (5)	1.00
O36	0.37228 (8)	0.10763 (8)	0	0.0283 (8)	1.00
O37	0.38975 (5)	0.12868 (5)	0.10128 (7)	0.0222 (5)	1.00
O38	0.42113 (5)	0.17162 (5)	0.08730 (7)	0.0233 (5)	1.00
O39	0.33870 (5)	0.16091 (6)	0.09787 (8)	0.0306 (6)	1.00
O40	0.34934 (6)	0.12741 (6)	0.15921 (7)	0.0291 (5)	1.00
O41	0.32393 (6)	0.18363 (6)	0.16960 (8)	0.0331 (6)	1.00
O42	0.37482 (6)	0.19680 (6)	0.22090 (7)	0.0307 (6)	1.00
O43	0.39783 (6)	0.13898 (6)	0.20674 (7)	0.0282 (5)	1.00
O44	0.43249 (6)	0.18690 (6)	0.19230 (7)	0.0297 (6)	1.00
O45	0.38524 (7)	0.16211 (7)	0.27626 (8)	0.0385 (7)	1.00
O46	0.36494 (7)	0.21727 (7)	0.28751 (8)	0.0425 (7)	1.00
O47	0.42016 (6)	0.20758 (7)	0.26266 (8)	0.0385 (7)	1.00
O48	0.40857 (6)	0.24984 (6)	0.20747 (8)	0.0374 (6)	1.00
O49	0.36352 (6)	0.23509 (6)	0.15336 (8)	0.0323 (6)	1.00
O50	0.42131 (6)	0.22304 (5)	0.12817 (7)	0.0300 (6)	1.00
O51	0.37555 (6)	0.21037 (6)	0.08142 (8)	0.0310 (6)	1.00
O52	0.39870 (7)	0.27755 (6)	0.13863 (9)	0.0425 (7)	1.00
O53	0.35381 (7)	0.26514 (6)	0.09289 (9)	0.0444 (7)	1.00
O54	0.30102 (7)	0.24263 (7)	0.16872 (9)	0.0433 (7)	1.00
O55	0.28382 (6)	0.17063 (7)	0.12170 (9)	0.0430 (7)	1.00
O56	0.27111 (6)	0.19329 (7)	0.19253 (9)	0.0455 (7)	1.00
O57	0.29424 (6)	0.13693 (7)	0.18322 (9)	0.0423 (7)	1.00
O58	0.33182 (6)	0.15175 (6)	0.24011 (8)	0.0385 (7)	1.00
O59	0.31440 (6)	0.19985 (7)	0.24760 (8)	0.0399 (7)	1.00
O60	0.27133 (7)	0.15439 (8)	0.25196 (10)	0.0554 (9)	1.00

Table SI3.1 Fractional atomic coordinates and isotropic or equivalent isotropic displacement parameters of Na_2SO_4@MK-A, Space group $P4_2/mmc$.(Continued)

Atom	***x***	***y***	***z***	U_{iso}/U_{eq} **(Å^2)**	**Occupancy**
O61	0.31014 (6)	0.22439 (7)	0.10796 (8)	0.0405 (7)	1.00
O62	0.25111 (7)	0.22184 (8)	0.12945 (10)	0.0568 (9)	1.00
O63	0.34309 (7)	0.28732 (6)	0.16250 (9)	0.0437 (7)	1.00
O64	0.29780 (8)	0.28456 (8)	0.11080 (10)	0.0617 (10)	1.00
O65	0.41067 (8)	0.25857 (6)	0.06665 (9)	0.0463 (8)	1.00
O66	0.36042 (7)	0.25874 (6)	0.22953 (8)	0.0388 (7)	1.00
O67	0.38956 (8)	0.30841 (7)	0.20439 (10)	0.0545 (9)	1.00
O68	0.40400 (7)	0.26385 (7)	0.28413 (10)	0.0517 (8)	1.00
O69	0.33279 (8)	0.17101 (8)	0.31503 (9)	0.0525 (9)	1.00
O70	0.44312 (6)	0.15146 (7)	0.25450 (7)	0.0377 (7)	1.00
O71	0.30367 (6)	0.11300 (7)	0.11175 (9)	0.0438 (7)	1.00
O72	0.5	0.19174 (8)	0.06377 (10)	0.0290 (8)	1.00
O73	0.34993 (7)	0.08810 (7)	0.07144 (9)	0.0436 (7)	1.00
O74	0.34600 (8)	0.04394 (9)	0.11144 (11)	0.0682 (11)	1.00
O75	0.35719 (9)	0.03926 (8)	0.04459 (11)	0.0669 (11)	1.00
S9	0.5	0.06106 (13)	0.03751 (17)	0.0859 (14)	0.50
O86	0.5	0.0776 (2)	0	0.097 (3)	1.00
O105	0.4739 (2)	0.0406 (2)	0.0367 (3)	0.098 (3)	0.50
O7BA	0.5	0.0736 (3)	0.0674 (4)	0.056 (3)	0.50
S8	0.36546 (3)	0.08012 (3)	0.26001 (4)	0.0540 (3)	1.00
O82	0.39517 (8)	0.08046 (7)	0.24266 (9)	0.0472 (8)	1.00
O83	0.34336 (8)	0.09097 (8)	0.23199 (11)	0.0596 (9)	1.00
O84	0.35778 (10)	0.05016 (9)	0.27272 (13)	0.0752 (12)	1.00
O85	0.36704 (11)	0.10182 (10)	0.29261 (11)	0.0794 (13)	1.00
S7	0.29471 (3)	0.29471 (3)	0.25	0.0435 (4)	1.00
O80	0.29956 (7)	0.26249 (7)	0.24337 (9)	0.0481 (8)	1.00
O81	0.31184 (7)	0.30411 (7)	0.28383 (9)	0.0486 (8)	1.00
O95	0.4200 (3)	0.2373 (2)	0.3537 (3)	0.189 (6)	0.731
O97	0.3917 (4)	0.3529 (2)	0.1541 (3)	0.150 (6)	0.561
O98	0.3692 (2)	0.1815 (3)	0.3736 (2)	0.200 (7)	0.731
O100	0.37234 (9)	0.31704 (10)	0.27779 (13)	0.0778 (13)	1.00
O101	0.32852 (13)	0.25424 (11)	0.32980 (12)	0.0967 (17)	1.00
O102	0.32828 (11)	0.04354 (11)	0.18641 (16)	0.0949 (15)	1.00
O103	0.5	0.1300 (2)	0.39854 (18)	0.109 (3)	1.00
O104	0.4110 (2)	0	0.0424 (3)	0.076 (4)	0.564
O106	0.4023 (4)	0.3172 (3)	0.0578 (5)	0.207 (9)	0.561
O107	0.3131 (3)	0	0	0.143 (11)	0.564
Na1	0.36808 (12)	0.31673 (8)	0.10939 (14)	0.0812 (18)	0.561
Na2	0.40687 (8)	0.19180 (8)	0.32808 (8)	0.0698 (12)	0.731
Na3	0.3668 (2)	0	0	0.064 (3)	0.564
S0AA	0.49644 (16)	0.23654 (7)	0.22634 (9)	0.0941 (11)	0.5
O4	0.52717 (17)	0.22646 (18)	0.2256 (2)	0.070 (2)	0.5
O7	0.4807 (2)	0.2231 (2)	0.2581 (3)	0.103 (3)	0.5
O3AA	0.4787 (2)	0.2335 (2)	0.1928 (3)	0.097 (3)	0.5
O10	0.4969 (8)	0.2712 (3)	0.2344 (4)	0.098 (6)	0.25

Table SI3.1 Fractional atomic coordinates and isotropic or equivalent isotropic displacement parameters of Na_2SO_4@MK-A, Space group $P4_2/mmc$.(Continued)

Atom	***x***	***y***	***z***	U_{iso}/U_{eq} **(Å^2)**	**Occupancy**
S1	0.31284 (14)	0.20433 (16)	0.0042 (4)	0.058 (2)	0.1721
O6AA	0.3308 (6)	0.2258 (6)	0.0273 (7)	0.086 (6)	0.1721
O3	0.2819 (3)	0.2147 (5)	0.0035 (11)	0.065 (6)	0.1721
O109	0.3251 (5)	0.2009 (6)	−0.0337 (4)	0.038 (5)	0.1721
O108	0.3150 (5)	0.1735 (4)	0.0241 (7)	0.067 (7)	0.1721
S3AA	0.3196 (3)	0.2297 (3)	−0.0051 (6)	0.079 (4)	0.1093
O0BA	0.2868 (3)	0.2313 (6)	−0.0077 (8)	0.051 (8)	0.1093
O1BA	0.3346 (4)	0.2568 (4)	−0.0189 (6)	0.026 (5)	0.1093
O1	0.3322 (8)	0.2029 (6)	−0.0216 (10)	0.074 (13)	0.1093
O6AB	0.3273 (9)	0.2269 (9)	0.0375 (6)	0.086 (6)	0.1093
S1X	0.30584 (10)	0.18824 (11)	0.0053 (2)	0.0460 (14)	0.2186
O6AX	0.3221 (5)	0.2108 (5)	0.0289 (5)	0.065 (6)	0.2186
O3X	0.2742 (3)	0.1977 (4)	0.0037 (10)	0.080 (5)	0.2186
O10X	0.3183 (4)	0.1871 (6)	−0.0326 (4)	0.068 (6)	0.2186
O2	0.3098 (4)	0.1583 (4)	0.0262 (5)	0.072 (5)	0.2186
O6	0.4560 (3)	0.1679 (3)	0.3254 (3)	0.232 (8)	0.731
O7AA	0.4740 (3)	0.2538 (3)	0.1187 (3)	0.107 (3)	0.50
O2BA	0.3217 (3)	0.3378 (3)	0.0886 (5)	0.177 (7)	0.561
O4BA	0.5	0.1372 (3)	0	0.030 (2)	0.50
O15	0.1919 (4)	0.2444 (4)	0.2033 (5)	0.169 (6)	0.50
O17	0.2263 (4)	0.2761 (4)	0.1478 (5)	0.181 (7)	0.50
O3BA	0.43012 (19)	0.06667 (19)	0	0.110 (3)	1.00
O6BA	0.5	0.1217 (3)	0	0.037 (3)	0.50
O8BA	0.5	0.0710 (3)	0.0834 (4)	0.063 (3)	0.50

SI3.2 Selected bond distances and bond angles in Na_2SO_4@MK-A structure

Table SI3.2 List of Na—O bond distances and O—Na—O angles in Na_2SO_4@MK-A structure.

Bond	**Bond Distance (Å)**	**Bond**	**Bond Distance (Å)**
Na1—O106	2.361 (16)	Na2—O95	2.299 (10)
Na1—O2BA	2.390 (13)	Na2—O98	2.361 (10)
Na1—O52	2.447 (5)	Na3—O104	2.468 (13)
Na1—O53	2.462 (5)	Na3—O104^{ii}	2.468 (13)
Na1—O63	2.531 (5)	Na3—O107	2.405 (18)
Na1—O97	2.483 (13)	Na3—O75	2.384 (4)
Na2—O45	2.442 (4)	Na3—O75^{ii}	2.384 (4)
Na2—O46	2.610 (5)	Na3—O75^{iii}	2.384 (4)
Na2—O47	2.459 (4)	Na3—O75^{vi}	2.384 (4)
Na2—O6	2.445 (11)		
Bond	**Angle (°)**	**Bond**	**Angle (°)**
O52—Na1—O53	64.59 (14)	O98—Na2—O46	86.3 (3)
O52—Na1—O63	64.55 (14)	O98—Na2—O47	148.4 (3)
O52—Na1—O97	88.1 (3)	O98—Na2—O6	125.6 (5)
O53—Na1—O63	64.48 (14)	O6—Na2—O46	144.7 (3)

Table SI3.2 List of Na—O bond distances and O—Na—O angles in Na_2SO_4@MK-A structure. (Continued)

Bond	Angle (°)	Bond	Angle (°)
O53—Na1—O97	150.2 (3)	O6—Na2—O47	82.7 (3)
O97—Na1—O63	93.9 (3)	$O75^{vi}$—Na3—$O75^{iii}$	81.4 (2)
O106—Na1—O52	87.7 (4)	O75—Na3—$O75^{vi}$	159.2 (5)
O106—Na1—O53	89.9 (4)	O75—Na3—$O75^{ii}$	81.4 (2)
O106—Na1—O63	148.0 (3)	$O75^{vi}$—Na3—$O75^{ii}$	94.9 (2)
O106—Na1—O97	101.3 (6)	O75—Na3—$O75^{iii}$	94.9 (2)
O106—Na1—O2BA	109.2 (6)	$O75^{iii}$—Na3—$O75^{ii}$	159.2 (5)
O2BA—Na1—O52	153.4 (4)	$O75^{ii}$—Na3—$O104^{ii}$	75.8 (2)
O2BA—Na1—O53	94.2 (4)	$O75^{vi}$—Na3—$O104^{ii}$	75.8 (2)
O2BA—Na1—O63	92.5 (4)	O75—Na3—O104	75.8 (2)
O2BA—Na1—O97	107.6 (5)	$O75^{iii}$—Na3—O104	75.8 (2)
O45—Na2—O46	63.39 (12)	$O75^{iii}$—Na3—$O104^{ii}$	122.3 (3)
O45—Na2—O47	64.30 (12)	$O75^{ii}$—Na3—O104	122.3 (3)
O45—Na2—O6	95.2 (2)	O75—Na3—$O104^{ii}$	122.3 (3)
O47—Na2—O46	63.03 (12)	$O75^{vi}$—Na3—O104	122.3 (3)
O95—Na2—O45	150.4 (3)	$O75^{ii}$—Na3—O107	79.6 (2)
O95—Na2—O46	90.4 (3)	$O75^{vi}$—Na3—O107	79.6 (2)
O95—Na2—O47	92.5 (3)	$O75^{iii}$—Na3—O107	79.6 (2)
O95—Na2—O98	95.4 (5)	O75—Na3—O107	79.6 (2)
O95—Na2—O6	100.0 (5)	O104—Na3—$O104^{ii}$	73.6 (6)
O98—Na2—O45	96.2 (3)	O107—Na3—O104	143.2 (3)

Symmetry codes: (i) −x+1, y, z; (ii) x, y, −z; (iii) x, −y, z; (iv) −x+1, −y, z; (v) y, x, −z+1/2; (vi) x, −y, −z.

SI3.3 Fractional atomic coordinates and isotropic or equivalent isotropic displacement parameters of K_2SO_4@MK-A structure

Table SI3.3 Fractional atomic coordinates and isotropic or equivalent isotropic displacement parameters of K_2SO_4@MK-A, Space group $P4_2/mmc$.

Atom	*x*	*y*	*z*	U_{iso}/U_{eq} (Å^2)	Occupancy
S5	0.5	0.13072 (5)	0.18619 (8)	0.0388 (6)	1.00
S4	0.36107 (6)	0.05839 (6)	0.07788 (8)	0.0733 (7)	1.00
S6	0.43307 (6)	0.20633 (6)	0	0.0419 (7)	1.00
Al13	0.37833 (5)	0.17031 (5)	0.08816 (7)	0.0411 (6)	1.00
Al12	0.42954 (5)	0.18377 (5)	0.13825 (7)	0.0401 (6)	1.00
Al1	0.42040 (5)	0.06168 (5)	0.12821 (7)	0.0450 (6)	1.00
Al5	0.5	0	0.27046 (15)	0.0563 (13)	1.00
Al17	0.41032 (5)	0.17319 (5)	0.23147 (7)	0.0472 (6)	1.00
Al14	0.40000 (6)	0.14285 (7)	0	0.0368 (7)	1.00
Al4	0.42869 (9)	0	0.26390 (10)	0.0539 (9)	1.00
Al24	0.30112 (6)	0.17011 (6)	0.21484 (8)	0.0567 (7)	1.00
Al16	0.36160 (5)	0.19840 (5)	0.17174 (7)	0.0427 (6)	1.00
Al19	0.39026 (6)	0.23361 (6)	0.24698 (8)	0.0525 (7)	1.00
Al2	0.46102 (6)	0.03308 (5)	0.20408 (7)	0.0469 (6)	1.00

Table SI3.3 Fractional atomic coordinates and isotropic or equivalent isotropic displacement parameters of K_2SO_4@MK-A, Space group $P4_2/mmc$.(Continued)

Atom	***x***	***y***	***z***	U_{iso}/U_{eq} **(Å^2)**	**Occupancy**
Al15	0.31660 (5)	0.14852 (6)	0.13898 (8)	0.0553 (7)	1.00
Al20	0.37787 (6)	0.27088 (5)	0.18224 (8)	0.0572 (7)	1.00
Al3	0.40571 (8)	0	0.18304 (10)	0.0495 (9)	1.00
Al10	0.43225 (5)	0.12979 (5)	0.08736 (6)	0.0366 (5)	1.00
Al18	0.35075 (6)	0.18311 (6)	0.26396 (7)	0.0522 (7)	1.00
Al9	0.39042 (5)	0.13144 (5)	0.15410 (7)	0.0410 (6)	1.00
Al6	0.46767 (7)	−0.06158 (5)	0.29425 (8)	0.0600 (7)	1.00
Al11	0.5	0.16375 (6)	0.10533 (9)	0.0351 (7)	1.00
Al8	0.46091 (10)	0	0.12322 (13)	0.0674 (11)	1.00
Al23	0.28971 (6)	0.20720 (7)	0.14860 (8)	0.0636 (8)	1.00
Al21	0.38813 (6)	0.24428 (5)	0.10886 (7)	0.0517 (7)	1.00
Al22	0.32694 (7)	0.25761 (6)	0.13241 (8)	0.0607 (8)	1.00
Al7	0.5	−0.03249 (9)	0.35583 (12)	0.0680 (12)	1.00
O40	0.42261 (10)	0.12290 (10)	0.03738 (14)	0.0381 (11)	1.00
O42	0.38968 (10)	0.12931 (10)	0.10021 (13)	0.0373 (12)	1.00
O25	0.5	0.03310 (15)	0.1870 (2)	0.0474 (19)	1.00
O30	0.47142 (11)	0.14064 (11)	0.07974 (15)	0.0445 (13)	1.00
O10	0.44913 (16)	0	0.1714 (2)	0.0444 (18)	1.00
O62	0.29538 (12)	0.13781 (13)	0.18263 (17)	0.0600 (16)	1.00
O60	0.28383 (13)	0.17152 (15)	0.12259 (18)	0.0702 (18)	1.00
O74	0.33388 (14)	0.17191 (15)	0.31219 (18)	0.0736 (19)	1.00
O58	0.35358 (15)	0.26542 (12)	0.09341 (16)	0.0646 (17)	1.00
O69	0.29695 (17)	0.28423 (17)	0.11125 (19)	0.091 (2)	1.00
O78	0.35748 (19)	0.03937 (16)	0.0441 (2)	0.099 (3)	1.00
O16	0.5	−0.08819 (16)	0.2910 (2)	0.060 (2)	1.00
O19	0.5	−0.0405 (2)	0.4088 (3)	0.079 (3)	1.00
O79	0.34530 (17)	0.04607 (18)	0.1110 (2)	0.100 (3)	1.00
O9	0.44897 (11)	0.06005 (10)	0.16735 (14)	0.0443 (13)	1.00
O45	0.34971 (11)	0.12766 (11)	0.15754 (15)	0.0452 (13)	1.00
O41	0.37206 (16)	0.10881 (16)	0	0.0481 (19)	1.00
O53	0.40976 (12)	0.25042 (11)	0.20602 (17)	0.0562 (15)	1.00
O28	0.43163 (10)	0.14084 (10)	0.14017 (13)	0.0376 (11)	1.00
O29	0.44063 (11)	0.09090 (10)	0.10065 (14)	0.0426 (12)	1.00
O49	0.43286 (11)	0.18675 (11)	0.18970 (15)	0.0475 (13)	1.00
O31	0.5	0.13521 (16)	0.1447 (2)	0.064 (2)	1.00
O48	0.39841 (11)	0.13940 (11)	0.20367 (14)	0.0441 (13)	1.00
O44	0.33895 (11)	0.16200 (12)	0.09696 (15)	0.0480 (13)	1.00
O8	0.39250 (12)	0.06029 (12)	0.08633 (15)	0.0535 (14)	1.00
O63	0.33317 (12)	0.15147 (12)	0.23876 (16)	0.0554 (15)	1.00
O55	0.42188 (12)	0.22339 (11)	0.12733 (16)	0.0502 (14)	1.00
O13	0.46719 (18)	0	0.2400 (2)	0.054 (2)	1.00
O80	0.34932 (14)	0.08957 (13)	0.07013 (19)	0.0705 (18)	1.00
O14	0.5	−0.03198 (16)	0.2987 (2)	0.057 (2)	1.00
O38	0.40531 (18)	0.22273 (18)	0	0.063 (2)	1.00
O64	0.31600 (12)	0.20032 (12)	0.24638 (15)	0.0515 (14)	1.00

Table SI3.3 Fractional atomic coordinates and isotropic or equivalent isotropic displacement parameters of K_2SO_4@MK-A, Space group $P4_2/mmc$.(Continued)

Atom	***x***	***y***	***z***	U_{iso}/U_{eq} **(Å^2)**	**Occupancy**
O27	0.39879 (11)	0.09091 (11)	0.15583 (15)	0.0461 (13)	1.00
O43	0.42161 (10)	0.17174 (10)	0.08608 (13)	0.0372 (11)	1.00
O72	0.39065 (15)	0.30850 (13)	0.20375 (19)	0.0727 (19)	1.00
O71	0.36124 (12)	0.25903 (12)	0.22704 (15)	0.0514 (14)	1.00
O52	0.42154 (12)	0.20776 (12)	0.25884 (16)	0.0548 (15)	1.00
O61	0.27190 (12)	0.19349 (14)	0.19207 (18)	0.0657 (17)	1.00
O35	0.38604 (10)	0.17513 (10)	0.14295 (14)	0.0390 (12)	1.00
O76	0.30382 (12)	0.11427 (14)	0.11122 (19)	0.0655 (17)	1.00
O39	0.44918 (13)	0.21357 (13)	0.03383 (16)	0.0608 (16)	1.00
O36	0.37648 (11)	0.16166 (11)	0.03730 (15)	0.0476 (13)	1.00
O50	0.38630 (13)	0.16194 (12)	0.27321 (15)	0.0553 (15)	1.00
O37	0.42884 (17)	0.17491 (16)	0	0.056 (2)	1.00
O32	0.5	0.15840 (17)	0.2064 (3)	0.070 (3)	1.00
O56	0.37583 (12)	0.21099 (11)	0.08131 (15)	0.0501 (14)	1.00
O17	0.46987 (15)	−0.05972 (13)	0.34685 (17)	0.0673 (18)	1.00
O70	0.41104 (15)	0.25935 (12)	0.06692 (17)	0.0693 (18)	1.00
O34	0.47040 (11)	0.18685 (11)	0.12919 (15)	0.0463 (13)	1.00
O23	0.44322 (15)	0.03148 (11)	0.10225 (17)	0.0657 (18)	1.00
O22	0.36536 (18)	0	0.2009 (2)	0.055 (2)	1.00
O11	0.39798 (12)	0.03100 (11)	0.15123 (15)	0.0487 (14)	1.00
O51	0.36645 (13)	0.21761 (12)	0.28503 (15)	0.0564 (15)	1.00
O21	0.3884 (2)	0	0.2807 (2)	0.065 (2)	1.00
O67	0.25155 (14)	0.22225 (17)	0.13043 (18)	0.081 (2)	1.00
O68	0.34343 (14)	0.28744 (12)	0.16275 (16)	0.0632 (17)	1.00
O26	0.46622 (13)	0.06125 (11)	0.24145 (16)	0.0522 (14)	1.00
O54	0.36384 (12)	0.23527 (11)	0.15241 (15)	0.0493 (14)	1.00
O57	0.39924 (14)	0.27776 (12)	0.13821 (18)	0.0682 (18)	1.00
O15	0.43794 (14)	−0.03102 (12)	0.29499 (16)	0.0610 (16)	1.00
O65	0.27273 (14)	0.15435 (15)	0.2509 (2)	0.078 (2)	1.00
O77	0.5	0.19119 (15)	0.06369 (19)	0.0433 (17)	1.00
O18	0.4746 (2)	0	0.3596 (2)	0.069 (3)	1.00
O59	0.30189 (13)	0.24289 (13)	0.16924 (17)	0.0613 (16)	1.00
O73	0.40558 (13)	0.26408 (14)	0.27998 (18)	0.0670 (17)	1.00
O46	0.32451 (11)	0.18441 (12)	0.16872 (15)	0.0473 (13)	1.00
O12	0.41968 (12)	0.02659 (11)	0.22201 (15)	0.0513 (14)	1.00
O47	0.37596 (11)	0.19705 (11)	0.21841 (14)	0.0459 (13)	1.00
O75	0.44407 (12)	0.15173 (12)	0.25057 (14)	0.0519 (14)	1.00
O20	0.43813 (15)	−0.09233 (13)	0.29576 (18)	0.0712 (18)	1.00
O33	0.47334 (12)	0.11358 (12)	0.19534 (19)	0.0631 (17)	1.00
O24	0.5	0	0.1189 (4)	0.089 (4)	1.00
O66	0.31053 (12)	0.22499 (14)	0.10847 (17)	0.0627 (16)	1.00
S7	0.36617 (7)	0.08034 (6)	0.25652 (8)	0.0757 (8)	1.00
O81	0.36768 (18)	0.10150 (16)	0.28939 (19)	0.095 (2)	1.00
O82	0.35867 (18)	0.05055 (14)	0.2691 (2)	0.098 (3)	1.00
O83	0.39582 (14)	0.08057 (12)	0.23880 (18)	0.0671 (17)	1.00

Table SI3.3 Fractional atomic coordinates and isotropic or equivalent isotropic displacement parameters of K_2SO_4@MK-A, Space group $P4_2/mmc$.(Continued)

Atom	***x***	***y***	***z***	U_{iso}/U_{eq} (Å^2)	**Occupancy**
O84	0.34471 (15)	0.09074 (15)	0.2287 (2)	0.086 (2)	1.00
S2	0.5	0.06234 (19)	0.0367 (2)	0.047 (3)	0.34
S1	0.4668 (5)	0.0549 (5)	0	0.069 (7)	0.17
O4AA	0.4422 (8)	0.0721 (7)	0	0.075 (9)	0.33
O6AA	0.4739 (3)	0.0406 (3)	0.0359 (4)	0.083 (4)	0.17
O1	0.5	0.0781 (4)	0	0.102 (5)	0.33
O2A	0.4739 (3)	0.0406 (3)	0.0359 (4)	0.083 (4)	0.34
O1A	0.5	0.0781 (4)	0	0.102 (5)	0.67
S10	0.31962 (19)	0.2319 (2)	0.0065 (3)	0.073 (4)	0.25
O91	0.3296 (9)	0.2053 (7)	0.0280 (11)	0.19 (3)	0.25
O91A	0.3307 (5)	0.2285 (5)	−0.0315 (5)	0.045 (5)	0.25
O92	0.2869 (3)	0.2314 (5)	0.0096 (5)	0.052 (6)	0.25
O94	0.3315 (5)	0.2600 (4)	0.0186 (6)	0.082 (8)	0.25
S10A	0.3138 (3)	0.2062 (3)	0.0034 (7)	0.126 (5)	0.25
O91B	0.3118 (8)	0.1753 (5)	0.0179 (10)	0.161 (19)	0.25
O91C	0.3277 (5)	0.2072 (5)	−0.0332 (6)	0.045 (5)	0.25
O92A	0.2819 (4)	0.2152 (6)	0.0036 (15)	0.092 (9)	0.25
O94A	0.3296 (9)	0.2280 (9)	0.0252 (11)	0.19 (3)	0.25
S3	0.50541 (15)	0.23723 (10)	0.22440 (13)	0.0792 (16)	0.50
O6	0.5074 (4)	0.2702 (2)	0.2271 (4)	0.104 (6)	0.50
O8AA	0.5226 (3)	0.2299 (3)	0.1908 (4)	0.084 (4)	0.50
O5AA	0.4731 (2)	0.2295 (3)	0.2206 (4)	0.077 (4)	0.50
O4A	0.5173 (3)	0.2243 (3)	0.2580 (4)	0.095 (5)	0.50
S9	0.4660 (2)	0.1417 (2)	0.3589 (3)	0.118 (4)	0.36
O87	0.4953 (4)	0.1403 (3)	0.3407 (4)	0.073 (5)	0.36
O88	0.4622 (5)	0.1705 (4)	0.3781 (6)	0.110 (8)	0.36
O89	0.4652 (4)	0.1153 (4)	0.3850 (5)	0.086 (6)	0.36
O90	0.4399 (4)	0.1383 (5)	0.3369 (6)	0.100 (7)	0.36
O118	0.4263 (5)	0.1281 (5)	0.3519 (6)	0.091 (6)	0.36
S8	0.29528 (5)	0.29528 (5)	0.25	0.0556 (8)	1.00
O85	0.29965 (13)	0.26323 (12)	0.24372 (17)	0.0597 (16)	1.00
O95	0.5	0.0760 (4)	0.0732 (6)	0.078 (5)	0.67
O96	0.5	0.0720 (7)	0.0886 (10)	0.058 (8)	0.33
O97	0.4012 (6)	0.3101 (6)	0.0404 (8)	0.135 (9)	0.39
O98	0.4271 (5)	0.3176 (5)	0.0602 (6)	0.108 (7)	0.39
O117	0.4165 (4)	0.2513 (4)	0.3506 (5)	0.067 (5)	0.36
O119	0.4371 (7)	0.2510 (7)	0.3391 (9)	0.143 (11)	0.36
O99	0.2996 (5)	0.3645 (6)	0.0919 (7)	0.049 (7)	0.22
O100	0.3082 (5)	0.3311 (5)	0.0743 (6)	0.097 (6)	0.39
O101	0.5	0.1372 (3)	0	0.076 (4)	1.00
O102	0.3750 (6)	0.3810 (7)	0.0652 (8)	0.325 (14)	0.78

Table SI3.3 Fractional atomic coordinates and isotropic or equivalent isotropic displacement parameters of K_2SO_4@MK-A, Space group $P4_2/mmc$.(Continued)

Atom	***x***	***y***	***z***	U_{iso}/U_{eq} **(Å^2)**	**Occupancy**
O103	0.3714 (2)	0.3189 (2)	0.2753 (2)	0.110 (3)	1.00
O104	0.33104 (18)	0.25572 (19)	0.3275 (2)	0.103 (3)	1.00
O105	0.2387 (3)	0.2387 (3)	0.25	0.153 (6)	1.00
O106	0.3649 (4)	0.1829 (4)	0.3761 (5)	0.182 (7)	0.72
O107	0.4074 (2)	0	0.0434 (3)	0.094 (3)	1.00
O108	0.32926 (19)	0.04458 (19)	0.1860 (2)	0.110 (3)	1.00
O110	0.4554 (4)	0.2959 (4)	0.1471 (5)	0.231 (7)	1.00
O111	0.4058 (4)	0.0315 (4)	0.3620 (5)	0.111 (6)	0.50
O112	0.3133 (7)	0	0.0696 (9)	0.060 (8)	0.28
O115	0.3932 (3)	0.3557 (3)	0.1590 (3)	0.127 (4)	0.78
O116	0.4423 (6)	0.1974 (6)	0.4085 (8)	0.122 (9)	0.36
K1	0.41759 (14)	0.19228 (10)	0.33381 (12)	0.0893 (17)	0.72
K2	0.36840 (12)	0.32599 (7)	0.09897 (14)	0.121 (2)	0.78
K3	0.3276 (2)	0	0	0.082 (3)	0.55
O0AA	0.4254 (4)	0.0661 (4)	0	0.088 (5)	0.67
O1AA	0.4796 (3)	0.1836 (3)	0.2957 (4)	0.051 (4)	0.36
O2AA	0.4788 (4)	0.2508 (4)	0.1179 (5)	0.122 (6)	1.00
O3AA	0.5	0.2583 (6)	0.3233 (8)	0.134 (10)	0.50
O7AA	0.2584 (4)	0.2552 (4)	0.0632 (5)	0.123 (6)	0.50
O4	0.2269 (5)	0.2775 (5)	0.1522 (6)	0.140 (7)	0.50
O2	0.2635 (5)	0.1763 (5)	0.0479 (6)	0.136 (7)	0.50
O3	0.5	0.2151 (6)	0.3899 (8)	0.131 (9)	0.50
O0BA	0.3043 (7)	0	0.0935 (9)	0.062 (8)	0.28
O9AA	0.2739 (7)	0.0285 (10)	0.0154 (15)	0.22 (3)	0.28
O1BA	0.3136 (7)	0.3435 (7)	0.1005 (8)	0.142 (10)	0.39
O2BA	0.3816 (7)	0.3320 (7)	0.1230 (10)	0.065 (8)	0.22
O3BA	0.4064 (5)	0.1854 (6)	0.3384 (7)	0.031 (6)	0.28

SI3.4 Selected bond distances and bond angles in K_2SO_4@MK-A structure

Table 3.4 List of K—O bond distances and O—K—O angles in K_2SO_4@MK-A structure.

Bond	**Bond Distance (Å)**	**Bond**	**Bond Distance (Å)**
K1—O106	2.78 (2)	K2—O115	2.695 (13)
K1—O116	2.90 (3)	K2—O97	2.65 (3)
K1—O117	2.746 (18)	K2—O98	3.01 (2)
K1—O118	3.06 (3)	K3—O112	2.52 (3)
K1—O119	2.87 (3)	K3—O112^{ii}	2.52 (3)
K1—O1AA	3.200 (15)	K3—O78^{ii}	2.724 (8)
K1—O88	2.79 (2)	K3—O78^{iv}	2.724 (8)
K1—O90	2.708 (19)	K3—O78^{vi}	2.724 (8)
K2—O100	2.80 (2)	K3—O9AA	2.803 (19)
K2—O102	2.77 (3)		

Table3.4 List of K—O bond distances and O—K—O angles in K_2SO_4@MK-A structure. (Continued)

Bond	Angle (°)	Bond	Angle (°)
O100—K2—O57	131.2 (5)	O50—K1—O1AA	92.6 (3)
O100—K2—O58	81.2 (5)	O50—K1—O51	53.65 (16)
O100—K2—O68	84.8 (5)	O51—K1—O1AA	116.8 (3)
O102—K2—Al20	156.6 (6)	O52—K1—O116	143.4 (6)
O102—K2—O100	82.4 (7)	O52—K1—O118	116.7 (5)
O102—K2—O57	146.1 (6)	O52—K1—O119	77.4 (7)
O102—K2—O58	145.4 (7)	O52—K1—O1AA	62.5 (3)
O102—K2—O68	152.8 (6)	O52—K1—O50	55.69 (17)
O102—K2—O98	77.9 (8)	O52—K1—O51	54.23 (16)
O106—K1—O119	111.8 (8)	O52—K1—S9	112.0 (3)
O106—K1—O50	86.7 (4)	O57—K2—O68	53.56 (17)
O106—K1—O51	74.7 (4)	O57—K2—O98	73.5 (5)
O106—K1—O52	127.7 (5)	O58—K2—O57	55.22 (19)
O106—K1—O88	106.9 (6)	O58—K2—O68	54.34 (17)
O106—K1—S9	110.2 (5)	O58—K2—O98	93.2 (5)
$O112^{ii}$—K3—O112	150.6 (15)	$O78^{ii}$—K3—O78	70.7 (4)
$O112^{ii}$—K3—O78	133.2 (4)	$O78^{ii}$—K3—$O78^{iv}$	121.2 (5)
$O112^{ii}$—K3—$O78^{ii}$	64.2 (5)	$O78^{ii}$—K3—O9AA	105.0 (10)
$O112^{ii}$—K3—$O78^{iv}$	133.2 (4)	$O78^{iv}$—K3—O78	81.3 (4)
$O112^{ii}$—K3—$O78^{vi}$	64.2 (5)	$O78^{iv}$—K3—O9AA	126.5 (10)
$O112^{ii}$—K3—O9AA	89.2 (12)	O78—K3—O9AA	90.7 (10)
O112—K3—O78	64.2 (5)	$O78^{vi}$—K3—O78	121.2 (5)
O112—K3—$O78^{ii}$	133.2 (4)	$O78^{vi}$—K3—$O78^{ii}$	81.3 (4)
Bond	**Angle (°)**	**Bond**	**Angle (°)**
O112—K3—$O78^{iv}$	64.2 (5)	$O78^{vi}$—K3—$O78^{iv}$	70.7 (4)
O112—K3—$O78^{vi}$	133.2 (4)	$O78^{vi}$—K3—O9AA	147.3 (10)
O112—K3—O9AA	64.7 (12)	O88—K1—O119	92.1 (7)
O115—K2—O100	123.4 (5)	O88—K1—O50	128.4 (4)
O115—K2—O102	84.8 (7)	O88—K1—O51	177.1 (4)
O115—K2—O57	79.4 (3)	O88—K1—O52	124.6 (5)
O115—K2—O58	129.6 (3)	O90—K1—O106	97.8 (6)
O115—K2—O68	82.4 (3)	O90—K1—O119	138.2 (7)
O115—K2—O98	94.0 (5)	O90—K1—O50	79.4 (4)
O116—K1—O118	83.4 (7)	O90—K1—O51	132.4 (4)
O116—K1—O1AA	91.0 (6)	O90—K1—O52	107.6 (4)
O116—K1—O51	141.5 (6)	O90—K1—O88	50.0 (4)
O117—K1—O116	73.3 (7)	O90—K1—S9	25.0 (3)
O117—K1—O118	155.7 (6)	O97—K2—Al20	111.8 (6)
O117—K1—O1AA	101.2 (5)	O97—K2—Al21	71.4 (5)
O117—K1—O50	127.6 (4)	O97—K2—Al22	107.0 (6)
O117—K1—O51	75.3 (4)	O97—K2—O100	108.7 (7)
O117—K1—O52	86.9 (4)	O97—K2—O102	78.0 (8)
O118—K1—O1AA	85.7 (6)	O97—K2—O115	121.9 (7)
O118—K1—O51	122.4 (5)	O97—K2—O57	85.2 (6)
O119—K1—O50	129.3 (7)	O97—K2—O58	78.8 (6)
O119—K1—O51	85.0 (6)	O97—K2—O68	129.1 (6)
O50—K1—O116	157.4 (6)	O98—K2—O68	126.8 (5)
O50—K1—O118	74.6 (5)		

Symmetry codes: (i) −x+1, y, z; (ii) x, y, −z; (iii) −x+1, −y, z; (iv) x, −y, z; (v) y, x, −z+1/2; (vi) x, −y, −z.

SI3.5 Fractional atomic coordinates and isotropic or equivalent isotropic displacement parameters of Rb_2SO_4@MK-A structure

Table SI3.5 Fractional atomic coordinates and isotropic or equivalent isotropic displacement parameters of Rb_2SO_4@MK-A, Space group $P4_2/mmc$.

Atom	***x***	***y***	***z***	U_{iso}/U_{eq} **(Å^2)**	**Occupancy**
Al0B	0.12160 (7)	0.32895 (7)	0.08708 (9)	0.0308 (8)	1.00
Al1	0.03883 (9)	0.46676 (7)	0.19979 (10)	0.0415 (9)	1.00
Al12	0.11216 (9)	0.25494 (7)	0.10820 (10)	0.0435 (10)	1.00
Al13	0.03916 (17)	0.5	0.12043 (18)	0.0702 (19)	1.00
Al14	0.17341 (10)	0.24180 (9)	0.13189 (11)	0.0582 (12)	1.00
Al15	0	0.46759 (13)	0.34946 (16)	0.081 (2)	1.00
Al16	0.09416 (12)	0.5	0.17933 (14)	0.0427 (13)	1.00
Al1A	0.07058 (7)	0.31555 (7)	0.13658 (9)	0.0291 (8)	1.00
Al1B	0	0.33543 (9)	0.10415 (12)	0.0245 (10)	1.00
Al2	0.10979 (8)	0.26631 (8)	0.24444 (10)	0.0444 (10)	1.00
Al2A	0	0.5	0.2650 (2)	0.053 (2)	1.00
Al2B	0.10002 (9)	0.35596 (9)	0	0.0256 (10)	1.00
Al3	0.12241 (9)	0.22873 (8)	0.18066 (11)	0.0508 (11)	1.00
Al3A	0.07971 (8)	0.43772 (7)	0.12579 (9)	0.0371 (9)	1.00
Al4	0.14866 (8)	0.31694 (8)	0.26059 (10)	0.0445 (10)	1.00
Al4A	0.08964 (8)	0.32656 (8)	0.22836 (9)	0.0372 (9)	1.00
Al5	0.21045 (9)	0.29224 (10)	0.14688 (12)	0.0581 (12)	1.00
Al5A	0.19853 (8)	0.32988 (9)	0.21223 (11)	0.0506 (10)	1.00
Al6	0.07089 (15)	0.5	0.25916 (15)	0.0544 (16)	1.00
Al7	0.18345 (8)	0.35098 (9)	0.13721 (11)	0.0467 (10)	1.00
Al7A	0.06773 (7)	0.36953 (6)	0.08583 (8)	0.0248 (7)	1.00
Al8A	0.10958 (7)	0.36800 (7)	0.15193 (9)	0.0307 (8)	1.00
Al9	0.03239 (11)	0.43869 (8)	0.28865 (11)	0.0603 (12)	1.00
Al9A	0.13826 (7)	0.30133 (7)	0.16989 (9)	0.0340 (8)	1.00
O0AA	0.11043 (14)	0.36990 (14)	0.09873 (18)	0.0272 (16)	1.00
O0BA	0.18415 (16)	0.29969 (16)	0.2431 (2)	0.043 (2)	1.00
O1	0.1684 (3)	0.2447 (3)	0.3254 (3)	0.109 (4)	1.00
O10	0.0459 (5)	0.2014 (5)	0.2185 (6)	0.206 (8)	1.00
O101	0.1431 (3)	0.4592 (2)	0.0440 (3)	0.091 (3)	1.00
O102	0.1405 (3)	0.4506 (3)	0.2629 (4)	0.146 (7)	1.00
O103	0.1552 (2)	0.4531 (3)	0.1080 (3)	0.115 (5)	1.00
O104	0	0.4179 (7)	0.0700 (9)	0.060 (10)	0.50
O105	0.1315 (3)	0.3992 (3)	0.2841 (3)	0.132 (6)	1.00
O108	0	0.2300 (4)	0.2297 (5)	0.123 (6)	1.00
O116	0.0249 (4)	0.2707 (3)	0.2013 (5)	0.148 (6)	1.00
O117	0.0270 (4)	0.4571 (4)	0.0348 (5)	0.069 (5)	0.50
O120	0.0210 (4)	0.2780 (4)	0.2519 (5)	0.184 (7)	1.00
O15	0.0391 (7)	0.3861 (7)	0.3800 (9)	0.074 (9)	0.32
O16	0.0537 (9)	0.2445 (8)	0.3249 (10)	0.092 (11)	0.32
O17	0	0.4668 (2)	0.1829 (3)	0.037 (3)	1.00
O18	0.2182 (6)	0.2680 (6)	0.3523 (7)	0.260 (11)	1.00

Table SI3.5 Fractional atomic coordinates and isotropic or equivalent isotropic displacement parameters of Rb_2SO_4@MK-A, Space group $P4_2/mmc$.(Continued)

Atom	***x***	***y***	***z***	U_{iso}/U_{eq} **(Å^2)**	**Occupancy**
O19	0.1350 (4)	0.3173 (4)	0.3718 (5)	0.201 (8)	1.00
O1AA	0.05977 (15)	0.40815 (14)	0.09860 (18)	0.0307 (17)	1.00
O1BA	0.2247 (16)	0.5	0	0.15 (3)	0.44
O2	0.0085 (6)	0.3626 (5)	0.3339 (6)	0.057 (8)	0.32
O20	0.0888 (10)	0.1849 (9)	0.0404 (12)	0.053 (12)	0.20
O21	0.14995 (15)	0.37203 (15)	0.1553 (2)	0.0382 (19)	1.00
O22	0.16110 (16)	0.33762 (16)	0.0964 (2)	0.0402 (19)	1.00
O23	0.05113 (16)	0.44009 (15)	0.16338 (19)	0.0359 (19)	1.00
O24	0.06756 (15)	0.31241 (15)	0.18714 (19)	0.0343 (18)	1.00
O26	0.10112 (16)	0.40882 (14)	0.1537 (2)	0.0372 (19)	1.00
O28	0.07868 (16)	0.29195 (16)	0.2552 (2)	0.042 (2)	1.00
O29	0	0.3637 (2)	0.1431 (3)	0.053 (3)	1.00
O2AA	0.02883 (14)	0.35827 (14)	0.07848 (19)	0.0308 (17)	1.00
O2BA	0	0.4282 (8)	0.0788 (9)	0.065 (10)	0.50
O3	0.0471 (5)	0.1983 (5)	0.1402 (6)	0.225 (9)	1.00
O30	0.07878 (14)	0.32718 (14)	0.08569 (18)	0.0262 (16)	1.00
O31	0.1283 (2)	0.3898 (2)	0	0.036 (3)	1.00
O32	0.0716 (2)	0.3244 (2)	0	0.044 (3)	1.00
O33	0.10120 (16)	0.36027 (15)	0.2014 (2)	0.0376 (19)	1.00
O34	0.07749 (14)	0.37575 (14)	0.03688 (18)	0.0271 (16)	1.00
O35	0.16685 (18)	0.34815 (17)	0.2354 (2)	0.049 (2)	1.00
O36	0.02974 (15)	0.31214 (15)	0.1272 (2)	0.0358 (19)	1.00
O37	0.1887 (9)	0.1616 (9)	0.0834 (11)	0.151 (15)	0.39
O38	0.05065 (18)	0.28546 (18)	0.0335 (2)	0.053 (2)	1.00
O39	0.06832 (14)	0.35868 (14)	0.13891 (18)	0.0271 (16)	1.00
O3AA	0.0620 (7)	0.3685 (6)	0.3438 (8)	0.050 (7)	0.32
O3BA	0.0818 (11)	0.3792 (10)	0.3457 (12)	0.120 (14)	0.32
O4	0.1687 (3)	0.4550 (3)	0.1835 (4)	0.140 (5)	1.00
O41	0	0.3074 (2)	0.0631 (3)	0.035 (3)	1.00
O42	0.11386 (14)	0.32454 (14)	0.14141 (18)	0.0264 (16)	1.00
O43	0.0898 (2)	0.23983 (17)	0.0664 (2)	0.060 (3)	1.00
O44	0.19975 (18)	0.23650 (18)	0.2422 (2)	0.054 (2)	1.00
O45	0.1512 (2)	0.4093 (2)	0.0689 (3)	0.069 (3)	1.00
O46	0.0515 (2)	0.5	0.1677 (3)	0.035 (3)	1.00
O47	0.12466 (17)	0.28841 (15)	0.0808 (2)	0.0391 (19)	1.00
O48	0.10188 (17)	0.46878 (15)	0.1477 (2)	0.040 (2)	1.00
O49	0.03363 (19)	0.43866 (16)	0.2364 (2)	0.048 (2)	1.00
O4AA	0.09028 (16)	0.24946 (16)	0.2038 (2)	0.047 (2)	1.00
O4BA	0.0567 (13)	0.3515 (13)	0.3230 (16)	0.17 (2)	0.32
O50	0.1045 (2)	0.41988 (19)	0.2345 (2)	0.072 (3)	1.00
O51	0.10765 (18)	0.43823 (17)	0.0847 (2)	0.048 (2)	1.00
O52	0.07835 (16)	0.27596 (15)	0.1263 (2)	0.0386 (19)	1.00
O53	0.12324 (15)	0.33743 (16)	0.03697 (19)	0.0362 (18)	1.00
O54	0.12381 (16)	0.30284 (15)	0.21610 (19)	0.0379 (19)	1.00
O55	0.0353 (9)	0.3314 (10)	0.3761 (12)	0.119 (14)	0.32

Table SI3.5 Fractional atomic coordinates and isotropic or equivalent isotropic displacement parameters of Rb_2SO_4@MK-A, Space group $P4_2/mmc$.(Continued)

Atom	***x***	***y***	***z***	U_{iso}/U_{eq} (Å^2)	**Occupancy**
O56	0.0618 (2)	0.46888 (17)	0.2894 (2)	0.059 (3)	1.00
O57	0.08041 (18)	0.47321 (15)	0.2171 (2)	0.045 (2)	1.00
O58	0.02656 (16)	0.38717 (17)	0.1913 (3)	0.055 (2)	1.00
O59	0.17547 (15)	0.31521 (16)	0.1669 (2)	0.0388 (19)	1.00
O5AA	0.0947 (2)	0.2761 (2)	0	0.045 (3)	1.00
O5BA	0.0639 (8)	0.4308 (8)	0	0.078 (11)	0.50
O6	0.1089 (5)	0.1435 (5)	0.1544 (6)	0.064 (7)	0.39
O60	0.13884 (17)	0.24118 (15)	0.2256 (2)	0.045 (2)	1.00
O61	0.1570 (2)	0.21215 (17)	0.1624 (2)	0.056 (2)	1.00
O63	0.1013 (2)	0.22189 (16)	0.1376 (2)	0.060 (3)	1.00
O65	0.13662 (16)	0.26420 (15)	0.1512 (2)	0.0388 (19)	1.00
O66	0.22784 (18)	0.3059 (2)	0.1896 (2)	0.059 (2)	1.00
O67	0	0.5324 (2)	0.2919 (3)	0.062 (4)	1.00
O68	0.05533 (16)	0.34760 (16)	0.2471 (2)	0.0398 (19)	1.00
O69	0.11335 (18)	0.33819 (17)	0.26898 (19)	0.046 (2)	1.00
O6AA	0.1943 (9)	0.5	0.0833 (12)	0.123 (14)	0.44
O6BA	0.1915 (17)	0.4246 (18)	0	0.24 (3)	0.44
O7	0.0184 (4)	0.3164 (4)	0.2924 (6)	0.207 (9)	1.00
O70	0	0.3418 (2)	0.2035 (3)	0.072 (4)	1.00
O71	0.1098 (2)	0.19091 (18)	0.2019 (3)	0.075 (3)	1.00
O72	0.19583 (19)	0.18717 (19)	0.2176 (2)	0.056 (2)	1.00
O73	0.2480 (2)	0.2770 (3)	0.1301 (3)	0.084 (3)	1.00
O74	0.1339 (3)	0.5	0.1970 (3)	0.054 (3)	1.00
O75	0.19836 (18)	0.25628 (18)	0.1678 (2)	0.055 (2)	1.00
O76	0.0568 (2)	0.46771 (16)	0.0992 (2)	0.059 (3)	1.00
O77	0.19638 (17)	0.3852 (2)	0.1094 (3)	0.062 (3)	1.00
O78	0.13379 (17)	0.28267 (17)	0.2811 (2)	0.045 (2)	1.00
O79	0.0309 (2)	0.44014 (18)	0.3403 (2)	0.068 (3)	1.00
O7AA	0.2180 (7)	0.2775 (6)	0	0.191 (11)	1.00
O7BA	0.0712 (13)	0.2479 (13)	0.3399 (16)	0.17 (2)	0.32
O8	0.1707 (5)	0.2850 (5)	0.0341 (6)	0.214 (9)	1.00
O80	0	0.3610 (5)	0	0.088 (7)	1.00
O81	0.18970 (19)	0.2742 (2)	0.1078 (2)	0.059 (2)	1.00
O82	0.1654 (2)	0.3285 (2)	0.3078 (2)	0.060 (2)	1.00
O83	0.09475 (19)	0.23585 (19)	0.2778 (3)	0.061 (2)	1.00
O84	0	0.5	0.1144 (5)	0.086 (7)	1.00
O85	0.1109 (3)	0.5	0.2758 (3)	0.063 (4)	1.00
O86	0.20464 (18)	0.36195 (18)	0.1797 (2)	0.056 (2)	1.00
O87	0.0625 (2)	0.40766 (18)	0.2898 (3)	0.078 (3)	1.00
O88	0.1463 (2)	0.23428 (18)	0.0928 (2)	0.062 (3)	1.00
O89	0	0.4203 (4)	0	0.075 (6)	1.00
O8AA	0.2620 (3)	0.2620 (3)	0.25	0.113 (6)	1.00
O8BA	0.1165 (18)	0.1951 (18)	0.025 (2)	0.16 (3)	0.20
O90	0.21615 (17)	0.3283 (2)	0.1209 (2)	0.064 (3)	1.00
O91	0	0.4120 (2)	0.2861 (3)	0.058 (3)	1.00

Table SI3.5 Fractional atomic coordinates and isotropic or equivalent isotropic displacement parameters of Rb_2SO_4@MK-A, Space group $P4_2/mmc$.(Continued)

Atom	*x*	*y*	*z*	U_{iso}/U_{eq} (Å^2)	Occupancy
O92	0.2030 (2)	0.2151 (2)	0.1116 (3)	0.089 (4)	1.00
O93	0.0776 (7)	0.4331 (6)	0	0.057 (8)	0.50
O94	0.22713 (19)	0.3451 (2)	0.2478 (3)	0.069 (3)	1.00
O96	0.1276 (2)	0.1817 (2)	0.2728 (3)	0.087 (3)	1.00
O97	0	0.4597 (3)	0.4013 (3)	0.095 (6)	1.00
O98	0.0266 (3)	0.5	0.3538 (3)	0.064 (4)	1.00
O99	0.1557 (2)	0.4095 (2)	0.2253 (3)	0.091 (3)	1.00
O9AA	0.0320 (2)	0.5	0.2355 (3)	0.037 (3)	1.00
O9BA	0.2716 (4)	0.3572 (4)	0.1503 (5)	0.246 (7)	1.00
Rb0A	0.08038 (8)	0.30721 (7)	0.33267 (7)	0.0990 (15)	0.63
Rb25	0.0929 (2)	0.5	0.0411 (3)	0.087 (4)	0.27
Rb6A	0.17774 (13)	0.5	0	0.055 (2)	0.44
Rb95	0.1342 (3)	0.17062 (16)	0.0966 (3)	0.230 (6)	0.39
S0AA	0.1782 (5)	0.2711 (5)	0	0.294 (9)	1.00
S1	0	0.36936 (8)	0.18315 (10)	0.0286 (9)	1.00
S10	0.20463 (7)	0.20463 (7)	0.25	0.0481 (12)	1.00
S11	0.13420 (13)	0.42052 (10)	0.25182 (13)	0.0945 (17)	1.00
S14	0.0334 (5)	0.3587 (5)	0.3532 (7)	0.144 (8)	0.32
S16	0	0.26349 (16)	0.2230 (2)	0.095 (2)	1.00
S2	0.06682 (9)	0.29240 (8)	0	0.0297 (9)	1.00
S4	0.0319 (7)	0.4413 (7)	0	0.032 (10)	0.11
S64	0	0.4371 (2)	0.0356 (3)	0.040 (4)	0.39
S8	0.13923 (10)	0.44092 (9)	0.07633 (12)	0.0703 (11)	1.00

SI3.6 Selected bond distances in Rb_2SO_4@MK-A structure

Table SI3.2 List of Rb—O bond distances in Rb_2SO_4@MK-A structure.

Bond	Bond Distance (Å)	Bond	Bond Distance (Å)
Rb6A—O101^{iii}	2.863 (10)	Rb25—O51^{iv}	3.237 (10)
Rb6A—O101	2.863 (10)	Rb25—O51	3.237 (10)
Rb6A—O101^{ii}	2.863 (10)	Rb25—O76^{iv}	2.998 (12)
Rb6A—O101^{iv}	2.863 (10)	Rb25—O76	2.998 (12)
Rb6A—O6AA	3.07 (4)	Rb25—O101^{iv}	2.890 (13)
Rb6A—O6AA^{ii}	3.07 (4)	Rb25—O101	2.890 (13)
Rb6A—O1BA	2.10 (7)	Rb25—O117	3.52 (2)
Rb6A—O6BA	3.43 (8)	Rb25—O117^{iv}	3.52 (2)
Rb6A—O6BA^{iii}	3.43 (8)	Rb25—O93	3.40 (3)
Rb95—O6	2.65 (3)	Rb25—O93^{iii}	3.40 (3)
Rb95—O20	2.93 (4)	Rb0A—O28	2.853 (8)
Rb95—O37	2.51 (4)	Rb0A—O69	3.044 (8)
Rb95—O8BA	2.89 (8)	Rb0A—O78	3.209 (8)
Rb95—O61	3.162 (11)	Rb0A—O7	3.147 (19)
Rb95—O88	2.899 (12)	Rb0A—O19	2.85 (2)
Rb95—O63	3.091 (12)	Rb0A—O16	3.06 (4)
Rb25^{ii}—O93	3.40 (3)	Rb0A—O3BA	3.25 (4)

Table SI3.2 List of Rb—O bond distances in Rb_2SO_4@MK-A structure. (Continued)

Bond	Bond Distance (Å)	Bond	Bond Distance (Å)
Rb0A—O4BA	2.27 (6)	Rb0A—O55	2.76 (4)
Rb0A—O7BA	2.69 (6)	Rb0A—O3AA	2.89 (3)

Symmetry codes: (i) *−x, y, z;* (ii) *x, y, −z;* (iii) *x, −y+1, −z;* (iv) *x, −y+1, z;* (v) *−x, −y+1, z;* (vi) *y, x, −z+1/2.*

SI3.7 Fractional atomic coordinates and isotropic or equivalent isotropic displacement parameters of Cs_2SO_4@MK-A structure

Table SI3.7 Fractional atomic coordinates and isotropic or equivalent isotropic displacement parameters of Cs_2SO_4@MK-A, Space group $P4_2/mmc$.

Atom	*x*	*y*	*z*	U_{iso}/U_{eq} (Å^2)	Occupancy
Al1	0.06221 (5)	0.41984 (6)	0.37433 (6)	0.0405 (7)	1.00
Al10	0.13047 (4)	0.43230 (5)	0.41398 (6)	0.0257 (6)	1.00
Al11	0.16431 (6)	0.5	0.39542 (8)	0.0254 (8)	1.00
Al12	0.14406 (7)	0.40031 (6)	0.5	0.0274 (8)	1.00
Al13	0.17114 (5)	0.37846 (5)	0.41291 (6)	0.0329 (6)	1.00
Al14	0.18435 (5)	0.42950 (5)	0.36312 (6)	0.0310 (6)	1.00
Al15	0.17327 (5)	0.41006 (5)	0.27172 (6)	0.0406 (7)	1.00
Al16	0.19866 (5)	0.36161 (5)	0.33061 (6)	0.0366 (6)	1.00
Al17	0.14926 (6)	0.31650 (5)	0.36346 (8)	0.0506 (8)	1.00
Al18	0.17025 (6)	0.30095 (6)	0.28891 (8)	0.0566 (8)	1.00
Al19	0.18272 (6)	0.35054 (6)	0.24001 (7)	0.0489 (7)	1.00
Al2	0.03318 (5)	0.46084 (6)	0.30038 (6)	0.0463 (7)	1.00
Al20	0.23360 (6)	0.39005 (6)	0.25576 (7)	0.0476 (7)	1.00
Al21	0.27109 (5)	0.37805 (6)	0.31908 (7)	0.0523 (8)	1.00
Al22	0.24500 (5)	0.38820 (6)	0.39161 (7)	0.0462 (7)	1.00
Al23	0.25858 (6)	0.32703 (7)	0.36838 (8)	0.0618 (9)	1.00
Al24	0.20805 (7)	0.28973 (6)	0.35384 (8)	0.0625 (9)	1.00
Al3	0	0.40597 (9)	0.32048 (10)	0.0497 (10)	1.00
Al4	0	0.42879 (11)	0.24122 (10)	0.0630 (13)	1.00
Al5	0	0.5	0.23563 (13)	0.0599 (17)	1.00
Al6	0.06143 (6)	0.46741 (9)	0.21192 (7)	0.0715 (10)	1.00
Al7	0.03249 (10)	0.5	0.15120 (11)	0.0917 (19)	1.00
Al8	0	0.46015 (11)	0.38000 (12)	0.0685 (13)	1.00
Al9	0.13177 (5)	0.39020 (5)	0.34825 (6)	0.0326 (6)	1.00
Cs0A	0	0.31614 (19)	0.5	0.097 (4)	0.18
Cs1	0.2721 (2)	0.3533 (2)	0.5003 (5)	0.189 (7)	0.14
Cs2	0.23377 (7)	0.23377 (7)	0.25	0.194 (4)	0.37
Cs3	0.19582 (6)	0.42080 (8)	0.16221 (6)	0.1113 (12)	0.44
Cs97	0.1379 (3)	0.5	0.5	0.103 (7)	0.12
O0AA	0	0.4039 (4)	0.5384 (5)	0.138 (6)	0.82
O0BA	0.2574 (6)	0.2607 (6)	0.4407 (7)	0.075 (8)	0.25
O0CA	0.0635 (3)	0.2924 (3)	0.3274 (4)	0.090 (4)	0.50
O0DA	−0.058 (3)	0.401 (3)	0.5	0.21 (5)	0.18

Table SI3.7 Fractional atomic coordinates and isotropic or equivalent isotropic displacement parameters of Cs_2SO_4@MK-A, Space group $P4_2/mmc$. (Continued)

Atom	***x***	***y***	***z***	U_{iso}/U_{eq} (Å^2)	**Occupancy**
O1	0.2976 (4)	0.4562 (4)	0.2843 (5)	0.246 (7)	1.00
O10	0.2216 (3)	0.4802 (3)	0.2452 (4)	0.080 (4)	0.50
O102	0.2703 (5)	0.5	0.4613 (6)	0.216 (8)	1.00
O104	0.1812 (4)	0.3601 (4)	0.1283 (5)	0.102 (6)	0.44
O105	0.1323 (5)	0.4405 (4)	0.1576 (6)	0.043 (6)	0.22
O108	0.1902 (7)	0.2487 (7)	0.2050 (8)	0.056 (8)	0.18
O109	0.3160 (9)	0.4353 (10)	0.4471 (11)	0.206 (16)	0.36
O11	0.2676 (2)	0.4927 (4)	0.2684 (4)	0.092 (6)	0.50
O111	0.1368 (7)	0.2290 (7)	0.3514 (9)	0.133 (11)	0.32
O12	0.2293 (3)	0.4777 (3)	0.3120 (4)	0.093 (4)	0.50
O12A	0.2243 (4)	0.5261 (3)	0.2820 (5)	0.093 (5)	0.50
O13	0.06171 (13)	0.39164 (12)	0.41469 (16)	0.0547 (16)	1.00
O14	0.06006 (10)	0.44893 (12)	0.33666 (13)	0.0405 (13)	1.00
O15	0	0.2989 (6)	0.5935 (9)	0.098 (7)	0.50
O16	0.1143 (7)	0.4738 (7)	0.1147 (8)	0.128 (14)	0.22
O18	0	0.4677 (2)	0.2653 (2)	0.053 (2)	1.00
O19	0.03249 (16)	0.5	0.2080 (2)	0.073 (3)	1.00
O1AA	0.0745 (3)	0.5	0.4124 (5)	0.085 (5)	0.75
O1B	0.2086 (8)	0.3306 (7)	0.5332 (9)	0.064 (5)	0.19
O1BA	0.2174 (8)	0.3239 (9)	0.4686 (10)	0.064 (5)	0.14
O1C	0.2332 (7)	0.3299 (8)	0.4730 (9)	0.064 (5)	0.19
O1CA	0	0.235 (2)	0.461 (2)	0.15 (3)	0.18
O1D	0.2286 (9)	0.3379 (8)	0.5315 (11)	0.068 (14)	0.16
O1DA	−0.0574 (13)	0.3081 (13)	0.5	0.084 (17)	0.18
O1E	0.2646 (7)	0.3321 (10)	0.4820 (15)	0.12 (3)	0.16
O2	0.2586 (4)	0.4731 (4)	0.3726 (5)	0.262 (8)	1.00
O20	0.06115 (12)	0.46609 (15)	0.26383 (14)	0.0587 (17)	1.00
O21	0.08796 (17)	0.5	0.2141 (2)	0.068 (3)	1.00
O22	0.1373 (4)	0.4919 (4)	0.1678 (5)	0.036 (6)	0.22
O23	0.05952 (14)	0.4692 (2)	0.15980 (17)	0.098 (3)	1.00
O25	0.0398 (2)	0.5	0.0987 (3)	0.116 (5)	1.00
O26	0.03113 (12)	0.43810 (17)	0.21090 (16)	0.076 (2)	1.00
O27	0	0.3887 (2)	0.2248 (2)	0.075 (3)	1.00
O28	0	0.3659 (2)	0.3032 (2)	0.062 (2)	1.00
O29	0.03225 (11)	0.44253 (14)	0.40096 (15)	0.0554 (17)	1.00
O2AA	−0.0102 (10)	0.3999 (10)	0.5	0.067 (16)	0.18
O2B	0.1801 (6)	0.3143 (8)	0.4815 (11)	0.099 (14)	0.19
O2BA	0.1918 (5)	0.4047 (5)	0.1565 (6)	0.123 (11)	0.56
O2C	0.2112 (9)	0.3243 (10)	0.4700 (12)	0.064 (5)	0.16
O2CA	0.1960 (10)	0.3200 (8)	0.5317 (7)	0.064 (5)	0.14
O2DA	0.13619 (16)	0.5	0.35632 (19)	0.054 (2)	1.00
O3	0.0677 (5)	0.4316 (5)	0.5	0.124 (8)	0.75
O30	0	0.5	0.3834 (4)	0.090 (5)	1.00
O31	0.3135 (8)	0.4113 (8)	0.4594 (10)	0.037 (9)	0.14
O32	0	0.3027 (7)	0.4355 (10)	0.115 (10)	0.14

Table SI3.7 Fractional atomic coordinates and isotropic or equivalent isotropic displacement parameters of Cs_2SO_4@MK-A, Space group $P4_2/mmc$. (Continued)

Atom	***x***	***y***	***z***	U_{iso}/U_{eq} **(Å^2)**	**Occupancy**
O33	0.14114 (10)	0.43154 (10)	0.36141 (12)	0.0299 (12)	1.00
O34	0.09170 (10)	0.44030 (11)	0.40138 (13)	0.0349 (13)	1.00
O35	0.14113 (10)	0.47139 (10)	0.42101 (13)	0.0329 (12)	1.00
O36	0.3276 (15)	0.4115 (15)	0.5147 (18)	0.14 (3)	0.14
O37	0.11334 (12)	0.47339 (12)	0.30759 (18)	0.0599 (17)	1.00
O38	0.3163 (14)	0.3016 (14)	0.5	0.17 (2)	0.29
O39	0.18746 (10)	0.47020 (10)	0.37234 (13)	0.0346 (13)	1.00
O3AA	0.0757 (5)	0.4425 (5)	0.5	0.015 (7)	0.25
O3B	0.2173 (5)	0.2842 (3)	0.5060 (9)	0.030 (7)	0.19
O3BA	0	0.2934 (8)	0.3817 (11)	0.128 (12)	0.41
O3C	0.2367 (7)	0.2903 (4)	0.5081 (10)	0.058 (11)	0.16
O3CA	0.1640 (5)	0.3145 (8)	0.4807 (11)	0.074 (14)	0.14
O3DA	0.15781 (17)	0.5	0.2965 (2)	0.076 (3)	1.00
O4	0.2283 (6)	0.2779 (6)	0.1554 (8)	0.108 (8)	0.32
O40	0.19193 (15)	0.5	0.43772 (19)	0.0387 (18)	1.00
O41	0.12448 (10)	0.42258 (10)	0.46351 (13)	0.0297 (12)	1.00
O42	0.17546 (16)	0.42887 (16)	0.5	0.052 (2)	1.00
O43	0.22365 (17)	0.40551 (17)	0.5	0.052 (2)	1.00
O44	0.21469 (13)	0.44994 (13)	0.46617 (15)	0.0591 (17)	1.00
O45	0.16284 (11)	0.37677 (10)	0.46317 (13)	0.0369 (13)	1.00
O46	0.12987 (10)	0.38944 (10)	0.40151 (13)	0.0300 (12)	1.00
O47	0.17538 (10)	0.38610 (10)	0.35931 (13)	0.0307 (12)	1.00
O48	0.17250 (10)	0.42140 (10)	0.41452 (12)	0.0294 (12)	1.00
O49	0.18727 (11)	0.43282 (11)	0.31254 (13)	0.0380 (13)	1.00
O4AA	0.02683 (11)	0.42020 (13)	0.28242 (14)	0.0498 (16)	1.00
O4BA	0.1792 (11)	0.2102 (10)	0.3127 (12)	0.238 (19)	0.37
O4CA	0.03128 (11)	0.39765 (12)	0.35202 (14)	0.0453 (15)	1.00
O4DA	0.0313 (5)	0.4061 (5)	0.1430 (6)	0.151 (8)	0.50
O5	0.3049 (5)	0.4534 (4)	0.3617 (6)	0.291 (9)	1.00
O50	0.1689 (6)	0.4683 (8)	0.1206 (10)	0.138 (16)	0.22
O51	0.19711 (11)	0.37596 (11)	0.28423 (13)	0.0397 (13)	1.00
O52	0.18486 (12)	0.32466 (11)	0.33390 (15)	0.0459 (14)	1.00
O53	0.12839 (12)	0.35002 (11)	0.34482 (15)	0.0460 (14)	1.00
O54	0.16264 (12)	0.33897 (11)	0.40441 (14)	0.0443 (14)	1.00
O55	0.13814 (14)	0.29523 (12)	0.32107 (17)	0.0654 (18)	1.00
O56	0.15217 (12)	0.33277 (13)	0.26558 (15)	0.0542 (16)	1.00
O57	0.16142 (12)	0.38601 (13)	0.23150 (14)	0.0509 (15)	1.00
O58	0.21730 (12)	0.36547 (12)	0.21947 (14)	0.0515 (15)	1.00
O59	0.20779 (12)	0.42126 (12)	0.24465 (14)	0.0496 (15)	1.00
O5AA	0	0.44851 (17)	0.33280 (19)	0.0395 (19)	1.00
O5BA	0.3558 (4)	0.3909 (4)	0.3456 (5)	0.268 (8)	1.00
O5CA	0.03311 (15)	0.5	0.3178 (2)	0.0415 (19)	1.00
O5DA	0	0.4741 (3)	0.1473 (2)	0.088 (4)	1.00
O6	0	0.2808 (19)	0.5	0.23 (3)	0.41
O60	0.25907 (12)	0.36108 (12)	0.27450 (15)	0.0514 (15)	1.00

Table SI3.7 Fractional atomic coordinates and isotropic or equivalent isotropic displacement parameters of Cs_2SO_4@MK-A, Space group $P4_2/mmc$. (Continued)

Atom	***x***	***y***	***z***	U_{iso}/U_{eq} **(Å^2)**	**Occupancy**
O61	0.23580 (11)	0.36385 (11)	0.34854 (13)	0.0415 (14)	1.00
O62	0.22373 (10)	0.42155 (12)	0.37397 (14)	0.0413 (14)	1.00
O63	0.21172 (11)	0.37558 (11)	0.41895 (13)	0.0431 (14)	1.00
O64	0.27816 (11)	0.39921 (14)	0.36240 (16)	0.0599 (17)	1.00
O65	0.26594 (13)	0.35380 (15)	0.40683 (15)	0.0634 (18)	1.00
O66	0.22619 (14)	0.31034 (12)	0.39190 (16)	0.0608 (17)	1.00
O67	0.17263 (16)	0.28435 (12)	0.37981 (17)	0.0699 (19)	1.00
O68	0.19440 (15)	0.27226 (12)	0.31048 (17)	0.0674 (19)	1.00
O69	0.24375 (13)	0.30154 (13)	0.33270 (16)	0.0591 (17)	1.00
O6AA	0.3319 (2)	0.3652 (2)	0.4051 (3)	0.143 (4)	1.00
O6BA	0.0793 (5)	0.5	0.5	0.044 (5)	0.50
O6CA	0.09189 (13)	0.43789 (18)	0.21110 (18)	0.084 (2)	1.00
O70	0.22365 (19)	0.25187 (14)	0.3715 (2)	0.094 (3)	1.00
O71	0.28762 (13)	0.34272 (15)	0.33796 (16)	0.0655 (18)	1.00
O72	0.28672 (17)	0.29843 (17)	0.3885 (2)	0.096 (3)	1.00
O73	0.25955 (12)	0.41011 (15)	0.43395 (16)	0.0637 (19)	1.00
O74	0.25020 (11)	0.40978 (12)	0.29620 (15)	0.0503 (15)	1.00
O75	0.30880 (12)	0.39074 (15)	0.29796 (18)	0.0705 (19)	1.00
O76	0.26371 (13)	0.40438 (13)	0.22195 (17)	0.0657 (18)	1.00
O77	0.20007 (13)	0.31565 (13)	0.25732 (15)	0.0546 (16)	1.00
O78	0.17084 (15)	0.33412 (14)	0.19236 (16)	0.0689 (19)	1.00
O79	0.15540 (16)	0.27224 (15)	0.25458 (19)	0.084 (2)	1.00
O7AA	0.1990 (6)	0.2772 (3)	0.4940 (10)	0.028 (9)	0.14
O7BA	0.0431 (3)	0.5272 (3)	0.4649 (4)	0.078 (4)	0.50
O7CA	0.13921 (11)	0.39846 (11)	0.29883 (14)	0.0415 (14)	1.00
O8	0.0791 (6)	0.5	0.4310 (9)	0.025 (7)	0.25
O80	0.11543 (14)	0.30324 (13)	0.39135 (18)	0.0677 (19)	1.00
O81	0.15199 (11)	0.44414 (12)	0.25286 (14)	0.0435 (14)	1.00
O82	0.11002 (16)	0.37239 (15)	0.5	0.0408 (19)	1.00
O83	0.09179 (15)	0.34860 (16)	0.43104 (19)	0.080 (2)	1.00
O84	0.0480 (3)	0.3435 (2)	0.3905 (2)	0.157 (5)	1.00
O85	0.0415 (2)	0.3569 (3)	0.4575 (3)	0.148 (4)	1.00
O86	0.26363 (13)	0.30055 (13)	0.25758 (17)	0.0623 (18)	1.00
O87	0.30421 (13)	0.31306 (13)	0.21735 (16)	0.0623 (17)	1.00
O88	0.07962 (14)	0.39523 (17)	0.26581 (18)	0.083 (2)	1.00
O89	0.09111 (18)	0.34425 (19)	0.2750 (2)	0.104 (3)	1.00
O8AA	0.2246 (4)	0.2727 (4)	0.1850 (5)	0.073 (5)	0.37
O8BA	0.1237 (8)	0.4226 (8)	0.1521 (10)	0.090 (10)	0.22
O8CA	0.09121 (11)	0.39819 (11)	0.34671 (14)	0.0418 (14)	1.00
O8DA	0.1513 (13)	0.4728 (13)	0.1843 (16)	0.18 (2)	0.22
O90	0.0493 (2)	0.3582 (3)	0.2386 (4)	0.266 (10)	1.00
O91	0.0999 (2)	0.3678 (3)	0.2155 (2)	0.159 (5)	1.00
O93	0.2270 (6)	0.2463 (6)	0.4454 (8)	0.081 (8)	0.25
O98	0.31757 (18)	0.37273 (18)	0.2267 (2)	0.097 (2)	1.00

Table SI3.7 Fractional atomic coordinates and isotropic or equivalent isotropic displacement parameters of Cs_2SO_4@MK-A, Space group $P4_2/mmc$. (Continued)

Atom	***x***	***y***	***z***	U_{iso}/U_{eq} **(Å^2)**	**Occupancy**
O99	0.2551 (2)	0.3316 (2)	0.1742 (3)	0.121 (3)	1.00
O9AA	0.1817 (3)	0.4825 (3)	0.2078 (4)	0.071 (4)	0.44
O9BA	0.0437 (3)	0.3305 (3)	0.3172 (3)	0.066 (3)	0.50
O9CA	0.0228 (12)	0.5435 (12)	0.4684 (15)	0.19 (2)	0.25
S1	0.1945 (3)	0.3085 (2)	0.4946 (5)	0.029 (4)	0.14
S13	0.1386 (5)	0.4701 (4)	0.1404 (6)	0.183 (10)	0.22
S1B	0.2101 (3)	0.3144 (2)	0.4987 (8)	0.053 (4)	0.19
S1C	0.2343 (4)	0.3213 (3)	0.4985 (10)	0.101 (6)	0.16
S2	0.0569 (3)	0.4673 (3)	0.5	0.043 (3)	0.25
S3	0.0630 (3)	0.5	0.4641 (4)	0.048 (3)	0.25
S4	0.23546 (12)	0.4932 (2)	0.27743 (16)	0.082 (3)	0.50
S5	0.05993 (8)	0.36034 (9)	0.42302 (10)	0.0995 (11)	1.00
S6	0.13079 (6)	0.5	0.31647 (7)	0.0296 (7)	1.00
S7	0.20770 (6)	0.43355 (6)	0.5	0.0330 (7)	1.00
S8	0.29538 (6)	0.29538 (6)	0.25	0.0579 (10)	1.00
S9	0.07898 (7)	0.36540 (10)	0.24911 (10)	0.1108 (14)	1.00